ABSTRACT

Title of Dissertation:
Behavior of Square and L-shaped Slender Reinforced Concrete Columns under Combined Biaxial Bending and Axial Compression.

Wen Hu Tsao, Ph.D. in Civil Engineering, January 1992

Dissertation directed by: Dr. C.T.Thomas Hsu, Professor
Department of Civil and
Environmental Engineering

A numerical analysis was developed to evaluate the complete load-deflection and moment-curvature relationships for square and L-shaped slender reinforced concrete columns subjected to biaxial bending and axial load. This computer model can be used for any cross section geometry and material properties of normal concrete. The analysis was based on a deformation control and both the ascending and descending branches of curves can be studied. The finite difference method was introduced to calculate the deflections which satisfy the compatibility equations. Six square slender columns and eight L-shaped slender columns were tested to compare their experimental load-deformation results with the analytical results derived from the theoretical studies. A satisfactory agreement was achieved for the present study. The results of present study can be used for future design reference.

BEHAVIOR OF SQUARE AND L-SHAPED SLENDER REINFORCED CONCRETE COLUMNS UNDER COMBINED BIAXIAL BENDING AND AXIAL COMPRESSION

by
Wen Hu Tsao

Dissertation submitted to the Faculty of the Graduate studies
of the New Jersey Institute of Technology in partial fulfillment
of the requirements for the degree of
Doctor of Philosophy
December, 1991

Blank Page

APPROVAL SHEET

Title of Dissertation:

Behavior of Square and L-shaped Slender Reinforced Concrete Columns under Combined Biaxial Bending and Axial Compression.

Name of Candidate: Wen Hu Tsao
Ph.D. in Civil Engineering, December 1991

Dissertation and Abstract Approved by:

Dr. C.T.Thomas Hsu, Professor
Department of Civil and
Environmental Engineering

Date

Signatures of other members of the dissertation committee

Dr. F.Ansari, Professor
Department of Civil and
Environmental Engineering

Date

Dr. A. Saadeghvaziri, Assistant Professor
Department of Civil and
Environmental Engineering

Date

Dr. J. Schuring, Associate Professor
Department of Civil and
Environmental Engineering

Date

Dr. A. S. Ezeldin, Assistant Professor
Department of Civil and
Ocean Engineering
Stevens Institute of Technology

Date

VITA

Name : Wen-Hu Tsao

Degree and date to be conferred : Doctor of Philosophy, Jan. 26, 1992.

Secondary education :

Collegiate institutions attended	Dates	Degree	Date of degree
New Jersey Institute of Technology	1985-1991	Ph.D	Jan., 1992.
Stevens Institute of Technology	1983-1985	M. E.	June, 1985.
Taipei Institute of Technology	1977-1980	Diploma	June, 1980.

Major : Structural Engineering, Civil Engineering.

The fear of the LORD is the beginning of wisdom,

and knowledge of the Holy One is understanding.

Proverbs 9 : 10 NIV

Dedicated to the memory of my mother,

to my father and

to my wife.

ACKNOWLEDGEMENTS

The work presented in this thesis was carried out under the direction of Professor C. T. Thomas Hsu to whom the author wishes to express his deepest gratitude. His constant encouragement and discussions throughout the years contributed in a large part to the development of this study.

The author also wishes to express his appreciation and gratitude to the following persons and organizations :

The author's fellow graduate students, in particular Mr. Gang Wang who assisted the author in computer programming. Mrs. S. M. Lin-Hsu, Messrs. M. H. Lin, J.C. Hsu, T. Y. Lee, C. S. Chang, J. H. Fu, W. H. Chao, M. S. Parikh, H. P. Savalia and C. T. Chou, who assisted the author in experimental test. Mr. Allen Luke, the staff of the Structural Concrete Laboratory at NJIT who helped conduct the experimental tests. Mr. John Eimess, the staff of Strength of Material Laboratory who helped prepare test setup for the experimental tests. Their effects are greatly appreciated.

The experiments were performed using the MTS testing system which was purchased under the NSF grant, No. CEE 8308339. Financial support to purchase the research materials from several New Jersey corporations and companies, graduate assistantship from NJIT which enabled the author to carry out this study, are also greatly acknowledged.

Contents

NOTATIONS

a_k : area of element k.

$\mathbf{C_{ij}}, \mathbf{B_{ij}}$: stiffness coefficient.

CL : length of segment (i).

d_x, d_y : deflection in X, Y axis.

d_u, d_v : deflection in U, V axis.

$d_{x_{(i+1)}}, d_{x_{(i)}}, d_{x_{(i-1)}}$: deflection at segment $(i+1), (i), (i-1)$ in X axis.

$d_{y_{(i+1)}}, d_{y_{(i)}}, d_{y_{(i-1)}}$: deflection at segment $(i+1), (i), (i-1)$ in Y axis.

$d_{u_{(i+1)}}, d_{u_{(i)}}, d_{u_{(i-1)}}$: deflection at segment $(i+1), (i), (i-1)$ in U axis.

$d_{v_{(i+1)}}, d_{v_{(i)}}, d_{v_{(i-1)}}$: deflection at segment $(i+1), (i), (i-1)$ in V axis.

e_x, e_y : eccentricity in X, Y axis.

e_u, e_u : eccentricity in U, V axis.

$(E_s)_k$: secant modulus of elasticity for element k.

$H_{(i)}, G_{(i)}, A_{(i)}, D_{(i)}$: temporary matrix notations to simplify the expressions in the matrix operations.

I_x : moment of inertia about X axis.

I_y : moment of inertia about Y axis.

I_{xy} : product moment of inertia.

lc : nodal number for the middle segment.

lp : length for the plastic hinge.

$M_{x_{(c)}}, M_{y_{(c)}}$: the calculated value for the bending moment components in X, Y axis under biaxial bending and axial compression.

$M_{u_{(c)}}, M_{v_{(c)}}$: the calculated value for the bending moment components in U, V axis under biaxial bending and axial compression.

$P_{(c)}$: the calculated value for the axial load P under biaxial bending and axial compression.

$\phi_{x_{(i)}}, \phi_{y_{(i)}}$: curvature at segment (i) with respect to $M_{x_{(i)}}, M_{y_{(i)}}$.

UALL : allowable incompatibility for load $P_{(c)}$.

VALL : allowable incompatibility for strain at coordinate origin $\epsilon_{0_{(i)}}$.

WALL : allowable incompatibility for deflections $d_{x(i)}, d_{y(i)}, d_{u(i)}, d_{v(i)}$.

x,y : centroidal coordinates for any element in the cross section.

x_k, y_k : centroidal coordinates for element k in the cross section.

θ_p : the angle between principal axes U,V and X,Y axes.

ϵ_k : strain at element k which is subjected to biaxial bending and axial compression.

$\epsilon_{0_{(i)}}$: strain at coordinate origin in the principal axes for segment (i).

ϵ_0 : strain at coordinate origin in the principal axes.

ϕ_x, ϕ_y : curvature with respect to M_x, M_y.

ϕ_u, ϕ_v : curvature with respect to M_u, M_v.

$\phi_{u_{(i)}}, \phi_{v_{(i)}}$: curvature at segment (i) with respect to $M_{u_{(i)}}, M_{v_{(i)}}$.

LIST OF TABLES

LIST OF FIGURES

1 INTRODUCTIONS

1.1 STATEMENT OF ORIGINALITY

The irregular shaped slender columns are required for some particular structural design; however, the load and deformation behavior of irregular shaped slender reinforced concrete columns is rarely available in the literature. There is no published data up to date which discuss both linear and non-linear load-deformation behavior of L-shaped slender reinforced columns under combined biaxial bending and axial compression, particularly for descending branch of load-deformation curve.

The present research carries out not only experimental tests but also theoretical studies as well for complete load-deformation behavior of biaxially loaded slender reinforced concrete columns with square and L-shaped cross sections.

The finite difference method proposed herein for both standard and L-shaped columns has been found to be a very simple model to study the effects of plastic hinge and ductility behavior in columns.

1.2 LITERATURE REVIEW

1.2.1 BIAXIAL BENDING AND AXIAL LOAD

Many researchers have done a lot of investigations or designs for reinforced concrete members under biaxial bending and axial compression. Muller [63] proposed a design method by using a simple monograph. Chu [18] assumed the position of the neutral axis and stress distribution across the section to find the ultimate capacity due to axial load and moment. It can be extended to any sections of irregular shapes subjected to any kind of loading. However, the deformation behavior was not discussed.

Au [8] combined unsymmetrical bending in two direction, called skew bending, He assumed an equivalent uniform stress distribution over the compressive concrete section. Charts were provided to find the dimensions of the equivalent compressive stress block. This procedure can be solved by trial and error method.

Based on approximated failure surfaces, Bresler [15] derived some approximated mathematical expressions suggested by Pannell [66]. Two alternative methods are shown in the following:

Bresler load-contour method : A simple direct method is provided to calculate the ultimate strength of a reinforced concrete column subjected to axial compression and biaxial bending. The equation is given below:

$$\frac{1}{P_i} = \frac{1}{P_x} + \frac{1}{P_y} - \frac{1}{P_0}$$

P_x , P_y = the load carrying capacities under compression with uniaxial eccentricities e_x and e_y respectively.

P_0 = the load carrying capacity under pure axial compression.

Bresler failure surface method: A nondimensional interaction equation was proposed to represent the failure surface at a constant axial compression.

$$(\frac{M_x}{M_{x_0}})^{\alpha} + (\frac{M_y}{M_{y_0}})^{\beta} = 1.0$$

α , β are exponents that depends on the dimensions of the cross section, the reinforcement amount and location, concrete strength, steel yield stress and amount of concrete cover.

$$M_x = P_n e_y$$

$$M_y = P_n e_x$$

M_{x_0} = M_x capacity at axial load P_n when M_y is zero.

M_{y_0} = M_y capacity at axial load P_n when M_x is zero.

e_x, e_y = eccentricities along x and y axis respectively.

Furlong [31] assumed that the neutral axis is perpendicular to the resultant moments and simplified the biaxial bending on the square columns to an uniaxial bending. The interaction diagrams were proposed by all calculations for any arrangement of reinforced square columns.

Meek [60] assumed that the neutral axis coincides with the limit of the Whitney stress block and the e_x, e_y remain constant so that if P is increased, the bending moment M_x, M_y can be increased proportionately. By changing the inclination and location of neutral axis and finding α value, the interaction of biaxial eccentricity can be simplified to an uniaxial eccentricity.

$$\frac{M_y}{M_x} = \frac{e_x}{e_y} = \alpha = constant$$

Wiesinger [83] demonstrated the design of small eccentricities for symmetrical columns in one or two directions. where e'/t is not more than 2/3 in either direction.

e'= the eccentricity of the resultant load.

t= out-to-out dimension of column in the direction of bending.

Two dimensionless variables : "shape factor" for the gross area, g, and "pattern factor" for the steels were introduced for convenience. The design procedure was followed by those tables and calculated by trial and error method.

Pannell [66] could predict stress distributions by considering the interaction surface based on the three dimensional curves of failure load against the corresponding moments. The equation for transforming the actual moment is given below :

$$M_g = \frac{F M_y \sec\theta}{1 - N(\sin^2 2\theta)}$$

$$\theta = \tan^{-1}\frac{\phi M_x}{M_y}$$

where M_x, M_y are the components on the x and y axes of actual radial moment.

ϕ= the ratio M_{by}/M_{bx} of the balanced failure moments.

F= a factor adjusting for steel cover ratio.

$$F = \frac{M_{bb}}{M_{ba}}$$

M_{ba} = the balanced failure moment for the actural steel cover used.

M_{bb} = the equivalent moment for the ratio upon which the design curve is based.

N= a deviation factor.

M_g= the moment to be used in conjunction with the required failure load P.

Pannell [65] also extended Bresler's [29] equation to the following formula :

$$(\frac{M_y}{M_{f_y}})^n + (\frac{M_x}{M_{f_x}})^n = 1$$

where M_{f_y}, M_{f_x} = the failure moments for some load P acting in planes x and y respectively.

Rewriting

$$\frac{M_{f_y}}{M_y} = \sqrt[n]{1 + (\tan\theta)^n}$$

where

$$\tan\theta = \phi\frac{M_x}{M_y}$$

and

$$\frac{M_{f_y}}{M_y} = \frac{\sec\theta}{1 - N\sin^2 2\theta}$$

Both equations need to make load-moment interaction curve served for all depth-of-cover ratios. If the column has a different d_2/d ratio, then the quantity M_{f_y} shall be multiplied by F to obtain an appropriate value of M_{f_y}, where

d=over-all depth of column.

d_2 = concrete cover depth to the center line of steel.

Ang [7] proposed a method based on the "cracked section" theory to design a column under biaxial bending and axial load. The neutral axis for uncracked section was determined by using the familiar formula for eccentrically loaded column as follows :

$$\frac{P}{A} \pm \frac{M_y c_1}{I_x} \pm \frac{M_x c_2}{I_y}$$

Ang assumed the position of the neutral axis of the cracked section to be parallel to that of the uncracked section, and the final result may be obtained by trial and error method.

Aas-Jakobsen [1] assumed the equivalent moment M_e to simplify the design procedure of a column under a biaxially eccentric load.

A finite element approach was used by Warner [80] in which the concrete and steel areas in the cross section are broken into many small discrete areas. Axial force and biaxial moments can be determined by summation of the elemental forces acting on the elemental areas and summation of the moments of the elemental forces. Any desired form of stress-strain relations for concrete and steel can be used and any irregularities in the shape of cross section and in any arrangement of steel reinforcement can also be calculated.

Fleming and Werner [29] presented a simplified ultimate strength design procedure, for the most widely used ranges of concrete strength, steel yield and steel percentage. It can be directly obtained the size of section and area of reinforcing steel by the design curves. The neutral axis for the cross section was determined by trial and error approach.

Weber [81] has shown a set of charts for both analysis and design of columns with biaxial bending. There are some limitations for applying the chart. It's only good for square column with symmetrical reinforcing and for different combination.

Cranston [23] in 1967, presented the computer method by finding the relations between moment, axial load and curvature (M-P-ϕ) to form the governing differential equations. This method can take care of the columns with different materials, cross section varied along the length of the column, residual stresses existed, initial curved column and the moment developed in the end restraint systems. The cross section of column was divided into strips perpendicular to the principal axis. The bending moment of the column was limited to only about the principal axis. The computer procedure was followed by the inelastic analysis and could calculate all stages of behavior up to maximum load.

Ramamurthy [70] in 1966, proposed the design method of biaxially loaded columns by trial and error procedure and failure surface in order to determine the ultimate load. The approach was limited for rectangular and square cross section with symmetrical distribution of reinforcement.

Farah, Huggins [28] in 1969, studied the hinged reinforced concrete columns under biaxial bending and axial load by an integration method. Three simultaneous nonlinear equations was solved by the Newton-Raphson method. The flexure rigidity EI varied along the column and for each loading condition should be renovated. The strain distribution was first assumed and by successive iteration of the summation forces and moments which was compared to the applied loads and moments in order to obtain the equilibrium situations. The Newton-Raphson method was introduced to speed the convergence to equilibrium. The procedure could be extended for slender column just dividing the column into segments and again into sections.

Hsu [40,46] in 1973 and 1974, presented the determination of strain and curvature distribution in reinforced concrete sections under biaxial bending and axial load. The computer program was developed to study the ultimate strength, interaction diagrams and deformation behavior. The computer analysis can handle any concrete cross section geometry, steel arrangement and material properties. Taylor's expansion was introduced for calculating the summation of loads and moments and the Newton-Raphson method was used to accelerate the convergence.

Smith [77] in 1973, assumed a steel ratio for a given column size and used the equivalent uniaxial eccentricity to simplify the biaxial bending case.

Gouwens [32] in 1975, gave a design procedure for concrete column subject to biaxial bending. A couple of equations were illustrated to compare with the others researcher's results.

Furlong [30] in 1979, recommended a design procedure for biaxially loaded concrete columns. It followed the usage of a parabola-trapezoidal stress strain function for concrete compression zone instead of the traditional rectangular stress block and the results were found to be more accurate with the observed results than the other analytic stress strain functions.

Taylor [78] in 1985, proposed a direct design method by two approaches

: Firstly, the direct design contour charts was used to facilitate the design. Secondly, an automatic design procedure was proposed using the computer program that required some informations.

There are very few research studied the subject of reinforced concrete member under combined biaxial bending and tension. Hsu [41] in 1986, presented an important aspect in the development of the strength-interaction diagrams, load contours failure surface and design equations. The computer program was created for any geometry of cross section and material properties.

Ross and Yen [74] in 1986, proposed an interaction design of reinforced concrete columns with biaxial bending. The simplified approach was made by assuming the biaxial bending capacity to uniaxial bending capacity and thus obtained a mathematical description of a particular load contour representing the intersection of the failure surface. But the equilibrium and compatibility conditions were not always ensured and suggested for use in a square cross section only.

Recently, Hsu [45] proposed a general equation representing a three-dimensional failure surface of a column section. He provided a reasonable mathematical equation that can represent both the strength interaction diagrams and failure surface for the member under combined biaxial bending moments and axial load. The equation of failure surface method has been found to be a simpler and more logical approach for analysis and design of columns under combined biaxial bending and axial load. A general equation can be written as follows:

$$(\frac{P_n - P_{nb}}{P_0 - P_{nb}}) + (\frac{M_{nx}}{M_{nbx}})^{1.5} + (\frac{M_{ny}}{M_{nby}})^{1.5} = 1.0$$

where

P_n = nominal axial compression (positive), or tension (negative).

M_{nx}, M_{ny} = nominal bending moments about x- and y-axis, respectively.

P_0 = maximum norminal axial compression (positive), or axial tension (negative).

P_{nb} = norminal axial compression at balanced strain condition.

M_{nbx}, M_{nby} = norminal bending moments about x- and y-axis, respectively, at balanced strain condition.

1.2.2 BIAXIALLY LOADED L-SHAPED REINFORCED CONCRETE COLUMNS

The analysis and design of L-shaped columns under biaxial bending and axial load is sometime encountered in a building project. The corner columns in a framed structure and bridge piers are usually subjected to combined biaxial bending and axial load.

Muller [62] in 1959, proposed the design method of the L-shaped columns with small eccentricities. The application was limited for the column sections symmetrical about 45 degree axis. Three sets of tables could be found useful during the trial and error procedure.

Marin[56] in 1979, presented the design aids for L-shaped short columns subjected to biaxial bending and axial load. The idea was illustrated by an isobaric failure surface. The selected concrete cross sections were also symmetrical about the 45 degree axis and the steel distributions were limited to one kind for each thickness ratio studied. The design charts were only available to very simple geometries.

Ramamurthy [70] in 1983, presented two approaches: First method was based on failure surface in actual shapes of load contours using an inverse method of analysis. Second method was proposed to design the L-shaped section by the method of an equivalent square or rectangular cross section.

Hsu [38] in 1985, studied both the strength and deformational behavior of L-shaped tied columns under combined biaxial bending and axial compression. The computer program was developed to satisfy the equilibrium of forces and strain compatibility. The Newton-Raphson numerical method was again used to handle the nonlinear convergence. For given material stress-strain relationships for concrete and reinforcement steels, the L-shaped cross section was divided into elements for computer analysis. Since plane sections remain plane during bending, Hsu proposed :

$$\epsilon_k = \epsilon_p + \phi_u v_k + \phi_v u_k$$

where ϵ_p= uniform longitudinal strain at plastic centroid

ϕ_u, ϕ_v= the curvature produced by bending moment M_u, M_v respectively.

v_k, u_k= the coordinates about the principal axes for the element k. After

the strain distribution is assumed and by stress-strain curves the axial force P and bending moment M_u, M_v can be calculated by

$$P_{(c)} = \sum_{k=1}^{n} f_k a_k$$

$$M_{u(c)} = \sum_{k=1}^{n} f_k a_k v_k$$

$$M_{v(c)} = \sum_{k=1}^{n} f_k a_k u_k$$

The iteration procedure is required to meet the convergence for each assumed loading step with $P_{(s)}, M_{u(s)}, M_{v(s)}$ and can be accelerated by the extended Newton-Raphson method. where

$$M_{u(s)} = P_{(s)}e_v$$

$$M_{v(s)} = P_{(s)}e_u$$

where e_u, e_v are the load eccentricity components along u,v axes. The coordinate transformation is also needed to calculate the load, moment and curvature with respect to global coordinate axes x and y, respectively. They are shown in reference Hsu[38]. From the theoretical analysis results, the theoretical interaction curves could be obtained corresponding to centroidal axes.

For the experimental program, the demec gage method was used by Hsu [38] in order to obtain the strain distributions, and the curvature could be determined by the following equation :

$$\phi_x,\ or\ \phi_y = \frac{\epsilon_c}{kd}$$

kd=the distance between the location with the concrete strain ϵ_c and the point of zero strain along x or y axis.

The load contour interaction relating M_{nx}, M_{ny} can be obtained from cutting the failure surface at a constant load P_n,where

$$M_{nx} = P_n e_y$$

$$M_{ny} = P_n e_x$$

where M_{nx}, M_{ny} are nominal bending moment about x and y axis, respectively.

A general non-dimensional equation as proposed by Hsu [38] : the load contour can be again used for a design formula of L-section

$$(\frac{M_{nx}}{M_{ox}})^{\alpha_1} + (\frac{M_{ny}}{M_{oy}})^{\alpha_2} = 1.0$$

where α_1, α_2 are dependent on the dimension of the column, steel ratio and material properties etc.

$M_{ox} = M_{nx}$ capacity at axial load P_n when M_{ny} is zero.

$M_{oy} = M_{my}$ capacity at axial load P_n when M_{nx} is zero.

1.2.3 SLENDER REINFORCED CONCRETE COLUMNS

Broms and Viest [16] in 1958, introduced the ultimate strength analysis of long restrained ended reinforced concrete columns under bending and axial compression. The strength of a restrained column depends on both the properties of the column and the restraining members. The deflected shape of the column was assumed a part of cosine wave and the restraining moment was assumed proportional to the end rotations.

Chang and Ferguson [17] in 1963, presented the study for both eccentrically and concentrically loaded, slender reinforced concrete columns under short-time load. The concentrically loaded column analysis was based on von Kármán's theory and Hognestad's stress-strain relationship for concrete, and the idealized stress-strain curve for reinforcing steel. For the specific values of column load, the moment versus edge-strain curves were plotted. These curves were corrected between the moment and load for each in terms of edge strains which were derived by a couple of equations. At first they solved the load versus edge-strain equations, then obtained the moment versus edge-strain curves for a given critical load. By numerical integration of moment versus edge-strain curve, the deflection shape, length of cracking in the section and end slope of deflected column were determined.

Parme [68] in 1966, proposed the design aids for restrained eccentrically loaded slender column which provided the practical method for designers. He concluded that the design followed by the stability analysis was time consuming and the use of the ACI Code reduction formulas were too conservative to utilize.

MacGregor and Barter [53] in 1966, used the long column analysis by Pfrang and Siess [69] to determine the eccentrically loaded long columns bent in double curvature. The column was tended to bent in a single curvature, but in order to obtain the double curvature , the end restraints were introduced. A portion of moment applied to the joint was resisted by the restrained members. The column was stronger than a hinged column subjected to the same eccentricity. The second effect of bending moment was tended to strengthen the column, and the slenderness had less effect on restrained columns than on hinged column.

Martin and Olivieri [57] in 1966, tested the slender reinforced concrete columns under opposite eccentricity loading. A point of contraflexure between the ends of the column would produce the study of the difference in strength reduction for length of compression members depending on the location of the contraflexure. They used the computer program developed by Breen and Ferguson [14] to accomplish the theoretical analysis. The analysis was based on von Kármán's theory and Hognestad's stress block for concrete and an elasto-plastic stress strain relationship for steel.

Drysdale [26] in 1967, studied the behavior of slender reinforced concrete column subjected to sustained biaxial bending. The experiment was investigated by a single column size with constant material properties, and the columns were tested in pair to ensure the accuracy of results. The mathematical column model was developed to study the shrinkage, creep and elastic strains. Only half column length was used because the column bent in symmetric single curvature. The pinned-ended condition was used.

Abolitz [3] in 1968, presented the equations instead of the regular charts or table for working stress design of symmetrically reinforced short and long columns subjected to flexure. The design approaches were followed, one in accordance with ACI Code and the other was only for rectangular columns by an alternative method and could be modified later for square or circular sections. The biaxial bending followed the same formulas except the addition of the computation of weighted averages.

Warner [80] in 1969, presented a finite element approach by dividing the concrete cross section and steel areas into small elements and by summation of the elemental forces in order to determine the biaxial moments. It could be used for any stress-strain relations of concrete tensile strength and the extended unloading of concrete in compression at high strains.

MacGregor, Breen and Pfrang [50] in 1970, presented a proposal to revise the long column design procedures of the ACI 318-63. The columns was designed to carry the forces and moments based on a rational second order structural analysis. A moment magnifier δ was introduced for the design procedure which was similar to the one used in ACI 1963 Specifications. This moment magnifier was affected by the ratio of end moments and the deflected shape. The results of this proposed procedure led the designer to understand the basic behavior in slender columns and to evaluate the additional moment requirements in restraining members.

Colville [19] in 1975, developed a simplified procedure of estimating a deflection magnification factor and investigated the accuracy of the moment magnification in the design of square reinforced concrete columns. A finite element approach was used to study the effects of tension cracking, nonlinearity of the concrete in compression and yielding of the reinforcing steel. By including the effects of secondary bending and large displacement, the geometric nonlinearity was considered in this study.

MacGregor, Oelhafen and Hage [52] in 1975, presented the analysis of a step-by-step incremental rate-of-creep of a reinforced concrete columns subjected to sustained loads and they were able to work out a statistical evaluation of the flexural stiffness EI. A series of computer experiments were also carried out to derive the design equations for flexural stiffness EI, as given below :

$$EI = \frac{E_c I_g}{5\alpha} + E_s I_s$$

or

$$EI = \frac{E_c I_g}{5\alpha} + 1.2 E_s \rho_t I_g$$

where

$\alpha = 0.75 + 1.8\beta_p$ but not less than 1.0 .

β_p= the ratio of the design sustained load to the total design load.

ρ_t= total reinforcement ratio.

I_g= gross moment of inertia of uncracked concrete section.

I_s= moment of inertia of the reinforcing bars.

E_c, E_s= modulus of elasticity of concrete and steel.

EI= rotational stiffness of cross section.

It was recommended to use in the current ACI Code.

Basu and Suryanarayana [9] in 1975, proposed the computer method for analyzing the restrained long reinforced columns under biaxial bending. No sidesways were permitted. The load-deflection and moment-end rotation were studied by the results of the computer analysis. Only half of the column length was inputted according to the assumed symmetrically bent single curvature. The nonlinear governing equations were solved and the convergence for iteration was assured by the delta-square extrapolation procedure.

Abdel-Sayed [2] in 1975, proposed the improved method of slender reinforced concrete column under biaxially eccentric loading. A calibrating factor was presented for the use of the section property for square symmetrically reinforced concrete columns. the rectangular cross section could follow the second calibrating factor by using the same section property. The method took into account the compatibility of strains and lateral deformations. The designers could obtain a good initial estimate for the cross section by the section property curves. For different arrangement of reinforcement, it required an additional set of section properties curves.

Al-Noury [4] in 1982 and [5] in 1980, used the finite segment method to analyze the reinforced concrete column from a space structure. The cross was divided into finite elements to calculate its tangent stiffness by solving the governing differential equations about the principal axes. The modified tangent stiffness approach was used to handle the material plasticity and the geometrical change during the iterations.

The incremental tangent stiffness matrix was derived from

$$\{\delta F\} = [Q]\{\delta D\}$$

δF , δD= the infinitesimal changed in force and deformation.

[Q]= the incremental tangent stiffness matrix of each element.

From the force equilibrium of equations and the stress-strain relationships for each material, the change in forces are equal :

$$\delta M_x = \sum_{i=1}^{N_a}\sum_{j=1}^{N_b} y_j(G_c)_{ij}(\delta\epsilon_c)_{ij} + \rho'\sum_{k=1}^{N_s} y_k(G_s)_k(\delta\epsilon_s)_k - \rho'\sum_{k=1}^{N_s} y_k(G_c)_k(\delta\epsilon_c)_k\Delta A_c$$

$$\delta M_y = \sum_{i=1}^{N_a}\sum_{j=1}^{N_b} x_i(G_c)_{ij}(\delta\epsilon_c)_{ij} + \rho'\sum_{k=1}^{N_s} x_k(G_s)_k(\delta\epsilon_s)_k - \rho'\sum_{k=1}^{N_s} x_k(G_c)_k(\delta\epsilon_c)_k\Delta A_c$$

$$\delta P = \sum_{i=1}^{N_a}\sum_{j=1}^{N_b} (G_c)_{ij}(\delta\epsilon_c)_{ij} + \rho'\sum_{k=1}^{N_s} (G_s)_k(\delta\epsilon_s)_k - \rho'\sum_{k=1}^{N_s} (G_c)_k(\delta\epsilon_c)_k\Delta A_c$$

where

x_k, y_k, x_i, y_j= the coordinates for each element.

ρ' = the transformed steel ratio.($=N_c\rho/N_s$)

ρ = reinforcement ratio.

$(G_c)_{ij}, (G_s)_k, (G_c)_k$= the stiffness for concrete and steel.

$(\delta\epsilon_c)_k, (\delta\epsilon_c)_{ij}, (\delta\epsilon_s)_k$ = the incremental change of strain for concrete and steel.

N_a, N_b= the number of concrete element in rows and columns.

N_c, N_s= the number of cross section elements for concrete and steel.

ΔA_c= concrete element's area.

The strain distribution assumed to be linear,

$$\epsilon = \epsilon_0 + y\phi_x + x\phi_y$$

ϵ= strain at any point.

ϵ_0= strain from the compression loading only.

ϕ_x, ϕ_y= curvature with respect to x,y axes.

Then,

$$\begin{Bmatrix} \delta M_x \\ \delta M_y \\ \delta P \end{Bmatrix} = \begin{bmatrix} Q_{11} & Q_{12} & Q_{13} \\ Q_{21} & Q_{22} & Q_{23} \\ Q_{31} & Q_{32} & Q_{33} \end{bmatrix} \begin{Bmatrix} \delta\phi_x \\ \delta\phi_y \\ \delta\epsilon_0 \end{Bmatrix}$$

The incremental deformation can be solved by

$$\{\delta D\} = [Q]^{-1} \{\delta F\}$$

For biaxially loaded slender reinforced concrete columns, the original centroid of the cross section is moved to an instantaneous centroid due to the nonlinearity of concrete stress-strain relation.

The axes transformation and rotation are required to obtain the new principal axes. The segment stiffness matrix $[K(10 \times 10)]$ can be obtained by the following equation :

$$\left\{ \begin{array}{c} f_A(3) \\ m_A(2) \\ f_B(3) \\ m_B(2) \end{array} \right\} = \left[\begin{array}{c} \\ k(10 \times 10) \\ \\ \end{array} \right] \left\{ \begin{array}{c} u_A(3) \\ \theta_A(2) \\ u_B(3) \\ \theta_B(2) \end{array} \right\}$$

The axial deformation, shear deformation and the torsional effects were neglected by Al-Noury. He concluded that the tangent stiffness approach gave a lower bound solution and yielded the good results for slender reinforced concrete column under biaxial loads.

1.3 OBJECTIVES OF THE RESEARCH

1. To develop a non-linear computer analysis of slender reinforced concrete columns under combined biaxial bending and axial load. Both material and geometrical nonlinearity are included in the computer analysis. The analysis can also be used for any section geometry. The computer analysis will evaluate the complete behavior of the moment-curvature and load-deflection characteristics for biaxial loaded slender reinforced concrete columns with standard and L-shaped cross sections.

2. To test six 4 feet long square reinforced concrete columns and eight 4 feet long L-shaped reinforced concrete columns under combined biaxial bending and axial compression. The proportional loading and pinned-ended conditions are used. The experimental ultimate load, moment-curvature and load-deflection curves will be attained and compared with the results of the proposed computer analysis.

3. The main purpose of this research is to investigate the behavior of the square and L-shaped slender columns subjected to biaxial bending and axial compression. The experiment results and computer analysis derived from this study may contribute to the development of any future design method.

2 THEORETICAL ANALYSIS

2.1 Analysis of standard shaped slender column

To study the complete load-deflection and moment-curvature curves of standard shaped slender columns subjected to biaxial bending and axial compression with monotonic loadings, a strain compatibility and equilibrium of forces and moments which can account for any loading condition and material properties must be utilized.

The present computer analysis is based on the following assumptions :

1. Plane section remains plane before and after bending.
2. Strains in the steel and concrete at their interfaces are assumed to be compatible.
3. Effect of creep and shrinkage are neglected.
4. There is no initial deflection in the undeformed columns.
5. The axial deformation, shear deformation and torsional effect are all neglected.
6. Monotonic loading.

The cross section of a standard shaped slender column can be divided into several small elements as shown in Fig.(1) . Consider for each small element k, with its centroidal coordinates (x_k, y_k), the strain ϵ_k is assumed to be uniformly distributed across the element k. According to the assumptions that plane section remains plane , and for an element that is subjected to biaxial bending and axial compression, the strain ϵ_k can be expressed in the following form:

$$\epsilon_k = \epsilon_0 + \phi_x y + \phi_y x \tag{1}$$

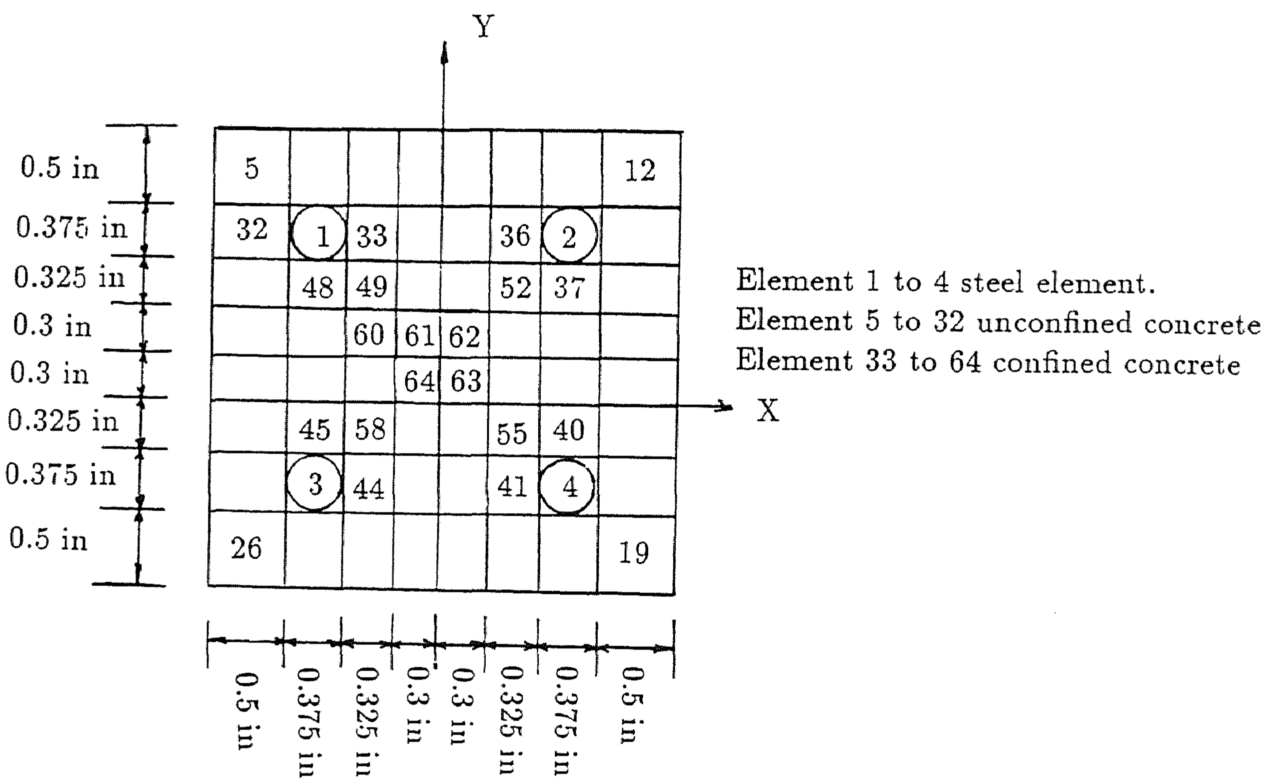

Figure 1: Cross section of square slender column.

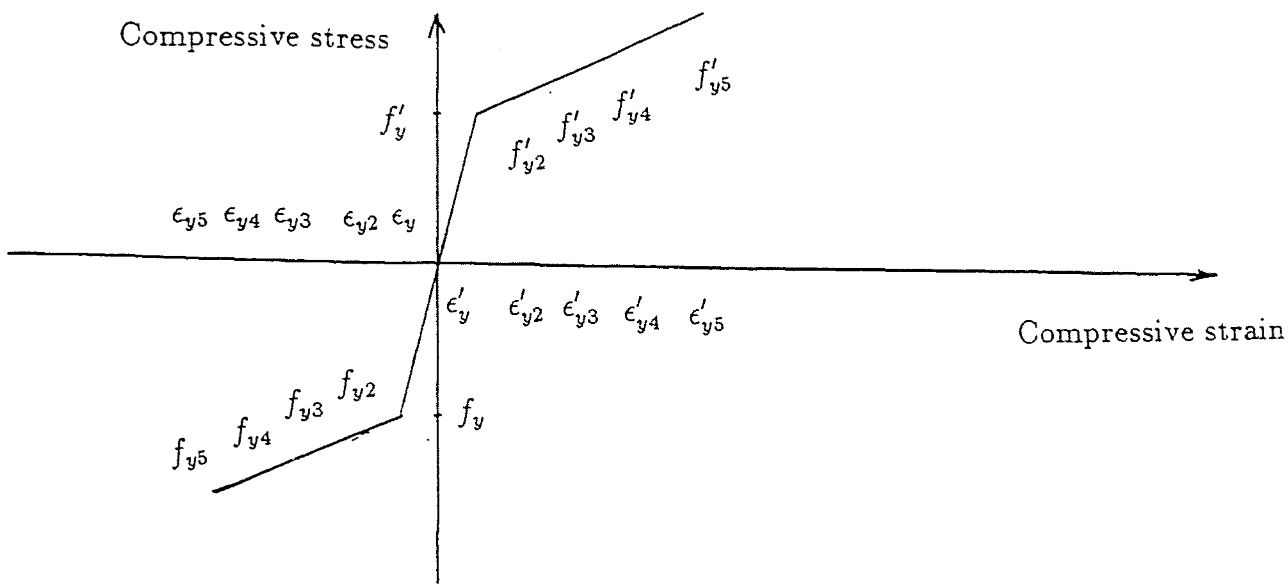

Figure 2: Idealized piecewise linear stress-strain curve

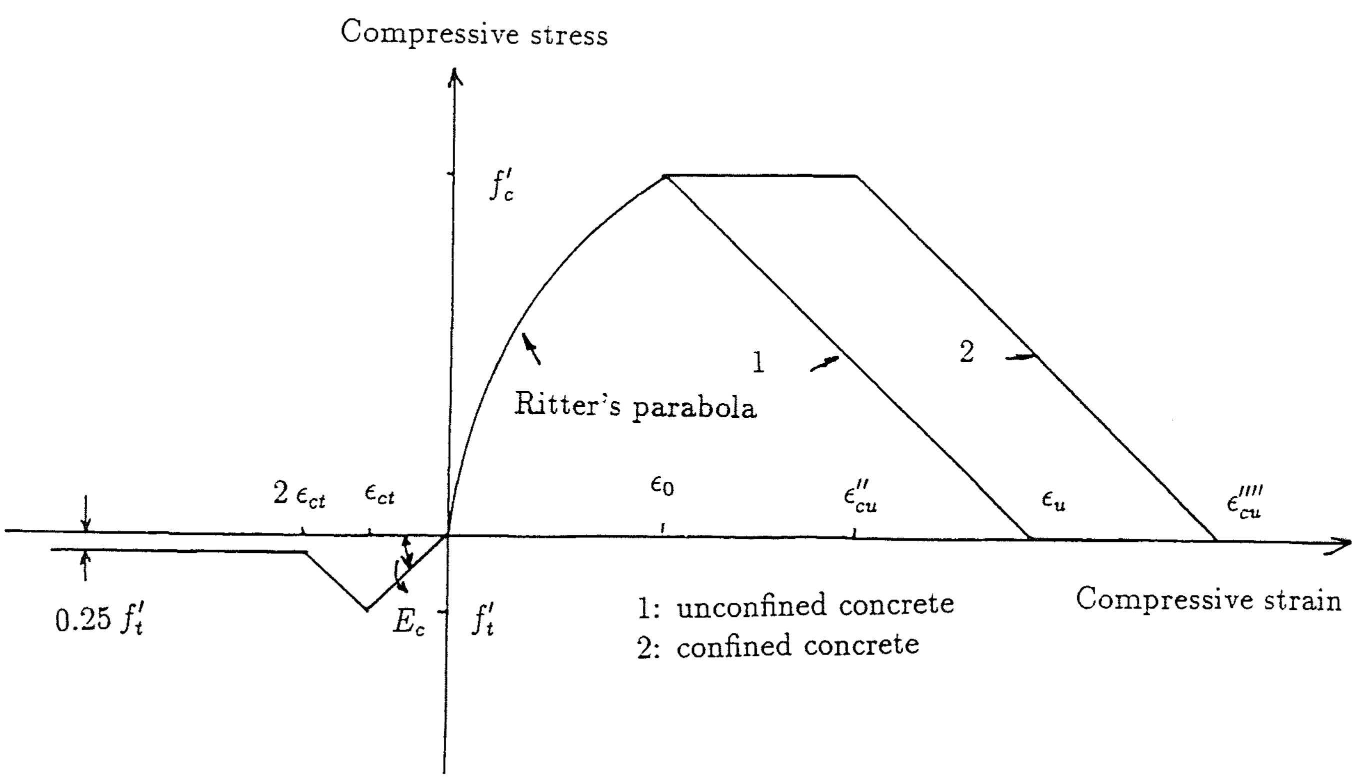

Figure 3: Modified Cranston-Chatterji stress-strain curve (Hsu [40])

where

ϵ_0 : strain at the coordinate origin of the principal axis.

ϕ_x : curvature with respect to M_x. ϕ_x is positive when it can produce compressive strains in the positive y direction.

ϕ_y : curvature with respect to M_y. ϕ_y is positive when it can produce compressive strains in the positive x direction.

Idealized piecewise linear stress-strain curve and modified Cranston-Chatterji stress-strain curve (see Appendix F.) have been used for reinforcing steel and concrete elements, respectively. For a value of strain ϵ_k , a value of the secant modulus of elasticity $(E_s)_k$ for steel or concrete elements can be obtained from Fig.(2) and Fig. (3). The secant modulus of elasticity can be assured to give the positive values of $(E_s)_k$ and to prevent the singularity problem in the matrix operation. The equilibrium equations in the cross section with n elements for the axial load P, bending moment components M_x, M_y can be expressed in the following forms :

$$\begin{aligned} P_{(c)} &= \sum_{k=1}^{n} (E_s)_k \epsilon_k a_k \\ M_{x_{(c)}} &= \sum_{k=1}^{n} (E_s)_k \epsilon_k a_k y_k \\ M_{y_{(c)}} &= \sum_{k=1}^{n} (E_s)_k \epsilon_k a_k x_k \end{aligned} \tag{2}$$

The subscript (c) from $P_{(c)}, M_{x_{(c)}}, M_{y_{(c)}}$ expresses the calculated values in an iteration cycle.

$(E_s)_k$: the secant modulus of elasticity in element k.

ϵ_k : strain of element k.

a_k : area of element k.

x_k, y_k : coordinates at the centroid of element k.

Substitute Eq.(1), in Eq. (2), Eq.(2) can be rewritten in the following matrix form.

$$\begin{Bmatrix} P_{(c)} \\ M_{x_{(c)}} \\ M_{y_{(c)}} \end{Bmatrix} = \begin{bmatrix} \sum_{k=1}^{n}(E_s)_k a_k & \sum_{k=1}^{n}(E_s)_k a_k y_k & \sum_{k=1}^{n}(E_s)_k a_k x_k \\ \sum_{k=1}^{n}(E_s)_k a_k y_k & \sum_{k=1}^{n}(E_s)_k a_k y_k^2 & \sum_{k=1}^{n}(E_s)_k a_k x_k y_k \\ \sum_{k=1}^{n}(E_s)_k a_k x_k & \sum_{k=1}^{n}(E_s)_k a_k x_k y_k & \sum_{k=1}^{n}(E_s)_k a_k x_k^2 \end{bmatrix} \begin{Bmatrix} \epsilon_0 \\ \phi x \\ \phi y \end{Bmatrix} \tag{3}$$

And let

$$\begin{aligned} C_{11} &= \sum_{k=1}^{n}(E_s)_k a_k \\ C_{12} &= C_{21} = \sum_{k=1}^{n}(E_s)_k a_k y_k \\ C_{13} &= C_{31} = \sum_{k=1}^{n}(E_s)_k a_k x_k \\ C_{22} &= \sum_{k=1}^{n}(E_s)_k a_k y_k^2 \\ C_{23} &= C_{32} = \sum_{k=1}^{n}(E_s)_k a_k x_k y_k \\ C_{33} &= \sum_{k=1}^{n}(E_s)_k a_k x_k^2 \end{aligned}$$

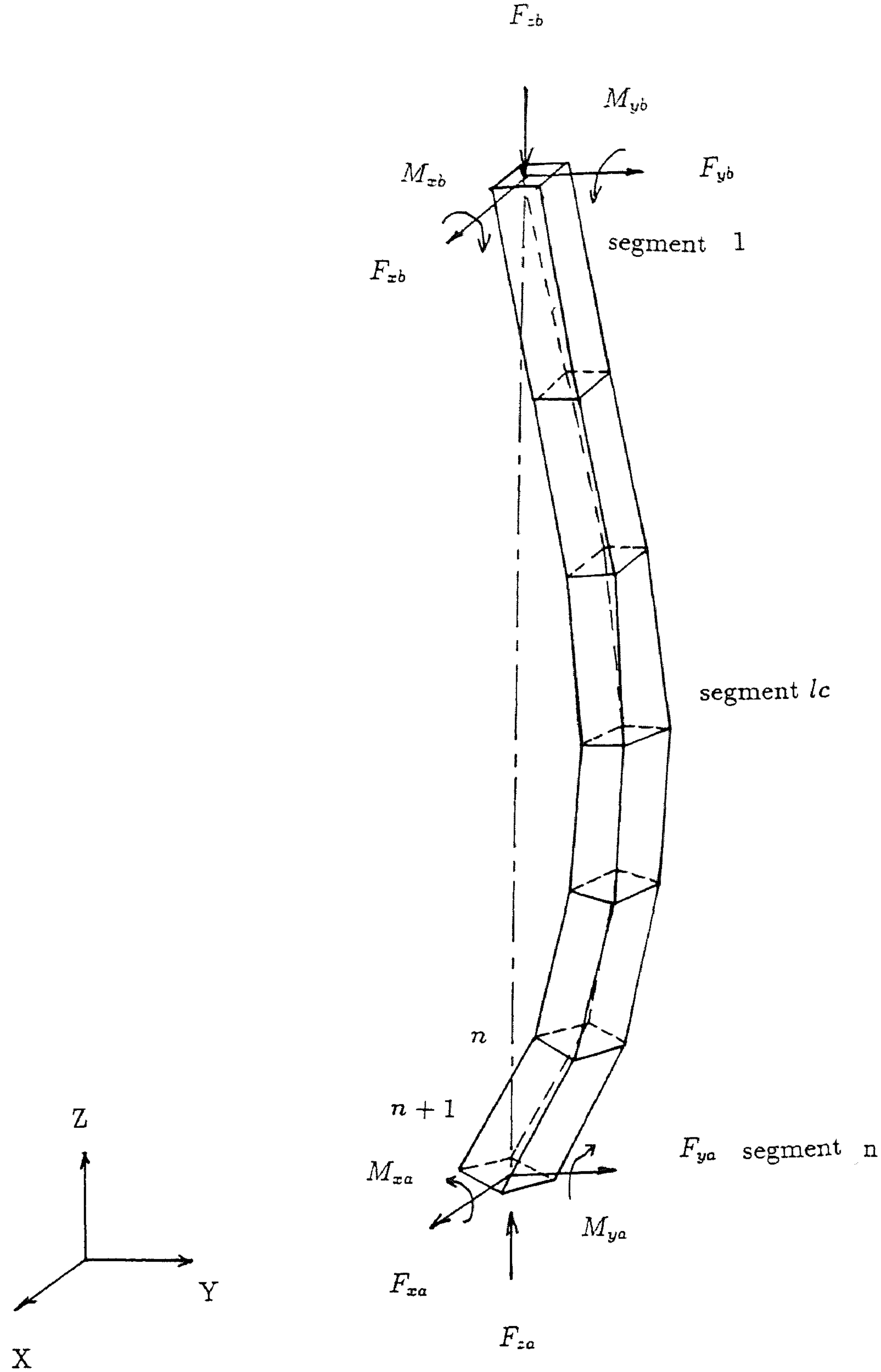

Figure 4: Slender square column divided into n segments

For slender column, the second order effect is important and for the case of proportional loading. Let d_x, d_y be expressed the deflections of column in x and y axis, respectively. Eq.(3) can be simplified in the following :

$$\left\{ \begin{array}{c} P_{(c)} \\ P_{(c)}(e_y + d_y) \\ P_{(c)}(e_x + d_x) \end{array} \right\} = \left[\begin{array}{ccc} C_{11} & C_{12} & C_{13} \\ C_{21} & C_{22} & C_{23} \\ C_{31} & C_{32} & C_{33} \end{array} \right] \left\{ \begin{array}{c} \epsilon_0 \\ \phi x \\ \phi y \end{array} \right\} \tag{4}$$

The finite difference method is hereby introduced to solve the three dimensional behavior of slender columns. As shown in Fig.(4), slender column is divided into several segments. The fundamental idea of this method is to replace the differential equation of the deflection curve by its finite difference approximation, and then to solve algebraically the finite difference equations obtained at serval segments along the column. So for the segment (i) :

$$\begin{aligned} \frac{d_{y(i+1)} - 2d_{y(i)} + d_{y(i-1)}}{(CL)^2} &= -(\phi_x)_{(i)} \\ \frac{d_{x(i+1)} - 2d_{x(i)} + d_{x(i-1)}}{(CL)^2} &= -(\phi_y)_{(i)} \end{aligned} \tag{5}$$

where

CL=the length of segment (i).

Substitute (5) in Eq.(4), one has

$$\left\{ \begin{array}{c} P_{(c)} \\ P_{(c)}(e_y + d_{y_{(i)}}) \\ P_{(c)}(e_x + d_{x_{(i)}}) \end{array} \right\} = \begin{bmatrix} C_{11} & C_{12} & C_{13} \\ C_{21} & C_{22} & C_{23} \\ C_{31} & C_{32} & C_{33} \end{bmatrix} \left\{ \begin{array}{c} \epsilon_{0_{(i)}} \\ -(d_{y_{(i+1)}} - 2d_{y_{(i)}} + d_{y_{(i-1)}})/(CL)^2 \\ -(d_{x_{(i+1)}} - 2d_{x_{(i)}} + d_{x_{(i-1)}})/(CL)^2 \end{array} \right\} \tag{6}$$

Expand Eq.(6) and rearrange it and for the segment (i)

$$(CL)^2 \left\{ \begin{array}{c} P_{(c)} \\ P_{(c)}(e_y + d_{y_{(i)}}) \\ P_{(c)}(e_x + d_{x_{(i)}}) \end{array} \right\} =$$

$$\begin{bmatrix} (CL)^2 C_{11_{(i)}} & -C_{12_{(i)}} & -C_{13_{(i)}} & 2C_{12_{(i)}} & 2C_{13_{(i)}} & -C_{12_{(i)}} & -C_{13_{(i)}} \\ (CL)^2 C_{21_{(i)}} & -C_{22_{(i)}} & -C_{23_{(i)}} & 2C_{22_{(i)}} & 2C_{23_{(i)}} & -C_{22_{(i)}} & -C_{23_{(i)}} \\ (CL)^2 C_{31_{(i)}} & -C_{32_{(i)}} & -C_{33_{(i)}} & 2C_{32_{(i)}} & 2C_{33_{(i)}} & -C_{32_{(i)}} & -C_{33_{(i)}} \end{bmatrix} \left\{ \begin{array}{c} \epsilon_{0_{(i)}} \\ d_{y_{(i-1)}} \\ d_{x_{(i-1)}} \\ d_{y_{(i)}} \\ d_{x_{(i)}} \\ d_{y_{(i+1)}} \\ d_{x_{(i+1)}} \end{array} \right\} \tag{7}$$

$$(CL)^2 \left\{ \begin{array}{c} P_{(c)} \\ P_{(c)}(e_y + d_{y_{(i)}}) \\ P_{(c)}(e_x + d_{x_{(i)}}) \end{array} \right\} =$$

$$\begin{bmatrix} 0 & -C_{12_{(i)}} & -C_{13_{(i)}} & (CL)^2 C_{11_{(i)}} & 2C_{12_{(i)}} & 2C_{13_{(i)}} & 0 & -C_{12_{(i)}} & -C_{13_{(i)}} \\ 0 & -C_{22_{(i)}} & -C_{23_{(i)}} & (CL)^2 C_{21_{(i)}} & 2C_{22_{(i)}} & 2C_{23_{(i)}} & 0 & -C_{22_{(i)}} & -C_{23_{(i)}} \\ 0 & -C_{32_{(i)}} & -C_{33_{(i)}} & (CL)^2 C_{31_{(i)}} & 2C_{32_{(i)}} & 2C_{33_{(i)}} & 0 & -C_{32_{(i)}} & -C_{33_{(i)}} \end{bmatrix} \left\{ \begin{array}{c} 0 \\ d_{y_{(i-1)}} \\ d_{x_{(i-1)}} \\ \epsilon_{0_{(i)}} \\ d_{y_{(i)}} \\ d_{x_{(i)}} \\ 0 \\ d_{y_{(i+1)}} \\ d_{x_{(i+1)}} \end{array} \right\} \tag{8}$$

And let

$$A_{(i)} = \begin{bmatrix} 0 & -C_{12_{(i)}} & -C_{13_{(i)}} \\ 0 & -C_{22_{(i)}} & -C_{23_{(i)}} \\ 0 & -C_{32_{(i)}} & -C_{33_{(i)}} \end{bmatrix}$$

$$D_{(i)} = \begin{bmatrix} (CL)^2 C_{11_{(i)}} & 2C_{12_{(i)}} & 2C_{13_{(i)}} \\ (CL)^2 C_{21_{(i)}} & 2C_{22_{(i)}} & 2C_{23_{(i)}} \\ (CL)^2 C_{31_{(i)}} & 2C_{32_{(i)}} & 2C_{33_{(i)}} \end{bmatrix}$$

For the pinned-ended boundary conditions,

$$d_{y_{(1)}} = d_{x_{(1)}} = 0$$

$$d_{y_{(n+1)}} = d_{x_{(n+1)}} = 0$$

Add i=2 to i=n, one has

$$(CL)^2 P_{(c)} \left\{ \begin{array}{c} 1 \\ (e_y + d_{y_{(2)}}) \\ (e_x + d_{x_{(2)}}) \\ \vdots \\ 1 \\ (e_y + d_{y_{(i)}}) \\ (e_x + d_{x_{(i)}}) \\ \vdots \\ 1 \\ (e_y + d_{y_{(n)}}) \\ (e_x + d_{x_{(n)}}) \end{array} \right\} = \begin{bmatrix} D_{(2)} & A_{(2)} & & & & & & 0 \\ A_{(3)} & D_{(3)} & A_{(3)} & & & & & \\ & \ddots & \ddots & \ddots & & & & \\ & & & A_{(i)} & D_{(i)} & A_{(i)} & & \\ & & & & \ddots & \ddots & \ddots & \\ & 0 & & & & & & \\ & & & & & & A_{(n)} & D_{(n)} \end{bmatrix} \left\{ \begin{array}{c} \epsilon_{0_{(2)}} \\ d_{y_{(2)}} \\ d_{x_{(2)}} \\ \vdots \\ \epsilon_{0_{(i)}} \\ d_{y_{(i)}} \\ d_{x_{(i)}} \\ \vdots \\ \epsilon_{0_{(n)}} \\ d_{y_{(n)}} \\ d_{x_{(n)}} \end{array} \right\} \tag{9}$$

For symmetrical case, the analysis can be simplified, let

lc $=(n/2)+1$

n = number of sections or segments in slender column.

where lc = the nodal number for the middle segment.

and

$$d_{y_{(lc+1)}} = d_{y_{(lc-1)}}$$

$$d_{x_{(lc+1)}} = d_{x_{(lc-1)}}$$

$$\epsilon_{0_{(lc+1)}} = \epsilon_{0_{(lc-1)}}$$

Eq.(9) can be expressed in the following :

$$(CL)^2 P_{(c)} \left\{ \begin{array}{c} 1 \\ (e_y + d_{y_{(2)}}) \\ (e_x + d_{x_{(2)}}) \\ \vdots \\ 1 \\ (e_y + d_{y_{(i)}}) \\ (e_x + d_{x_{(i)}}) \\ \vdots \\ 1 \\ (e_y + d_{y_{(lc)}}) \\ (e_x + d_{x_{(lc)}}) \end{array} \right\} = \begin{bmatrix} D_{(2)} & A_{(2)} & & & & & \\ A_{(3)} & D_{(3)} & A_{(3)} & & & & \\ & \ddots & \ddots & \ddots & & & \\ & & A_{(i)} & D_{(i)} & A_{(i)} & & \\ & & & \ddots & \ddots & \ddots & \\ & & & & A_{(lc-1)} & D_{(lc-1)} & A_{(lc-1)} \\ & & & & & 2A_{(lc)} & D_{(lc)} \end{bmatrix} \left\{ \begin{array}{c} \epsilon_{0_{(2)}} \\ d_{y_{(2)}} \\ d_{x_{(2)}} \\ \vdots \\ \epsilon_{0_{(i)}} \\ d_{y_{(i)}} \\ d_{x_{(i)}} \\ \vdots \\ \epsilon_{0_{(lc)}} \\ d_{y_{(lc)}} \\ d_{x_{(lc)}} \end{array} \right\} \qquad (10)$$

Select the deflection $d_{y_{(lc)}}$ as the control increment for each iteration step and interchange $d_{y_{(lc)}}$ and $P_{(c)}$ from Eq. (10), thus

$$
-d_{y_{(lc)}} \begin{Bmatrix} 0 \\ 0 \\ 0 \\ \vdots \\ \vdots \\ -C_{12_{(lc-1)}} \\ -C_{22_{(lc-1)}} \\ -C_{32_{(lc-1)}} \\ 2C_{12_{(lc)}} \\ 2C_{22_{(lc)}} \\ 2C_{32_{(lc)}} \end{Bmatrix} =
$$

known

$$
\begin{bmatrix}
(CL)^2C_{11_{(2)}} & 2C_{12_{(2)}} & 2C_{13_{(2)}} & & \cdots & -(CL)^2 & 0 \\
(CL)^2C_{21_{(2)}} & 2C_{22_{(2)}} & 2C_{23_{(2)}} & & \cdots & -(CL)^2(e_y + d_{y_{(2)}}) & 0 \\
(CL)^2C_{31_{(2)}} & 2C_{32_{(2)}} & 2C_{33_{(2)}} & & \cdots & -(CL)^2(e_x + d_{x_{(2)}}) & 0 \\
 & \ddots & \ddots & \ddots & & \vdots & \vdots \\
 & & & & & -(CL)^2 & -C_{13_{(lc-1)}} \\
 & & & & & -(CL)^2(e_y + d_{y_{(lc-1)}}) & -C_{23_{(lc-1)}} \\
 & & & & & -(CL)^2(e_x + d_{x_{(lc-1)}}) & -C_{33_{(lc-1)}} \\
 & & & & & -(CL)^2 & 2C_{13_{(lc)}} \\
 & 0 & & & & -(CL)^2(e_y + d_{y_{(lc)}}) & 2C_{23_{(lc)}} \\
 & & & & & -(CL)^2(e_x + d_{x_{(lc)}}) & 2C_{33_{(lc)}}
\end{bmatrix}
\begin{Bmatrix} \epsilon_{0_{(2)}} \\ d_{y_{(2)}} \\ d_{x_{(2)}} \\ \vdots \\ \epsilon_{0_{(i)}} \\ d_{y_{(i)}} \\ d_{x_{(i)}} \\ \vdots \\ \epsilon_{0_{(lc)}} \\ P_{(c)} \\ d_{x_{(lc)}} \end{Bmatrix} \quad (11)
$$

known unknown

After satisfying the convergence criteria, the load $P_{(c)}$, deflections $d_{x_{(i)}}, d_{y_{(i)}}$ and strain at origin $\epsilon_{0_{(i)}}$ are obtained. The biaxial bending moment $M_{x_{(lc)}}, M_{y_{(lc)}}$

at middle segment can be calculated as follows :

$$M_{x_{(lc)}} = P_{(c)}(e_y + d_{y_{(lc)}})$$

$$M_{y_{(lc)}} = P_{(c)}(e_x + d_{x_{(lc)}})$$

2.2 Analysis of L-shaped slender column

To study the complete load-deflection and moment-curvature curve of L-shaped slender columns subjected to biaxial bending and axial compression with monotonic loadings, a strain compatibility and equilibrium of forces and moments which can account for any loading condition and material properties can again be utilized.

The cross section of a L-shaped column can be divided into several small elements as shown in Fig. (5). According to Hsu [5], consider for each small element k, with its centroidal coordinates (x_k, y_k), the strain ϵ_k is again assumed to be uniformly distributed across the element k. Fig. (5) shows an angle θ_p which defines the angle between the x, y coordinate system and the principal axes u, v. The principal axes are defined as those axes for which the product of inertia has vanished. Thus

$$\tan 2\theta_p = \frac{-2I_{xy}}{I_y - I_x} \tag{12}$$

$$\theta_p = \frac{1}{2}\tan^{-1}\left(\frac{-2I_{xy}}{I_y - I_x}\right) \tag{13}$$

where

I_x = the moment of inertia about x axis.

I_y = the moment of inertia about y axis.

I_{xy} = the product moment of inertia.

According to the assumption that plane section remains plane during bending, and for an element which is subjected to biaxial bending and axial compression, the strain ϵ_k can be expressed as

$$\epsilon_k = \epsilon_0 + \phi_u v + \phi_v u \tag{14}$$

where

ϵ_0 : strain at the coordinate origin of the principal axes.

ϕ_u : curvature with respect to M_u. ϕ_u is positive when it can produce compressive strains in the positive v direction.

ϕ_v : curvature with respect to M_v. ϕ_v is positive when it can produce compressive strains in the positive u direction.

u,v : the coordinates for the principal axes. where

$$\left\{ \begin{array}{c} u \\ v \end{array} \right\} = \left[\begin{array}{cc} \cos\theta_p & -\sin\theta_p \\ \sin\theta_p & \cos\theta_p \end{array} \right] \left\{ \begin{array}{c} x \\ y \end{array} \right\} \tag{15}$$

Idealized piecewise linear stress-strain curve and modified Cranston-Chatterji stress-strain curve are again used for reinforcing steel and concrete elements, respectively. For a value of strain ϵ_k , a value of the secant modulus of elasticity $(E_s)_k$ for steel or concrete elements can be obtained from Fig.(2) and Fig. (3). The secant modulus of elasticity can be assured

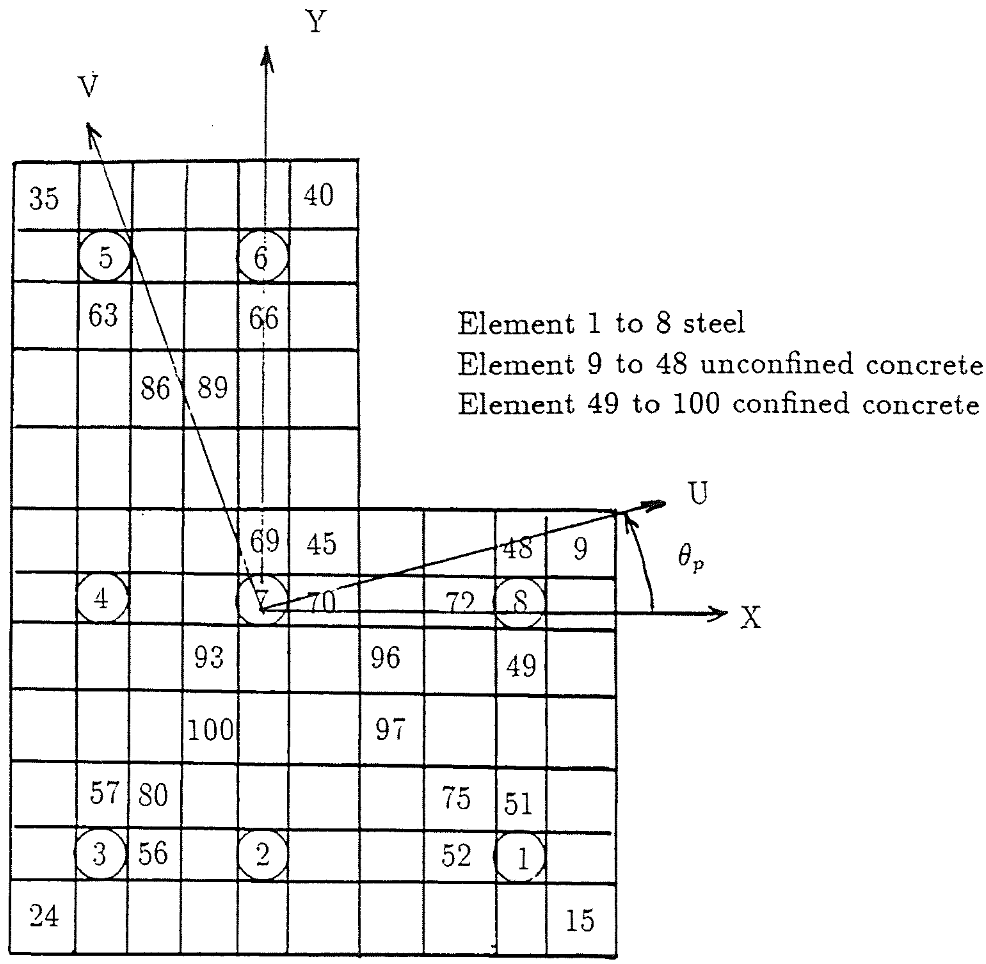

Figure 5. Cross section of L-shaped slender column.

to give the positive values and to prevent the singularity problem in the matrix operation.

The equilibrium equations in the cross section with n elements for the axial load P, bending moment components M_u, M_v can be expressed in the following forms :

$$\begin{aligned} P_{(c)} &= \sum_{k=1}^{n} (E_s)_k \epsilon_k a_k \\ M_{u_{(c)}} &= \sum_{k=1}^{n} (E_s)_k \epsilon_k a_k v_k \end{aligned} \qquad (16)$$

$$M_{v_{(c)}} = \sum_{k=1}^{n} (E_s)_k \epsilon_k a_k u_k$$

The subscript (c) from $P_{(c)}, M_{u_{(c)}}, M_{v_{(c)}}$ represents the calculated values in an iteration cycle.

$(E_s)_k$: the secant modulus of elasticity in element k.

ϵ_k : strain of element k.

a_k : area of element k.

u_k, v_k : the coordinates at the centroid of element k for the principal axes.

Based on the assumption that the plane section remains plane during bending, Eq. (16) can be rewritten in the following matrix form.

$$\begin{Bmatrix} P_{(c)} \\ M_{u_{(c)}} \\ M_{v_{(c)}} \end{Bmatrix} = \begin{bmatrix} \sum_{k=1}^{n}(E_s)_k a_k & \sum_{k=1}^{n}(E_s)_k a_k v_k & \sum_{k=1}^{n}(E_s)_k a_k u_k \\ \sum_{k=1}^{n}(E_s)_k a_k v_k & \sum_{k=1}^{n}(E_s)_k a_k v_k^2 & \sum_{k=1}^{n}(E_s)_k a_k u_k v_k \\ \sum_{k=1}^{n}(E_s)_k a_k u_k & \sum_{k=1}^{n}(E_s)_k a_k u_k v_k & \sum_{k=1}^{n}(E_s)_k a_k u_k^2 \end{bmatrix} \begin{Bmatrix} \epsilon_0 \\ \phi_u \\ \phi_v \end{Bmatrix} \tag{17}$$

And let

$$\begin{aligned} B_{11} &= \sum_{k=1}^{n} (E_s)_k a_k \\ B_{12} &= B_{21} = \sum_{k=1}^{n} (E_s)_k a_k v_k \\ B_{13} &= B_{31} = \sum_{k=1}^{n} (E_s)_k a_k u_k \end{aligned}$$

$$
\begin{aligned}
B_{22} &= \sum_{k=1}^{n} (E_s)_k a_k v_k^2 \\
B_{23} &= B_{32} = \sum_{k=1}^{n} (E_s)_k a_k u_k v_k \\
B_{33} &= \sum_{k=1}^{n} (E_s)_k a_k u_k^2
\end{aligned}
$$

For the slender column, the second order effect may be critical for the biaxial bending calculations, Eq.(17) can be simplified in the following form:

$$
\left\{ \begin{array}{c} P_{(c)} \\ P_{(c)}(e_v + d_v) \\ P_{(c)}(e_u + d_u) \end{array} \right\} = \left[\begin{array}{ccc} B_{11} & B_{12} & B_{13} \\ B_{21} & B_{22} & B_{23} \\ B_{31} & B_{32} & B_{33} \end{array} \right] \left\{ \begin{array}{c} \epsilon_0 \\ \phi_u \\ \phi_v \end{array} \right\} \tag{18}
$$

where

$$
\left\{ \begin{array}{c} e_u \\ e_v \end{array} \right\} = \left[\begin{array}{cc} \cos\theta_p & -\sin\theta_p \\ \sin\theta_p & \cos\theta_p \end{array} \right] \left\{ \begin{array}{c} e_x \\ e_y \end{array} \right\} \tag{19}
$$

The finite difference method is again used to solve the three dimensional behavior of slender columns. Fig.(6) shows the slender column that was divided into several portions. For the segment (i) :

$$
\begin{aligned}
\frac{d_{v_{(i+1)}} - 2d_{v_{(i)}} + d_{v_{(i-1)}}}{(CL)^2} &= -(\phi_u)_i \\
\frac{d_{u_{(i+1)}} - 2d_{u_{(i)}} + d_{u_{(i-1)}}}{(CL)^2} &= -(\phi_v)_i
\end{aligned} \tag{20}
$$

Substitute the above equation in Eq. (18), one obtains,

$$
\left\{ \begin{array}{c} P_{(c)} \\ P_{(c)}(e_v + d_{v_{(i)}}) \\ P_{(c)}(e_u + d_{u_{(i)}}) \end{array} \right\} = \left[\begin{array}{ccc} B_{11} & B_{12} & B_{13} \\ B_{21} & B_{22} & B_{23} \\ B_{31} & B_{32} & B_{33} \end{array} \right] \left\{ \begin{array}{c} \epsilon_{0_{(i)}} \\ -(d_{v_{(i+1)}} - 2d_{v_{(i)}} + d_{v_{(i-1)}})/(CL)^2 \\ -(d_{u_{(i+1)}} - 2d_{u_{(i)}} + d_{u_{(i-1)}})/(CL)^2 \end{array} \right\} \tag{21}
$$

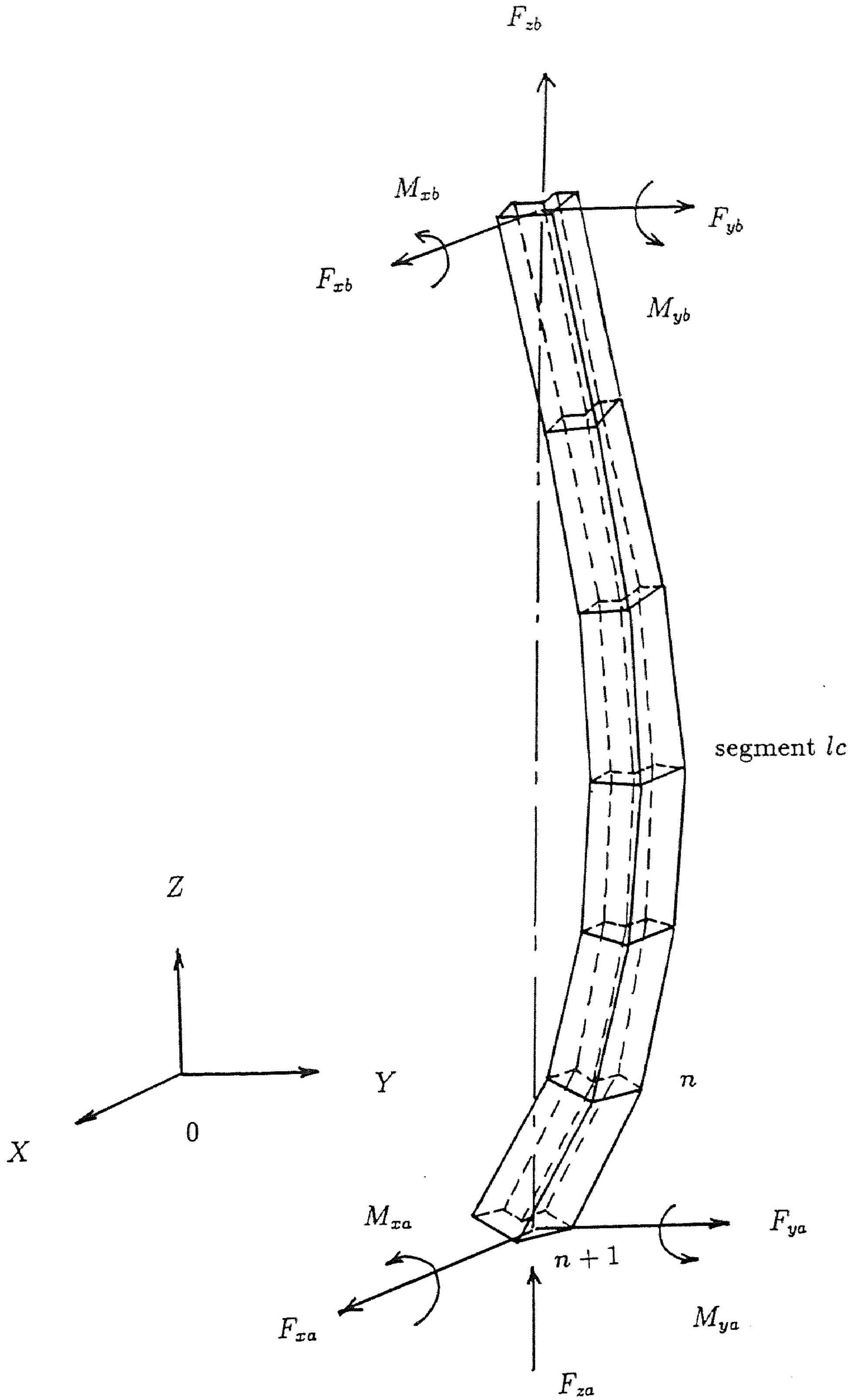

Figure 6. Slender L-shaped column divided into n segments.

Expand Eq.(21) and rearrange it, and for the segment (i),

$$(CL)^2 \left\{ \begin{array}{c} P_{(c)} \\ P_{(c)}(e_v + d_{v_{(i)}}) \\ P_{(c)}(e_u + d_{u_{(i)}}) \end{array} \right\} = \tag{22}$$

$$\left[\begin{array}{ccccccc} (CL)^2 B_{11_{(i)}} & -B_{12_{(i)}} & -B_{13_{(i)}} & 2B_{12_{(i)}} & 2B_{13_{(i)}} & -B_{12_{(i)}} & -B_{13_{(i)}} \\ (CL)^2 B_{21_{(i)}} & -B_{22_{(i)}} & -B_{23_{(i)}} & 2B_{22_{(i)}} & 2B_{23_{(i)}} & -B_{22_{(i)}} & -B_{23_{(i)}} \\ (CL)^2 B_{31_{(i)}} & -B_{32_{(i)}} & -B_{33_{(i)}} & 2B_{32_{(i)}} & 2B_{33_{(i)}} & -B_{32_{(i)}} & -B_{33_{(i)}} \end{array} \right] \left\{ \begin{array}{c} \epsilon_{0_{(i)}} \\ d_{v_{(i-1)}} \\ d_{u_{(i-1)}} \\ d_{v_{(i)}} \\ d_{u_{(i)}} \\ d_{v_{(i+1)}} \\ d_{u_{(i+1)}} \end{array} \right\}$$

$$(CL)^2 \left\{ \begin{array}{c} P_{(c)} \\ P_{(c)}(e_v + d_{v_{(i)}}) \\ P_{(c)}(e_u + d_{u_{(i)}}) \end{array} \right\} = \tag{23}$$

$$\left[\begin{array}{ccccccccc} 0 & -B_{12_{(i)}} & -B_{13_{(i)}} & (CL)^2 B_{11_{(i)}} & 2B_{12_{(i)}} & 2B_{13_{(i)}} & 0 & -B_{12_{(i)}} & -B_{13_{(i)}} \\ 0 & -B_{22_{(i)}} & -B_{23_{(i)}} & (CL)^2 B_{21_{(i)}} & 2B_{22_{(i)}} & 2B_{23_{(i)}} & 0 & -B_{22_{(i)}} & -B_{23_{(i)}} \\ 0 & -B_{32_{(i)}} & -B_{33_{(i)}} & (CL)^2 B_{31_{(i)}} & 2B_{32_{(i)}} & 2B_{33_{(i)}} & 0 & -B_{32_{(i)}} & -B_{33_{(i)}} \end{array} \right] \left\{ \begin{array}{c} 0 \\ d_{v_{(i-1)}} \\ d_{u_{(i-1)}} \\ \epsilon_{0_{(i)}} \\ d_{v_{(i)}} \\ d_{u_{(i)}} \\ 0 \\ d_{v_{(i+1)}} \\ d_{u_{(i+1)}} \end{array} \right\}$$

And let

$$G_{(i)} = \left[\begin{array}{ccc} 0 & -B_{12_{(i)}} & -B_{13_{(i)}} \\ 0 & -B_{22_{(i)}} & -B_{23_{(i)}} \\ 0 & -B_{32_{(i)}} & -B_{33_{(i)}} \end{array} \right]$$

$$H_{(i)} = \left[\begin{array}{ccc} (CL)^2 B_{11_{(i)}} & 2B_{12_{(i)}} & 2B_{13_{(i)}} \\ (CL)^2 B_{21_{(i)}} & 2B_{22_{(i)}} & 2B_{23_{(i)}} \\ (CL)^2 B_{31_{(i)}} & 2B_{32_{(i)}} & 2B_{33_{(i)}} \end{array} \right]$$

For slender columns with pinned ends :

$$d_{v_{(1)}} = d_{u_{(1)}} = 0$$

$$d_{v_{(n+1)}} = d_{u_{(n+1)}} = 0$$

Add i=2 to $i = n$, it results in the following equations:

$$(CL)^2 P_{(c)} \left\{ \begin{array}{c} 1 \\ (e_v + d_{v_{(2)}}) \\ (e_u + d_{u_{(2)}}) \\ \vdots \\ 1 \\ (e_v + d_{v_{(i)}}) \\ (e_u + d_{u_{(i)}}) \\ \vdots \\ 1 \\ (e_v + d_{v_{(n)}}) \\ (e_u + d_{u_{(n)}}) \end{array} \right\} = \begin{bmatrix} H_{(2)} & G_{(2)} & & & & & & \\ G_{(3)} & H_{(3)} & G_{(3)} & & & & & \\ & \ddots & \ddots & \ddots & & & & \\ & & & G_{(i)} & H_{(i)} & G_{(i)} & & \\ & & & & \ddots & \ddots & \ddots & \\ & & & & & & G_{(n)} & H_{(n)} \end{bmatrix} \left\{ \begin{array}{c} \epsilon_{0_{(2)}} \\ d_{v_{(2)}} \\ d_{u_{(2)}} \\ \vdots \\ \epsilon_{0_{(i)}} \\ d_{v_{(i)}} \\ d_{u_{(i)}} \\ \vdots \\ \epsilon_{0_{(n)}} \\ d_{v_{(n)}} \\ d_{u_{(n)}} \end{array} \right\} \tag{24}$$

For symmetrical case, the analysis can be further simplified. Let

lc =(nnod/2)+1

where lc = nodal number for the middle segment of column.

nnod= number of sections or segments in slender column.

and

$$d_{v_{(lc+1)}} = d_{v_{(lc-1)}}$$

$$d_{u_{(lc+1)}} = d_{u_{(lc-1)}}$$

$$\epsilon_{0_{(lc+1)}} = \epsilon_{0_{(lc-1)}}$$

$$
(CL)^2 P_{(c)} \left\{ \begin{array}{c} 1 \\ (e_v + d_{v_{(2)}}) \\ (\epsilon_u + d_{u_{(2)}}) \\ \vdots \\ 1 \\ (e_v + d_{v_{(i)}}) \\ (e_u + d_{u_{(i)}}) \\ \vdots \\ 1 \\ (e_v + d_{v_{(lc)}}) \\ (e_u + d_{u_{(lc)}}) \end{array} \right\} = \begin{bmatrix} H_{(2)} & G_{(2)} & & & & & & \\ G_{(3)} & H_{(3)} & G_{(3)} & & & & & \\ & \ddots & \ddots & \ddots & & & & \\ & & & G_{(i)} & H_{(i)} & G_{(i)} & & \\ & & & & \ddots & \ddots & \ddots & \\ & & & & & & 2G_{(lc)} & H_{(lc)} \end{bmatrix} \left\{ \begin{array}{c} \epsilon_{0_{(2)}} \\ d_{v_{(2)}} \\ d_{u_{(2)}} \\ \vdots \\ \epsilon_{0_{(i)}} \\ d_{v_{(i)}} \\ d_{u_{(i)}} \\ \vdots \\ \epsilon_{0_{(lc)}} \\ d_{v_{(lc)}} \\ d_{u_{(lc)}} \end{array} \right\} \tag{25}
$$

Select the deflection $d_{v_{(lc)}}$ as the control increment for each iteration step and interchange $d_{v_{(lc)}}$ and $P_{(c)}$ from Eq. (10), one has

$$
\underbrace{-d_{v_{(lc)}} \left\{ \begin{array}{c} 0 \\ 0 \\ 0 \\ \vdots \\ \vdots \\ -B_{12_{(lc-1)}} \\ -B_{22_{(lc-1)}} \\ -B_{32_{(lc-1)}} \\ 2B_{12_{(lc)}} \\ 2B_{22_{(lc)}} \\ 2B_{32_{(lc)}} \end{array} \right\}}_{\text{known}} =
$$

$$\begin{bmatrix} (CL)^2B_{11_{(2)}} & 2B_{12_{(2)}} & 2B_{13_{(2)}} & \cdots & -(CL)^2 & 0 \\ (CL)^2B_{21_{(2)}} & 2B_{22_{(2)}} & 2B_{23_{(2)}} & \cdots & -(CL)^2(e_v+d_{v_{(2)}}) & 0 \\ (CL)^2B_{31_{(2)}} & 2B_{32_{(2)}} & 2B_{33_{(2)}} & \cdots & -(CL)^2(e_u+d_{u_{(2)}}) & 0 \\ & \ddots & \ddots & \ddots & \vdots & \vdots \\ & & & & -(CL)^2 & -B_{13_{(lc-1)}} \\ & & & & -(CL)^2(e_v+d_{v_{(lc-1)}}) & -B_{23_{(lc-1)}} \\ & & & & -(CL)^2(e_u+d_{u_{(lc-1)}}) & -B_{33_{(lc-1)}} \\ & & & & -(CL)^2 & 2B_{13_{(lc)}} \\ & 0 & & & -(CL)^2(e_v+d_{v_{(lc)}}) & 2B_{23_{(lc)}} \\ & & & & -(CL)^2(e_u+d_{u_{(lc)}}) & 2B_{33_{(lc)}} \end{bmatrix} \begin{Bmatrix} \epsilon_{0_{(2)}} \\ d_{v_{(2)}} \\ d_{u_{(2)}} \\ \vdots \\ \epsilon_{0_{(i)}} \\ d_{v_{(i)}} \\ d_{u_{(i)}} \\ \vdots \\ \epsilon_{0_{(lc)}} \\ P_{(c)} \\ d_{u_{(lc)}} \end{Bmatrix} \tag{26}$$

known unknown

Once the load-deflection and moment-curvature results in the principal axes are obtained, the deflection $d_{u_{(i)}}$ and $d_{v_{(i)}}$ are transformed into x,y coordinate systems. It is because all slender columns are tested in the x,y coordinate system. The deflection for the segments from *i=1* to n in the x,y coordinate system can be calculated as follows :

$$\begin{Bmatrix} d_{x(i)} \\ d_{y(i)} \end{Bmatrix} = \begin{bmatrix} \cos\theta_p & \sin\theta_p \\ -\sin\theta_p & \cos\theta_p \end{bmatrix} \begin{Bmatrix} d_{u(i)} \\ d_{v(i)} \end{Bmatrix} \tag{27}$$

And

$$(\phi_x)_i = -\frac{d_{y(i+1)} - 2d_{y(i)} + d_{y(i-1)}}{(CL)^2} \tag{28}$$

$$(\phi_y)_i = -\frac{d_{x(i+1)} - 2d_{x(i)} + d_{x(i-1)}}{(CL)^2}$$

For the proportional loading system, the biaxial bending moment $M_{x(lc)}$, $M_{y(lc)}$ at the middle segment can be obtained as follows:

$$M_{x(lc)} = P_{(c)}(e_y + d_{y(lc)})$$

$$M_{y(lc)} = P_{(c)}(e_x + d_{x(lc)})$$

2.3 ACCURACY AND CONVERGENCE CRITERIA

1. The assumption of uniform strain distribution in a small element can be modified by increasing the number of elements in the cross section. It will increase the CPU time for the computations. But the results as shown in Fig. (7) indicate the analysis results of present study are reasonably accurate.

2. The convergence criteria are developed to examine the iteration cycles and compare with allowable incompatibilities. The allowable incompatibilities are set in the present study as follows: UALL=0.01 for the load $P_{(c)}$, VALL= 10^{-7} for the strain at coordinate origin $\epsilon_{0_{(i)}}$ and WALL= 0.001 for the deflections $d_{x_{(i)}}, d_{y_{(i)}}, d_{u_{(i)}}$ and $d_{v_{(i)}}$. The computation will continue to go to the next increment only if the solutions satisfy allowable incompatibilities UALL, VALL and WALL all together.

3. It is well known that the assumption of the uniaxial stress-strain curves for both reinforcing bars and unconfined or confined concrete may cause a minor error since the slender columns undergo a three dimensional behavior.

4. The slender column is divided into a different number of segments for computing the deflections by the finite difference method. It is well-known that the more segments are divided in the column member , the

more accurate results are achieved as compared with the tests. Based on the present study, it has been found that it is true only for the ascending branch of the load-deformation curves until the maximum load. When the column starts to form a plastic hinge at mid-height, the behavior of column changes tremendously. Fig. (8) shows the analysis using different number of segments (nnod), the different results of deflections are obtained in the descending branch of the curve. When the column starts to form the plastic hinge, the curvature is increased tremendously within the range of plastic hinge, as seen in Fig. (9). From the observation of tested column , it is reasonable to assume the length of plastic hinge lp= 1.5d to 2d. The present computer model is corrected to set the lp after the column reaches the maximum load. In other words, the column is re-divided into segments which is equal to lp at the mid-height and the same length for the rest of column as shown in Fig. (10).

It can be seen in Fig. (11), for example for column B2, the load-deflection results are calculated from the different number of segments. The final convergence can be achieved for both 8 and 16 segments. However, the column with 8 segments gives a more reasonable and satisfactory results.

5. The effect of torsion on slender column is neglected. During present experimental setup, four dial gages #5,#6,#7 and #8 are arranged to

check if the column rotates during the test. As shown in Fig. (12), the column deforms as normal as the one without twisting moment applied to the column. The pinned-ends in the present experiment provide enough friction resistance to prevent the rotation of the column during testing. The present computer model does not consider the torsional effect in the analysis and the results of the present computer analysis and the present experimental results reflect a good agreements between them as shown in the study.

6. Two loading brackets were provided at each end of test column to assist with the application of biaxially eccentric loads, these brackets were heavily reinforced to prevent any premature failure. However, the effect of these brackets on the behavior of slender column is also neglected in the present computer analysis.

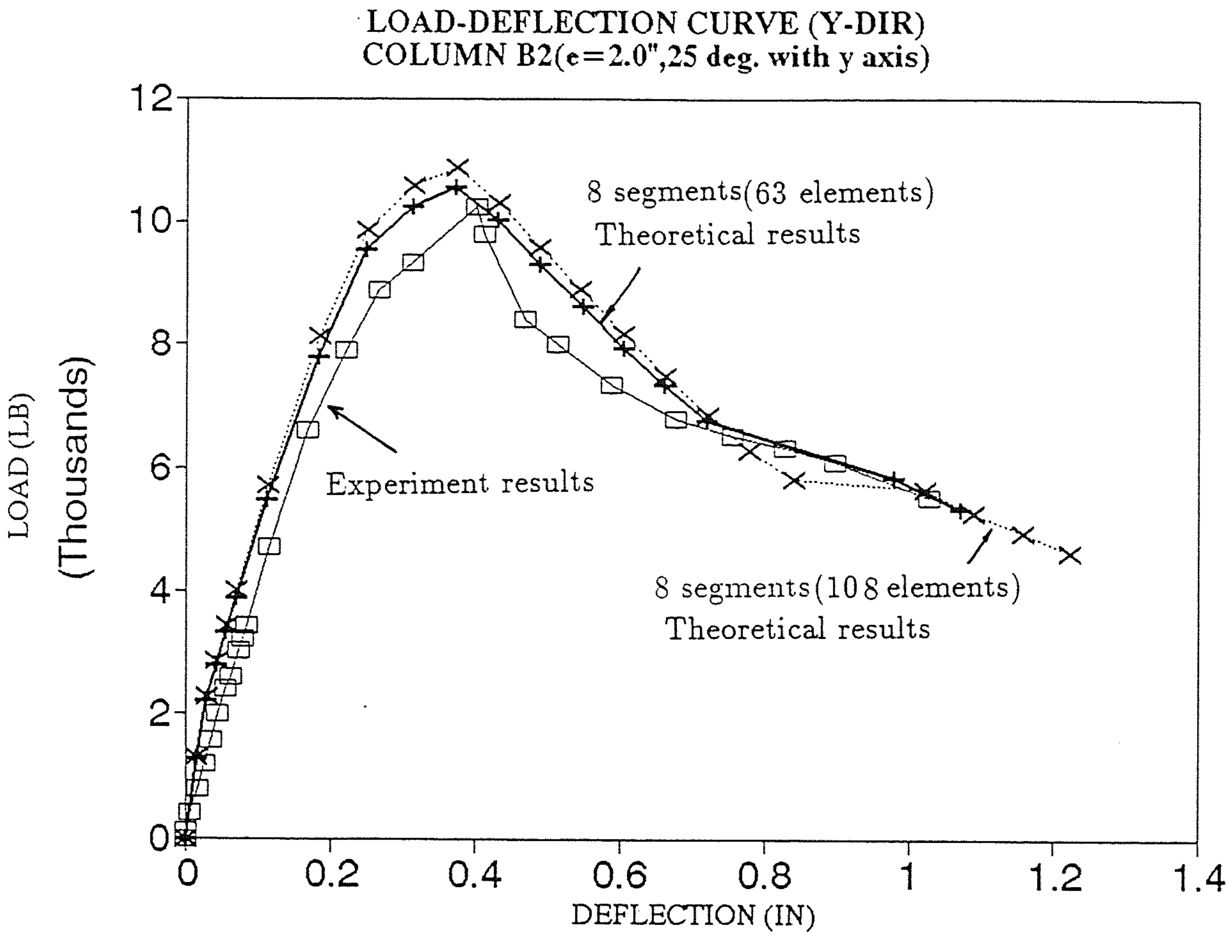

Figure 7. Analysis results by number of elements in cross section.

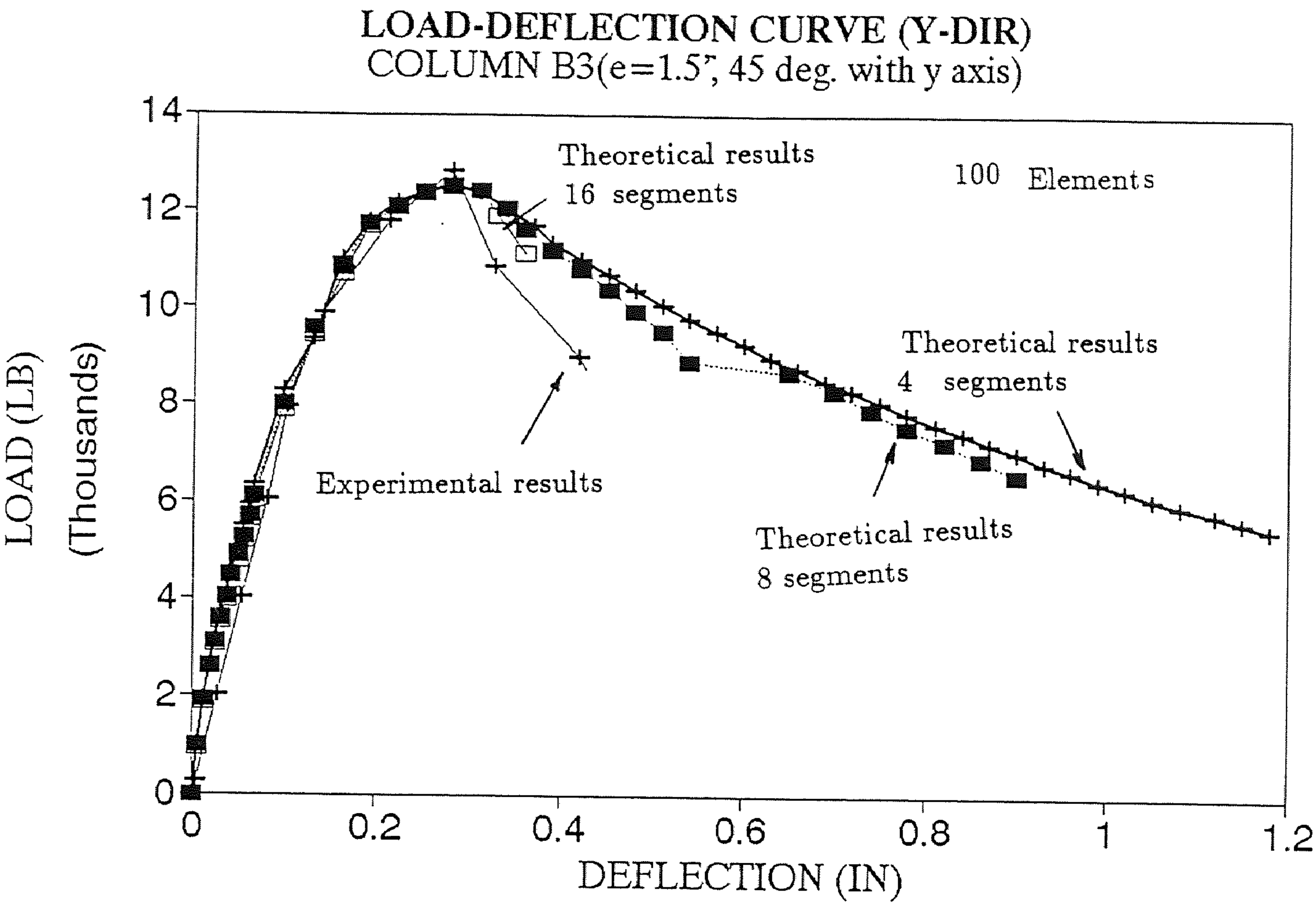

Figure 8. Analysis results by number of segments in column B3.

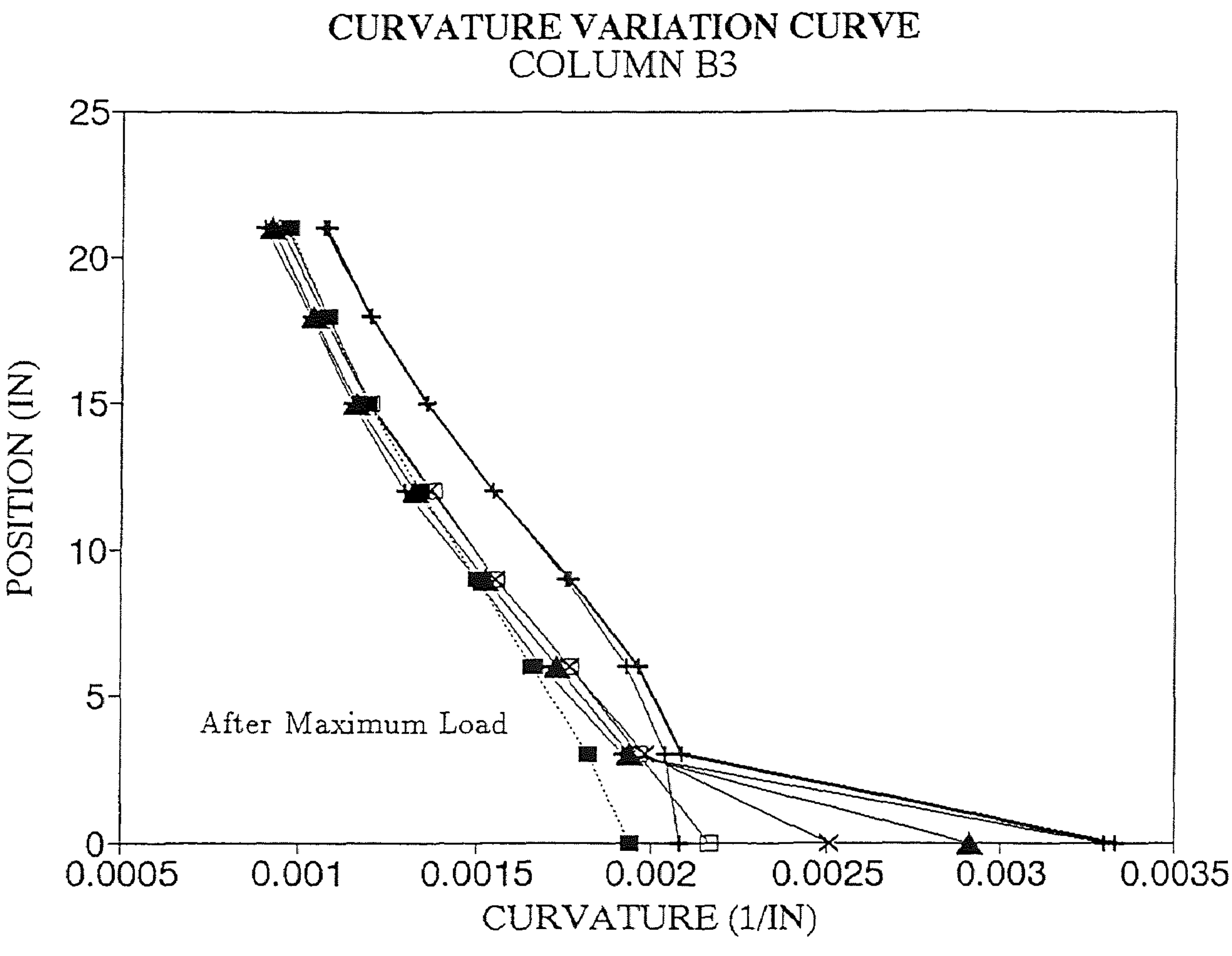

Figure 9. Curvature values along half column at various loading stages after maximum load.

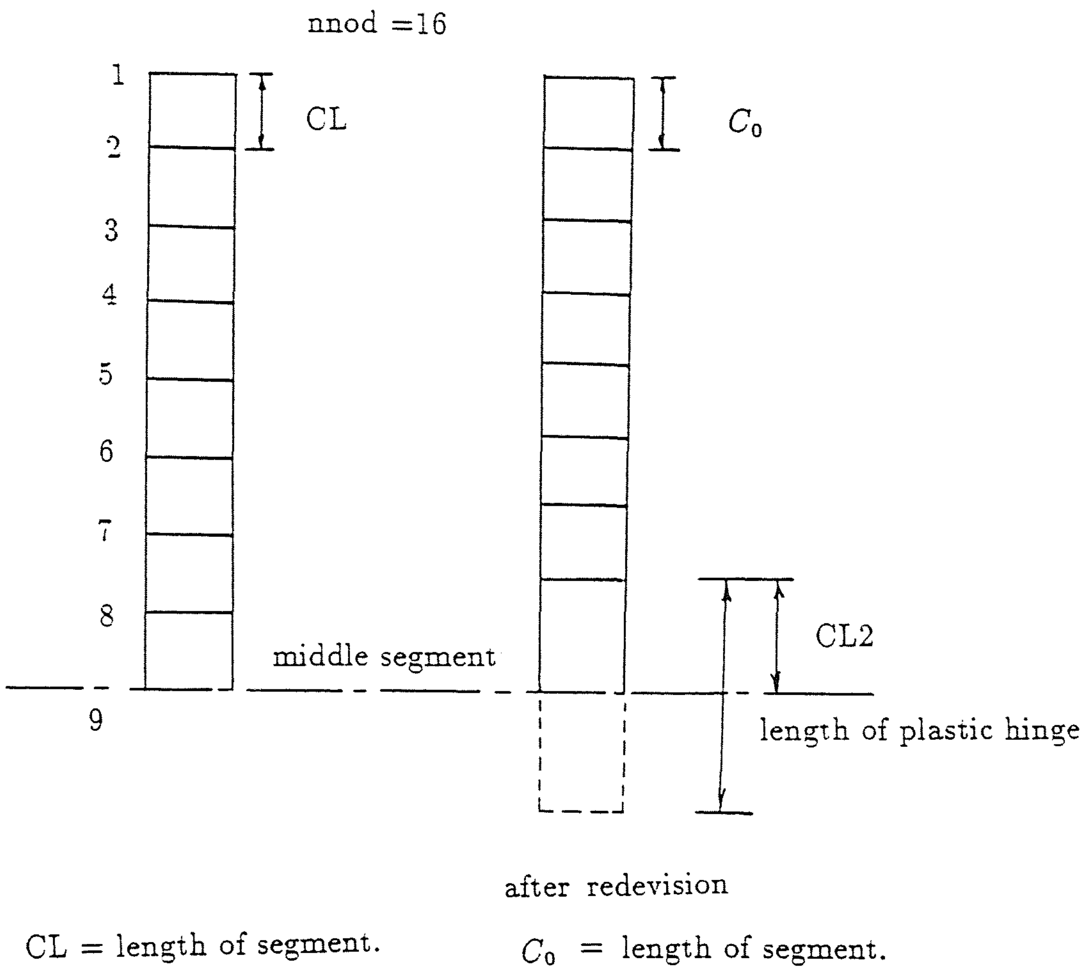

Figure 10. Segments are redivided when the plastic hinge forms.

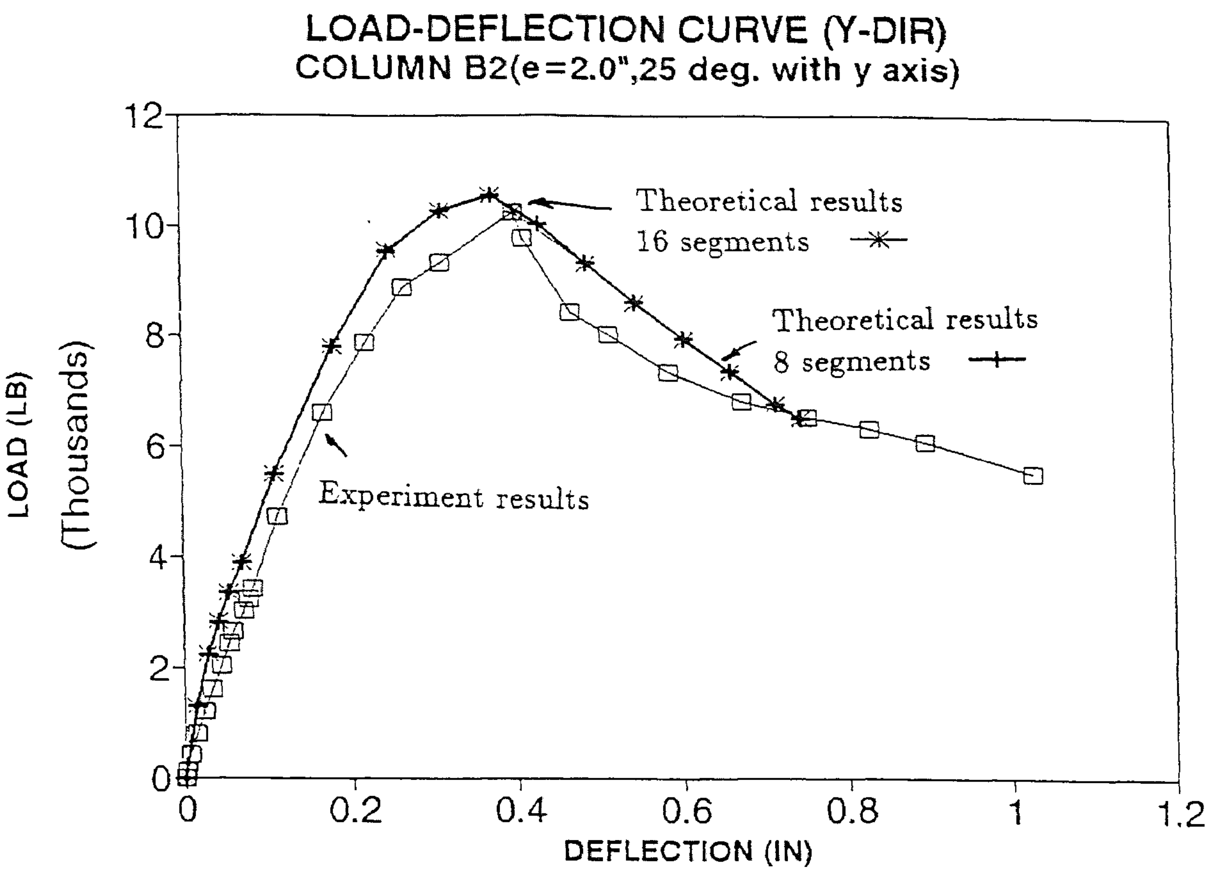

Figure 11. Convergence studies on column B2.

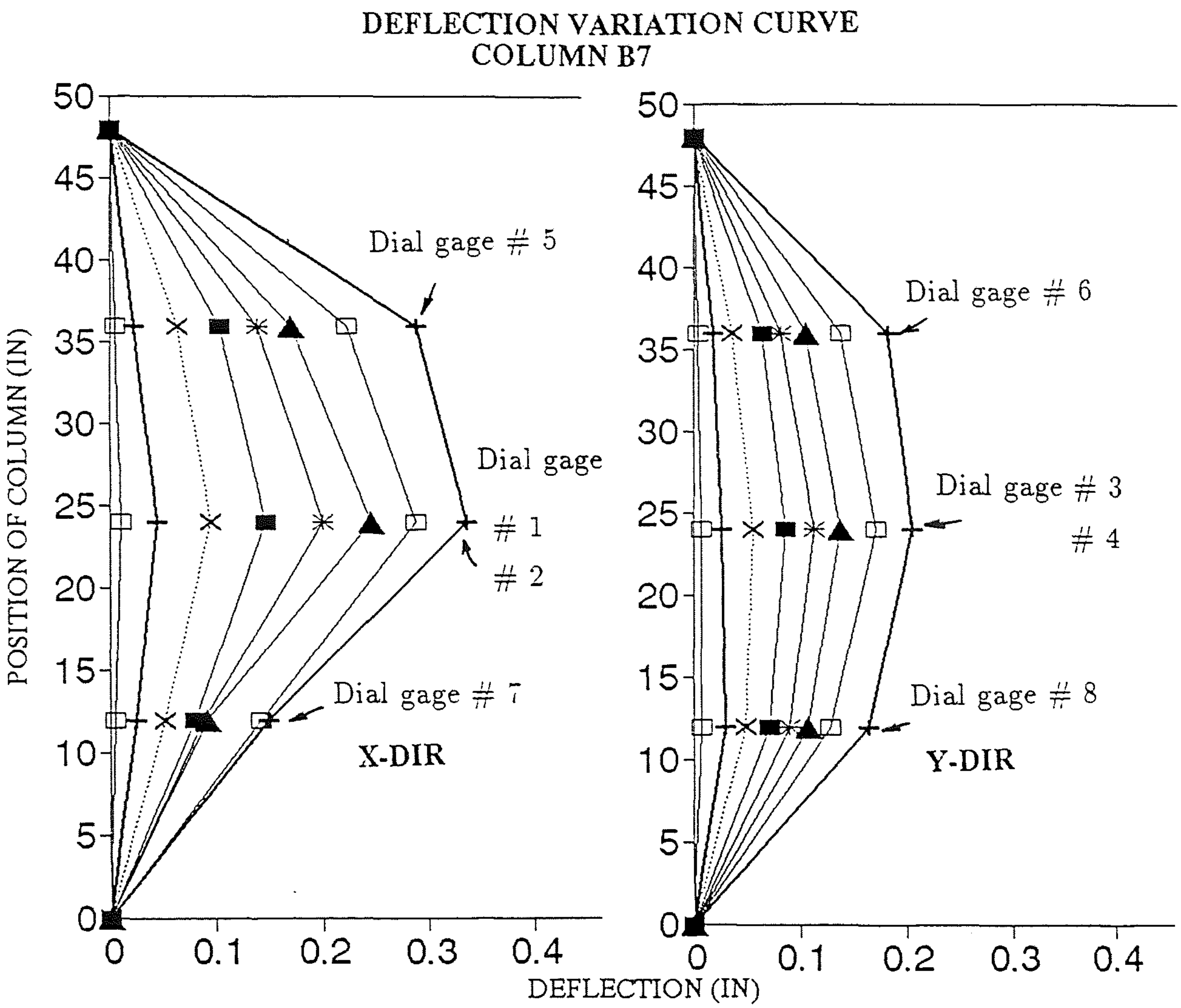

Figure 12. Deflection variations along column B7

2.4 DESCRIPTION OF COMPUTER PROGRAM

The present computer program was written in FORTRAN 77 and run in the NJIT Tesla system. It can be used at any IBM compatible personal computer using Microsoft FORTRAN.

The input data was created in a input file and the output file was generated by the program to store the results. The flow chart is given in Fig. 13 and the main notations are defined as follows :

- Read data : Read the input data file.
- Give initial value for boundary condition and control increment : The boundry condition is pinned-ended, the control deflection increment is the deflection d_y at the middle segment.
- IKEY=0 : IKEY controls the current increment step. If the convergence can not be reached, it will readjust the increment and go back to iteration process for convergence.
- Tolerance incompatibility : The incompatibility tolerances are Uall for $P_{(c)}$, Wall for $d_{x_{(i)}}, d_{y_{(i)}}, d_{u_{(i)}}$ and $d_{v_{(i)}}$ and Vall for $\epsilon_{0_{(i)}}$, respectively.
- 333 : This is the beginning to start the ISEC iteration.(usually 300 iterations was programmed)
- Do 999 : This is an iteration loop for ISEC.

- Do 888 : LC is the number of segments to be divided for column. This is a loop to relate the local to the global system.

- Check if sym. case : Check if the cross section is a symmetrical case.

- Rotate to the principal axes : Rotate the coordinate system to the principal axes system for computations.

- Find SUM* : This is a step to find the values of [**C**] matrix from Eq. (4), or [**B**] matrix from Eq. (18).

- CALL CALCAU : CALCAU is a subroutine to solve the unknowns from Eq. (11) or Eq. (26).

- Check convergence : The solutions should be the same or less than the allowable incompatibilities.

- Check ISEC = LP : If ISEC = LP, the convergence can not be reached, and the analysis must try a new increment for the control deflection.

- IKEY = IKEY + 1 : Go to the next increment step.

- Check curvature : If the curvature in the middle segment increases tremendously, set the length of plastic hinge and redivide the segments.

- Check IKEY : If the analysis reaches the final load, stop the computation.

FLOW CHART

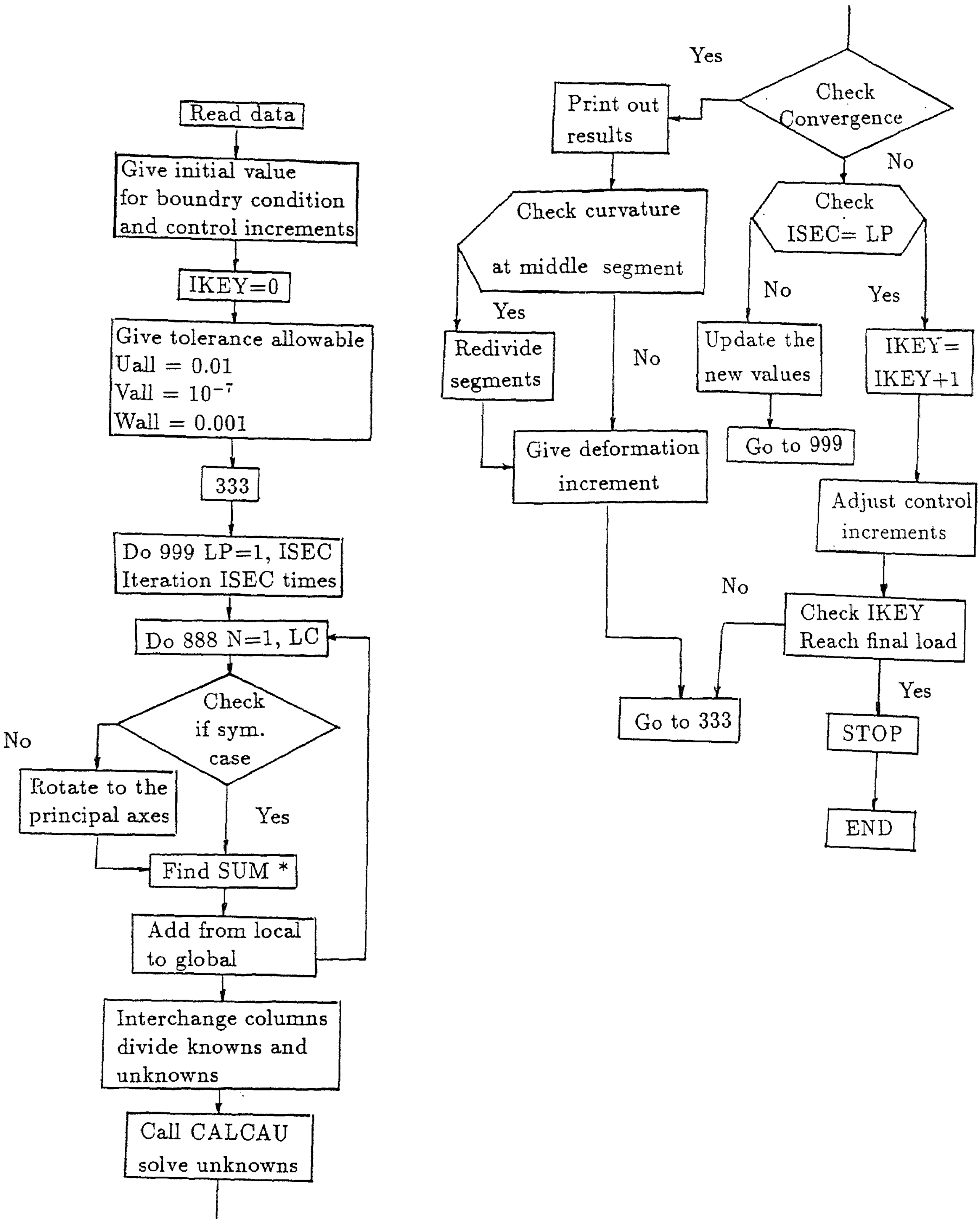

Figure 13. Flow chart for present computer program.

3 EXPERIMENTAL TESTS AND COMPARISON WITH COMPUTER ANALYSIS

3.1 Test program

3.1.1 Introduction

A test program was arranged to verify the accuracy of the theoretical analysis of this study. Eight L-shaped and six square slender columns were tested under combined biaxial bending and axial compression. Different eccentricities were used to examine the behavior of the slender columns. Two types of columns were tested, B series were for L-shaped slender columns and C series were for square slender columns. Specimens details are shown in Table. 1. The tension test for # 2 and # 3 reinforcing bars were done at Tinus & Olsen tension and compression test machine and all concrete cylinders and columns were tested using MTS loading system.

3.1.2 Experimental setup and loading arrangement

Several couple sets of Ames dial gages were used to measure the deflections at the beginning of brackets and at mid-height of column in both X and Y directions. The demec or mechanical gages were provided to measure the strains at central portion of column in order to calculate the average curvatures in both X and Y axes. Fig. 14 shows the demec or mechanical gages arrangements for L-shaped and square slender column specimens, respectively.

Specimen number	Main bars	f_y (ksi)	f'_c (psi)	s (in)	e_x (in)	e_y (in)	l (in)	ρ_g (%)	α (deg.)
B1	8-# 2	63	3600	3	0.634	1.359	48	4	25
B2	8-# 2	63	3636	3	0.845	1.813	48	4	25
B3	8-# 2	63	3886	3	1.061	1.061	48	4	45
B4	8-# 2	64	3886	3	1.414	1.414	48	4	45
B5	8-# 2	64	4256	3	0.354	0.354	48	4	45
B6	8-# 2	64	4256	3	0.707	0.707	48	4	45
B7	8-# 2	64	4237	3	0.609	0.793	48	4	37.5
B8	8-# 2	64	4237	3	1.218	1.587	48	4	37.5
C1	4-# 3	79	2771	3	0.383	0.924	48	4.9	22.5
C2	4-# 3	79	2695	3	0.707	0.707	48	4.9	45
C3	4-# 3	79	4212	3	1.414	1.414	48	4.9	45
C4	4-# 3	61	3700	3	0.707	0.707	48	4.9	45
C5	4-# 3	61	3700	3	0.765	1.848	48	4.9	22.5
C6	4-# 3	61	3700	3	0.383	0.924	48	4.9	22.5

$\alpha = \tan^{-1}(e_x/e_y)$
$l =$ total length of column.
$e_x =$ eccentricity along x-axis
$e_y =$ eccentricity along y-axis
s = spacing of lateral reinforcement
$f'_c =$ ultimate strength of concrete.
$f_y =$ steel yielding stress.
$\rho_g =$ steel percentage in gross cross section area.

Table 1. Details of specimens.

All biaxially loaded columns were tested on MTS loading system. The details of experimental setup are shown in Fig. 15 for L-shaped and square column tests, respectively. Stroke control was operated at the constant loading rate during testings. The readings from the dial gages and the demec gages were obtained at each loading increment.

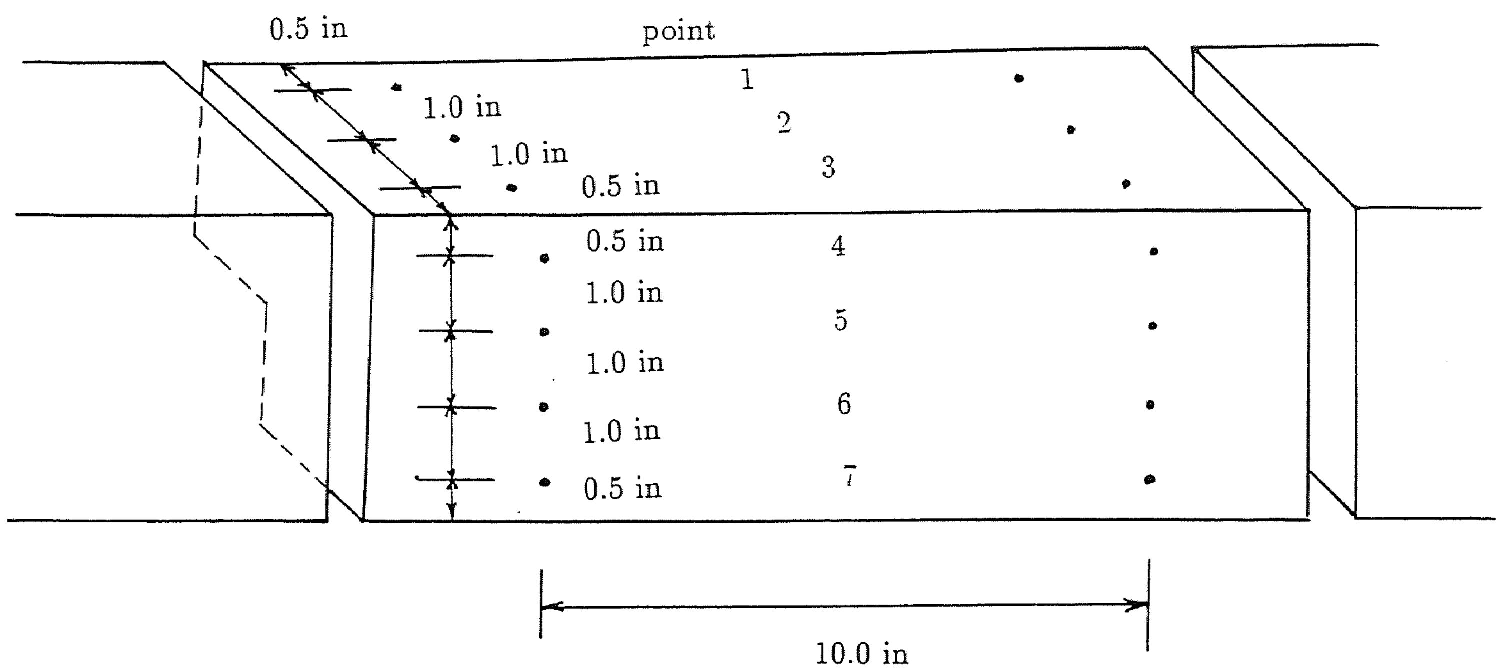

Figure 14a. Demec gage setup for L-shaped slender column specimens.

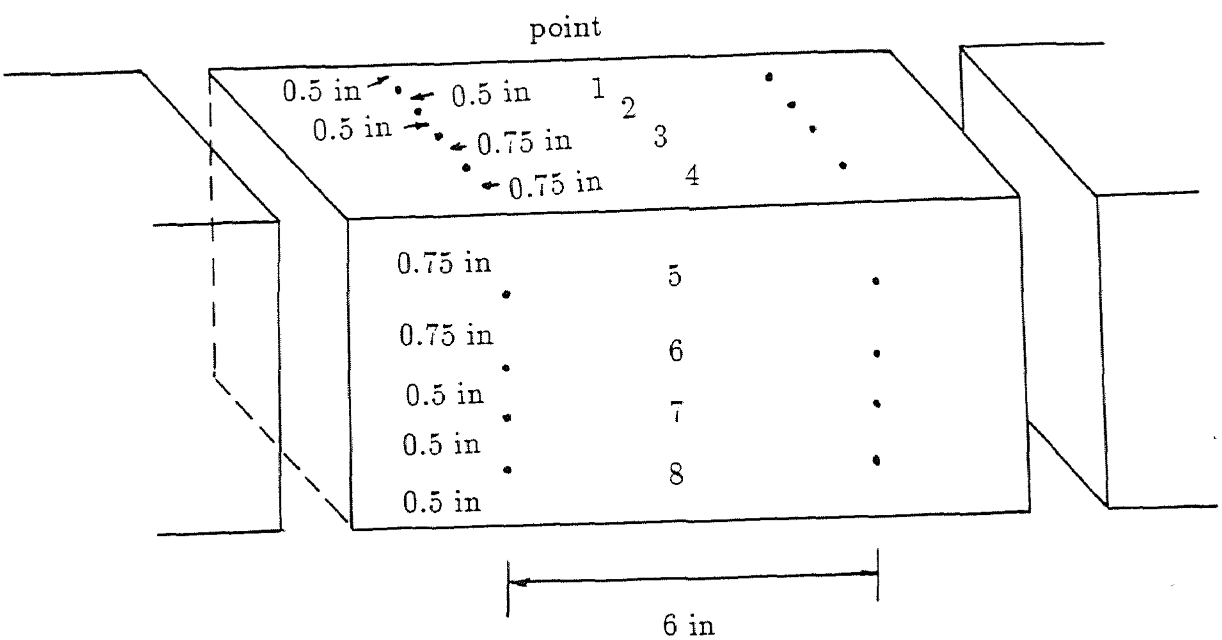

Figure 14b. Demec gage setup for square slender column specimens.

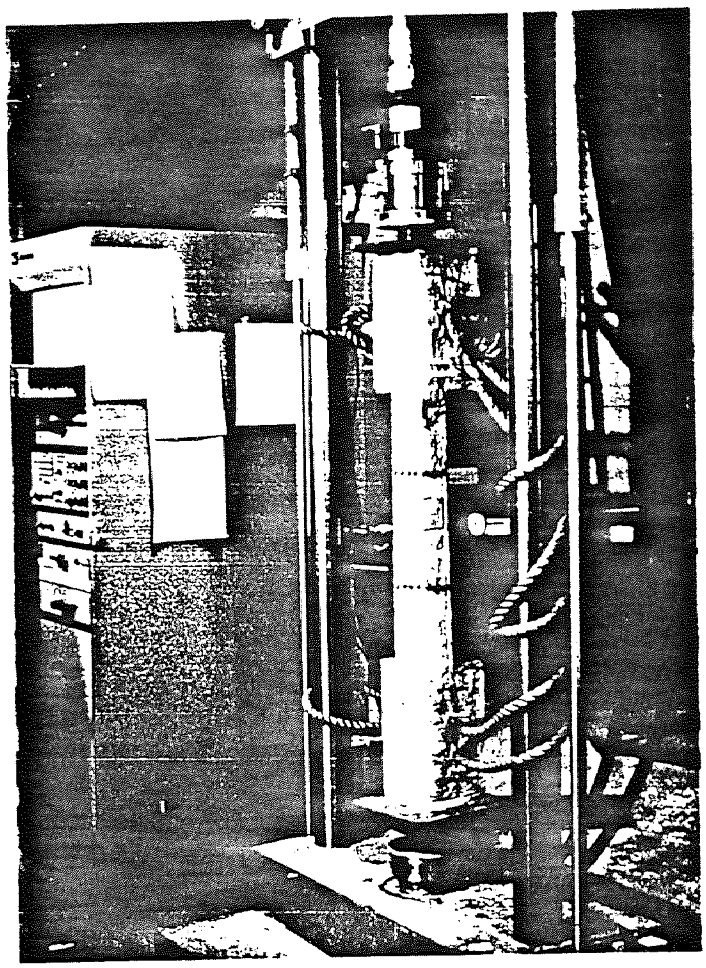

Figure 15a. Experimental setup for L-shaped slender columns.

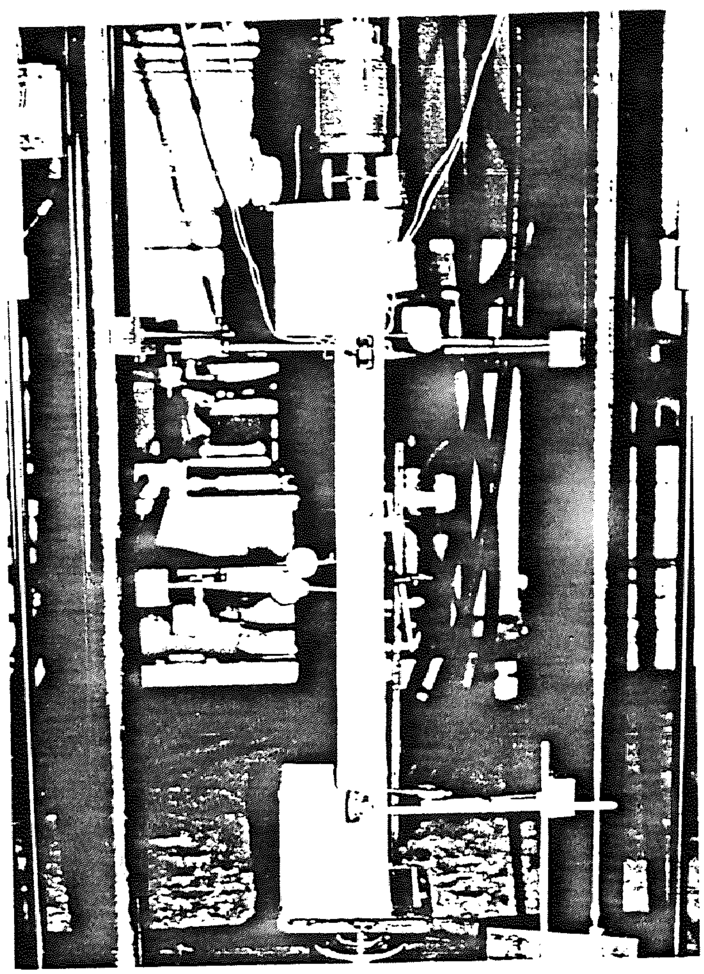

Figure 15b. Experimental setup for square slender columns.

3.1.3 L-shaped slender column test

L-shaped slender columns were made of 4 feet long, longitudinally reinforced by eight #2 bars which were tied by 14 gage steel wires at spacing 3-inch intervals. Cross section of test column is shown in Fig. 16. The typical stress-strain curves for # 2 reinforcing bars are shown in Fig. 17a and Fig. 17b. The brackets were one foot long on each end which were heavily reinforced to prevent local failure. The reinforcements were assembled into a unit before it was placed in the mold as shown in Fig. 18. The concrete used to cast the test specimens was prepared from sand, Portland cement Type III and water. The water cement ratio was 0.7 and the cement sand ratio was 3.0. The concrete properties and the stress-strain curves were determined by using 3 by 6 inches cylinder. The cylinders were to be cast by filling the mold in three equal layers and rodding each layer 25 times. After three days the molds of column were stripped and the cylinders were taken out for curing. Two days before the testing, the cylinders were capped and the column were dried. The failure conditions for each column specimens are shown in Table 2. Fig. 19. shows the test specimens after failure.

Test results of B-series columns			
Specimen number	location of plastic hinge	length of plastic hinge	no. of buckled bars
B1	close to upper bracket	6 inches	3
B2	near the middle	4 to 6 inches	none
B3	right at middle	5 to 6 inches	3
B4	close to lower bracket	5 inches	2
B5	near the middle	5 to 6 inches	1
B6	right at the middle	5 to 6 inches	2
B7	near the middle	3 to 6 inches	2
B8	near the middle	3 to 4 inches	2

Table 2. Failure conditions for L-shaped slender columns.

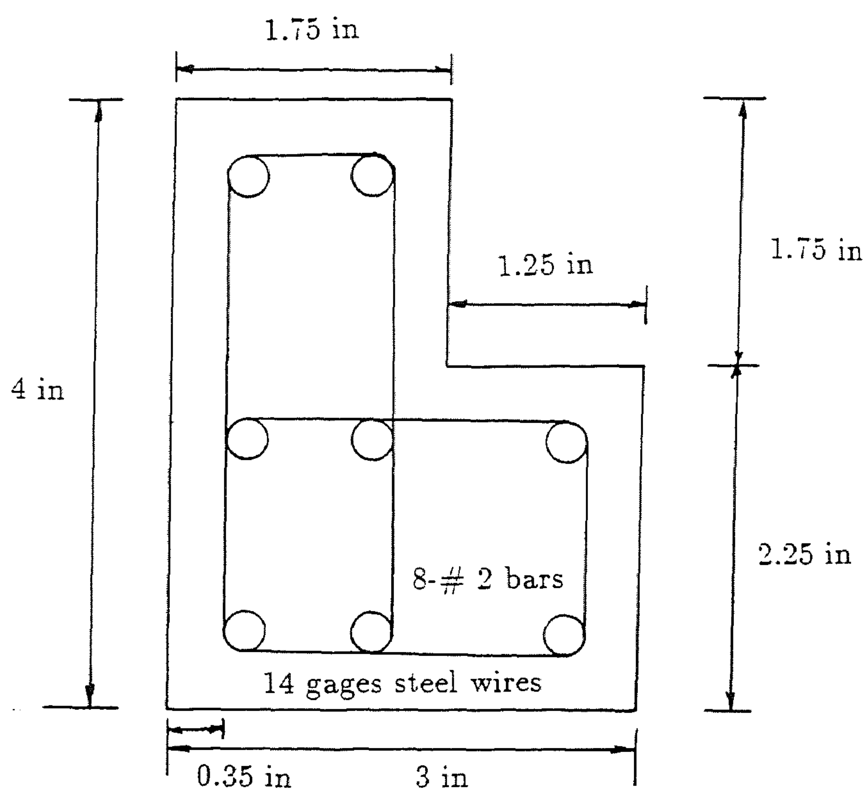

Figure 16. Test specimen details for L-shaped cross section.

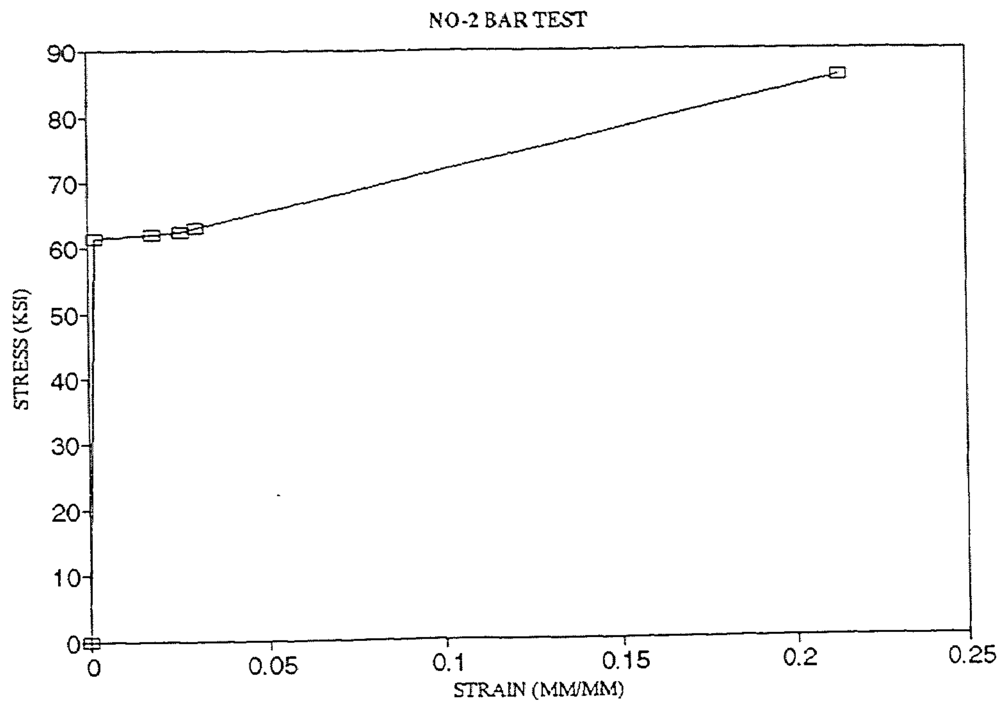

Figure 17a. Stress-strain curve of # 2 bar for B1, B2 and B3 column tests.

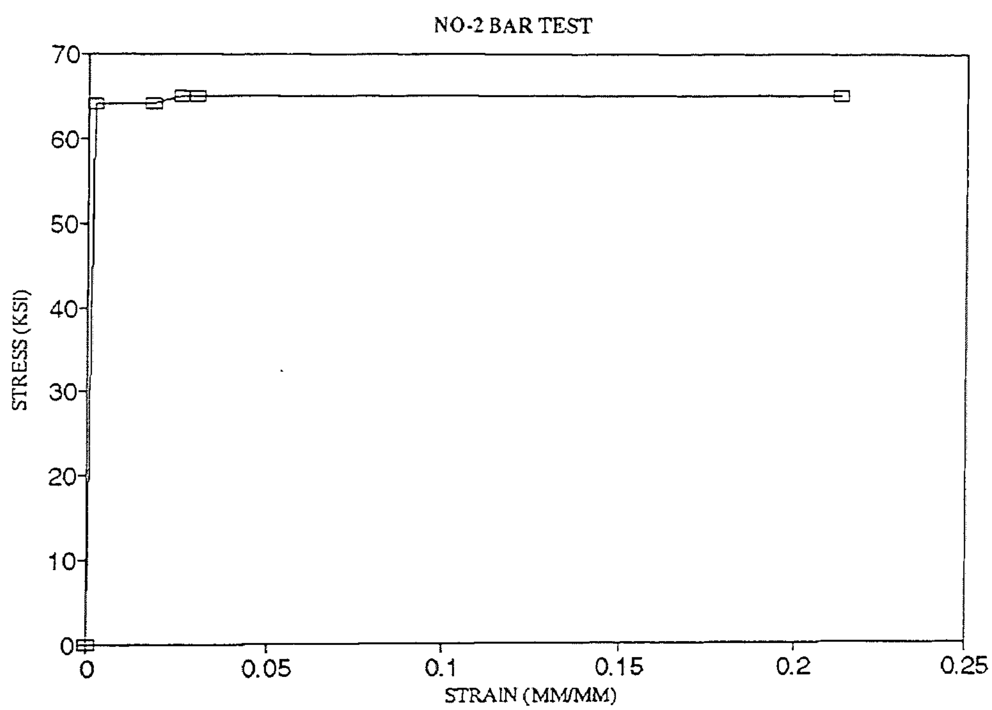

Figure 17b. Stress-strain curve of # 2 bar for B4 to B8 column tests.

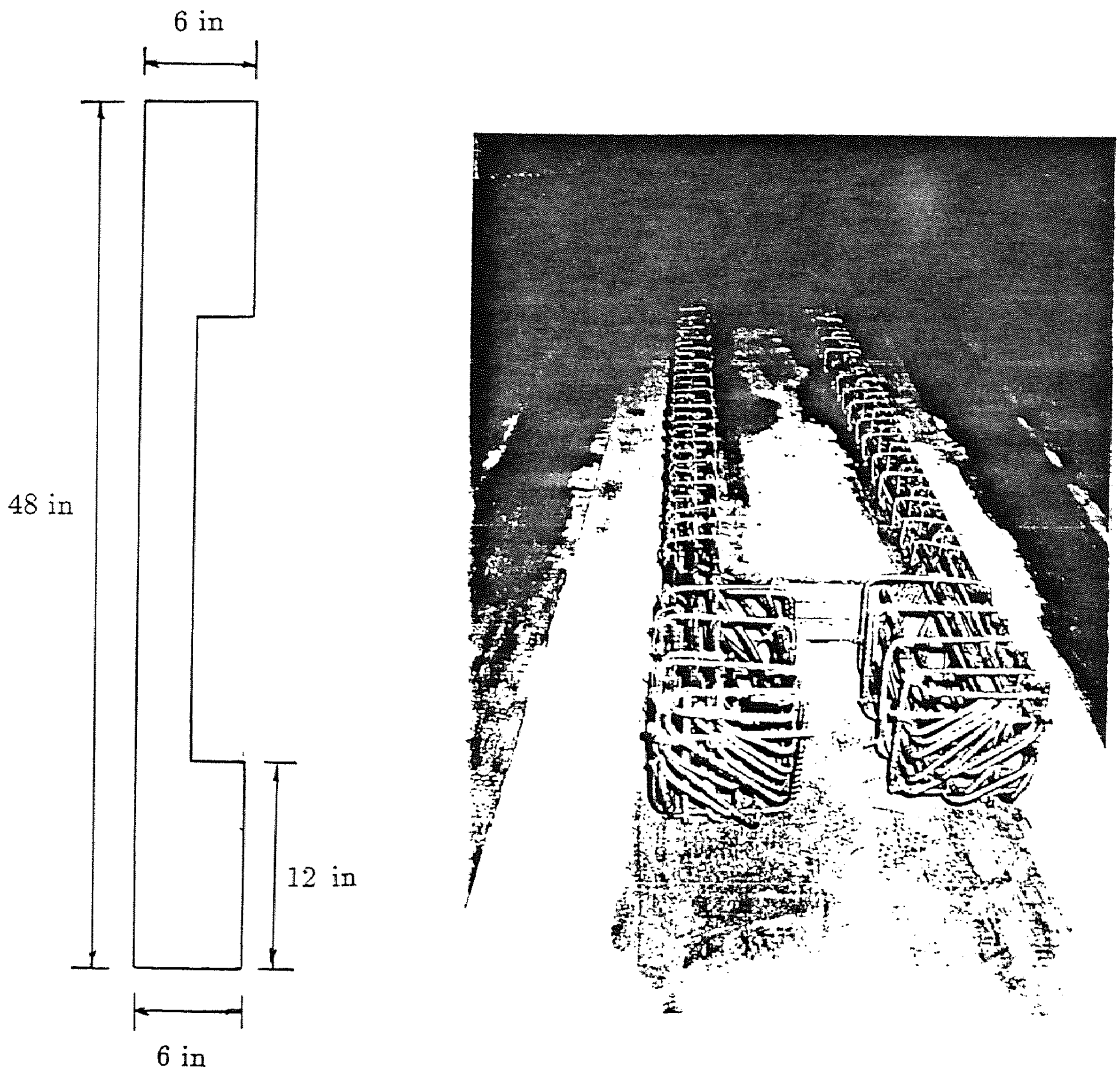

Figure 18. Reinforcement details for L-shaped slender columns.

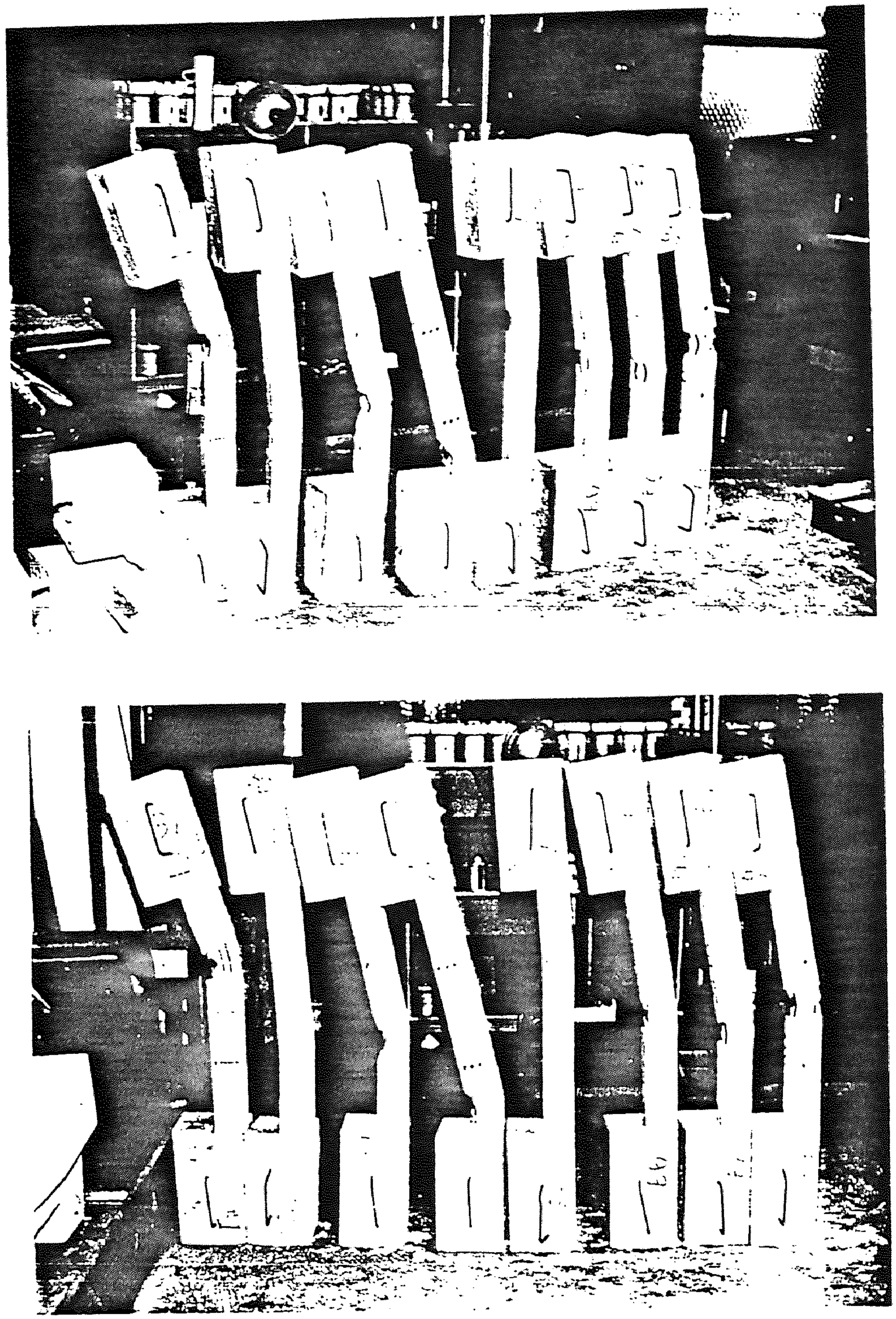

Figure 19. L-shaped slender columns after failure.

3.1.4 Square slender column test

Square slender columns were made of 4 feet long, longitudinally reinforced by four #3 bars which were tied by 14 gage steel wires at spacing 3-inch intervals. The typical stress-strain curves for # 3 reinforcing bars are shown in Fig. 20a. and Fig. 20b. The brackets were eight inches long at each end which were heavily reinforced to prevent local failure. The cross section of test column is shown in Fig. 21. The concrete used to cast the test specimens was prepared from a graded mixture of crushed quartz, sand, Portland cement Type III and water. The failure conditions are shown in Table 3. Fig. 22 illustrates the column specimens after testing.

Test results of C-series columns			
Specimen number	location of plastic hinge	length of plastic hinge	no. of buckled bars
C1	close to upper bracket	6 to 7 inches	none
C2	near the middle	8 to 9 inches	none
C3	close to lower bracket	8 to 9 inches	none
C4	right at the middle	8 to 10 inches	none
C5	right at the middle	6 to 8 inches	none
C6	right at the middle	7 to 8 inches	none

Table 3. Failure conditions for square slender columns.

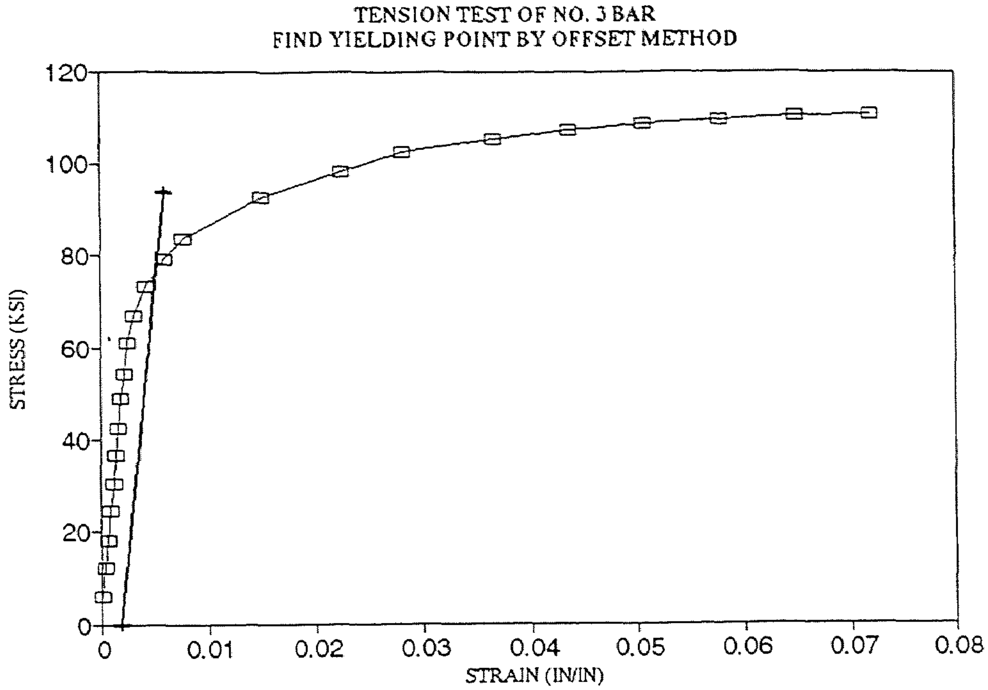

Figure 20a. Stress-strain curve of # 3 bars for C1 to C3 column test.

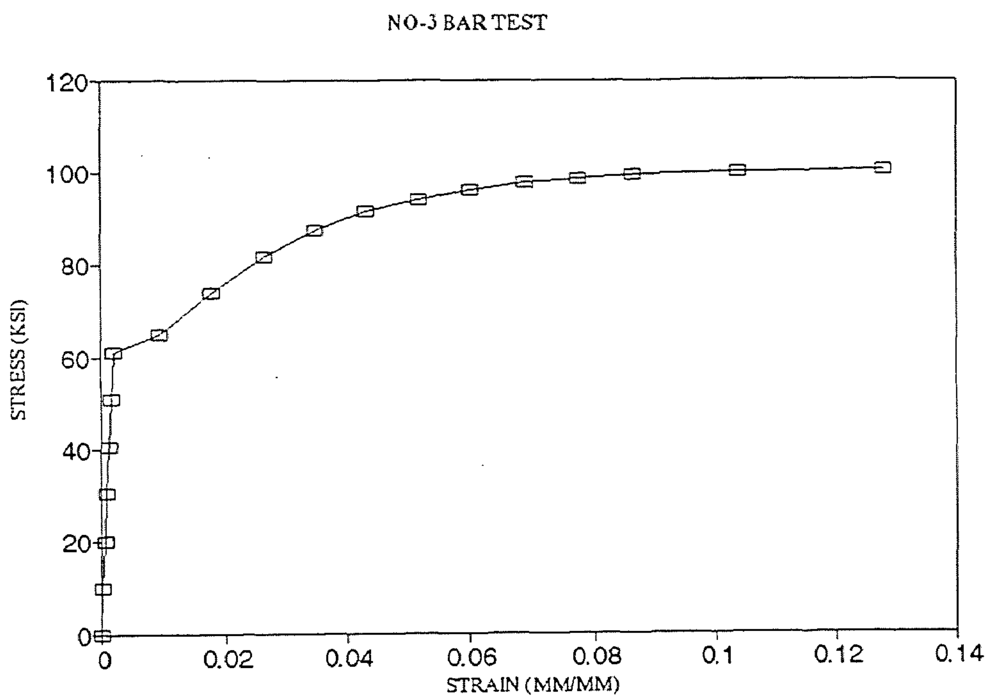

Figure 20b. Stress-strain curve of # 3 bars for C4 to C6 column test.

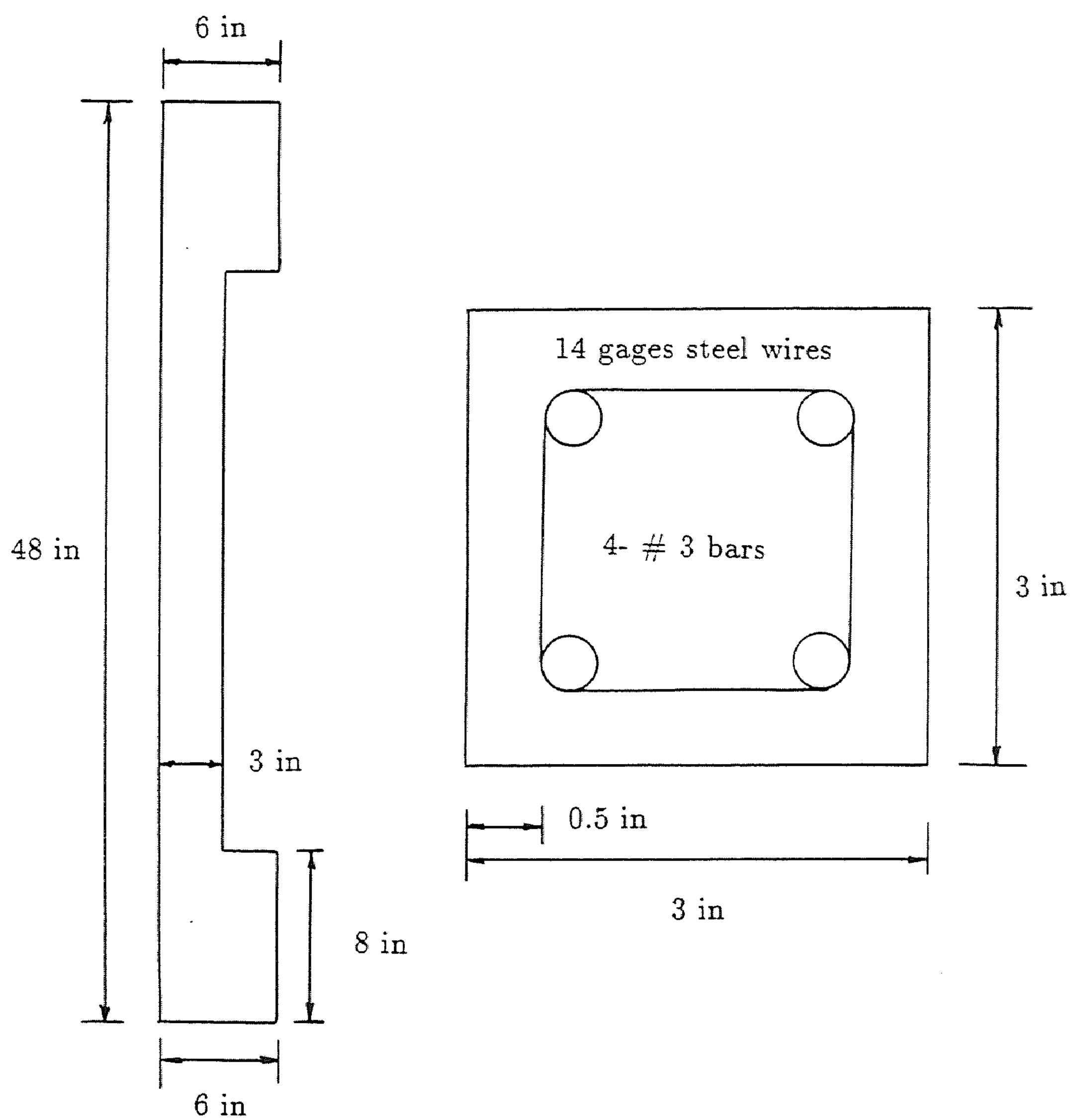

Figure 21. Test specimen details for square cross section.

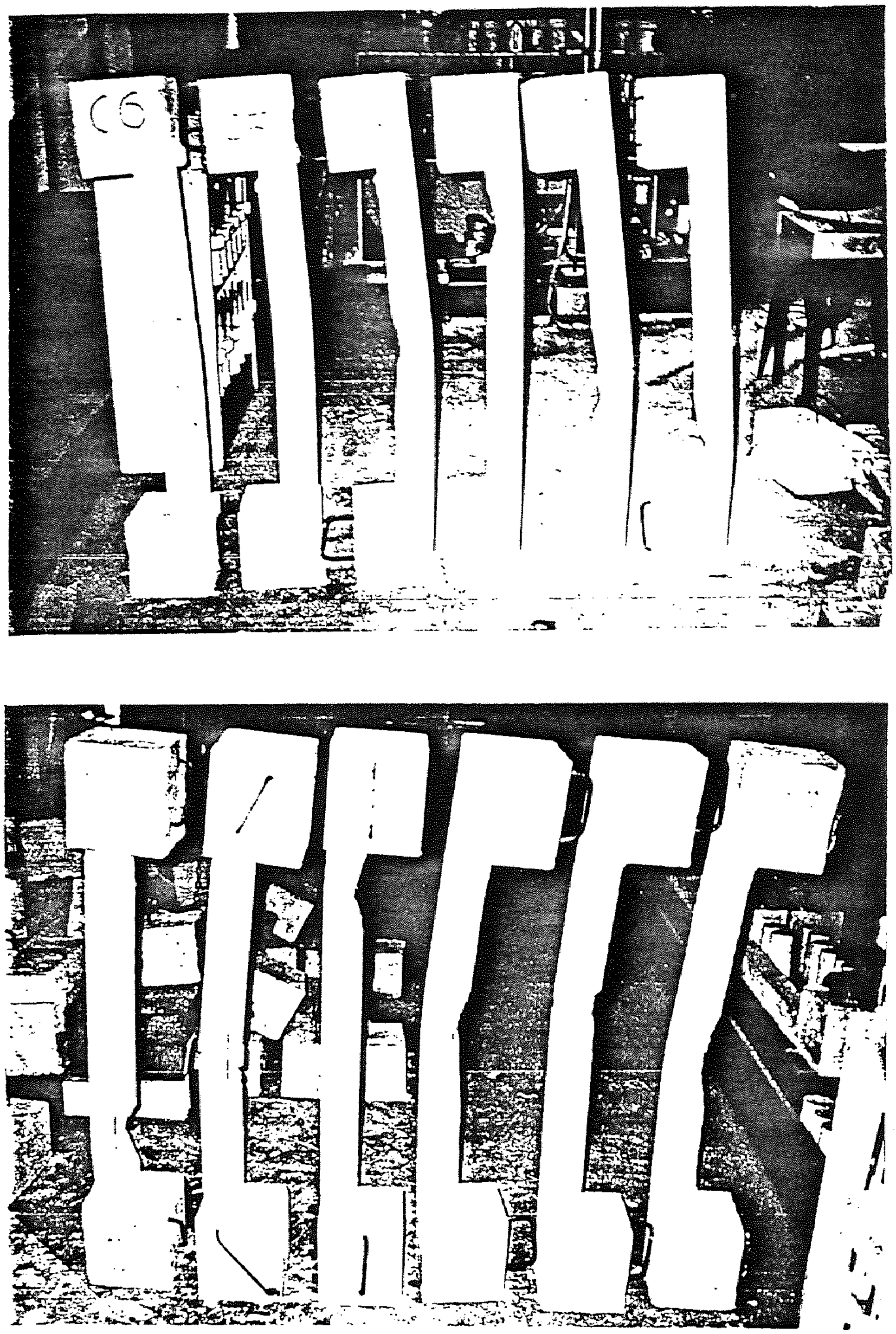

Figure 22. Square slender columns after failure.

3.2 Analysis of test results

3.2.1 Introduction

In all, eight L-shaped (B1 - B8 specimens) and six square (C1 - C6 specimens) slender reinforced concrete column were tested at the present study. Except B-1 specimen as a trial specimen, all other column test results were analyzed.

The applied loads were determined directly from the MTS loading system. Due to close-loop nature of the MTS loading system, which enables eliminating sudden collapse of the slender column specimen at maximum load. Thus both the ascending and descending branches of the biaxial load-deflection and moment-curvature curves were successfully determined.

The experimental values of M_x and M_y were computed using the experimental axial load values obtained from the load measurements and the load eccentricities were corrected for the mid-height deflection of the column. These experimental values at maximum are detailed in Table 4. Other experimental results can be found in Appendix A.

The deflection d can be calculated by $d = d_i - d_0$, where $d_i =$ the dial gage readings from each loading increments and $d_0 =$ the initial dial gage reading. There are two dial gages in both X and Y directions at mid-height of the column. Thus, the average deflection values were computed for each loading increments in X and Y-directions, respectively.

The strains ϵ from demec or mechanical gages can be determined by $\epsilon = (l_i - l_0)/l_0$, where l_i = length of demec gages at each loading step, and l_0 = initial length of demec gages at zero loading. After determinations of the strains at demec gage points 1-2-3 & 4-5-6-7 from B-series column specimens and point 1-2-3-4 & 5-6-7-8 from C-series column specimens in X and Y-directions, the strain-position curves were drawn as seen in Appendix B.

The curvature values at the present study were determined by the slope of the strain distribution diagrams as shown in Appendix B in both X and Y-direction. Usually, the linear strain distribution curves are obtained. If the strain distributions are not linear, the regression method of statistical analysis will be preformed to compute the curvature values.

The present test results were analyzed by the Lotus 1-2-3 and the final graphs were printed by Quattro. The crack and crush patterns for the series B and C are given in appendix C.

3.2.2 Test results of L-shaped slender column

The details of strain-position curves for L-shaped slender column tests are given in Appendix B. The complete biaxial load-deflection curves and moment-curvature curves are given in Appendix A.

3.2.3 Test results of square slender column

The details of strain-position curves for square slender column tests are given in Appendix B. The complete biaxial load-deflection curves and moment-curvature curves are also given in Appendix A.

Test results of B & C-series column tests			
Specimen number	P (LBS)	M_x (LB-IN)	M_y (LB-IN)
B2	10250	21771	15398
B3	12824	15071	21660
B4	10117	17172	21754
B5	28823	13598	16673
B6	16071	15254	21259
B7	16063	16509	15106
B8	10520	19011	17332
C1	15521	24357	9697
C2	12820	15315	15306
C3	8990	16267	15928
C4	19060	18992	19645
C5	10710	24343	11175
C6	18710	25311	11665

Table 4. Maximum axial load and moments from tests.

3.3 Comparison of test results and theoretical model

3.3.1 Introduction

The analytical values of load, bending moment components M_x and M_y, deflections and curvatures in both X and Y directions were computed for all specimens using the present computer analysis mentioned in the previous section.

For analysis purpose, the cross section of L-shaped column specimens was divided into 52 confined concrete elements, 40 unconfined concrete elements and 8 steel elements as shown in Fig. 5. Fig. 1 also shows that the square cross section consists of 32 confined concrete elements, 28 unconfined concrete elements and 4 steel elements. The slender column was also divided into a different number of segments for computing the deflections in X and Y directions. At present analysis, convergence can be achieved by dividing and redividing the segments for before and after the formation of plastic hinge as seen in Fig 10.

3.3.2 Maximum strength values

An examination of Tables 5, 6, 7 and 8 shows that good agreement was achieved between the experimental strengths and the computed values for all L-shaped and square reinforced concrete slender column specimens. Due to the second order effect, it should be noted that the loads to calculate the maximum moment values are not necessary to be the maximum load.

3.3.3 Biaxial load-deflection curves

The deflections components along the x and y axes were measured using dial gages with a least count of 0.001 in; the theoretical mid-height deflection components were calculated using the present numerical analysis. The experimental and theoretical load-deflection curves for L-shaped and square columns are shown in Appendix D and E. The comparisons show satisfactory agreement between experimental and theoretical curves. The descending branch of theoretical and experimental load-deflection curves were mostly successfully obtained for all specimens.

Maximum axial load and deflection results							
Specimen	Test			Analysis nnod*=6			
number	P_{max}	d_x	d_y	P_{max}	Ratio**	d_x	d_y
B2	10250	0.69	0.40	10479	1.022	0.48	0.37
B3	12824	0.72	0.28	11872	0.926	0.55	0.31
B4	10117	0.82	0.38	9400	0.929	0.54	0.31
B5	28823	0.37	0.20	25727	0.893	0.35	0.18
B6	16071	0.68	0.28	16721	1.040	0.44	0.25
B7	16063	0.48	0.27	17358	1.081	0.41	0.26
B8	10520	0.65	0.46	10051	0.955	0.55	0.35

Maximum axial load and deflection results								
Specimen	Analysis nnod*=8				Analysis nnod*=16			
number	P_{max}	Ratio**	d_x	d_y	P_{max}	Ratio**	d_x	d_y
B2	10500	1.024	0.48	0.37	10509	1.025	0.48	0.37
B3	11890	0.927	0.55	0.31	11907	0.928	0.55	0.31
B4	9416	0.931	0.54	0.31	9431	0.932	0.54	0.31
B5	25781	0.894	0.35	0.18	25841	0.897	0.35	0.18
B6	16718	1.040	0.44	0.25	16758	1.043	0.44	0.25
B7	17365	1.081	0.41	0.26	17400	1.083	0.41	0.26
B8	10055	0.956	0.55	0.35	10064	0.957	0.55	0.35

* nnod= number of segments for computations.

**Ratio= $P_{(analysis)}/P_{(test)}$

units : P_{max} (LBS), d_x, d_y (INCHES)

Table 5. Maximum axial load and deflection results for L-shaped slender columns.

Maximum axial load and deflection results							
Specimen number	Test			Analysis nnod*=8			
	P_{max}	d_x	d_y	P_{max}	Ratio**	d_x	d_y
C1	15521	0.24	0.68	14642	0.943	0.31	0.59
C2	12820	0.47	0.49	14085	1.099	0.47	0.47
C3	8990	0.52	0.56	10193	1.134	0.47	0.47
C4	19060	0.38	0.40	16431	0.862	0.35	0.35
C5	10710	0.38	0.64	10342	0.966	0.26	0.53
C6	18710	0.30	0.55	16907	0.904	0.24	0.47

Maximum axial load and deflection results								
Specimen number	Analysis nnod*=16				Analysis nnod*=32			
	P_{max}	Ratio**	d_x	d_y	P_{max}	Ratio**	d_x	d_y
C1	14659	0.944	0.31	0.59	14665	0.945	0.31	0.59
C2	14109	1.101	0.47	0.47	14114	1.101	0.47	0.47
C3	10195	1.134	0.47	0.47	10195	1.134	0.47	0.47
C4	16465	0.864	0.35	0.35	16468	0.864	0.35	0.35
C5	10345	0.966	0.26	0.53	10352	0.967	0.26	0.53
C6	16945	0.906	0.24	0.47	16947	0.906	0.24	0.47

* nnod= the number of segments for computations

** Ratio= $P_{(analysis)}/P_{(test)}$

units : P_{max} (LBS), d_x, d_y (INCHES)

Table 6. Maximum axial load and deflection results for square slender columns.

3.3.4 Biaxial moment-curvature curves

The experimental strain distribution along both axes for specimens was obtained using the data from demec or mechanical gages. A set of strain values in X and Y directions were first established before evaluating the moment-curvature relationships. The experimental and theoretical moment-curvature values for specimens B series and C series are shown in Appendix D and E. Good agreement was obtained between the theoretical and experimental curves from zero load up to failure. Both ascending and descending branches of moment-curvature curves were achieved. The terminations in the experimental curvature measurements were due to dislodging of demec or mechanical gages because of the crushing of concrete or because of severe tension cracks. The theoretical results of maximum moment with different number of segments and experimental results of maximum moment are shown in Table 7 and Table 8, respectively. It is noted that a good agreement is also achieved.

Maximum moment results						
Specimen number	Test		Analysis nnod*=6			
	M_x	M_y	M_x	$Ratio^1$	M_y	$Ratio^2$
B2	21771	15398	22911	1.052	13929	0.905
B3	15071	21660	16244	1.078	19089	0.881
B4	17172	21754	16215	0.944	18348	0.843
B5	13598	16673	13796	1.015	18073	1.084
B6	15254	21259	15944	1.045	19198	0.903
B7	16509	15106	18186	1.102	17711	1.172
B8	19011	17332	19483	1.025	17750	1.024

The results of maximum load and deflection								
Specimen number	theoretical nnod*=8				theoretical nnod*=16			
	M_x	$Ratio^1$	M_y	$Ratio^2$	M_x	$Ratio^1$	M_y	$Ratio^2$
B2	22956	1.054	13950	0.906	22976	1.055	13960	0.907
B3	16270	1.080	19112	0.882	16291	1.081	19137	0.884
B4	16242	0.946	19137	0.845	16270	0.947	18410	0.846
B5	13825	1.017	18379	1.087	13859	1.019	18168	1.090
B6	15940	1.045	19196	0.903	15980	1.048	19243	0.905
B7	18196	1.102	17715	1.173	18232	1.104	17754	1.175
B8	19487	1.025	17752	1.024	19493	1.025	17741	1.024

* nnod= number of segments for computations

$Ratio^1 = M_{x(analysis)}/M_{x(test)}$

$Ratio^2 = M_{y(analysis)}/M_{y(test)}$

units : M_x, M_y (LB-IN)

Table 7. Maximum moment results for L-shaped slender columns.

Maximum moment results						
Specimen number	Test		Analysis nnod*=8			
	M_x	M_y	M_x	$Ratio^1$	M_y	$Ratio^2$
C1	24357	9697	22168	0.914	10137	1.045
C2	15315	15306	16578	1.082	16578	1.083
C3	16267	15928	19204	1.181	19204	1.206
C4	18992	19645	17368	0.914	17368	0.884
C5	24343	11175	24592	1.010	10570	0.946
C6	25311	11665	23567	0.931	10503	0.900

The results of maximum load and deflection								
Specimen number	theoretical nnod*=16				theoretical nnod*=32			
	M_x	$Ratio^1$	M_y	$Ratio^2$	M_x	$Ratio^1$	M_y	$Ratio^2$
C1	22194	0.915	10158	1.048	22202	0.915	10163	1.048
C2	16606	1.084	16606	1.085	16612	1.085	16612	1.085
C3	19207	1.181	19207	1.206	19208	1.181	19208	1.206
C4	17404	0.916	17404	0.886	17407	0.917	17407	0.886
C5	24598	1.010	10578	0.947	24615	1.011	10584	0.947
C6	23620	0.933	10528	0.903	23623	0.933	10531	0.903

* nnod= number of segments for computations

$Ratio^1 = M_{x_{(analysis)}} / M_{x_{(test)}}$

$Ratio^2 = M_{y_{(analysis)}} / M_{y_{(test)}}$

units : M_x, M_y (LB-IN)

Table 8. Maximum moment results for square slender columns.

4 SUMMARY AND CONCLUSIONS

A computer model which simulates the biaxial load-deflection and moment-curvature behavior of standard and L-shaped slender reinforced concrete columns subjected to combined biaxial bending and axial load is presented. The secant stiffness method is used to determine the moment-curvature-thrust relationship for any column sections. The finite difference method is also used successful to study the three-dimensional load-deformation analysis. The present computer program can be used to compute both ascending and descending branches of load-deformation curves with the deformation increments control. Nonlinearity due to material plasticity and geometric change of the slender column are overcome by a successive iteration approach.

A total of six square and eight L-shaped slender reinforced concrete columns were tested to verify the accuracy of the theoretical analysis developed herein. Good agreement was achieved between theoretical results and test results. Based on the results presented, the following conclusions may be made :

1. The assumptions of the present theoretical analysis have been found reasonable and this computer model is able to predict the behavior of slender columns under combined biaxial bending and axial compression.

2. For determination of descending branch of the load-deformation curves,

the convergence criteria for the finite difference method in analysis is obtained by redividing the sections or segments once the plastic hinge starts forming at critical section.

3. Both the experimental results and computer analysis developed herein may be found useful in limit analysis and design of two or three dimensional reinforced concrete structures.

4. Using the suitable stress-strain curves for steels and concretes, the present computer program can be easily modified to study the behavior of slender composite reinforced concrete columns, behavior of slender prestressed reinforced concrete columns and behavior of slender high strength reinforced concrete columns with and without steel fibers.

BIBLIOGRAPH

[1] Aas-Jakobsen, A. " Biaxial eccentricities in ultimate loaded design.", ACI Journal proceedings,Vol.61, March 1964, pp. 293-315.

[2] Abdel-Sayed, Sadek Iskander," Behavior of slender reinforced concrete columns under biaxial eccentric loading. " Ph.D. Thesis, University of Ottawa, Feb. 1975. 181p.

[3] Abolitz, A. L., " Short and long column under uniaxial and biaxial flexure.", ACI Journal proceedings, Vol. 65, June 1968, pp. 462-469.

[4] Al-Noury, Soliman I., Chen, Wai F., " Finite segment method for biaxial loaded reinforced concrete columns.", Journal of the Structural Division, ASCE, Vol.108, No. ST4, April 1982,pp. 780-799.

[5] Al-Noury, Soliman I.," A study of reinforced concrete compression members under biaxial bending.", Ph.D. Thesis presented to Prudue University, 1980, 231p.

[6] Al-Noury, Soliman I., Chen, Wai F.,"Behavior and design of reinforced and composite concrete sections.",ASCE proceedings, Vol. 108, No. ST 6, June 1982, pp. 1266-1284.

[7] Ang, Charles Cho-Lim, " Square column with double eccentricities solved by numerical methods.", ACI Journal proceedings, Vol. 32, Feb. 1961, pp. 977-980.

[8] Au, Tung , " Ultimate strength of rectangular concrete members subjected to unsymmetrical bending.",ACI Journal proceedings, Vol. 54, Feb. 1958, pp. 657-674.

[9] Basu, A. K., Suryanarayana, P., " Analysis of restrained reinforced

concrete columns under biaxial bending.",Symposium on Reinforced Concrete Columns, ACI-SP-50-9, 1975, pp. 211-232.

[10] Batoz, Jean-louis, Dhatt, Gouri, " Incremental displacement algorithms for nonlinear problems.", International Journal for Numerical Method in Engineering., Short communications. Jan. 1979, pp. 1262-1267.

[11] Bellini, P. X., Chulya, A., " An improved automatic incremental algorithm for the efficient solution of nonlinear finite element equations.", Computers and Structures, Vol 26, No. 1/2, 1987, pp. 99-110.

[12] Bergan, P. G., Horrigmoe, G., Krakeland B., Soreide T.H., " Solution techniques for nonlinear finite element problems.", International Journal for Numerical Method in Engineering, Vol. 12, 1978, pp.1677-1696.

[13] Berwanger, Carl, " Effect of axial load on the moment-curvature relationship of reinforced concrete members.",Symposium on Reinforced Concrete Columns, ACI-SP-50-11, 1975, pp. 263-288.

[14] Breen, John E., Ferguson, Phil M., " The restrainted long concrete column as a part of a rectangular frame.", ACI Journal proceedings, Vol. 61, May 1964, pp. 563-587.

[15] Bresler, Boris, " Design criteria for reinforced columns under axial load and biaxial bending.",ACI Journal proceedings, Vol. 57, Nov. 1960, pp.481-490.

[16] Broms, Bengt, Viest, I. M., " Ultimate strength analysis of long restrained reinforced concrete columns.", ASCE proceedings, Vol. 84, ST 3, May 1958, pp. 1635-1-30.

[17] Chang, Wen F., Ferguson, Phil M., " Long hinged reinforced concrete columns.", ACI Journal proceedings, Vol. 60, Jan. 1963, pp. 1-25.

[18] Chu, Kuang-Han, Pabarcius Algis, "Biaxial loaded reinforced concrete columns.", ASCE proceeding, Vol. 85, ST 6, Dec. 1958, pp. 1865-1-27.

[19] Colville, James, " Slenderness effects in reinforced concrete square columns.", Symposium on Reinforced Concrete Columns, ACI-SP-50-7, 1975, pp. 165-183.

[20] Corley, W. Gene, "Rotational capacity of reinforced concrete beams. ",ASCE proceedings, Vol. 92, No. St 5, Oct. 1966, pp.121-146.

[21] Craemer, Hermann, " Skew bending in reinforced concrete computed by plasticity.", ACI Journal proceedings, Vol. 48, No. 7, Feb. 1952, pp. 516-519.

[22] Cranston, W. B., " Determining the relation between moment, axial load and cruvature for structural members.", Report TRA/395, Cement and Concrete Association, London, England, June 1966, 11p.

[23] Cranston, W. B.," A computer method for the analysis of restrained columns.", Report TRA/402, Cement and Concrete Association, London, England, April 1967.

[24] Crisfield, M. A., " A faster modified Newton-Raphson Iteration.", Computer Method in Applied Mechanics and Engineering, 20, 1979, pp.267-278.

[25] Czeriak, E., " Analytical approach to biaxial eccentricity .", ASCE proceedings, Vol. 104, ST 4, Aug. 1962, pp.105-158.

[26] Drysdale, R. G., " The behavior of slender reinforced columns subjected to sustained biaxial bending", Ph.D. Thesis, University of Toronto, Oct. 1967, 190p.

[27] El-Metwally, Salah E., Chen, Wai-Fah, "Load-Deformation relations for reinforced concrete sections.", ACI Structure Journal, Vol. 86,No. 2, March-April 1989, pp. 163-167.

[28] Farah, Anis, Huggins, M. W., " Analysis of reinforced concrete columns subjected to longitudinal load and biaxial bending.",ACI Journal ,No. 66-46, July 1969, pp. 569-575.

[29] Fleming, John F., Werner, Stuart D.," Design of columns subjected to biaxial bending.",ACI Journal proceedings, Vol 62, Mar. 1965, pp. 327-342.

[30] Furlong, Richard W., "Concrete columns under biaxiall y eccentric thrust.",ACI Journal, Vol. 76 No. 10 Oct. 1979, pp. 1093-1118.

[31] Furlong, Richard W., "Ultimate strength of square columns under biaxial eccentric loads.", ACI Journal proceedings, Vol. 32, March 1961, pp. 1129-1140.

[32] Gouwens, Albert J., " Biaxial bending simplified. ",Symposium on Reinforced Concrete Columns, ACI-SP-50-10, 1975, pp. 233-251.

[33] Gupta, S. R. Davalath, Murty, K. S. Madugula, " Analysis/Design of reinforced concrete circular cross sections.", ACI Structural Journal, Vol. 85, No. 6, Nov.-Dec. 1988, pp. 617-623.

[34] Gurfinkel, German , Robinson, Arthur, "Determination of strain distribution and curvature in a reinforced concrete section subjected to bending moment and longitudinal load.", ACI Journal,Proceedings, V. 64,

No. 7, July 1967, pp. 398-402.

[35] Hartz, B. J. "Matrix formulation of structural stability problems.", ASCE proceedings, Vol. 91, ST 6, Dec. 1965, pp. 141-157.

[36] Hognestad, Eivind, Hanson, N. W., McHenry, Douglas, " Concrete stress distribution in ultimate strength design." ACI Journal proceedings, Vol. 52, Nov. 1955, pp. 455-479.

[37] Horowitz, Bernardo, " Design of columns subjected to biaxial bending.", ACI Structural Journal, Vol. 86, No. 6, Nov.-Dec. 1989, pp. 717-722.

[38] Hsu, C. T. Thomas,"Biaxially loaded L-shaped reinforced concrete columns.", Journal of Structural Engineering, ASCE, Vol. 111, No. 12, Dec. 1985, pp. 2576-2595.

[39] Hsu, C. T. Thomas, Mirza, S. M.," Nonlinear behavior and analysis of reinforced concrete columns under combined loadings.", Study No. 14, M. S. Cohen,ed., University of Waterloo Press,1980, pp. 109-135.

[40] Hsu, C. T. Thomas," Behavior of structural concrete subjected to biaxial flexural and axial compression." Ph.D. Thesis,McGill University, August 1974, 479p.

[41] Hsu, C. T. Thomas, " Reinforced concrete members subject to combined biaxial bending and tension.", ACI Structural Journal, Vol. 83, No. 1, Feb. 1986, pp. 137-144.

[42] Hsu, C. T. Thomas, " Channel-shaped reinforced concrete compression members under biaxial bending.", ACI Structural Journal, Vol. 84, No. 3, May-June 1987, pp. 201-211.

[43] Hsu, C. T. Thomas,"T-Shaped reinforced concrete members under biaxial bending and axial compression.", ACI Structural Journal, Vol. 86, No. 4, July-Aug. 1989, pp. 460-468.

[44] Hsu, C. T. Thomas, " Lateral displacement for unbraced concrete frame buildings.", ACI Structural Journal, Vol.82, No. 6, Nov-Dec. 1985, pp. 853-862.

[45] Hsu, C. T. Thomas, "Analysis and design of square and rectangular columns by equation of failure surface. ", ACI Structural Journal, Vol. 85, March-April 1988, pp. 167-179.

[46] Hsu, Cheng-Tzu, Mirza, M. Saeed, " Structural concrete biaxial bending and compression.",ASCE proceedings, Vol. 99, ST2, Feb. 1973, pp. 285-290.

[47] Hu, Lu-Shien, " Eccentric bending in two directions of rectangular concrete columns.", ACI Journal proceedings, Vol. 26, May 1955, pp. 921-935.

[48] Koji, Sakai, Shamim, A. Sheikh, " What do we know about confinement in reinforced concrete columns ?", ACI Structural Journal, Vol. 86, No. 2, March-April 1989, pp. 192-206.

[49] Kwan, K. H., Liauw, T. C., " Computer aided design of reinforced concrete members subjected to axial compression and biaxial bending.", Structure Engineer, V. 63B, No. 2, June 1985, pp. 34-40.

[50] MacGregor, James G. ,Breen, John E. ,Pfrang, Edward O. , " Design of slender concrete columns.", ACI Journal Vol. 67, No. 2, Jan. 1970, pp. 6-28.

[51] MacGregor, James G., " Behavior of restrainted reinforced concrete

columns.", ASCE proceedings, Vol. 91, ST 3, June 1965, pp. 281-286.

[52] MacGregor, J. G., Oelhafen, U. H.,Hage, S. E., " A re-examination of the EI value for slender columns.", Symposium on Reinforced Concrete Columns, ACI-SP-50-1, pp. 1-40.

[53] MacGregor, J. G., Barter, S. L., " Long eccentrically loaded concrete columns bent in double curvature.",Symposium on Reinforced Concrete Columns, ACI-SP-13, 1966, pp. 139-156.

[54] Mander, J. B., Priestly, M. J. N., Park, R., " Theoretical stress-strain model for confined concrete.", ASCE proceedings, Vol. 114, No. 8, Aug. 1988, pp. 1804-1826.

[55] Manual, Robert F., MacGregor, James G., " Analysis of restrainted reinforced concrete columns under sustained load.", ACI Journal proceedings, Vol. 64, Jan. 1967, pp.12-24.

[56] Marin, Joaquin, "Design aids for L-shaped reinforced concrete columns.", ACI Journal, Vol. 76,No. 11 Nov. 1979, pp. 1197-1216.

[57] Martin, Ignacio , Olivieri, Elmer, " Test of slender reinforced concrete columns bent in double curvature. ",Symposium on Reinforced Concrete Columns,ACI-SP-13, 1966, pp. 121-138.

[58] Matthies, Hermann ,Strang, Gilbert, " The solution of nonlinear finite element equations.",International Journal for Numerical Method in Engineering, Vol. 14,1979, pp. 1613-1626.

[59] Mattock, Alan H., Kriz Ladislav B.,Hognestad Eivind, " Rectangular concrete stress distribution in ultimate strength design.", ACI Journal proceedings, Vol. 57, Feb. 1961, pp. 875-928.

[60] Meek, John L., "Ultimate strength of columns with biaxial eccentric loads.", ACI Journal proceedings, Vol. 60, Aug. 1963, pp.1053-1064.

[61] Mirza, S. Ali, MacGregor James G., " Slenderness and reliability of reinforced concrete columns.", ACI Structural Journal, Vol. 86, No. 4, July-Aug. 1989, pp. 428-438.

[62] Muller, L. S. ,"Design of L-shaped columns with small eccentricities.", ACI Journal, No. 56-31, Dec. 1959, pp. 487-498.

[63] Muller, L. S., " Eccentrical loaded corner columns.", ACI Journal proceedings, Vol. 47, March 1951, pp. 562-565.

[64] Nayak, G. C., Zienkiwicz, O. C., "Note on the 'ALPHA'-constant stiffness method for the analysis of nonlinear problems.", International Journal for Numerical Method in Engineering, Vol. 4, 1972, pp. 579-582.

[65] Pannell, F. N., " Failure surfaces for members in compression and biaxial bending.", ACI Journal proceedings, Vol. 60, Jan. 1963, pp. 129-140.

[66] Pannell, Frederick Norman, Discussion of "Biaxial loaded reinforced concrete columns.", ASCE proceedings ,Vol. 85, ST 6, June 1959, pp.47-54.

[67] Parme, Alfred L., Nieves Jose M., Gouwens Albert, "Capacity of reinforced rectangular columns subject to biaxial bending." ACI Journal, No.63-46, Sept. 1966, pp. 911-922.

[68] Parme, Alfred L., " Capacity of restrained eccentrically loaded long columns.", Symposium on Reinforced Concrete Columns, ACI-SP-13, 1966, pp. 325-367.

[69] Pfrang, E. O., Siess, C. P., Sozen, M. A., " Load-Moment-Curvature characteristics of reinforced concrete cross sections.", ACI Journal proceedings, Vol. 61, July 1964, pp. 763-778.

[70] Ramamurthy, L. N., " Investigation of the ultimate strength of square and rectangular columns under biaxial eccentric loads.", Symposium on Reinforced Concrete Columns, ACI-SP-13, 1966, pp. 263-298.

[71] Ramamurthy, L. N., Hafeez Khan T. A., " L-shaped column design for biaxial eccentricity.", ASCE proceeding, Vol 109, ST 8, Aug. 1983, pp. 1903-1917.

[72] Rangan, B., Vijaya, " Lateral deflection of slender reinforced concrete columns under sustained load.",ACI Structural Journal, Vol. 86, No. 6, Nov.-Dec. 1989, pp.660-663.

[73] Riad, Labib , " Eccentrically loaded reinforced concrete columns with variable cross section.", Symposium on Reinforced Concrete Columns, ACI-SP-13, 1966, pp. 245-262.

[74] Ross, David A. ,Yen, J. Richard, "Interactive design of reinforced concrete columns with biaxial bending." , ACI Journal proceedings, Vol. 83, No. 6, Nov-Dec. 1986, pp. 988-993.

[75] Ross, David A. ,Yen, J. Richard, " Computer aided design of reinforced concrete columns.", Concrete International, Vol. 6, No.3, Mar. 1984, pp. 47-54.

[76] Rotter, J. M., " Rapid exact inelastic biaxial bending analysis.", ASCE proceedings, Vol. 111, No. 2, Dec. 1985, pp. 2659-2674.

[77] Smith, K. N., Nelles, W. N., " Columns subjected to biaxial bending.", ACI Journal proceedings, Vol. 71, Aug.1974, pp. 411-413.

[78] Taylor. Michael A., "Direct Biaxial Design of Columns", Journal of Structural Engineering, ASCE, V. 111 No. 1, Jan. 1985, pp. 158-173.

[79] Wang Gary, C. T. Thomas Hsu, "Complete load-deformation behavior of biaxial loaded reinforced concrete columns.", Technical report structural series, No 90-2, New Jersey institute of Technology, Sep. 1990.

[80] Warner, R. F. ,"Biaxial moment thrust curvature relations", Journal of Structural Division, ASCE proceedings ST5 ,May. 1969, pp. 923-940.

[81] Weber, Donald C., "Ultimate strength design charts for columns with biaxial bending.", ACI Journal proceedings, Vol. 63, Nov. 1966, pp. 1205-1231.

[82] Whitney, Charles S., Cohen, Edward, " Guide for ultimate strength design of reinforced concrete.", ACI Journal proceedings, Vol. 53, Nov. 1956, pp. 455-490.

[83] Wiesinger, Frederick P. , "Design of symmetrical columns with small eccentricities in one or two directions. ", ACI Journal, Vol. 30, No. 2, Aug. 1958, pp. 273-284.

[84] Zahn, F. A., Park, R., Priestly, M. J. N., " Strength and ductility of square reinforced concrete column section subjected to biaxial bending.", ACI Structural Journal, Vol. 86, No. 2, March-April 1989, pp. 123-131.

APPENDICES

Appendix A. EXPERIMENTAL RESULTS

Experimental results of load-deflection and moment-curvature curves for L-shaped and square slender reinforced concrete columns are shown herein. Fig. A.1 through Fig. A.14 present B-series columns tests and Fig. A.15 through Fig. A.26 present C-series columns tests, respectively.

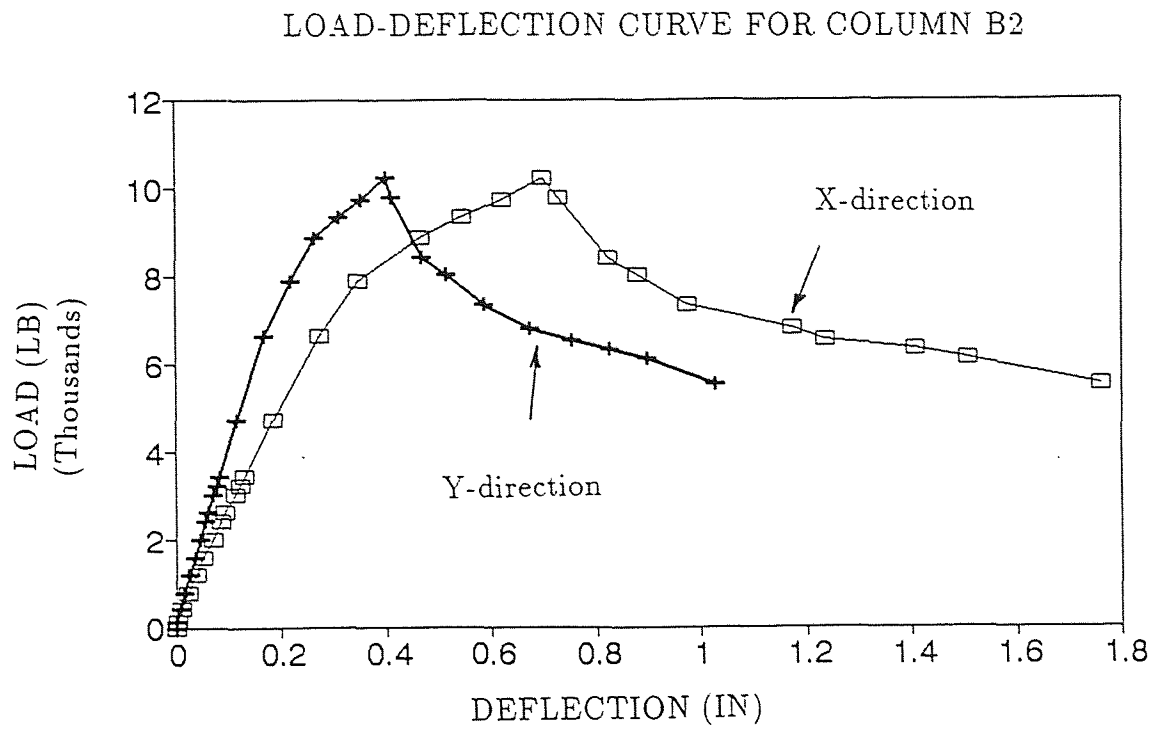

Figure A.1 Load-deflection curve for column B2

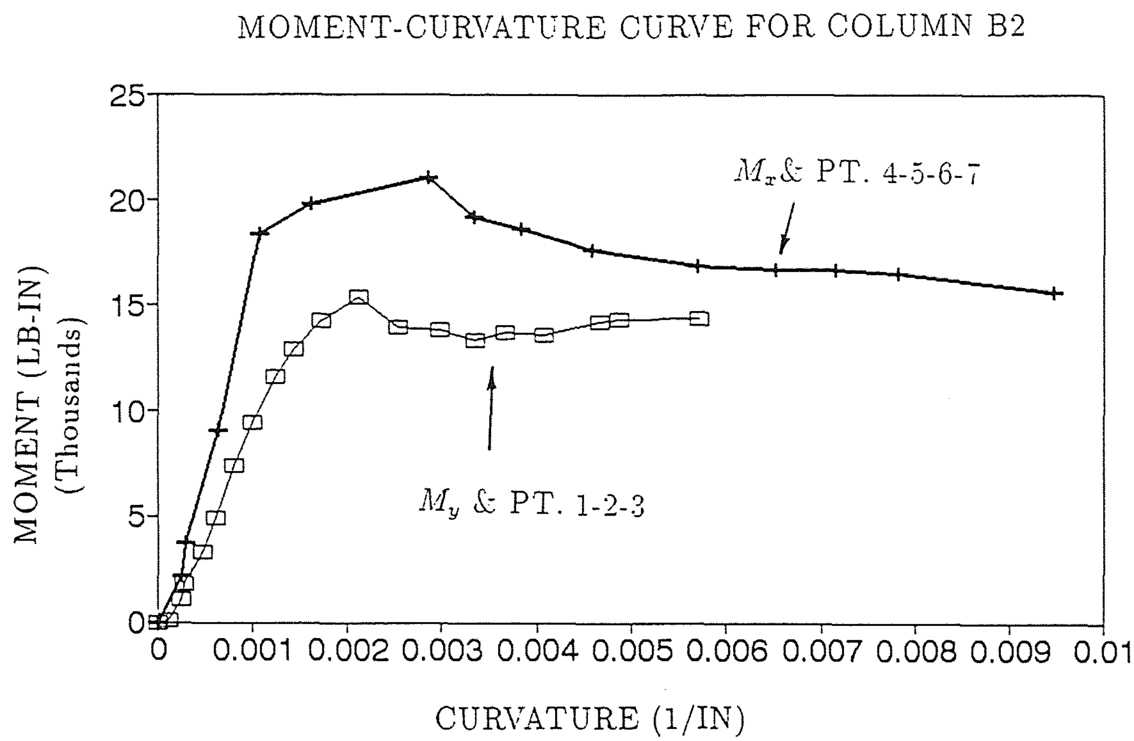

Figure A.2 Moment-curvature curve for column B2

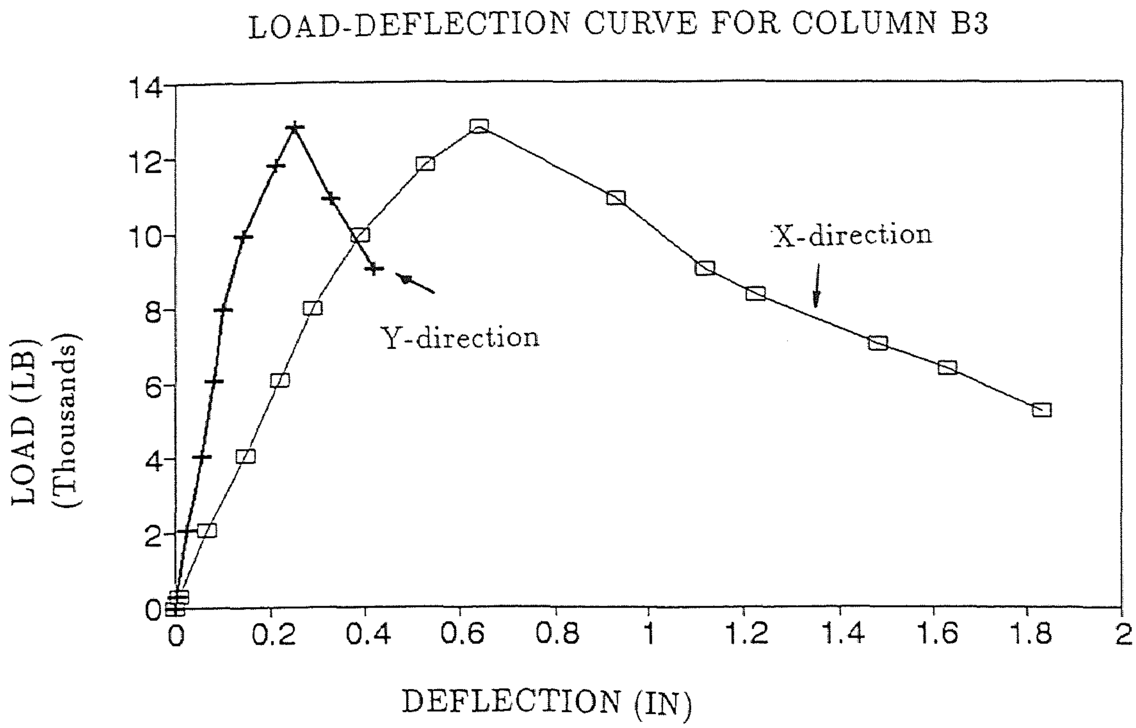

Figure A.3 Load-deflection curve for column B3

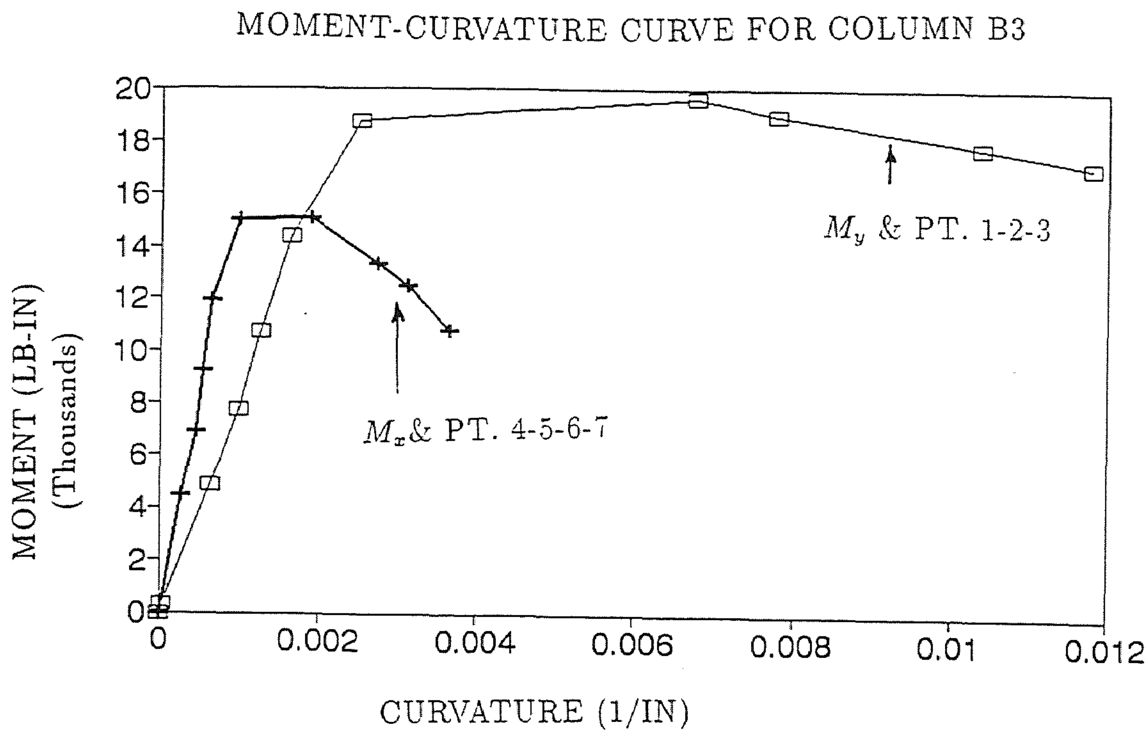

Figure A.4 Moment-curvature curve for column B3

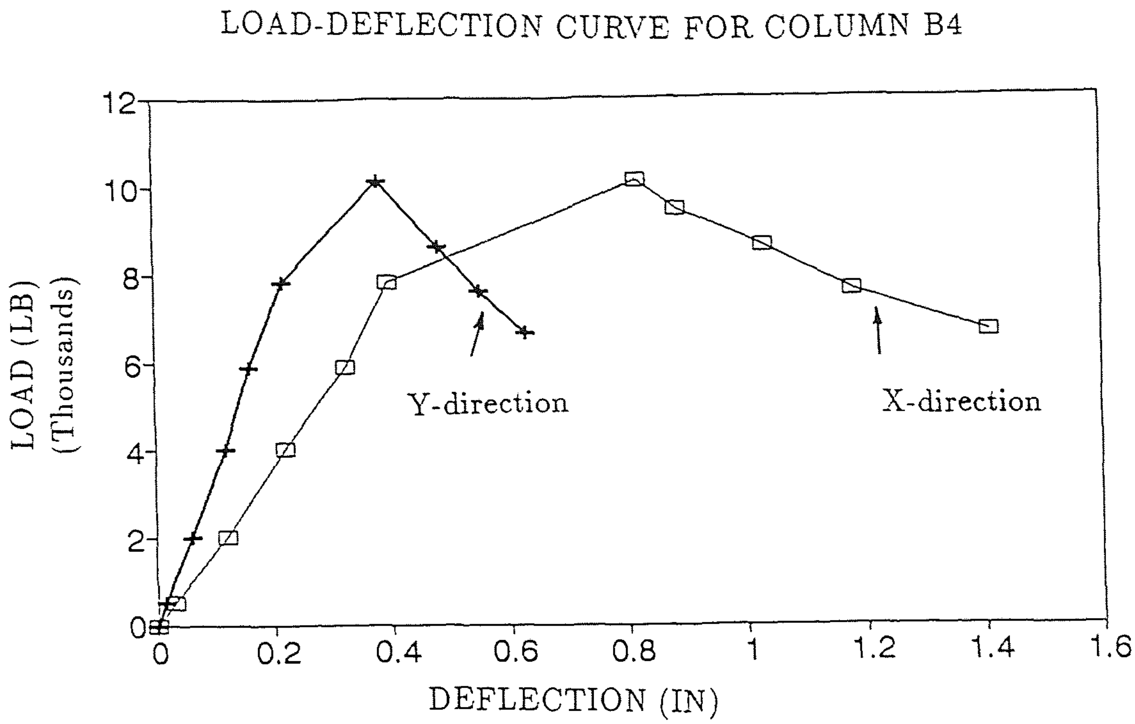

Figure A.5 Load-deflection curve for column B4

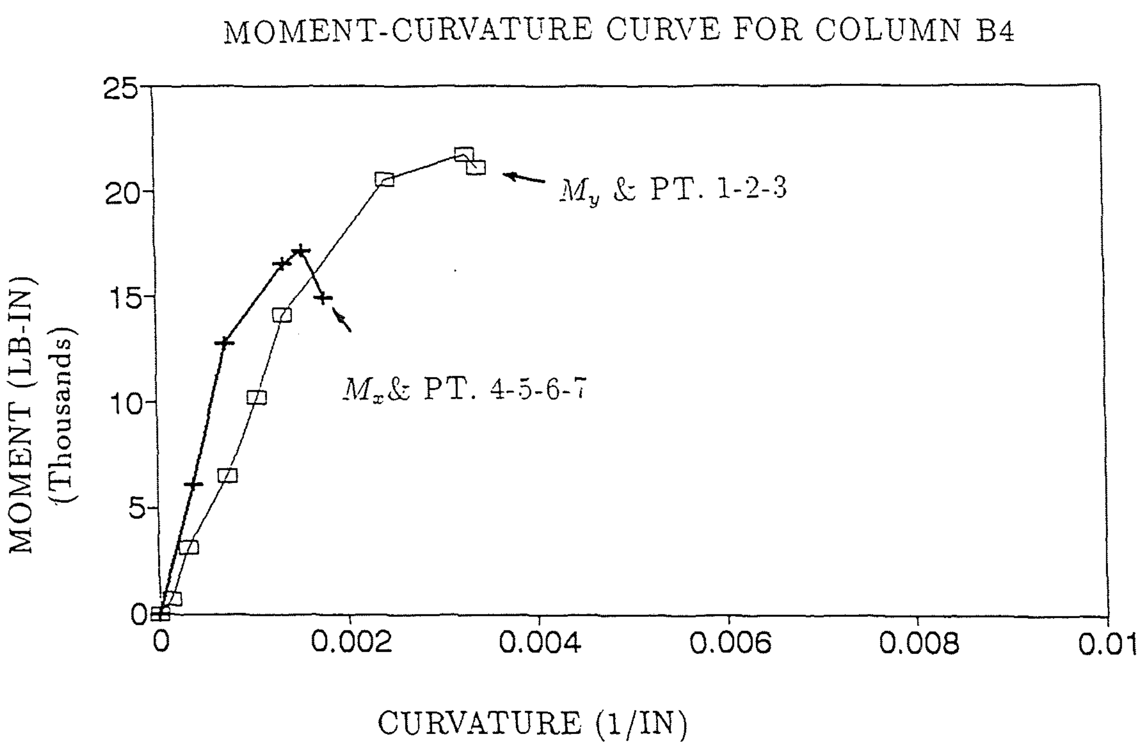

Figure A.6 Moment-curvature curve for column B4

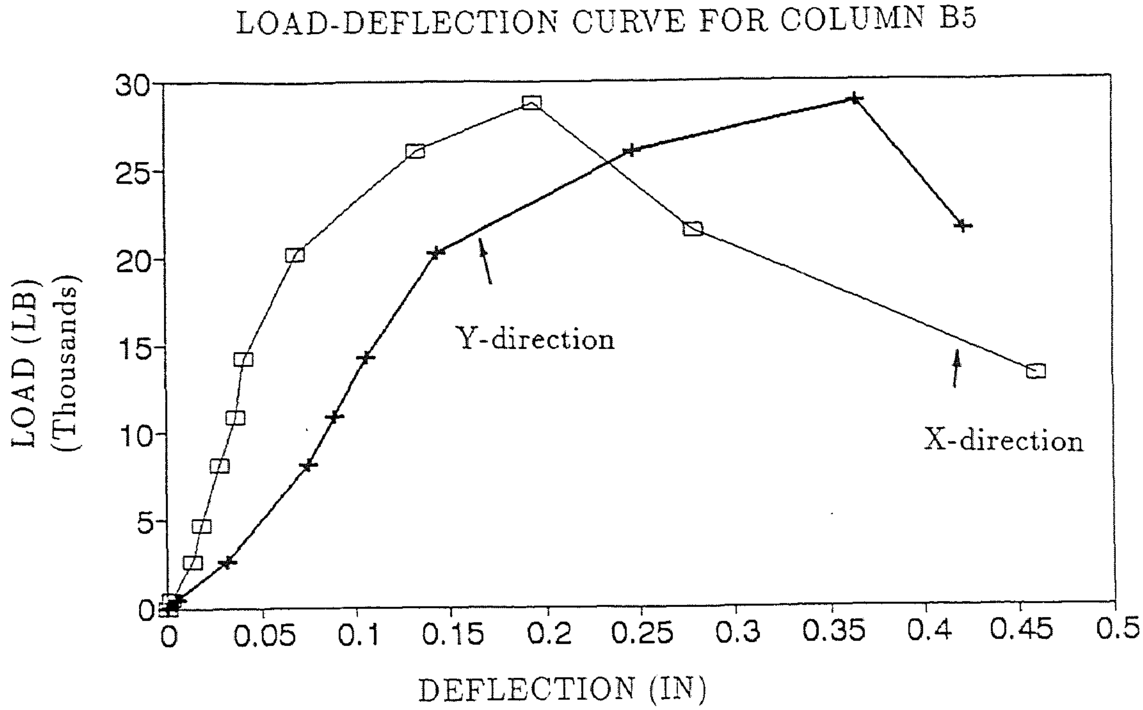

Figure A.7 Load-deflection curve for column B5

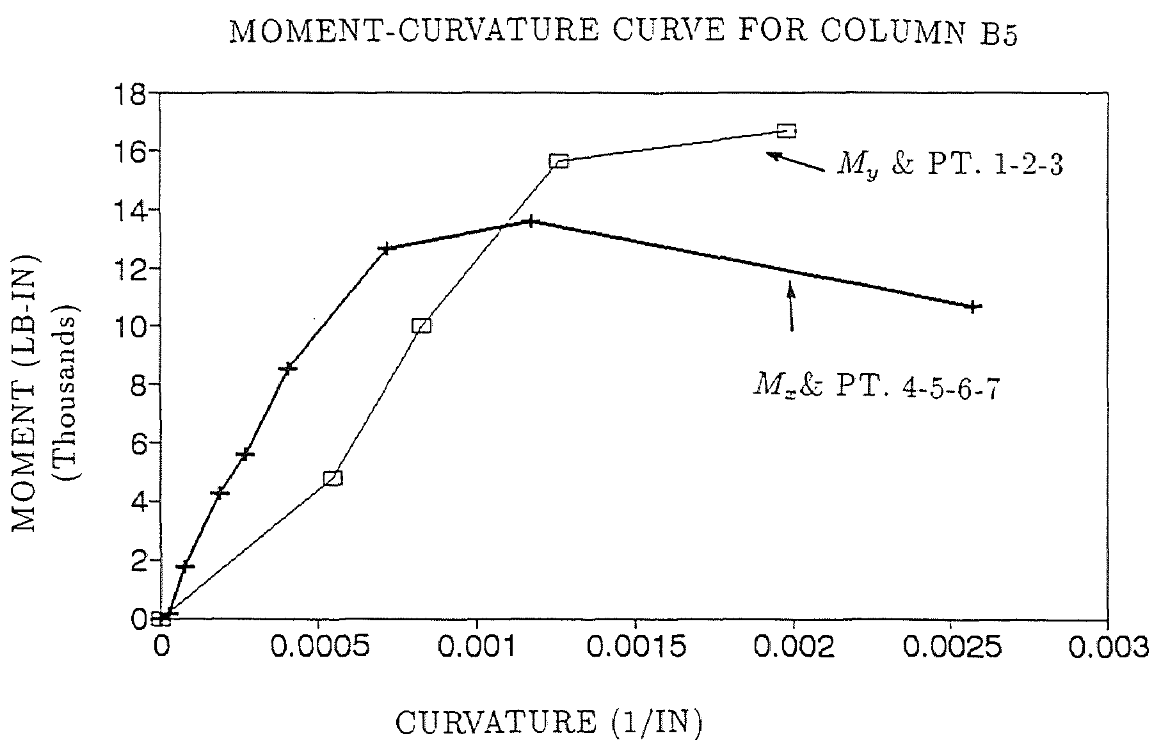

Figure A.8 Moment-curvature curve for column B5

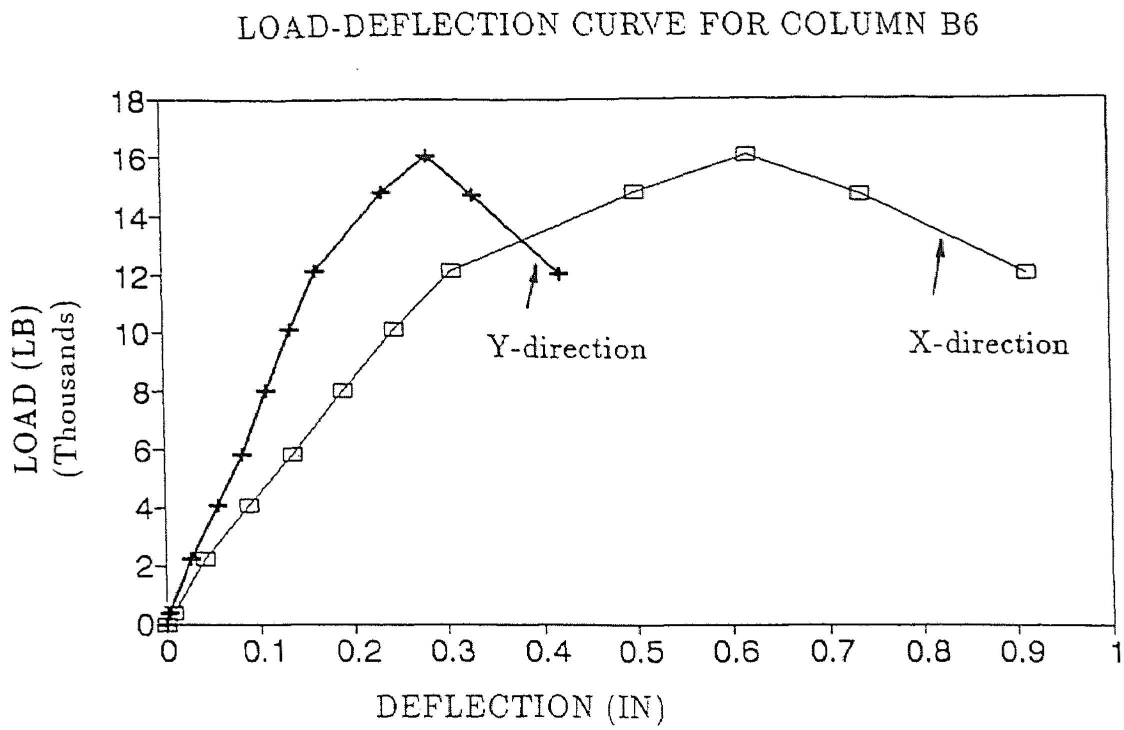

Figure A.9 Load-deflection curve for column B6

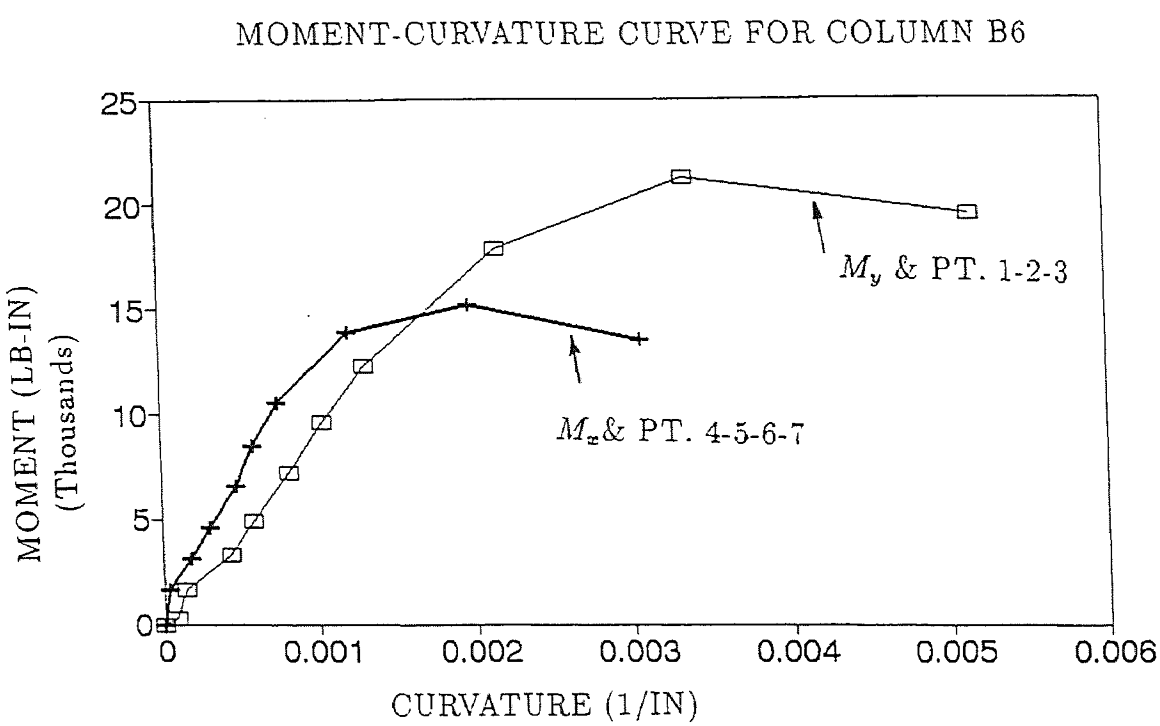

Figure A.10 Moment-curvature curve for column B6

LOAD-DEFLECTION CURVE FOR COLUMN B7

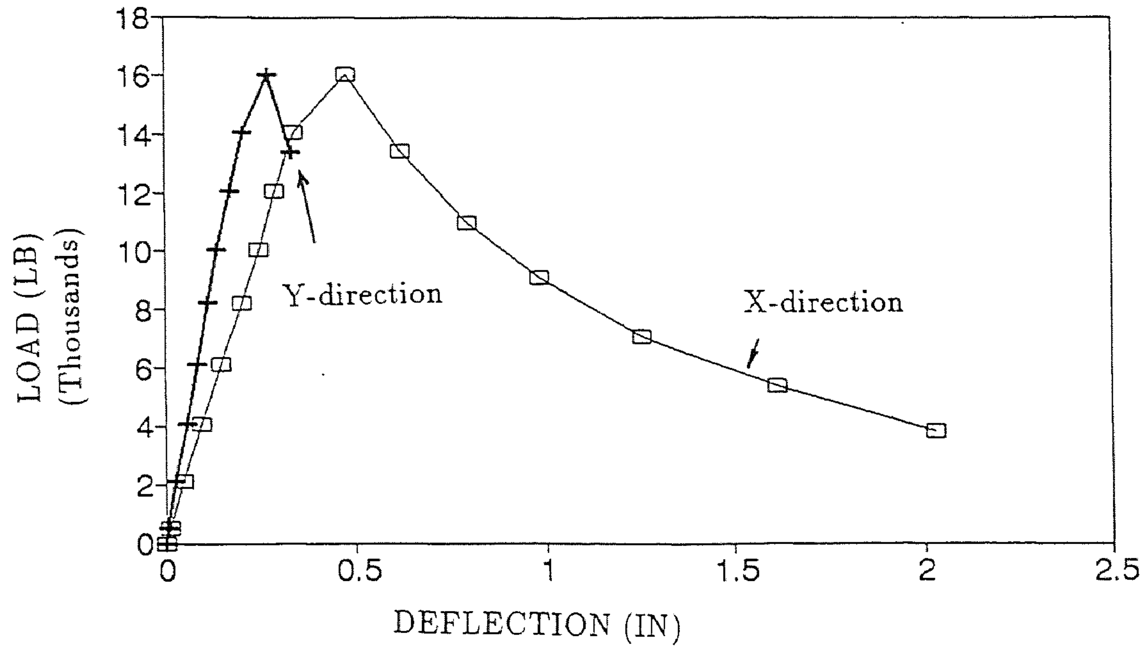

Figure A.11 Load-deflection curve for column B7

MOMENT-CURVATURE CURVE FOR COLUMN B7

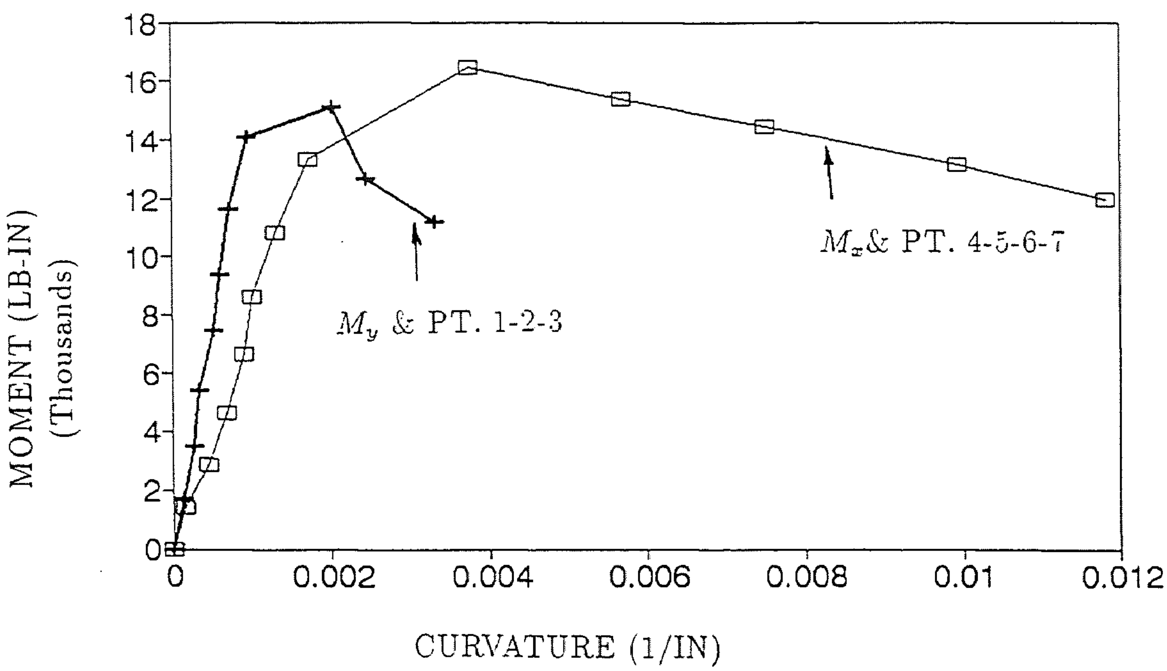

Figure A.12 Moment-curvature curve for column B7

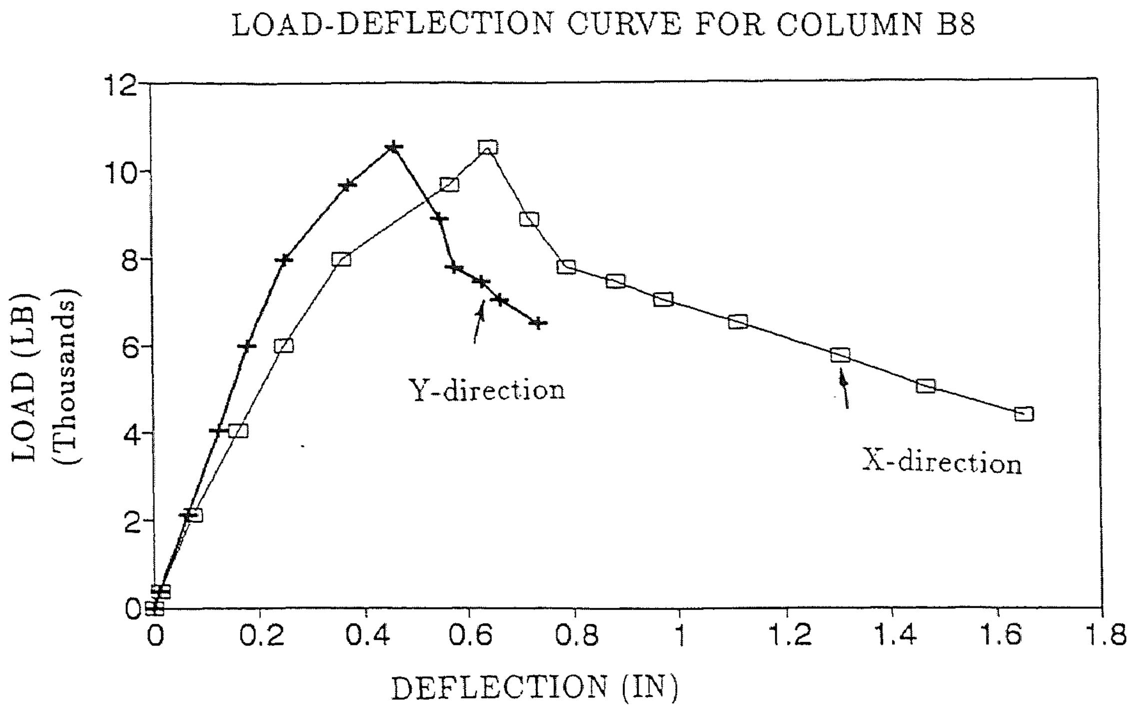

Figure A.13 Load-deflection curve for column B8

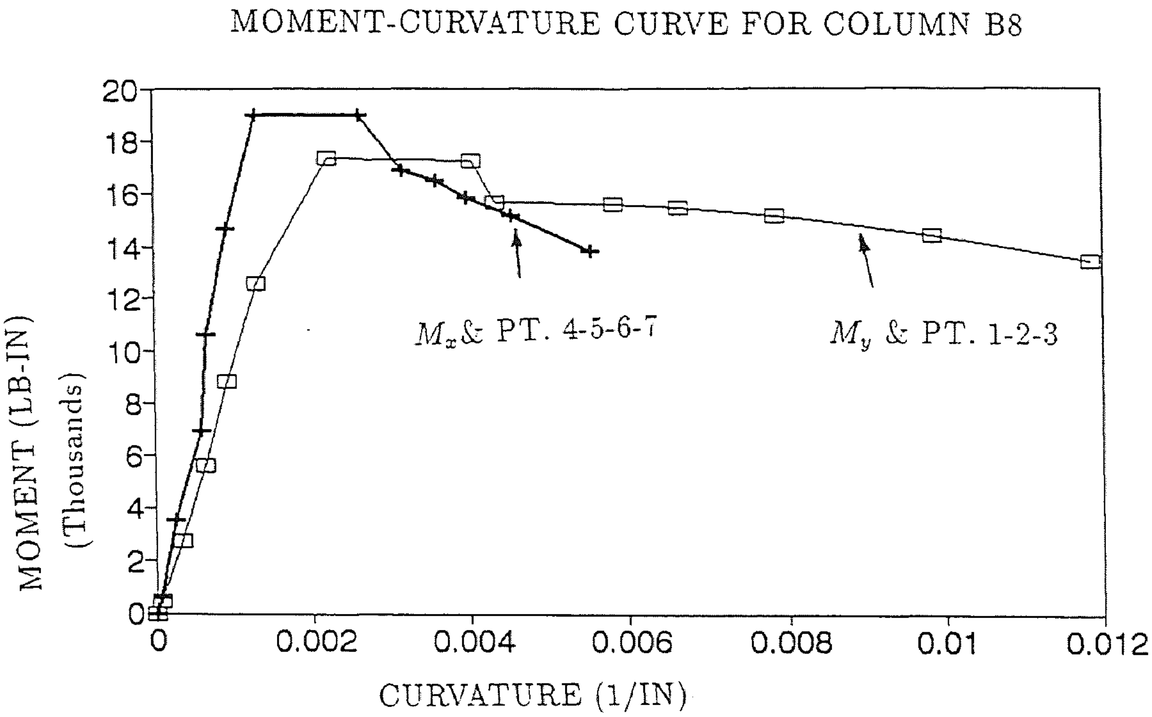

Figure A.14 Moment-curvature curve for column B8

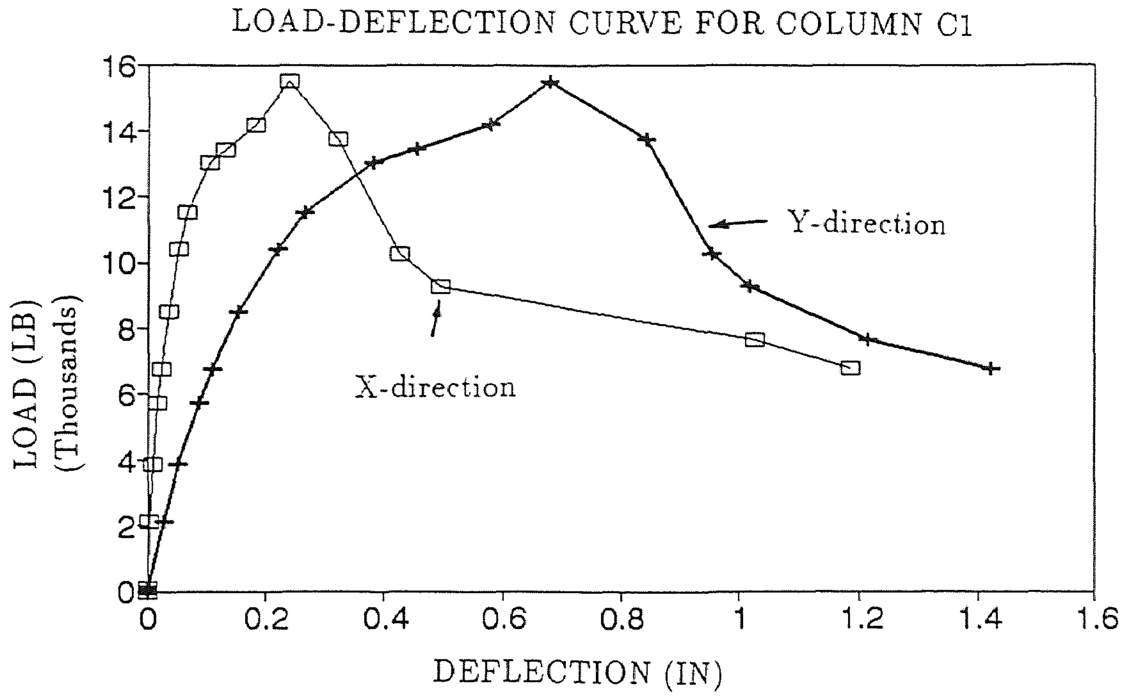

Figure A.15 Load-deflection curve for column C1

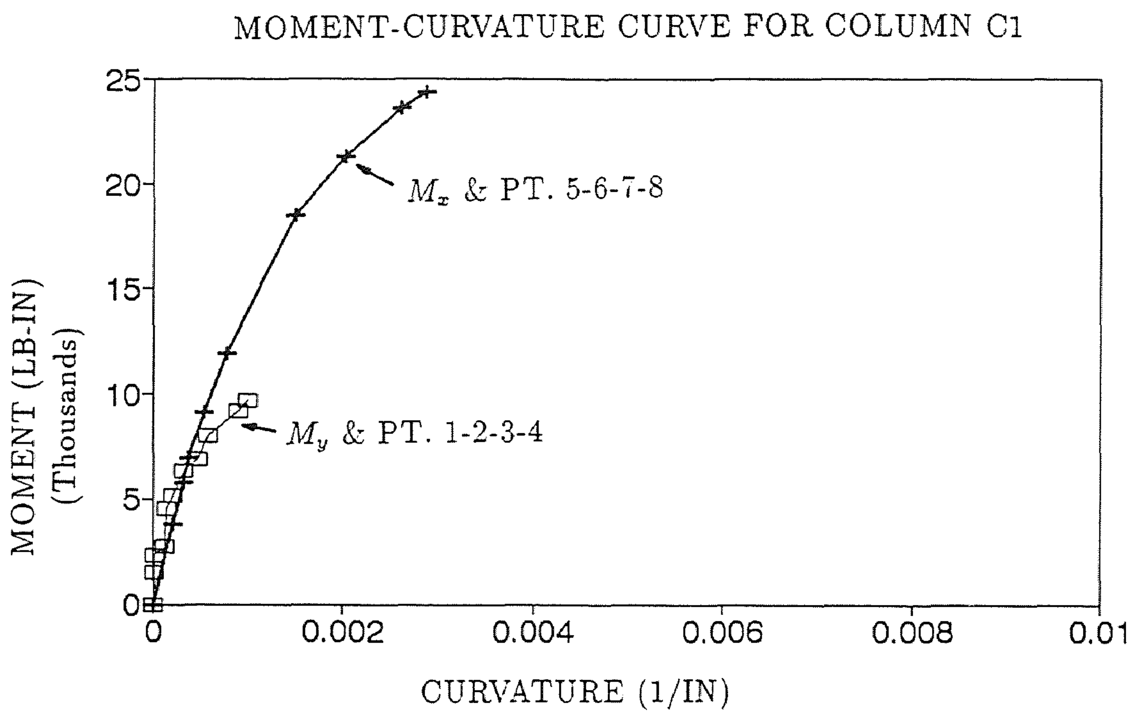

Figure A.16 Moment-curvature curve for column C1

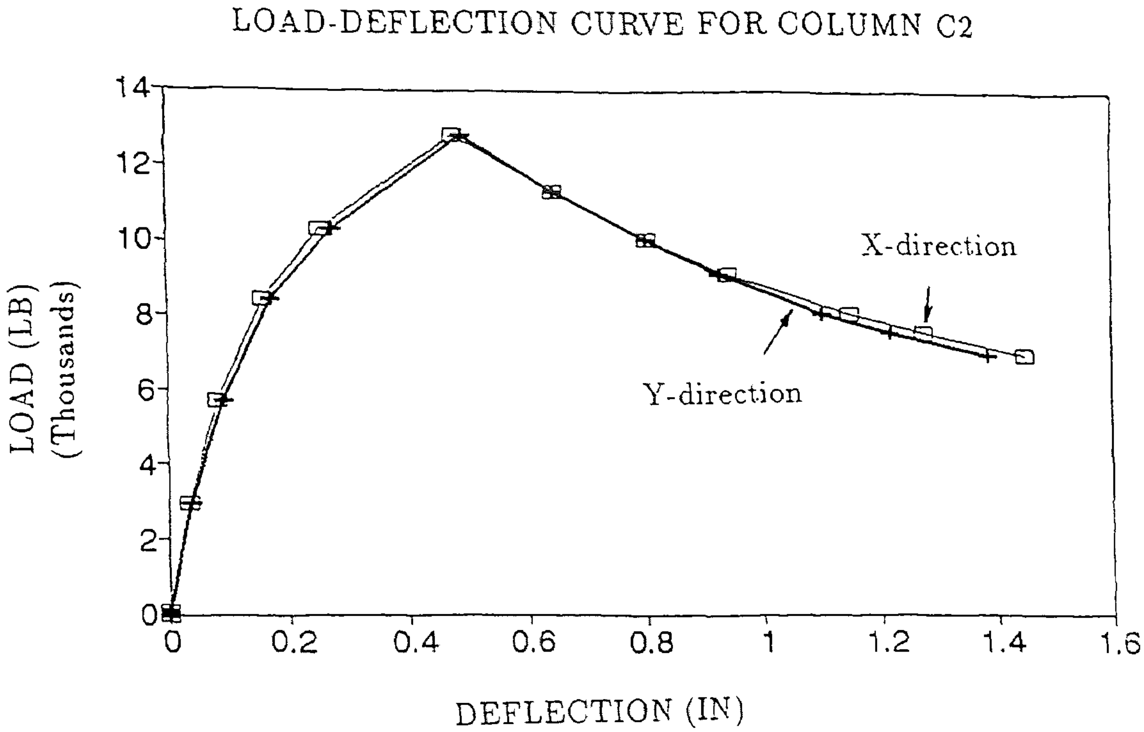

Figure A.17 Load-deflection curve for column C2

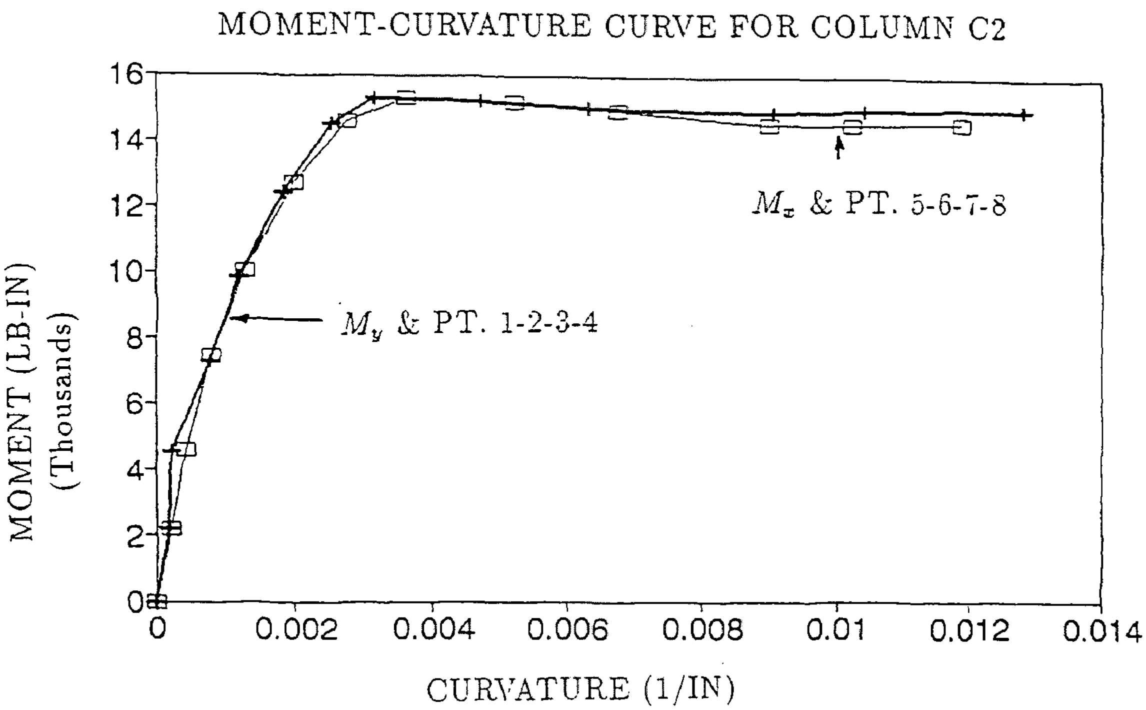

Figure A.18 Moment-curvature curve for column C2

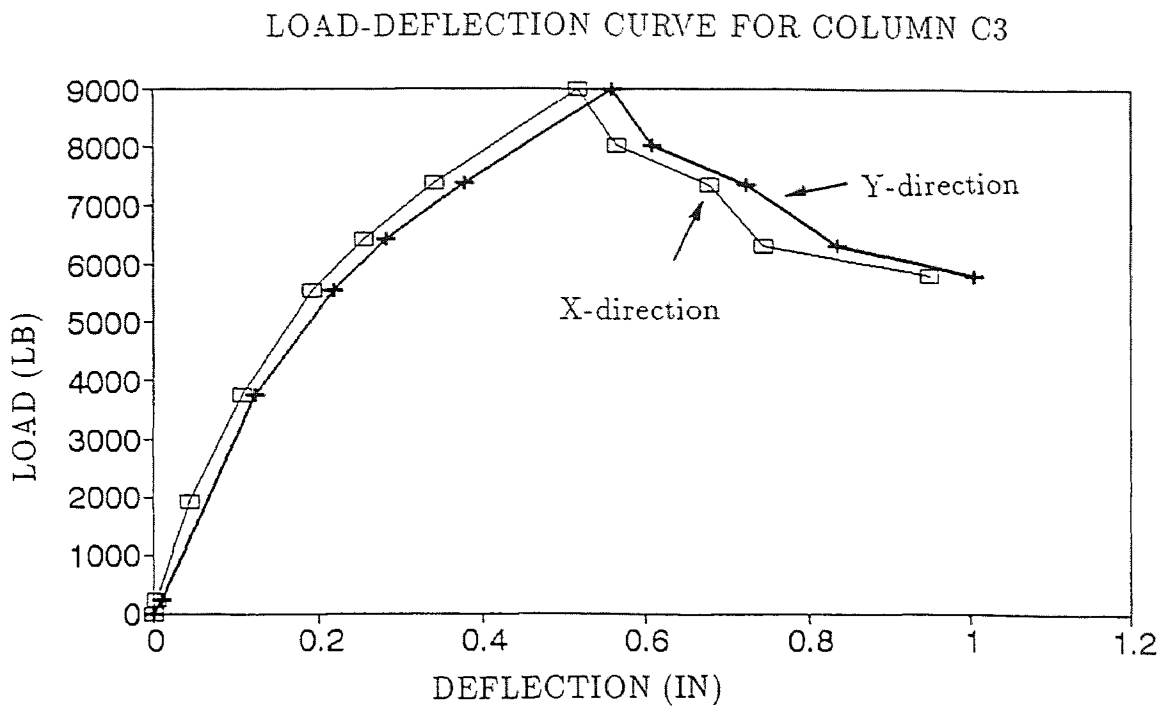

Figure A.19 Load-deflection curve for column C3

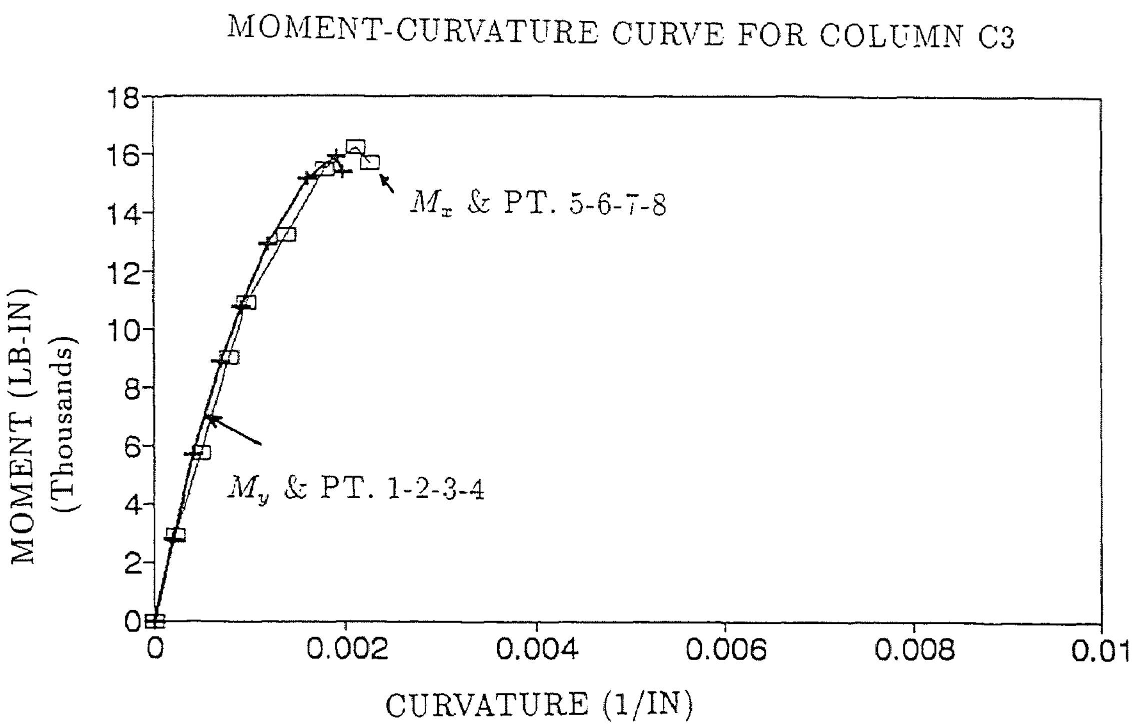

Figure A.20 Moment-curvature curve for column C3

LOAD-DEFLECTION CURVE FOR COLUMN C4

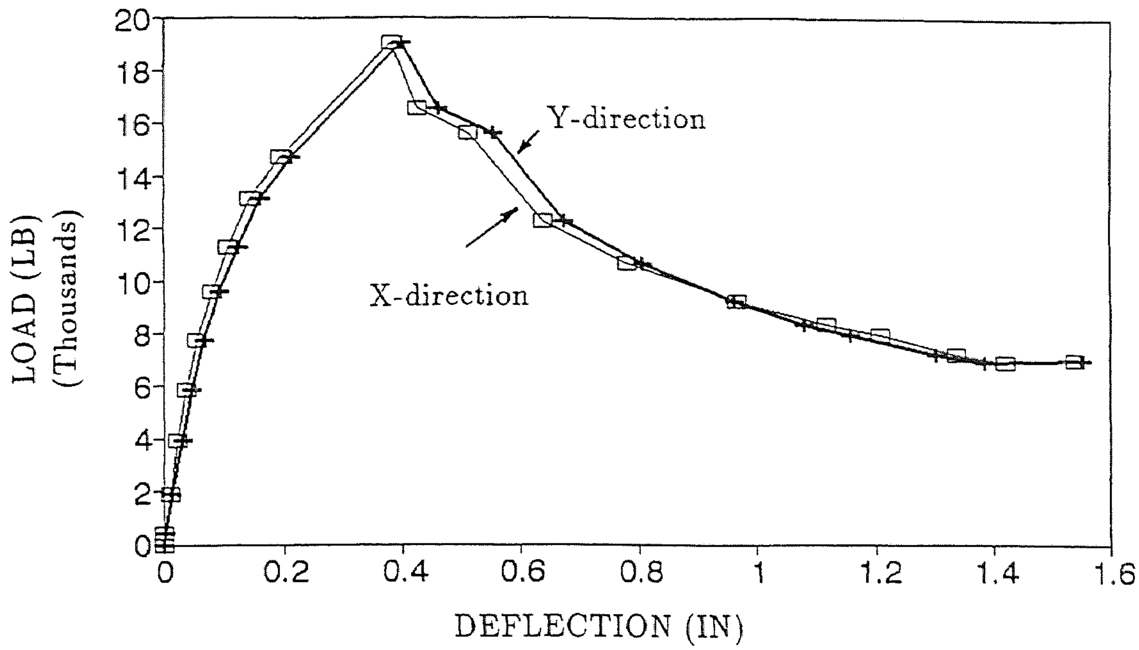

Figure A.21 Load-deflection curve for column C4

MOMENT-CURVATURE CURVE FOR COLUMN C4

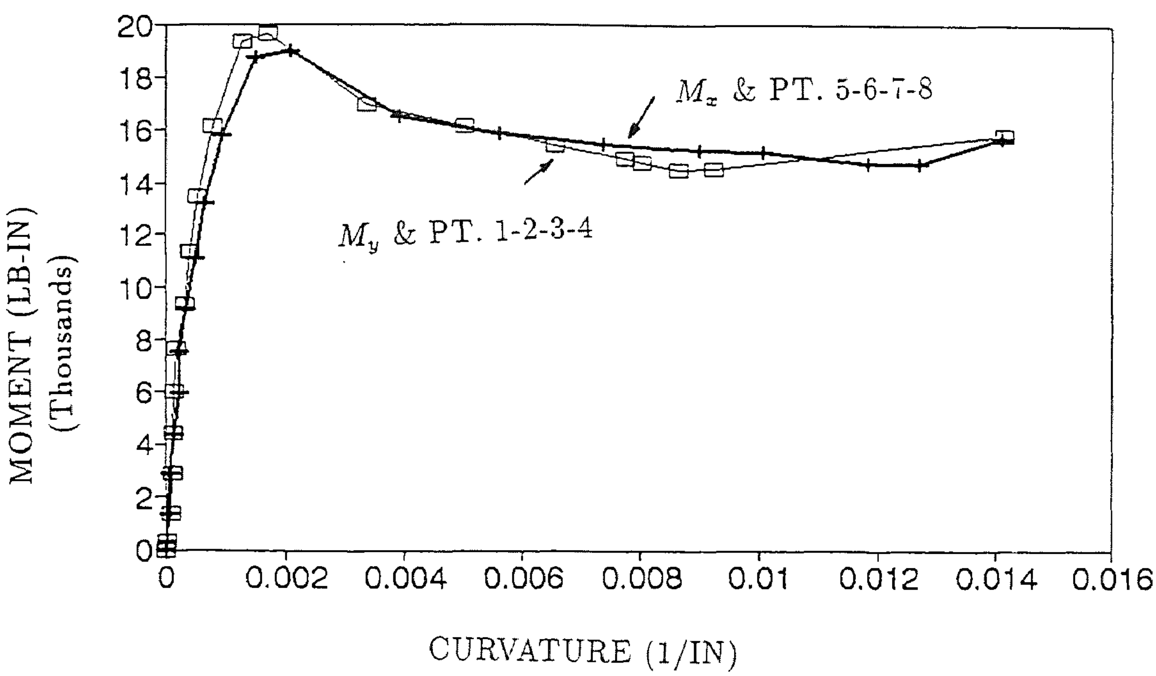

Figure A.22 Moment-curvature curve for column C4

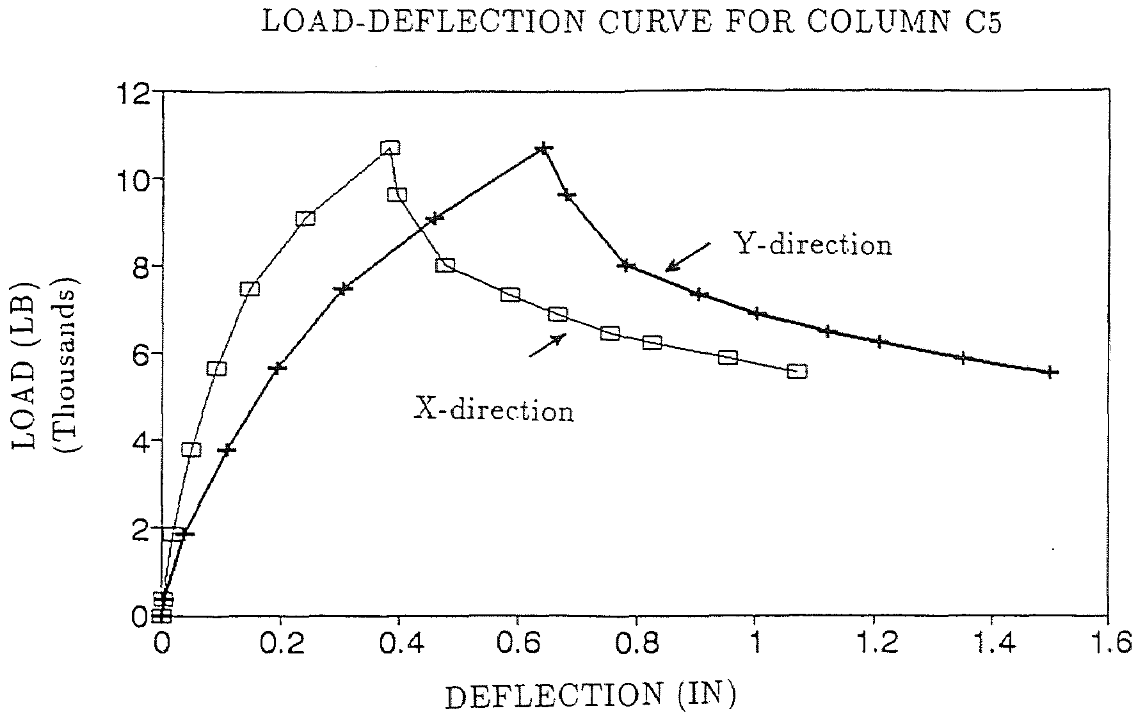

Figure A.23 Load-deflection curve for column C5

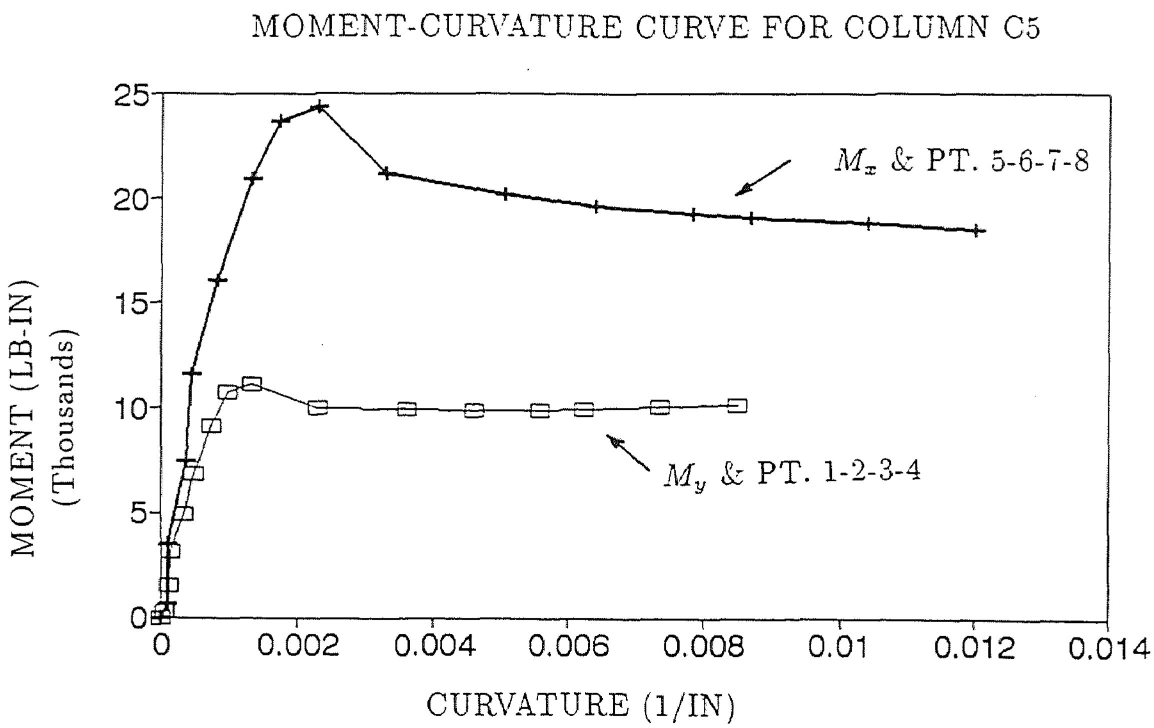

Figure A.24 Moment-curvature curve for column C5

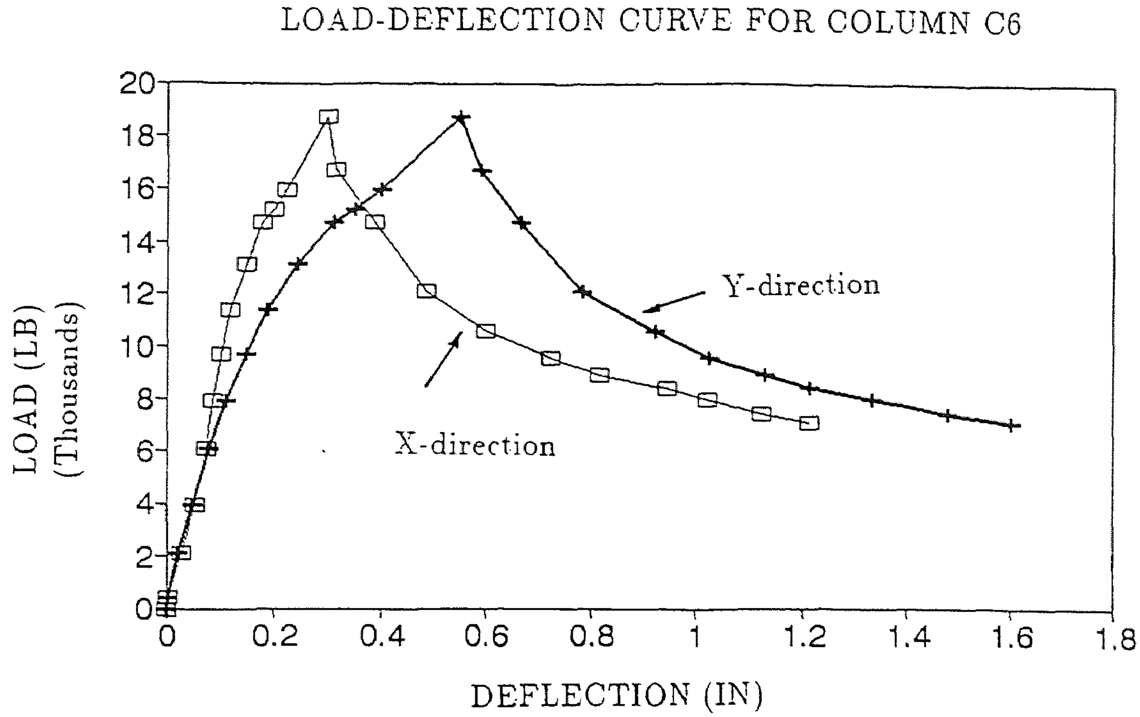

Figure A.25 Load-deflection curve for column C6

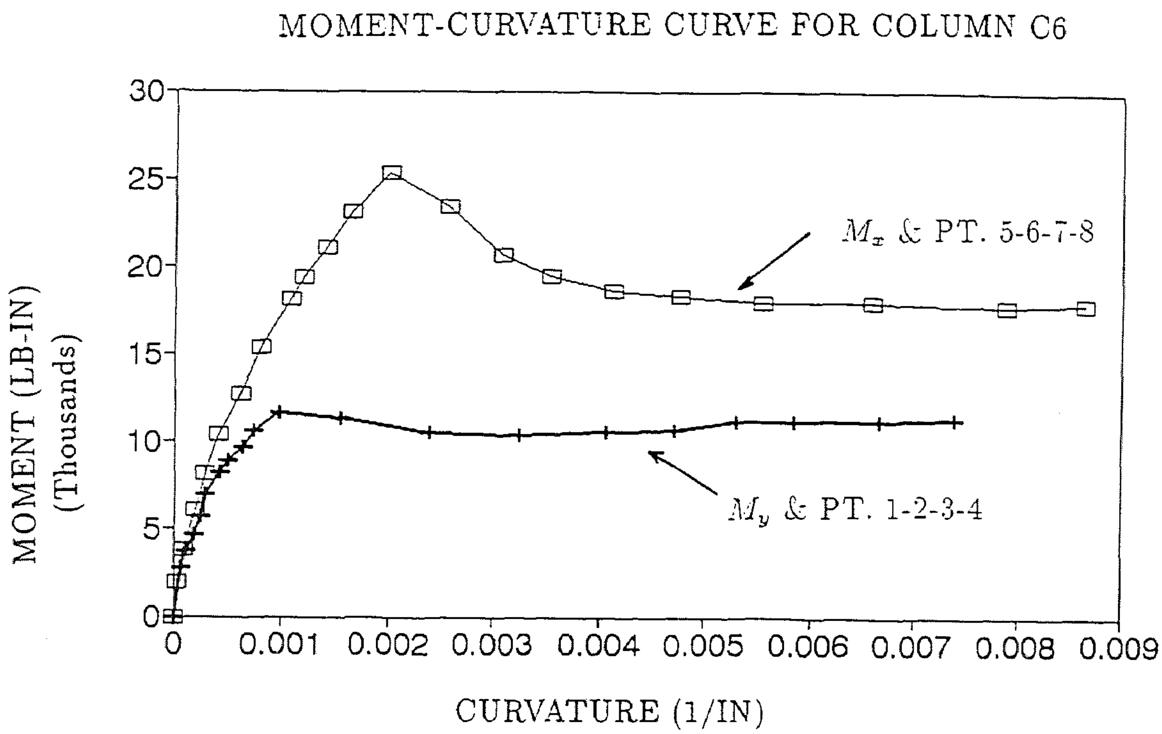

Figure A.26 Moment-curvature curve for column C6

Appendix B. Strain-position curve

Strain-position curves for L-shaped and square slender reinforced concrete columns are shown herein. Fig. B.1 through B.14 present B-series column tests and Fig. B.15 through B.26 present C-series column tests, respectively.

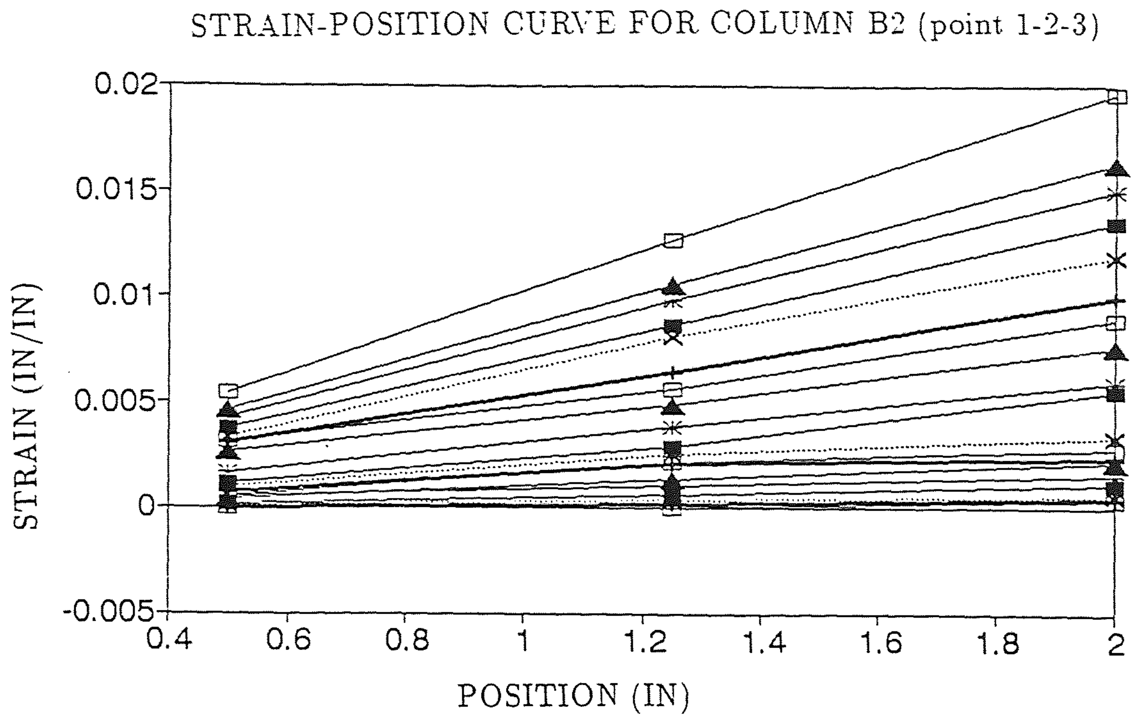

Figure B.1 Strain position curve for column B2 from point 1-2-3.

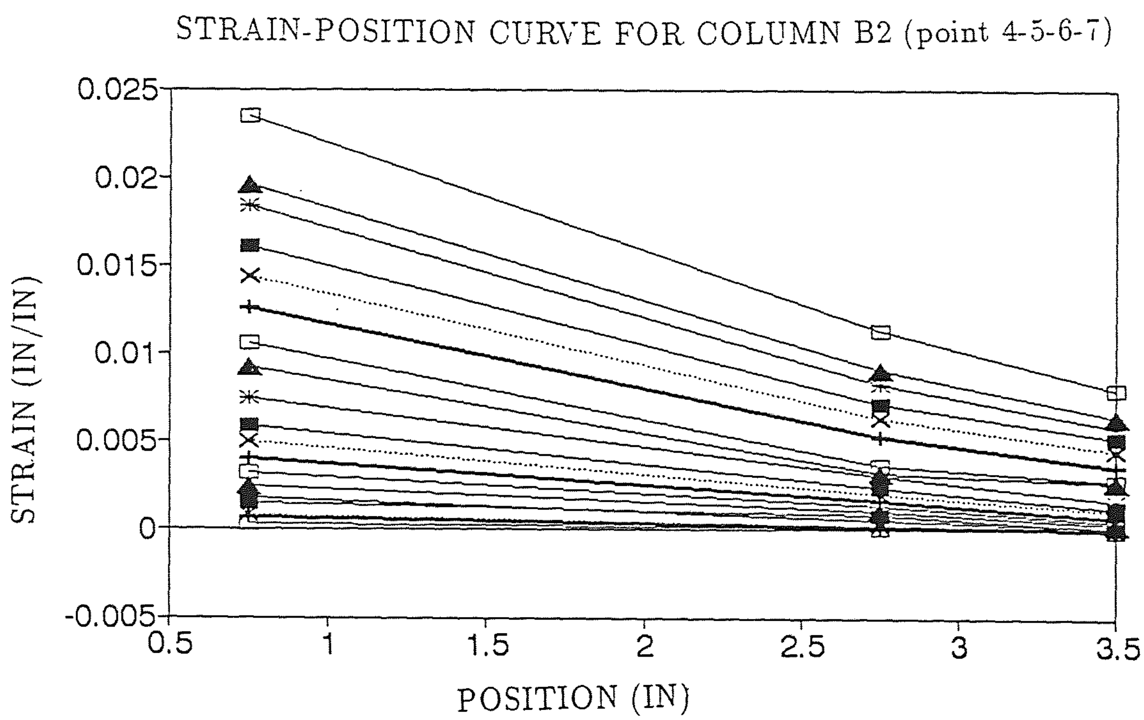

Figure B.2 Strain position curve for column B2 from point 4-5-6-7.

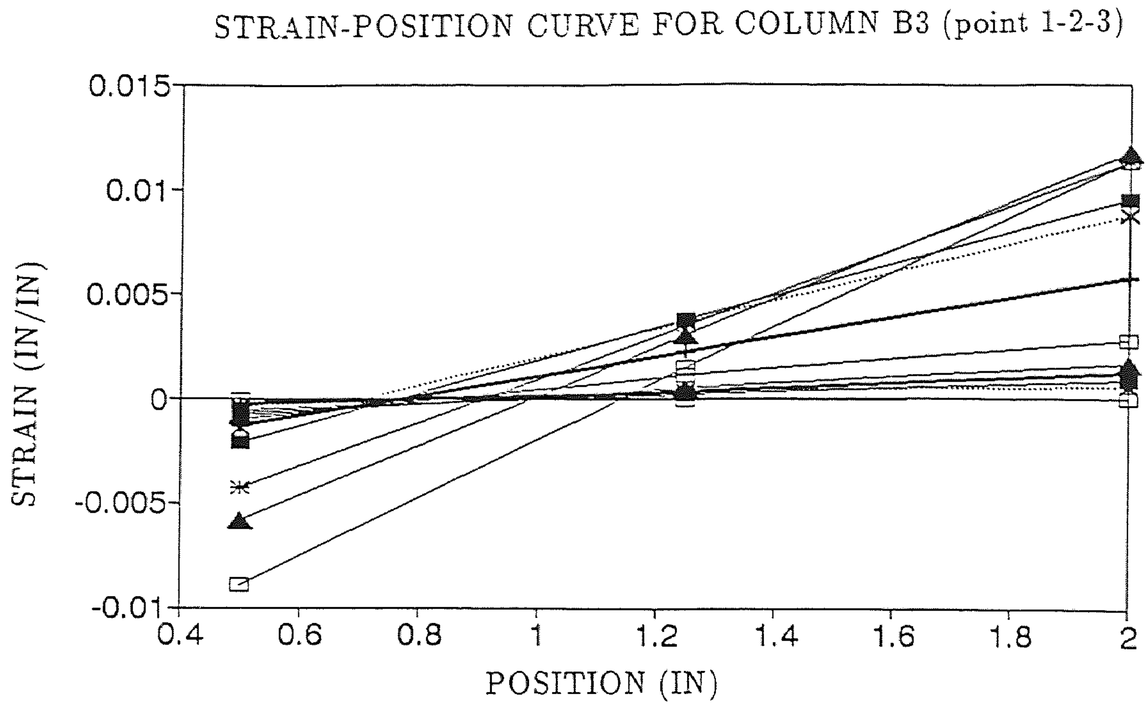

Figure B.3 Strain position curve for column B3 from point 1-2-3.

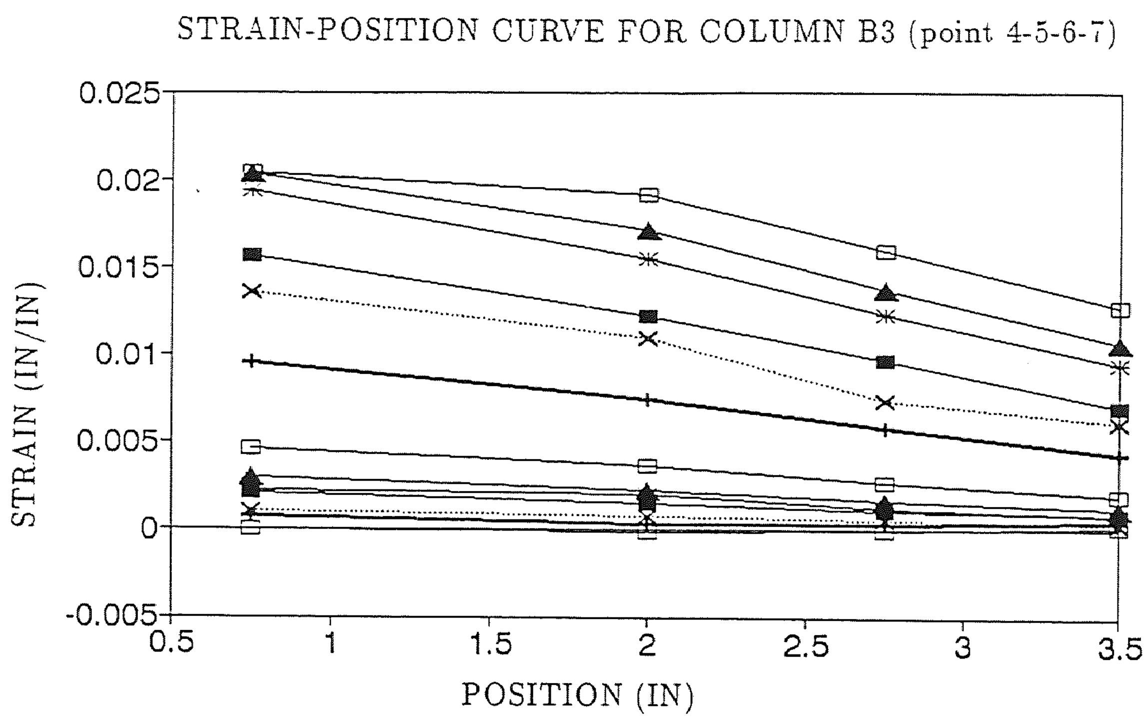

Figure B.4 Strain position curve for column B3 from point 4-5-6-7.

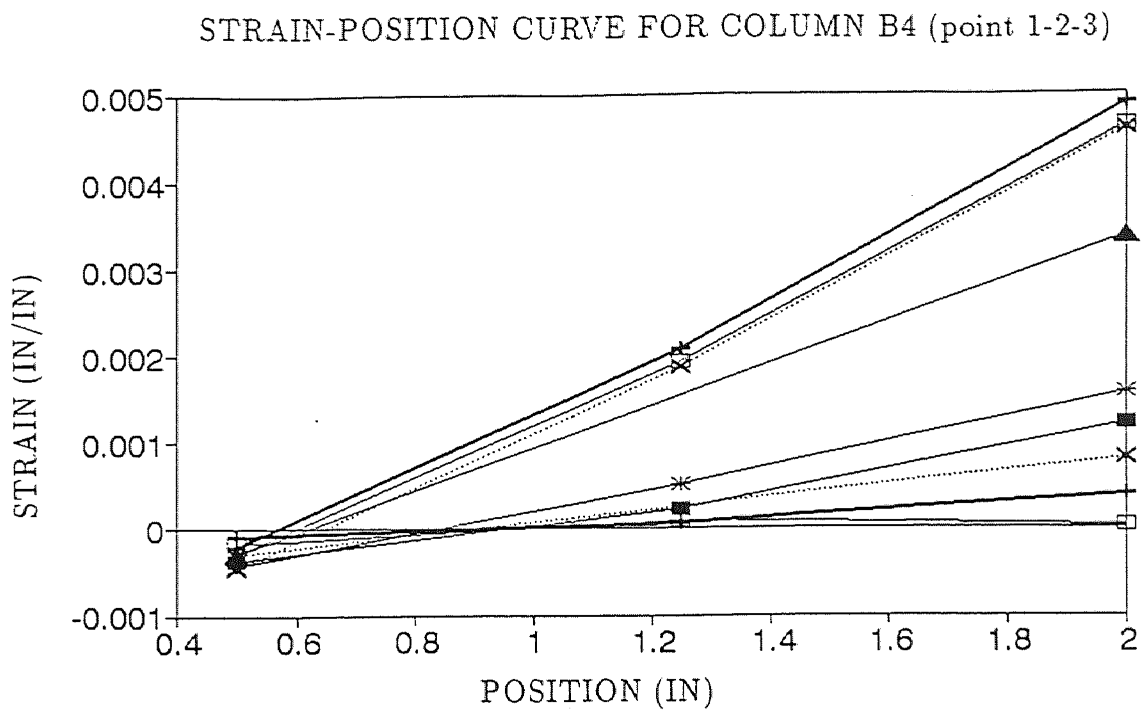

Figure B.5 Strain position curve tor column B4 from point 1-2-3.

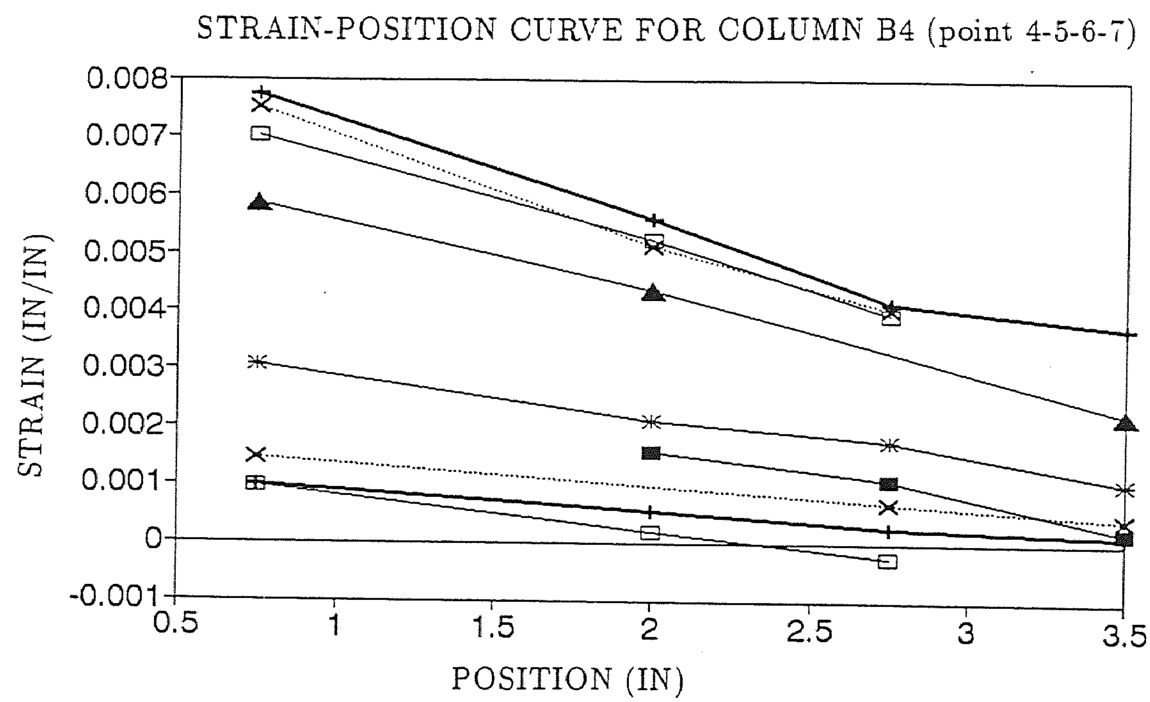

Figure B.6 Strain position curve for column B4 from point 4-5-6-7.

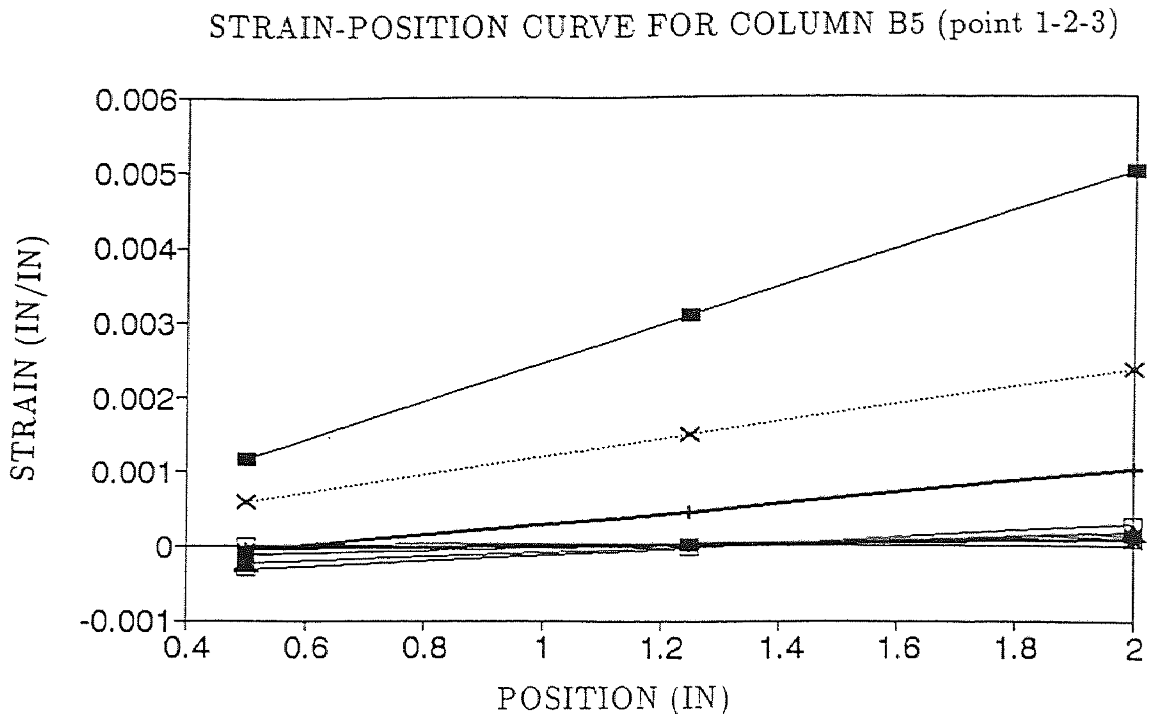

Figure B.7 Strain position curve for column B5 from point 1-2-3.

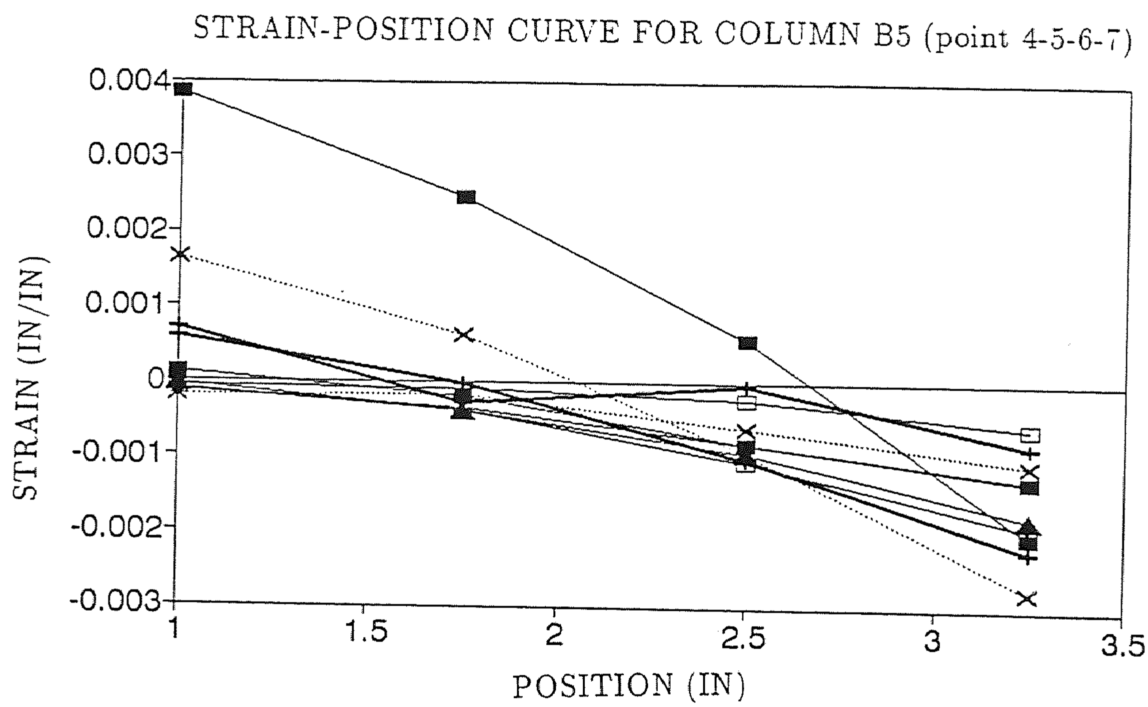

Figure B.8 Strain position curve for column B5 from point 4-5-6-7.

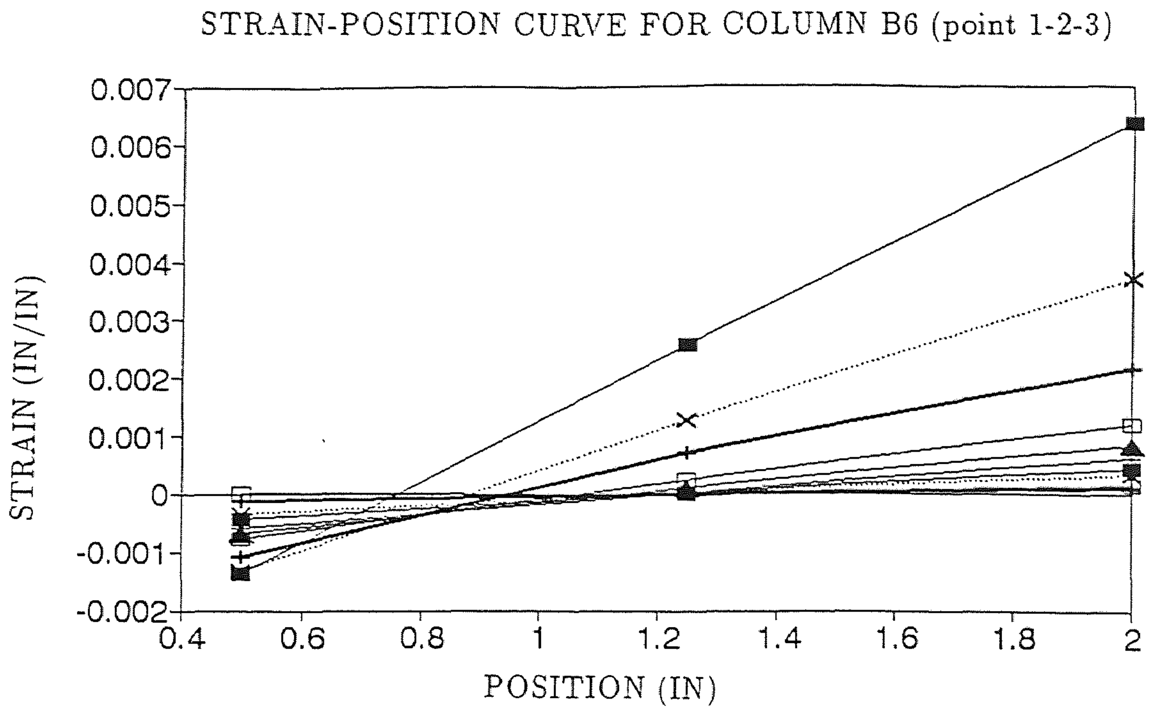

Figure B.9 Strain position curve for column B6 from point 1-2-3.

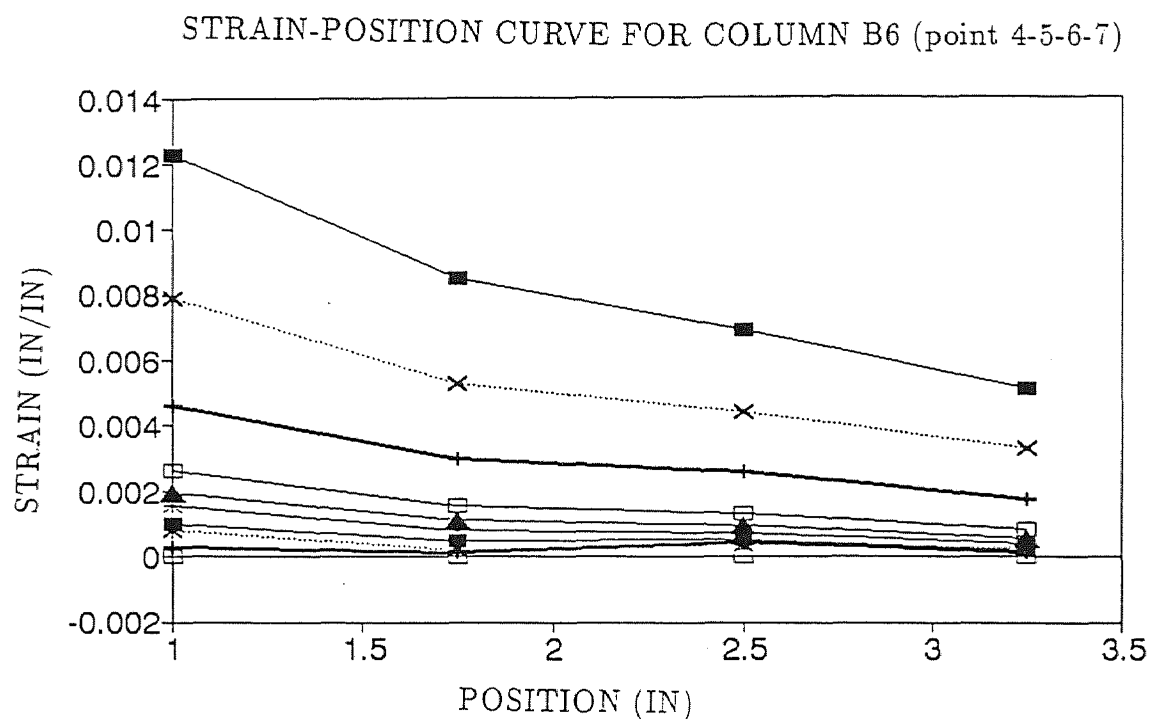

Figure B.10 Strain position curve for column B6 from point 4-5-6-7.

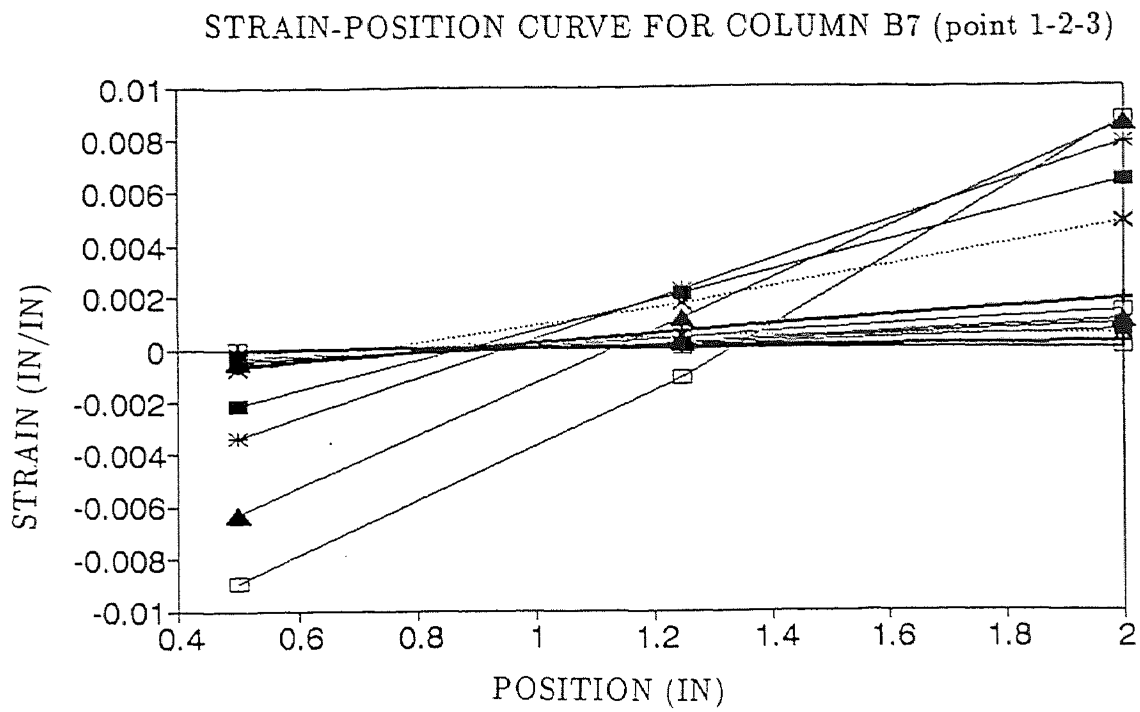

Figure B.11 Strain position curve for column B7 from point 1-2-3.

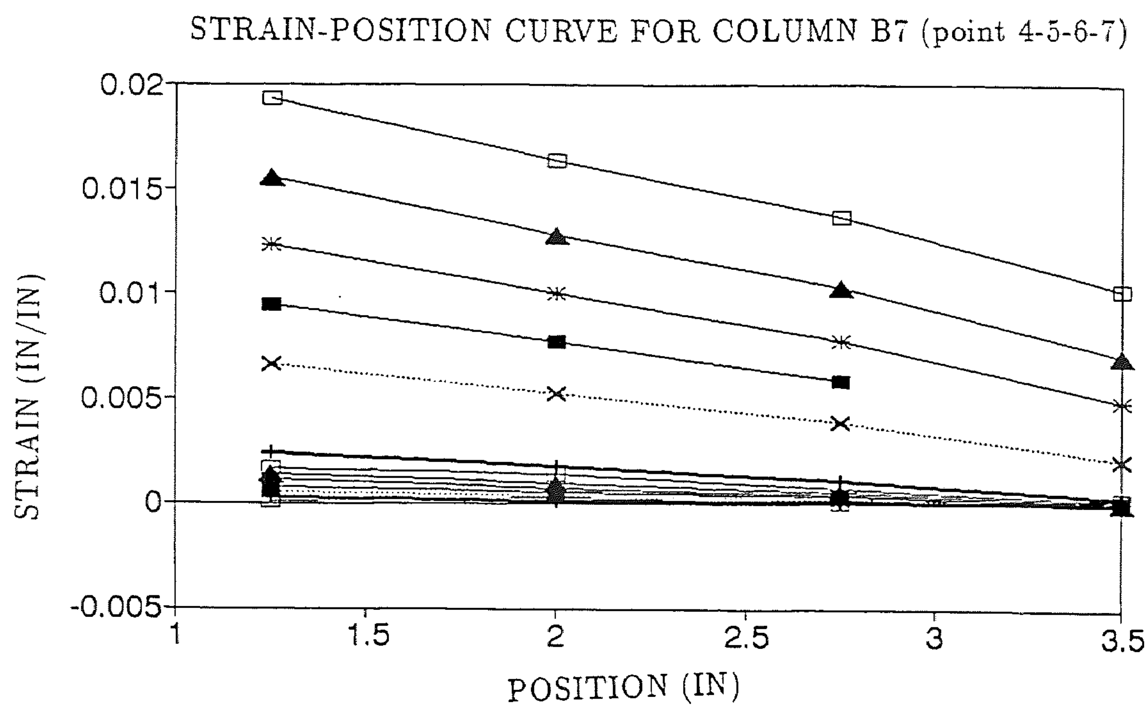

Figure B.12 Strain position curve for column B7 from point 4-5-6-7.

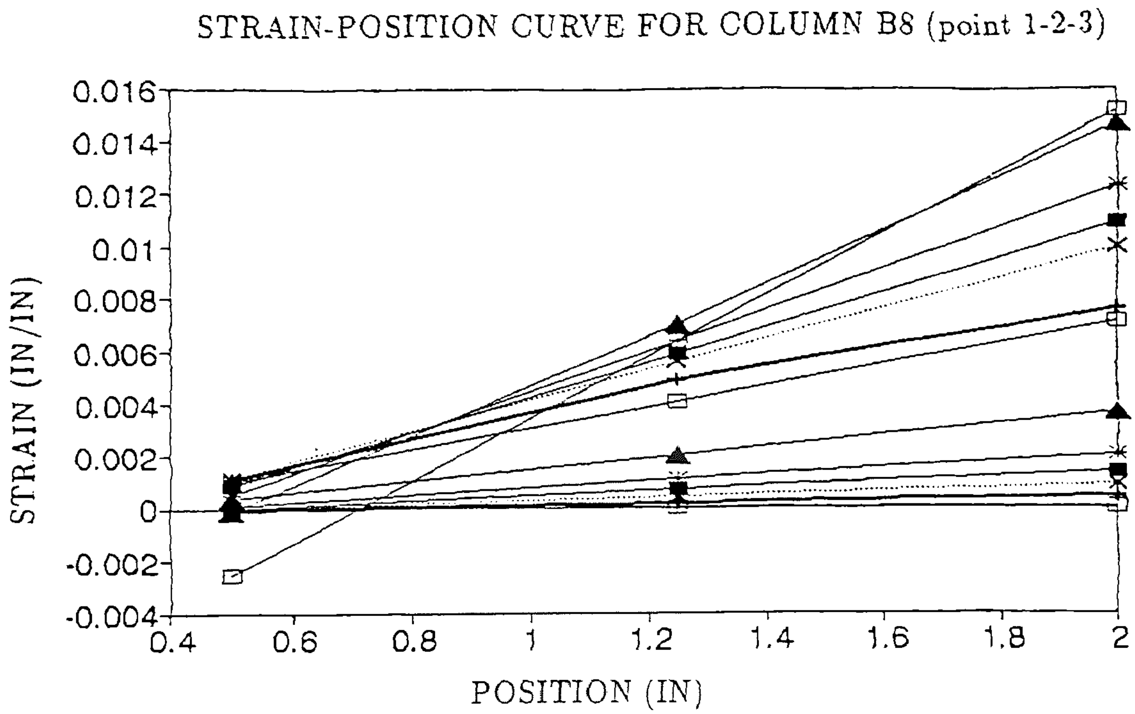

Figure B.13 Strain position curve for column B8 from point 1-2-3.

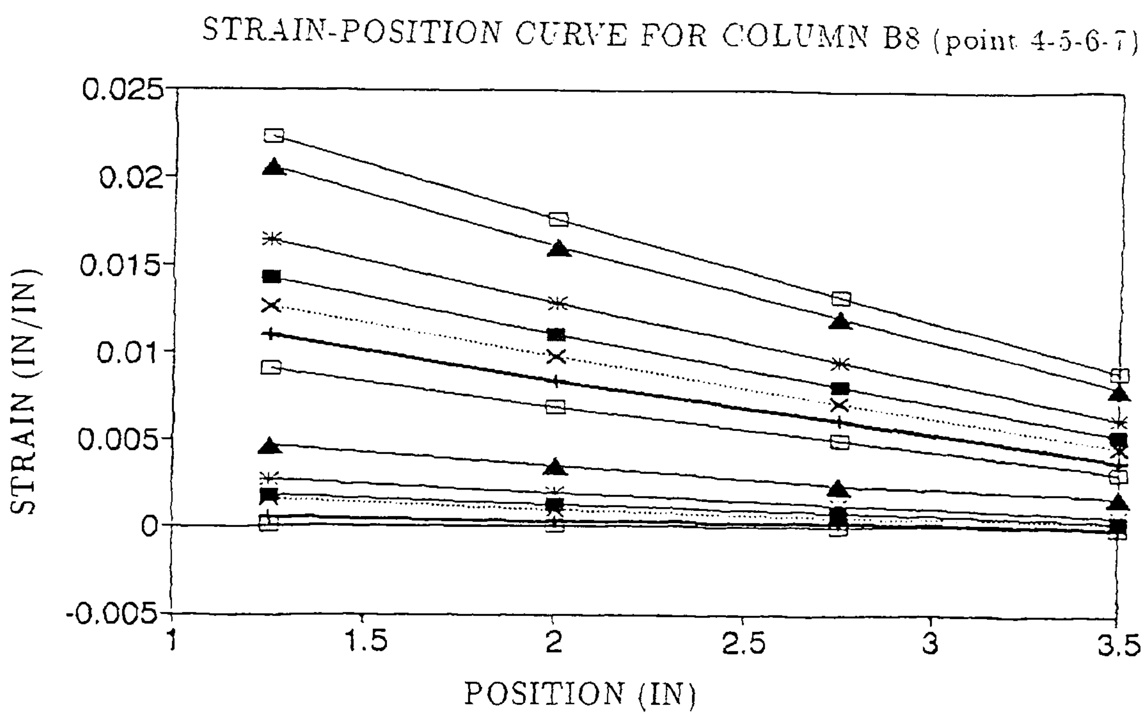

Figure B.14 Strain position curve for column B8 from point 4-5-6-7.

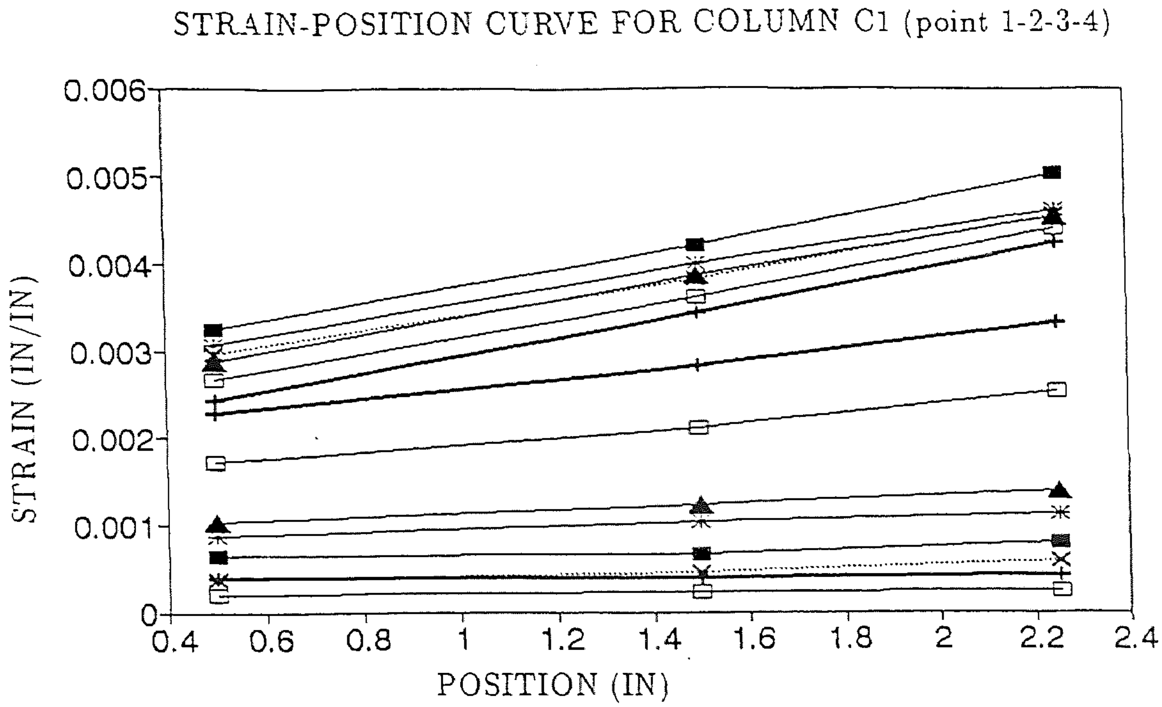

Figure B.15 Strain position curve for column C1 from point 1-2-3-4.

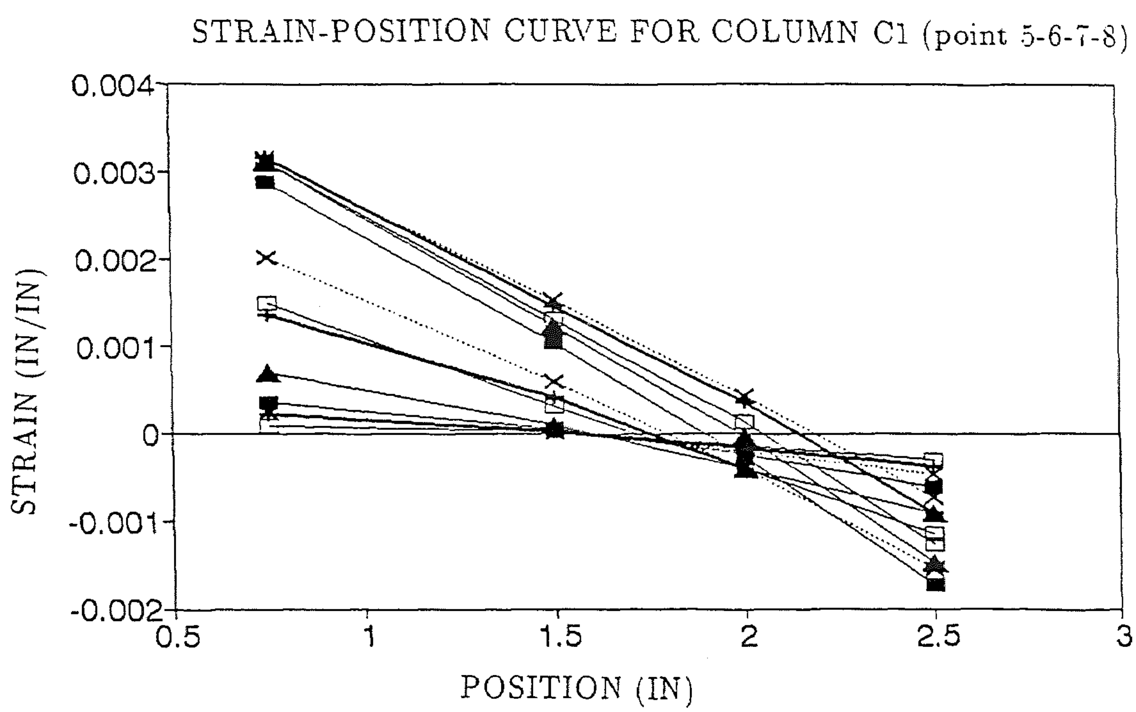

Figure B.16 Strain position curve for column C1 from point 5-6-7-8.

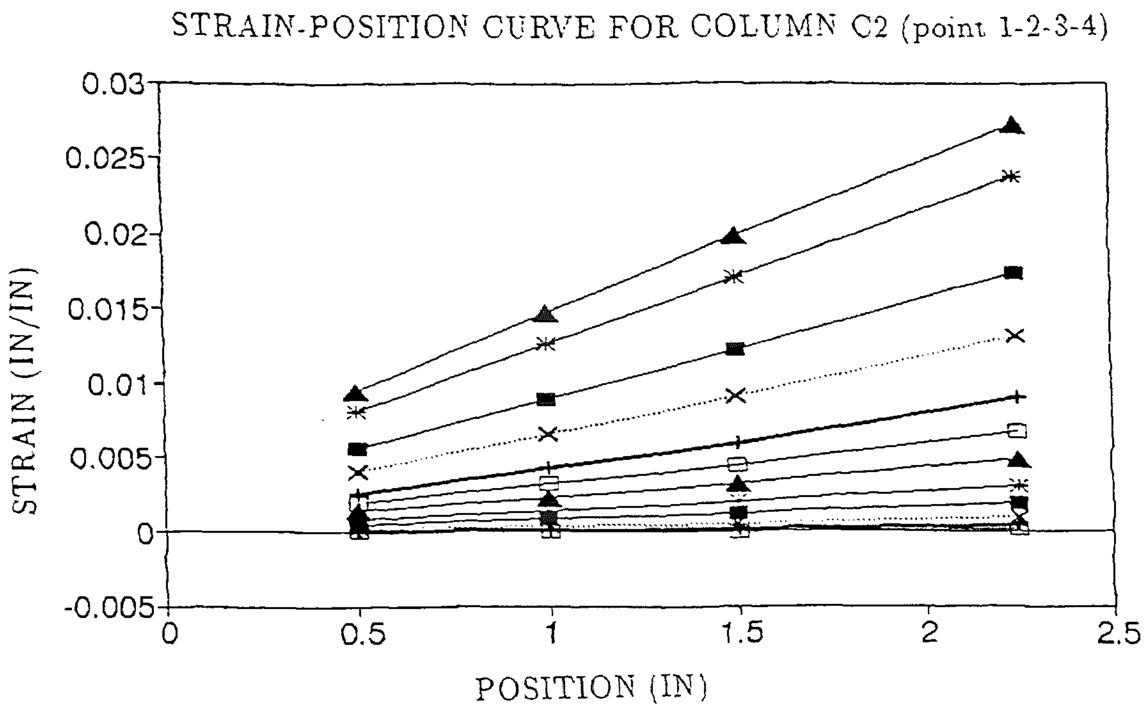

Figure B.17 Strain position curve for column C2 from point 1-2-3-4.

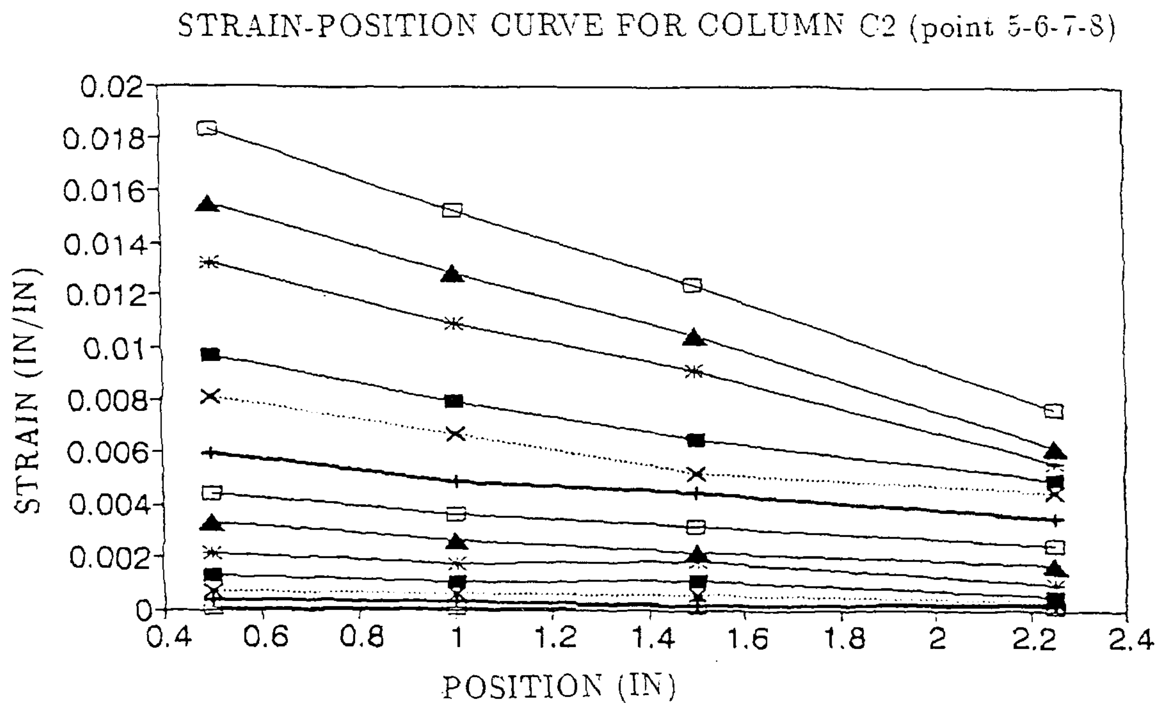

Figure B.18 Strain position curve for column C2 from point 5-6-7-8.

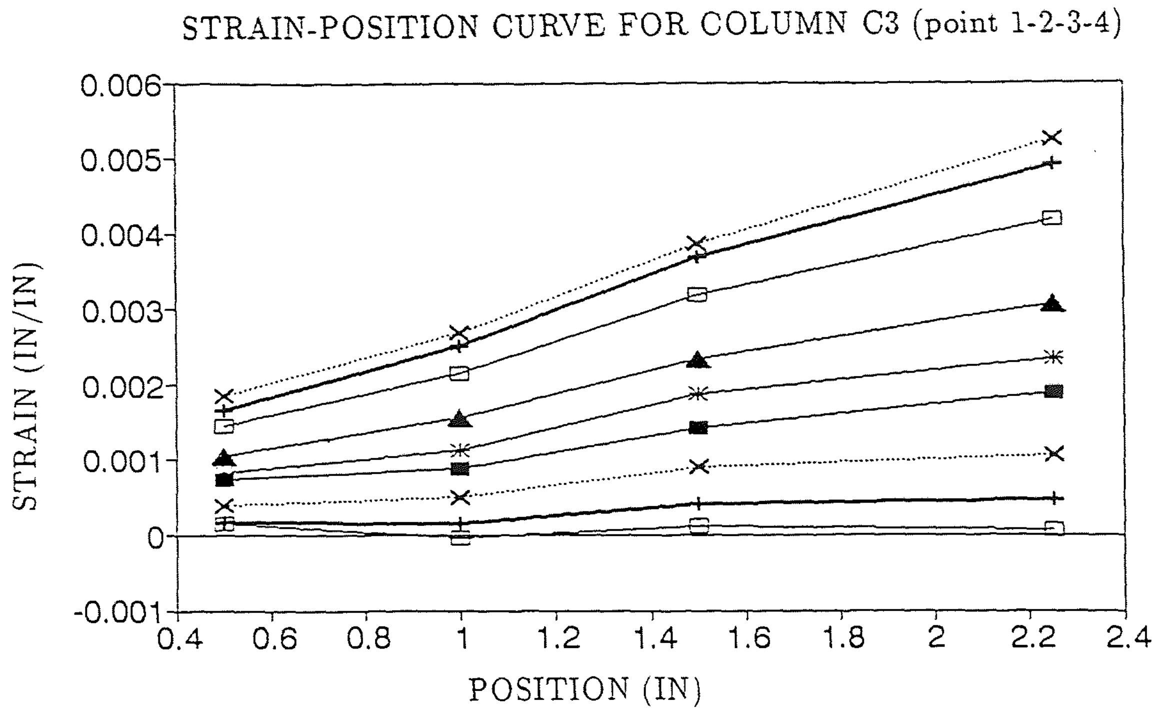

Figure B.19 Strain position curve for column C3 from point 1-2-3-4.

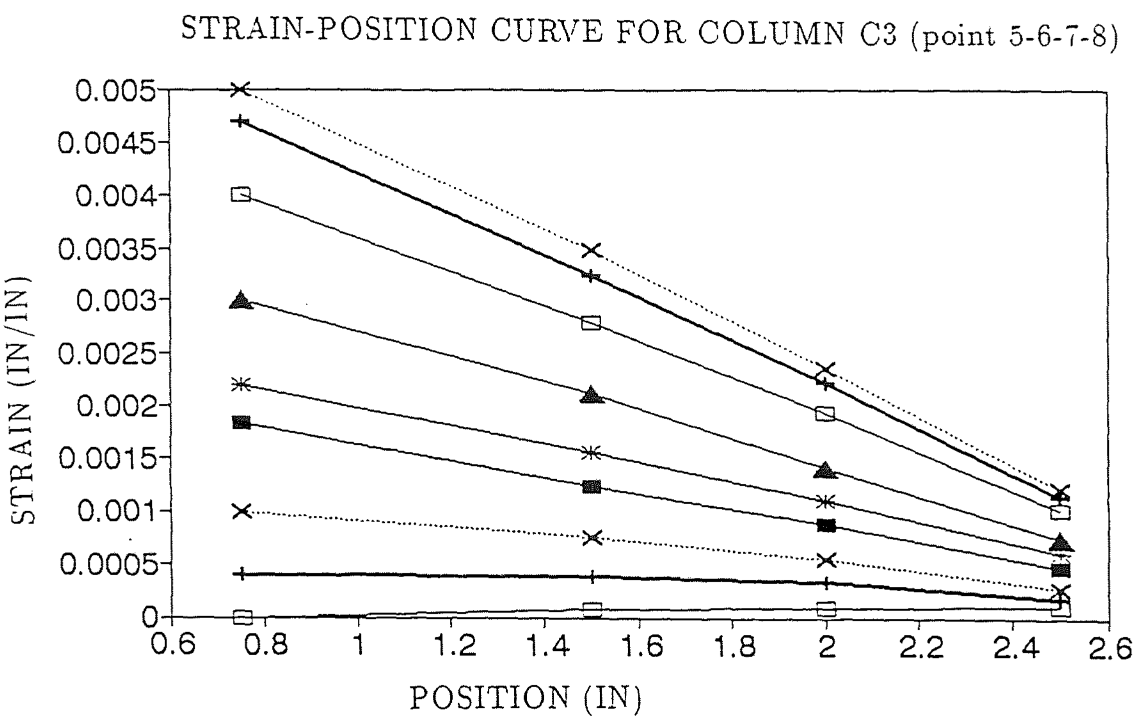

Figure B.20 Strain position curve for column C3 from point 5-6-7-8.

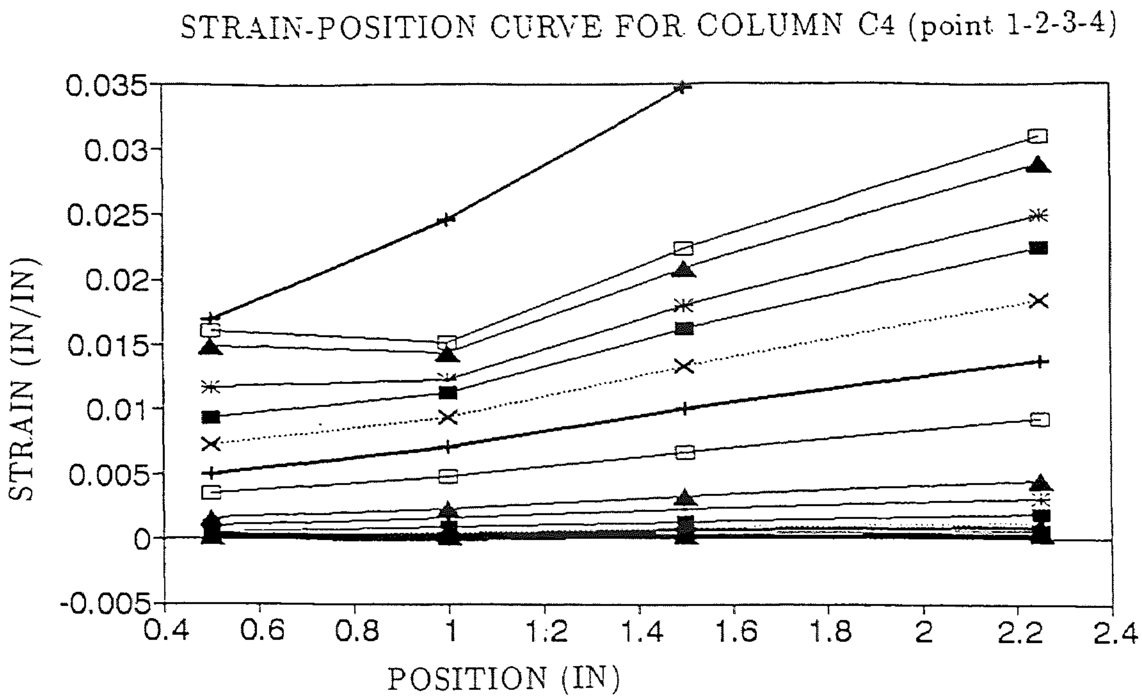

Figure B.21 Strain position curve for column C4 from point 1-2-3-4.

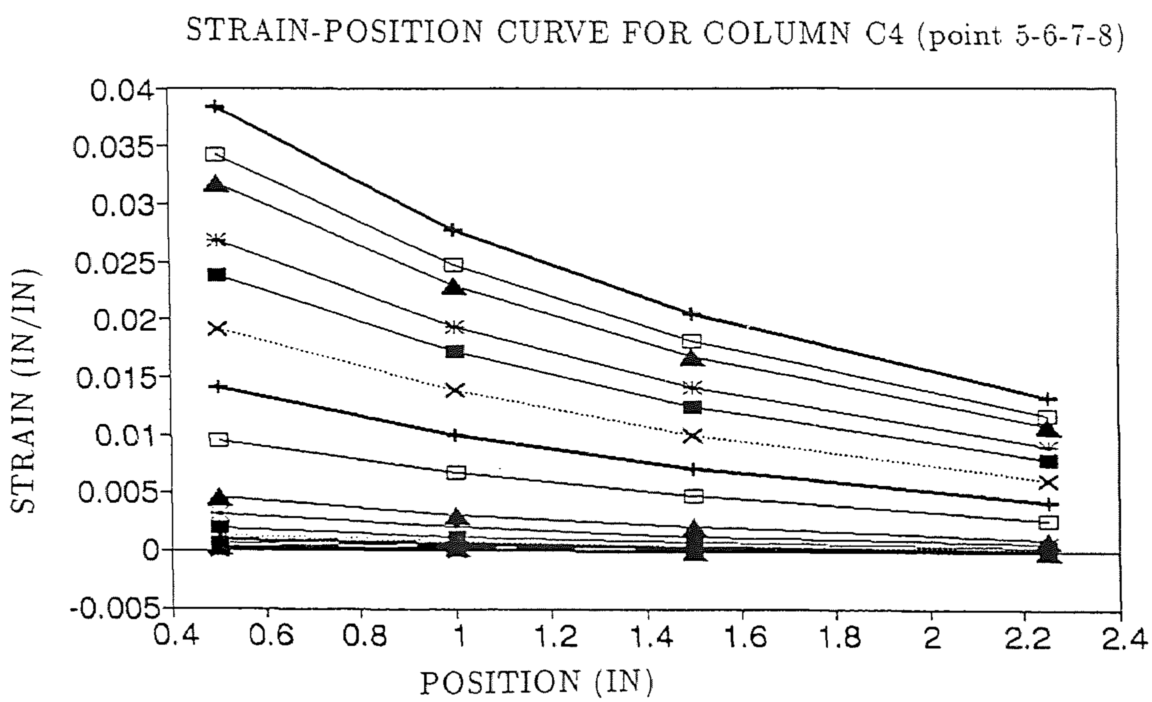

Figure B.22 Strain position curve for column C4 from point 5-6-7-8.

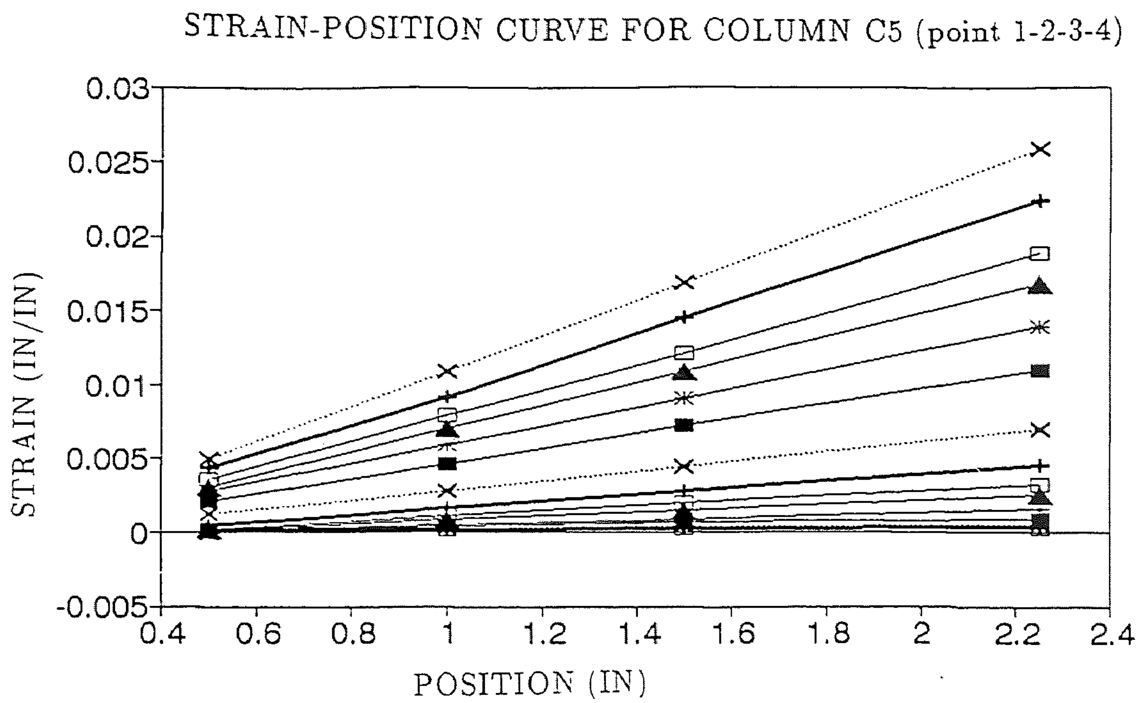

Figure B.23 Strain position curve for column C5 from point 1-2-3-4.

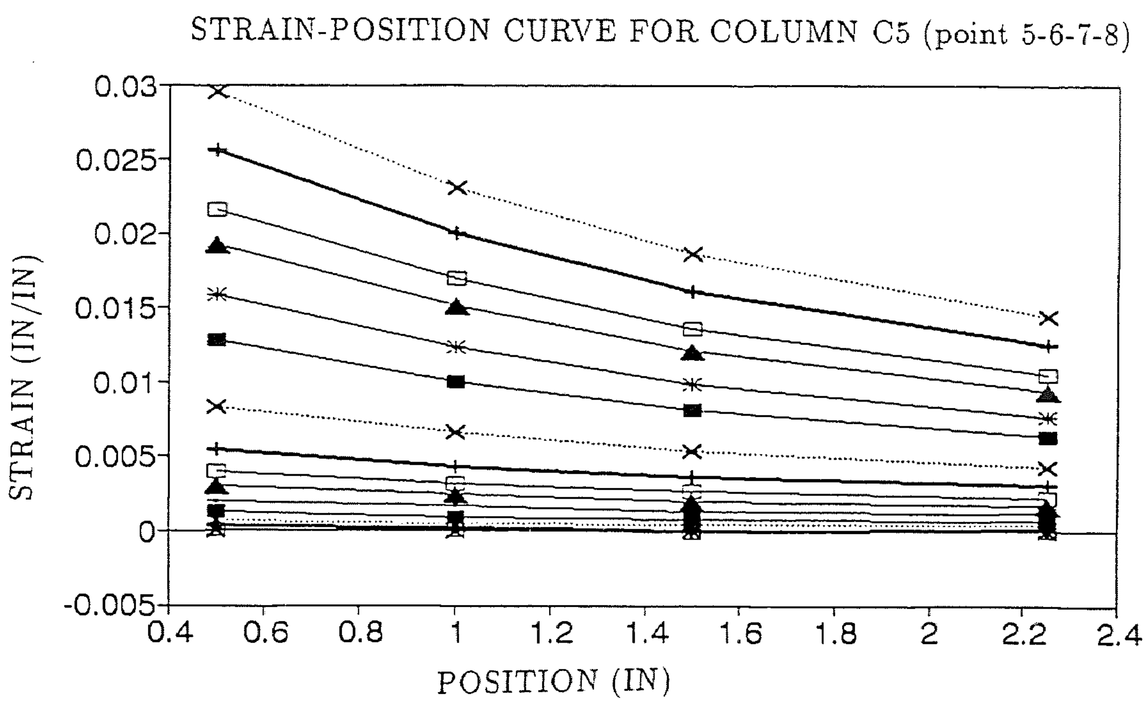

Figure B.24 Strain position curve for column C5 from point 5-6-7-8.

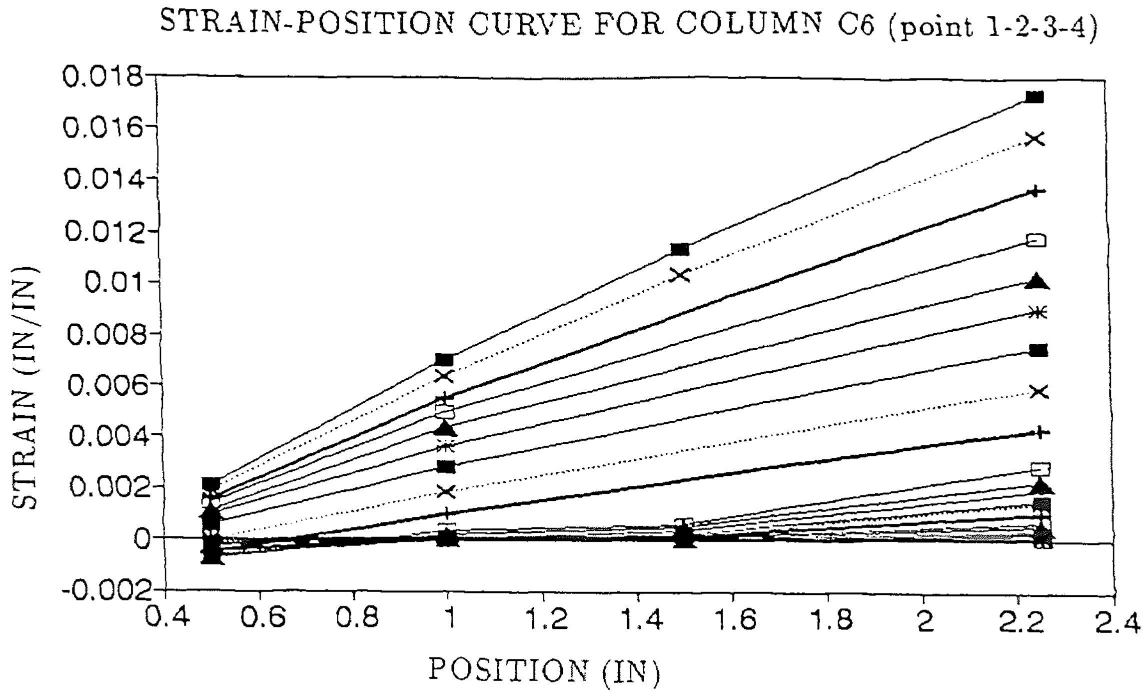

Figure B.25 Strain position curve for column C6 from point 1-2-3-4.

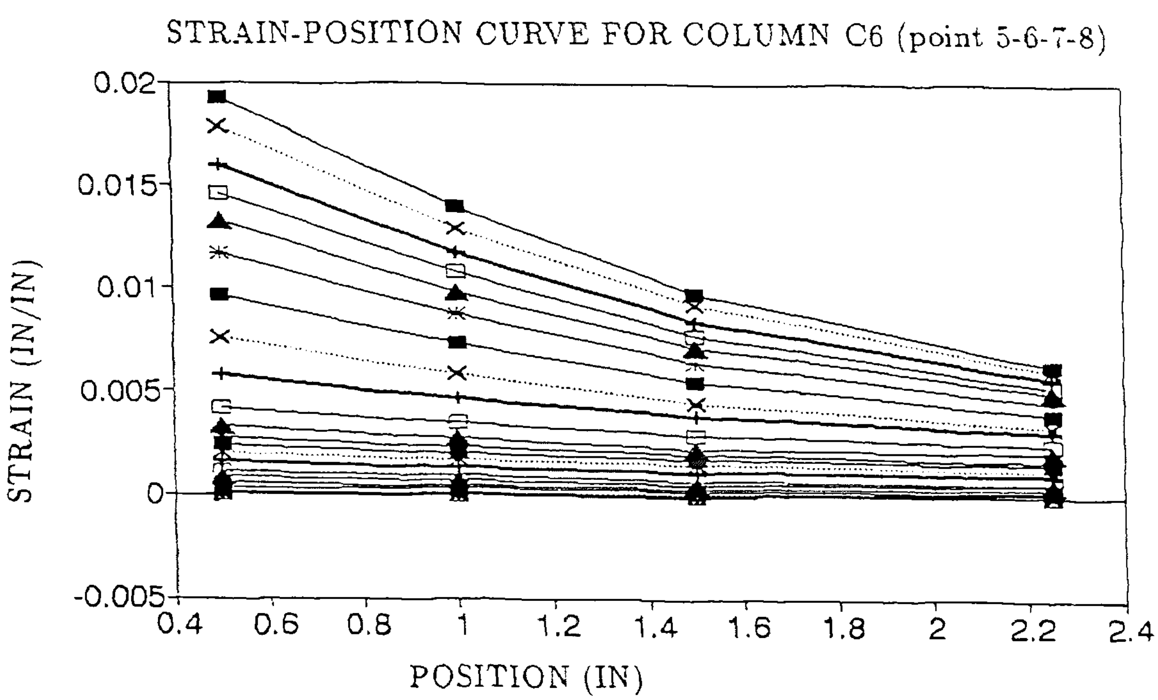

Figure B.26 Strain position curve for column C6 from point 5-6-7-8.

Appendix C. COLUMNS AFTER FAILURE

Crack and crushed patterns for L-shaped and square slender reinforced concrete columns are shown herein. Fig. C.1 through C.8 present B-series column tests and Fig. C.9 through C.14 present C-series column tests.

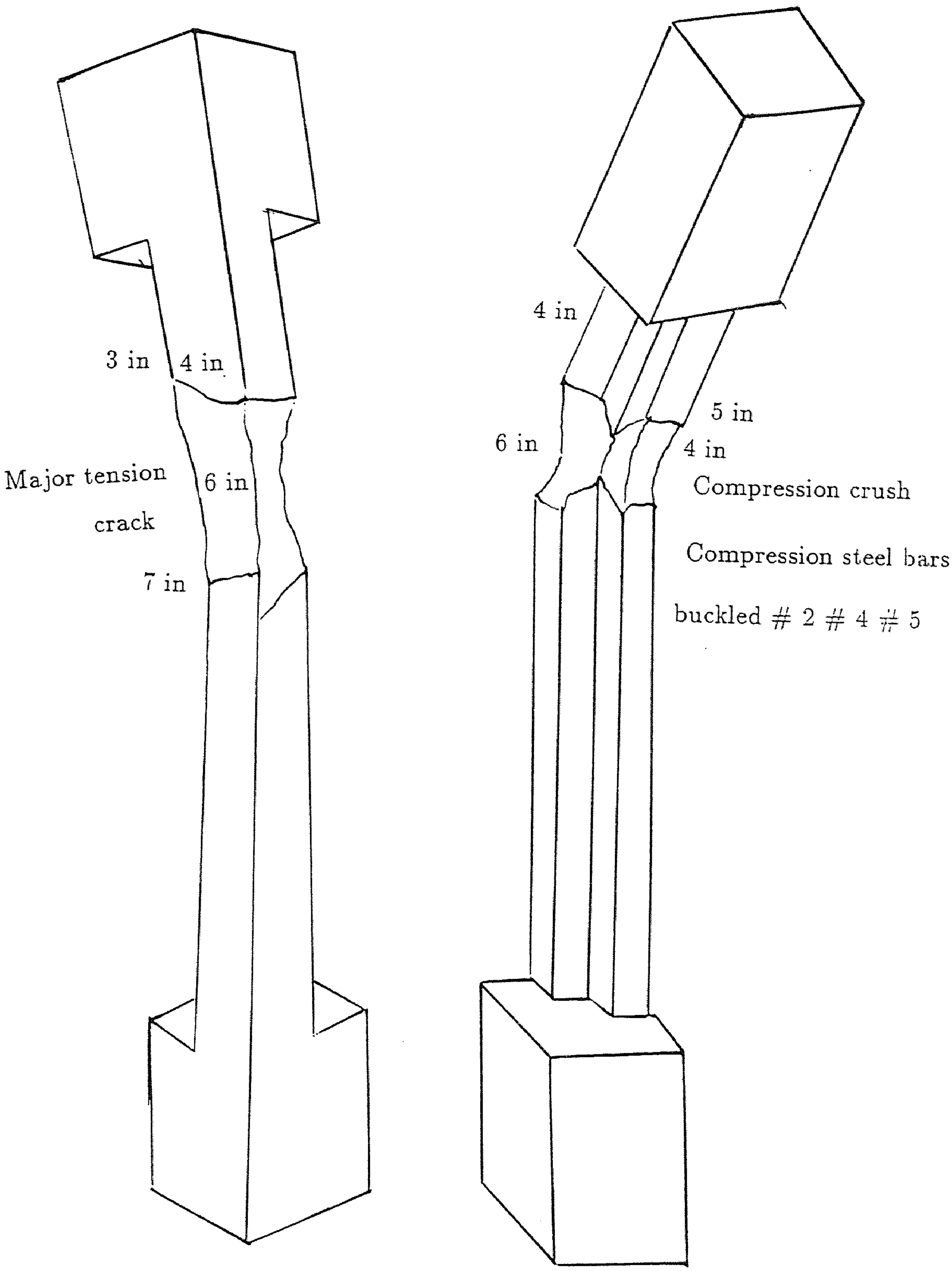

Figure C.1 Crack and crush patterns for column B1.

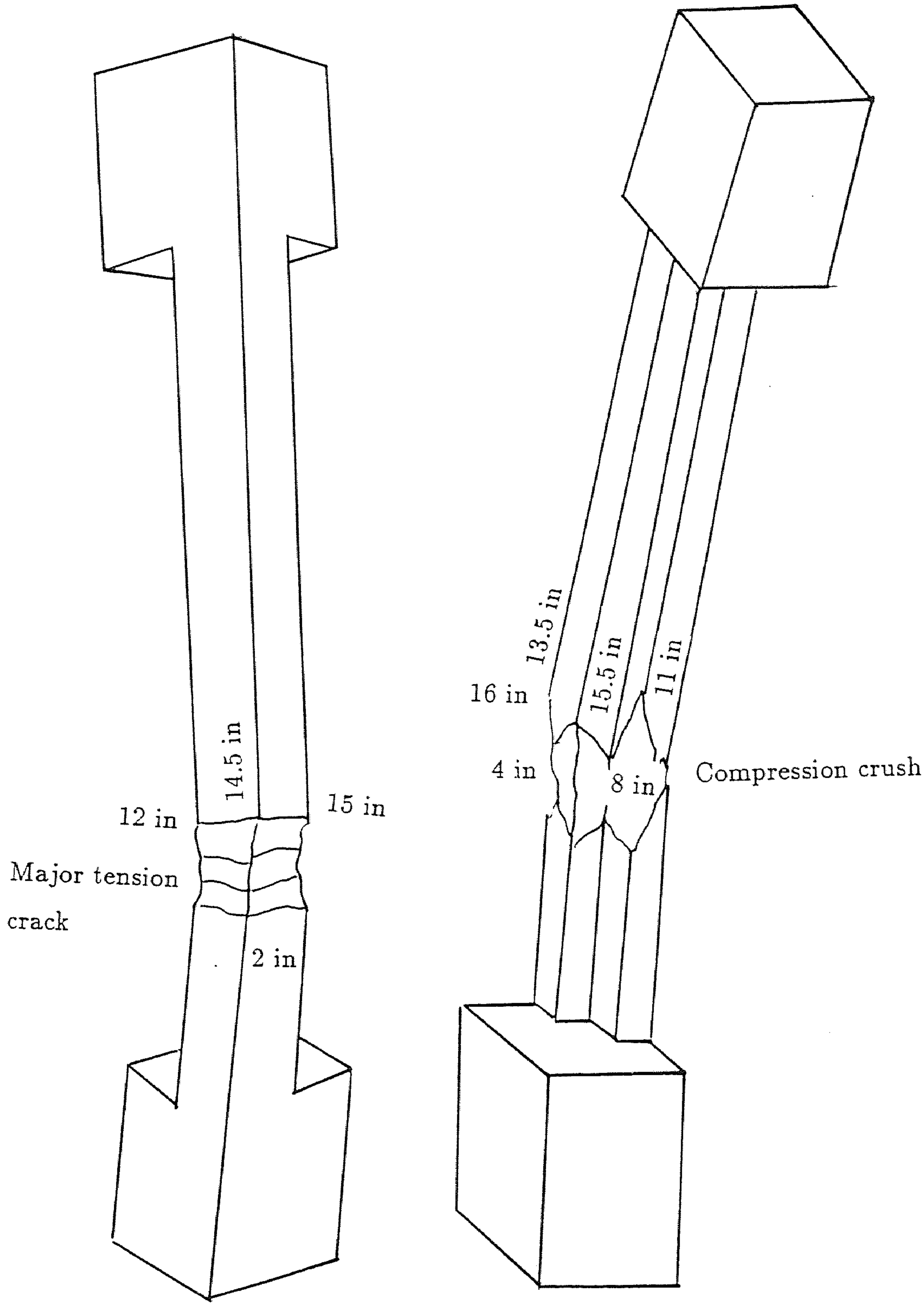

Figure C.2 Crack and crush patterns for column B2.

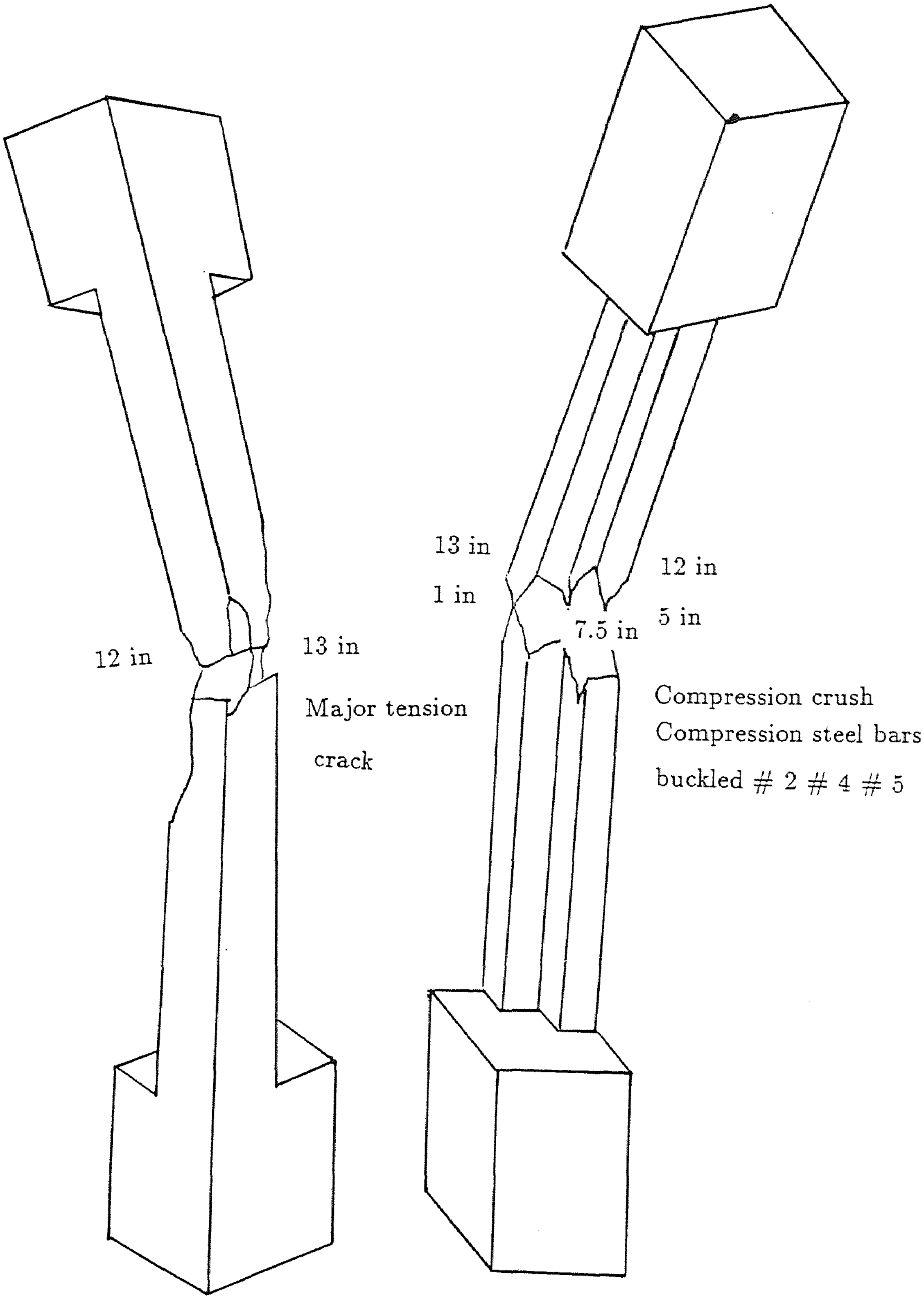

Figure C.3 Crack and crush patterns for column B3.

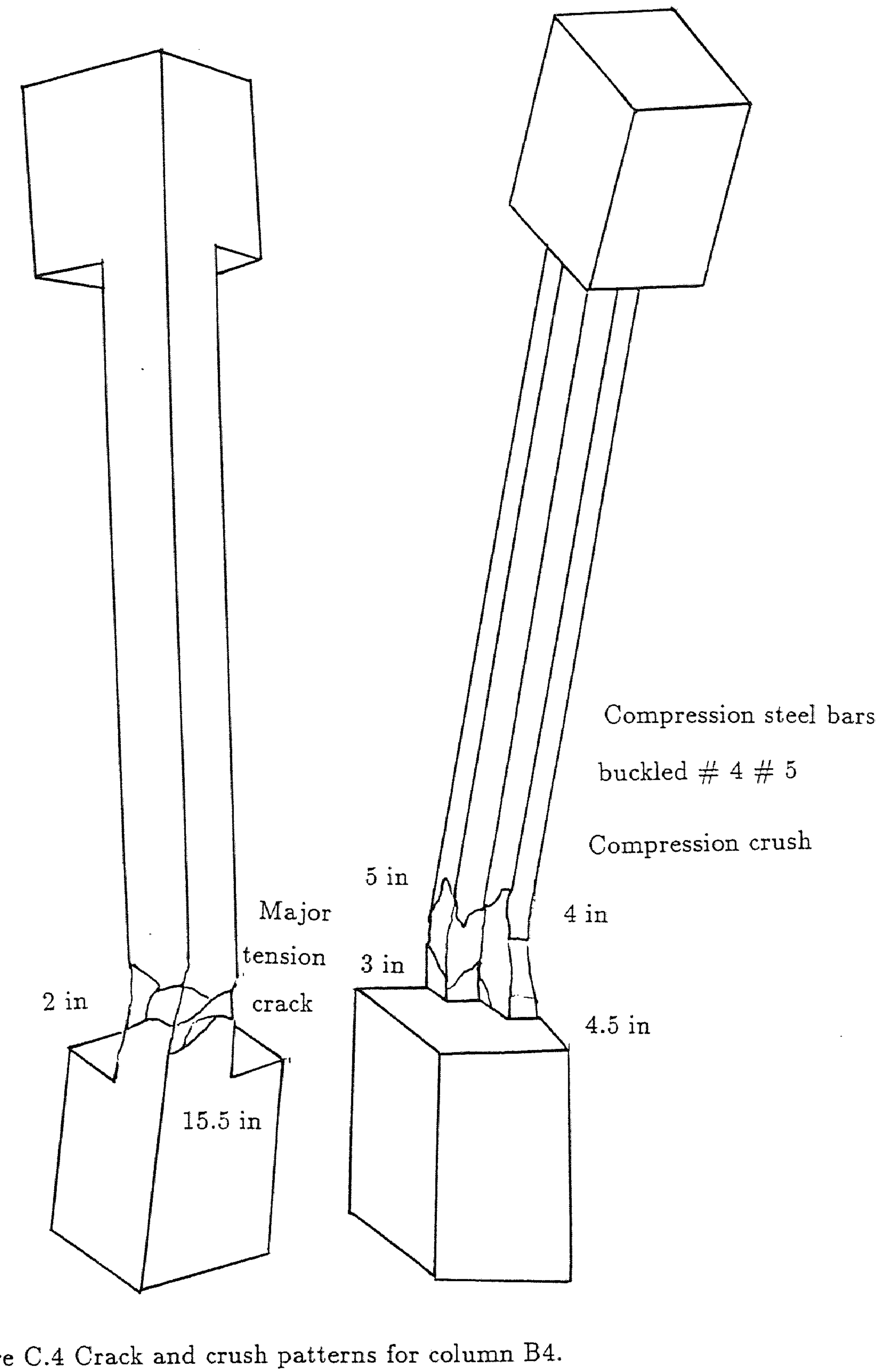

Figure C.4 Crack and crush patterns for column B4.

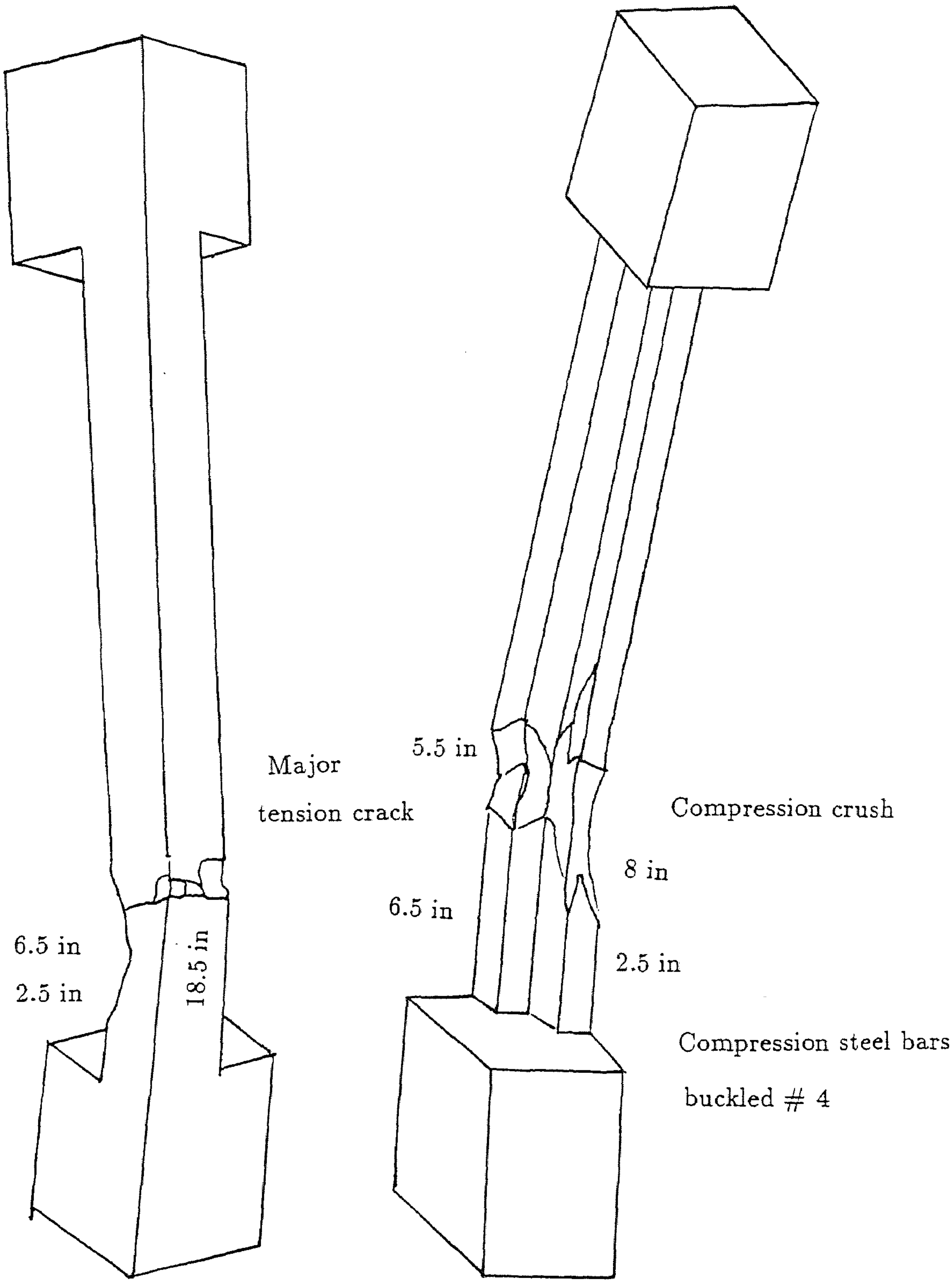

Figure C.5 Crack and crush patterns for column B5.

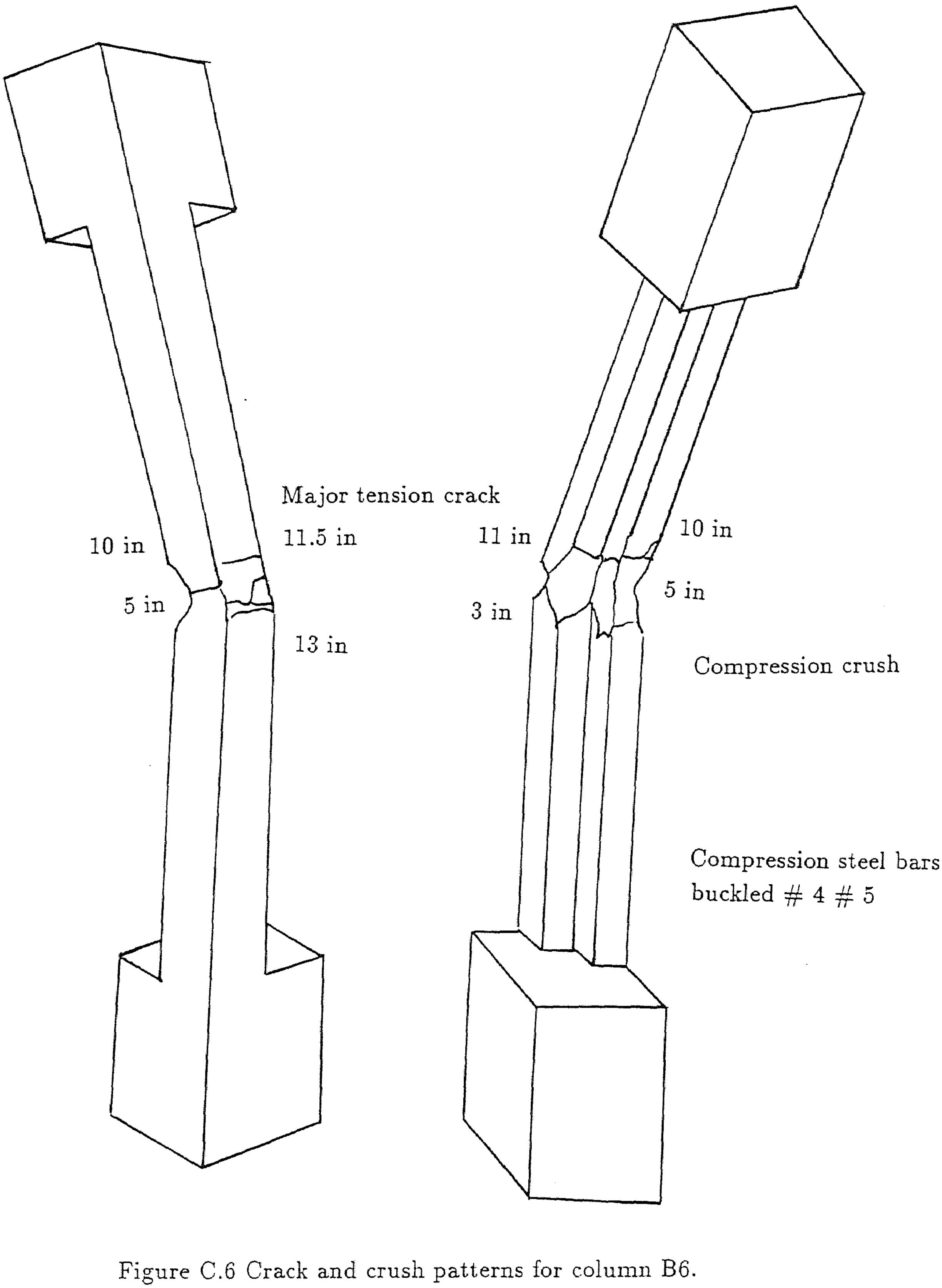

Figure C.6 Crack and crush patterns for column B6.

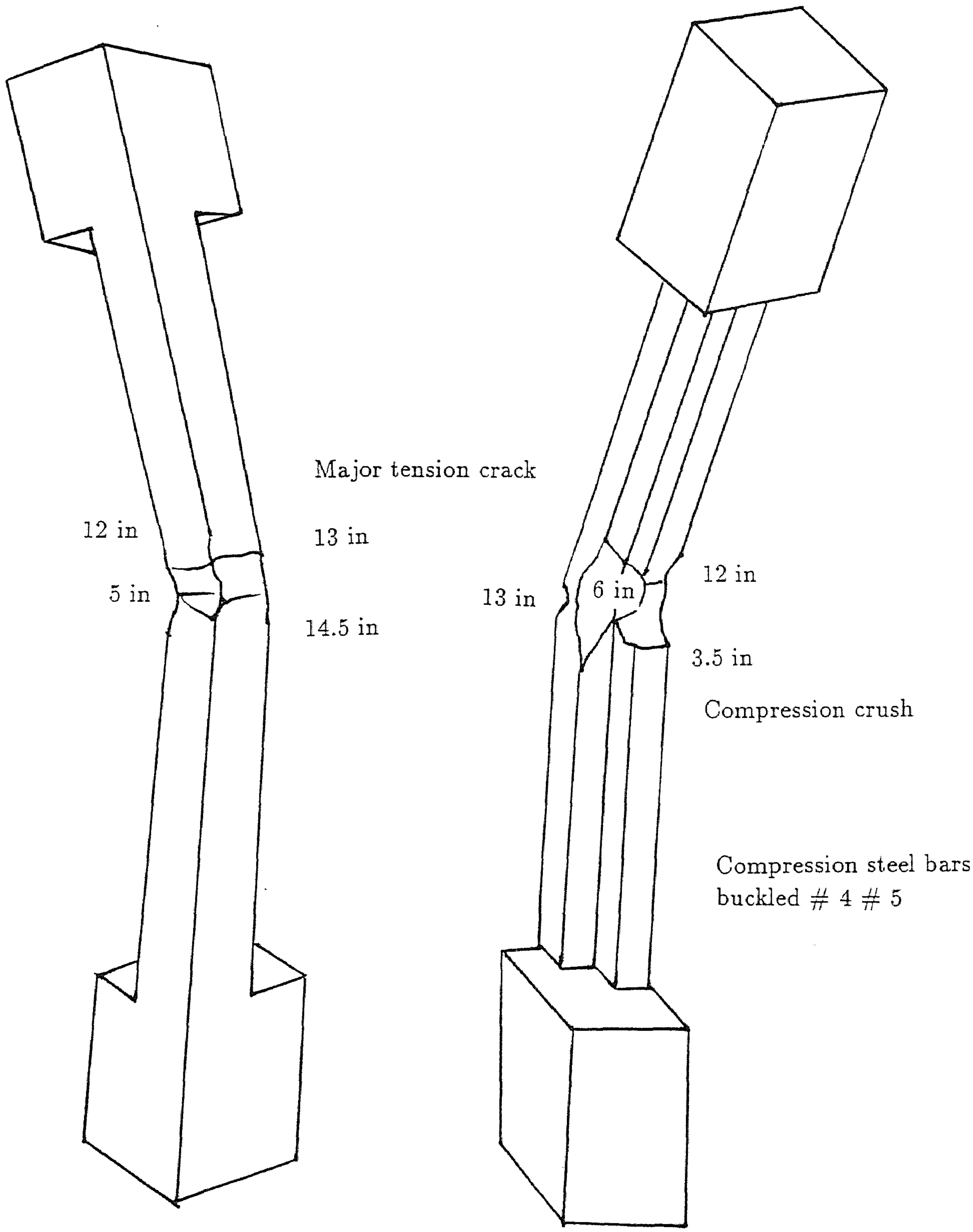

Figure C.7 Crack and crush patterns for column B7.

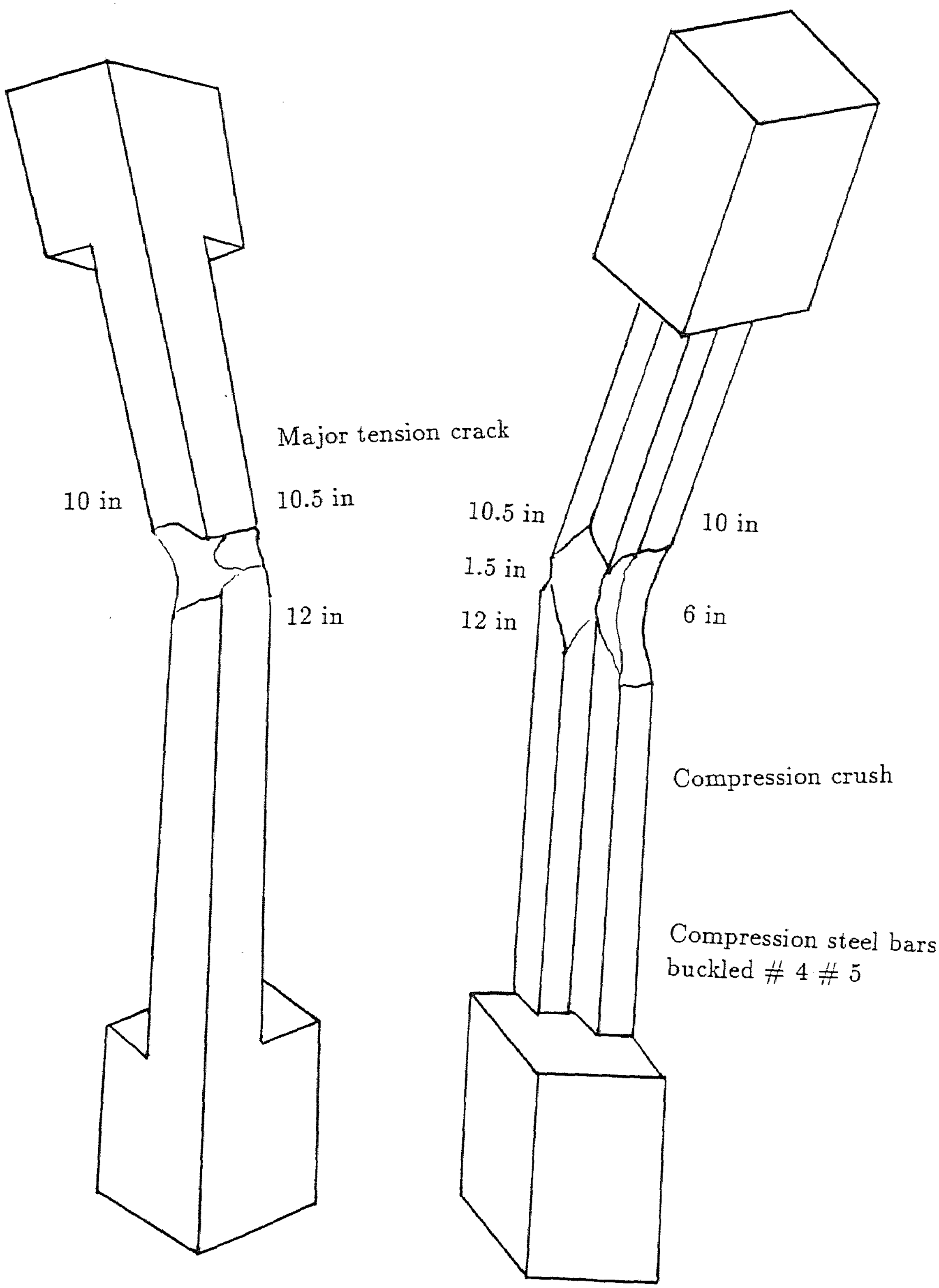

Figure C.8 Crack and crush patterns for column B8.

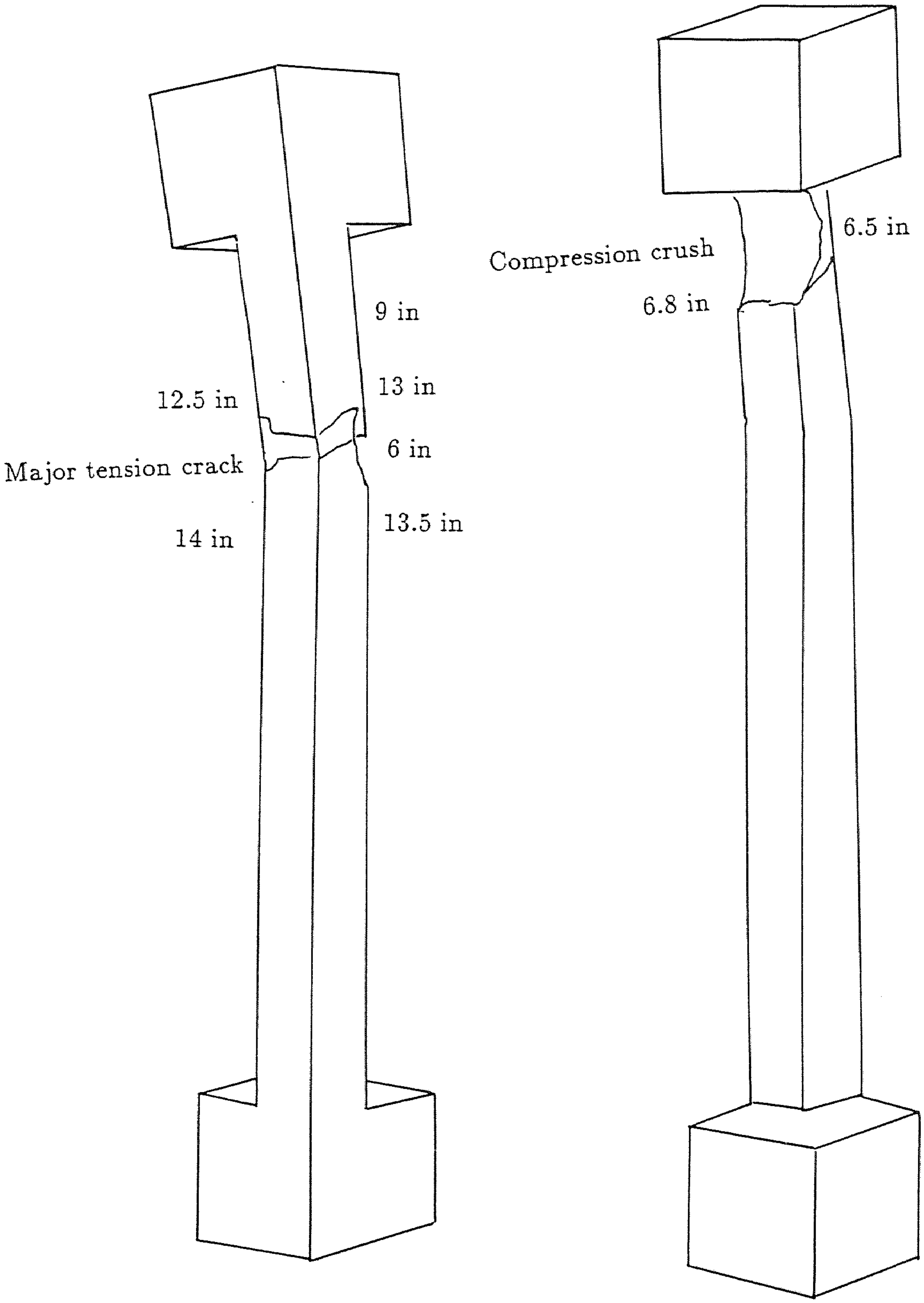

Figure C.9 Crack and crush patterns for column C1.

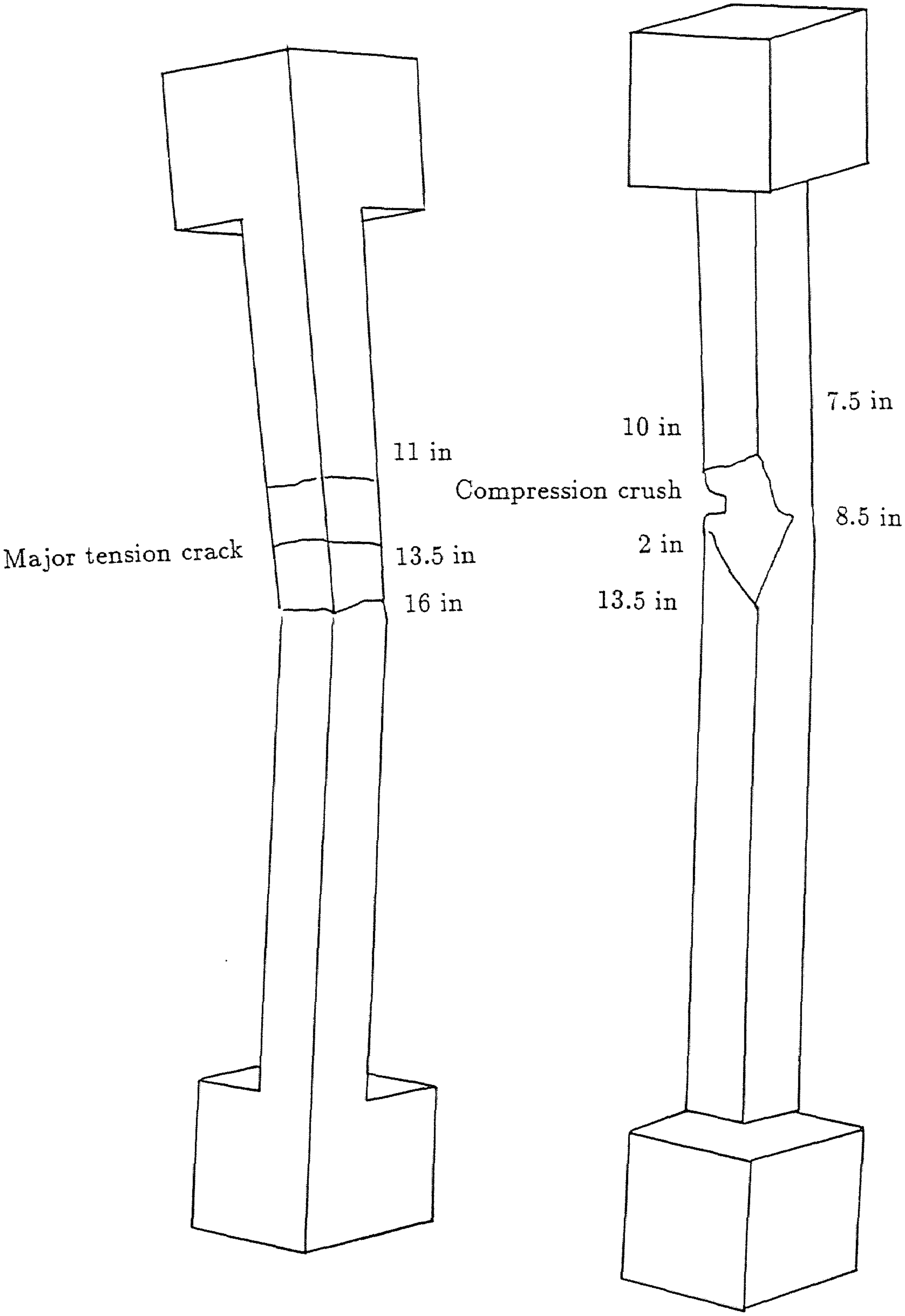

Figure C.10 Crack and crush patterns for column C2.

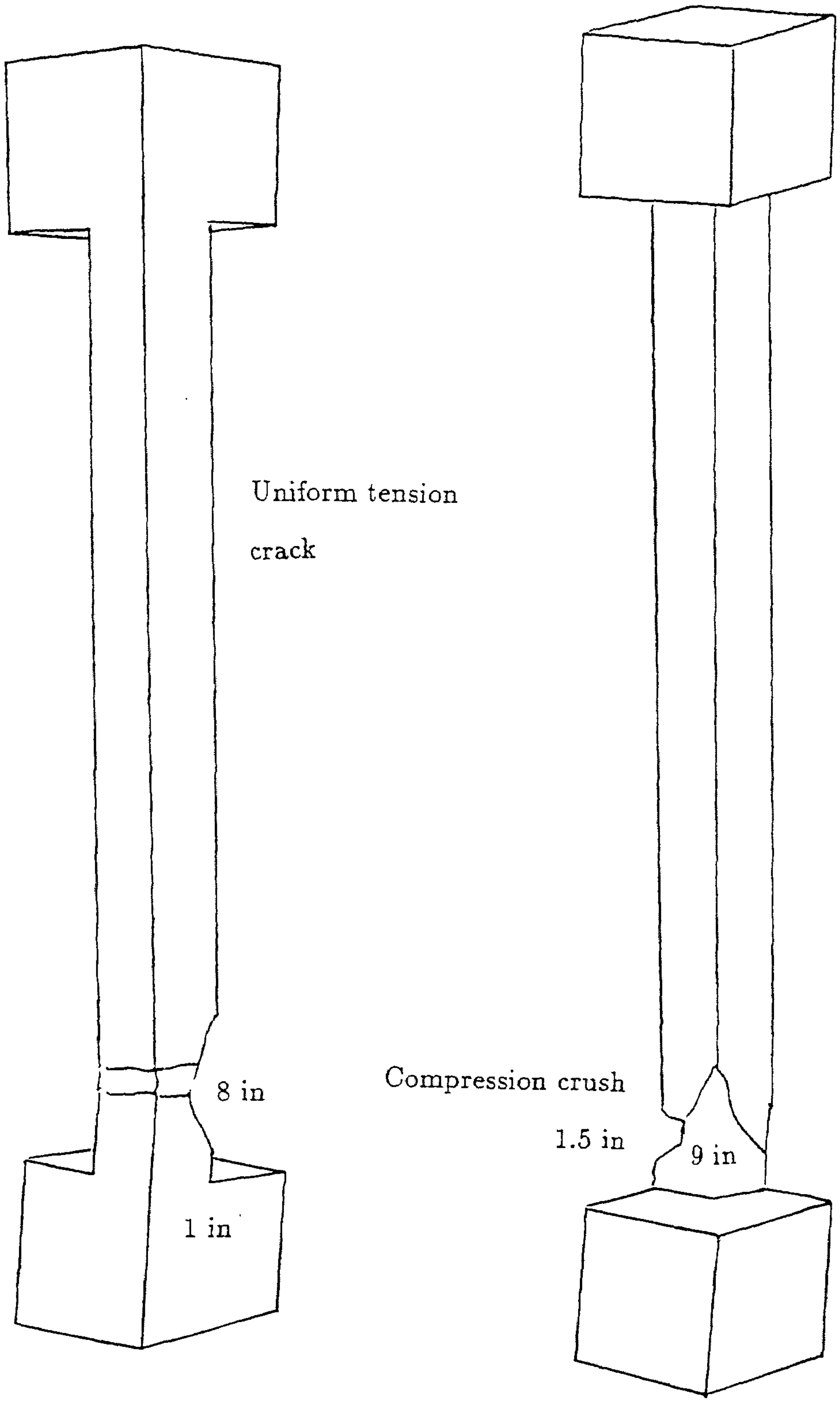

Figure C.11 Crack and crush patterns for column C3.

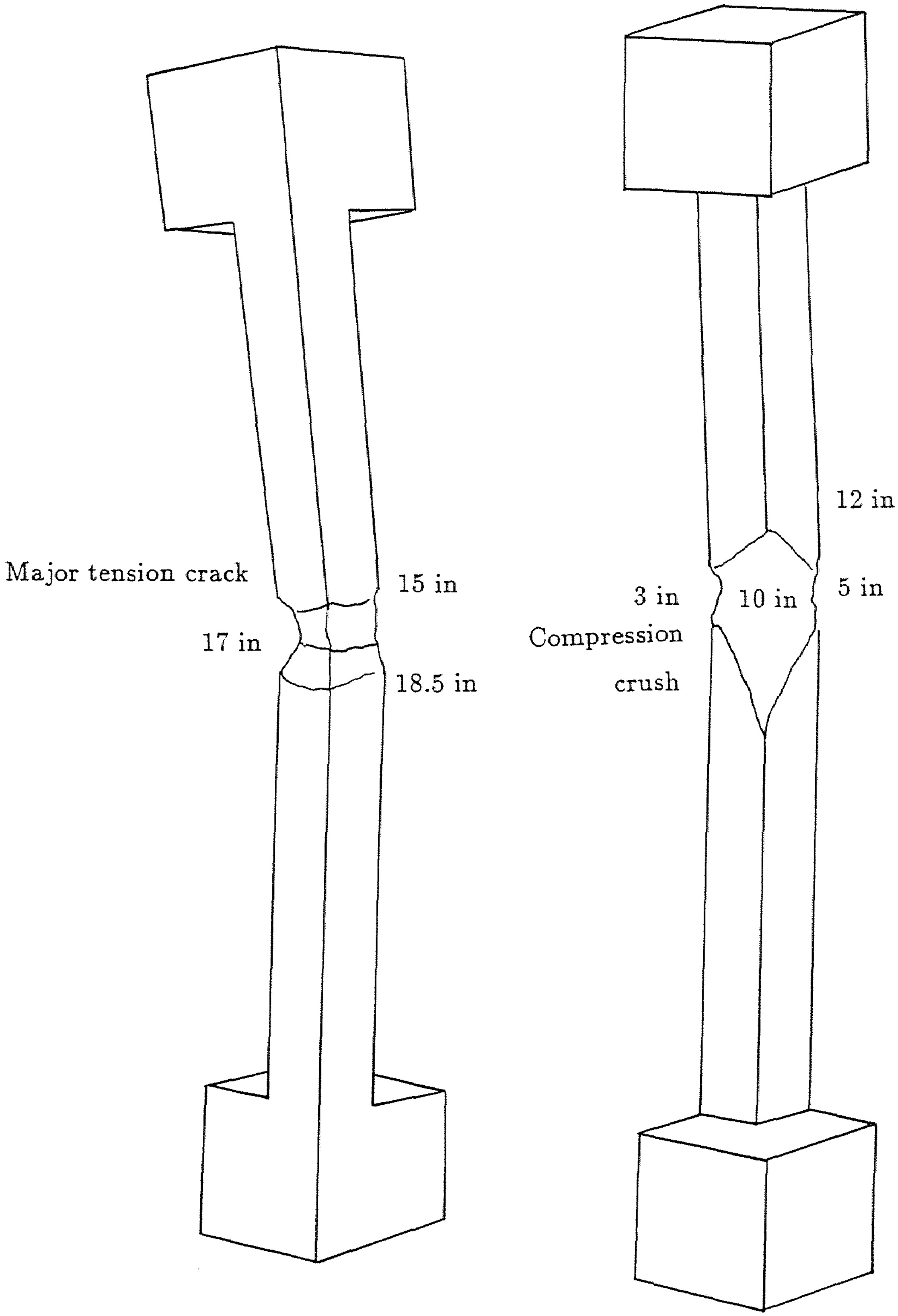

Figure C.12 Crack and crush patterns for column C4.

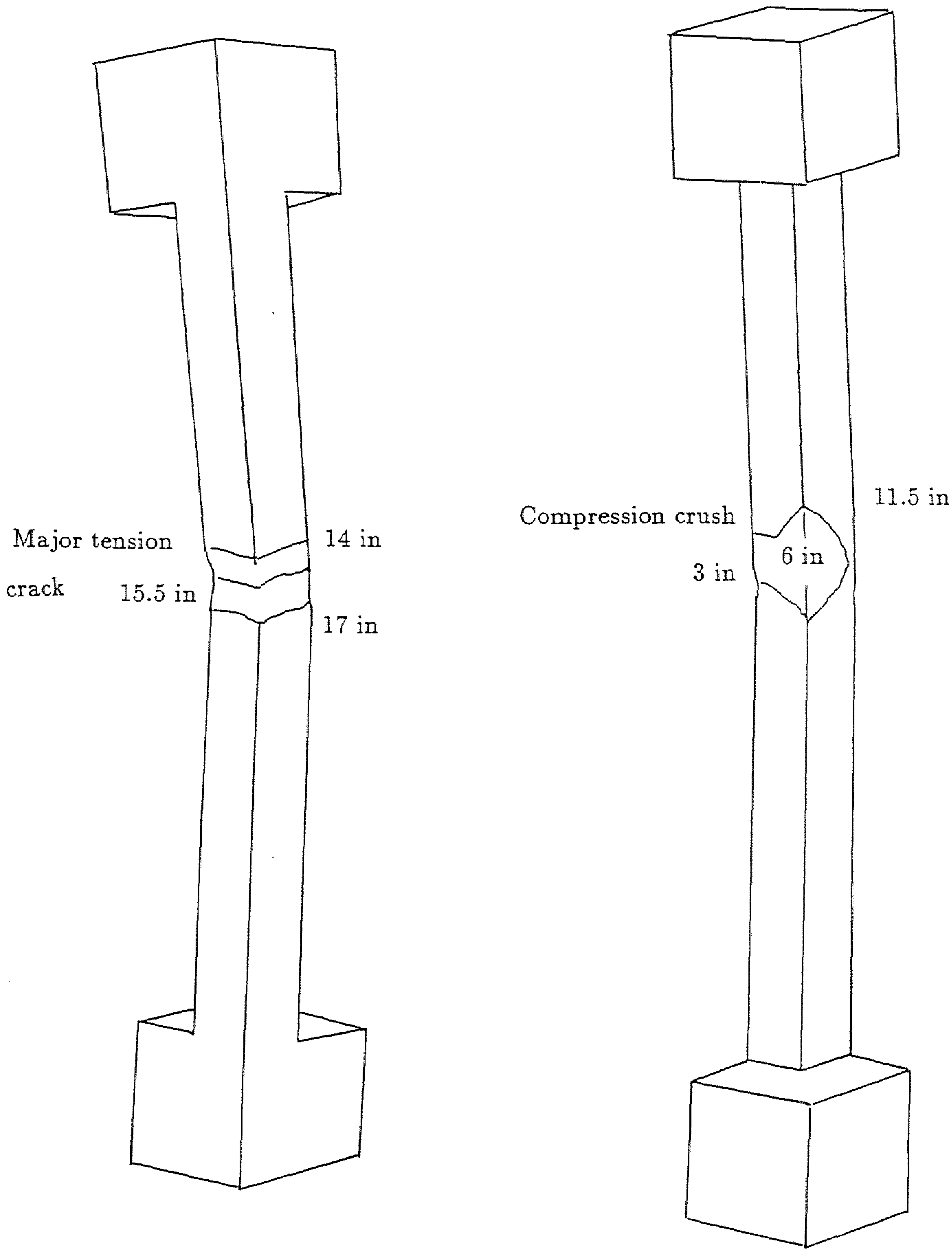

Figure C.13 Crack and crush patterns for column C5.

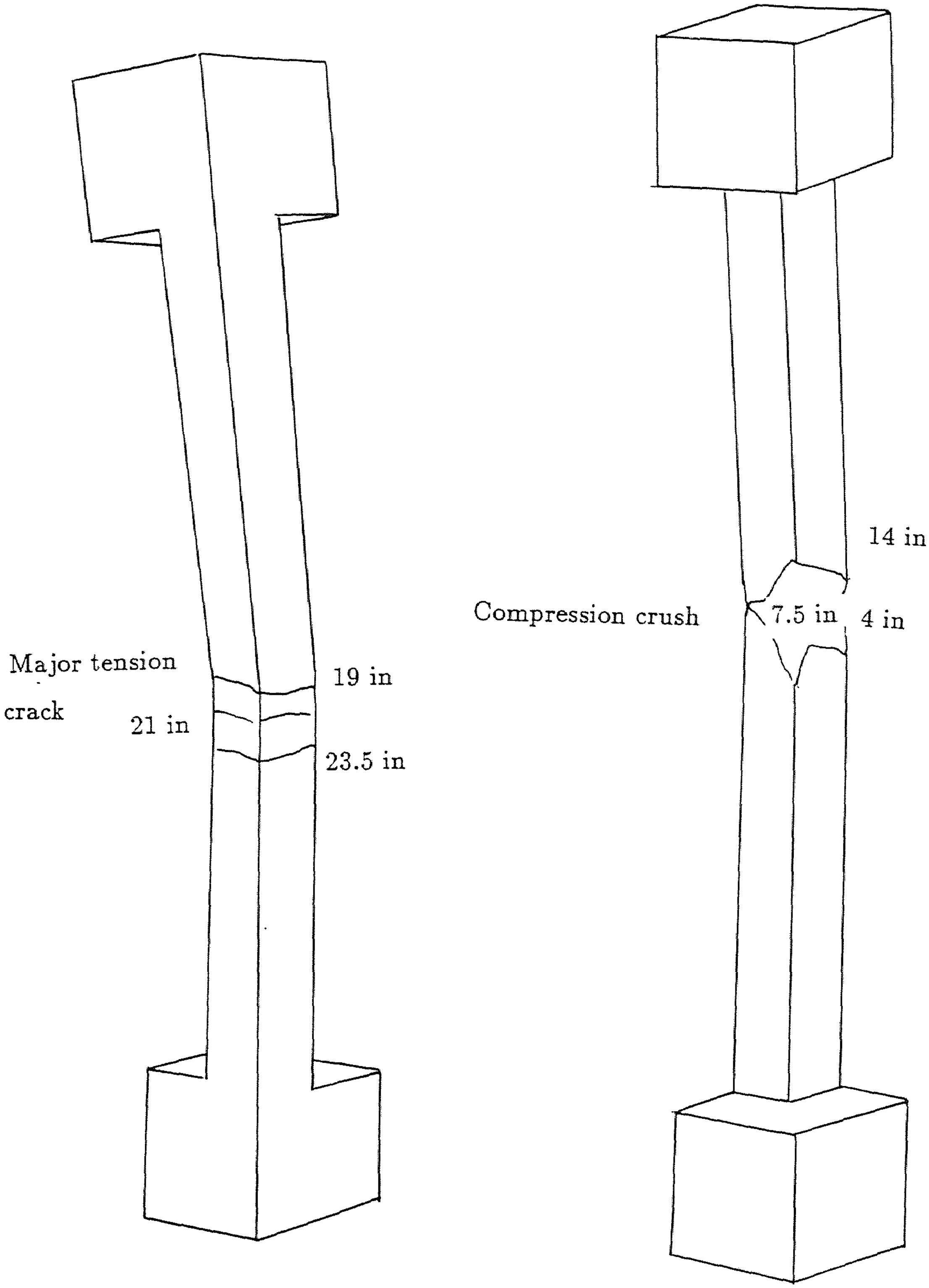

Figure C.14 Crack and crush patterns for column C6.

Appendix D.
Theoretical and Experimental Comparisons for B-series L-shaped Slender Columns.

Fig. D.1 through D.14 present theoretical and experimental comparisons of load-deflection curves and Fig. D.15 through D.28 present theoretical and experimental comparisons of moment-curvature curves.

-⊟- Experimental results.

-+- Theoretical results. (8 segments)

COMPARISON LOAD-DEFLECTION CURVE (X-DIR) FOR COLUMN B2.

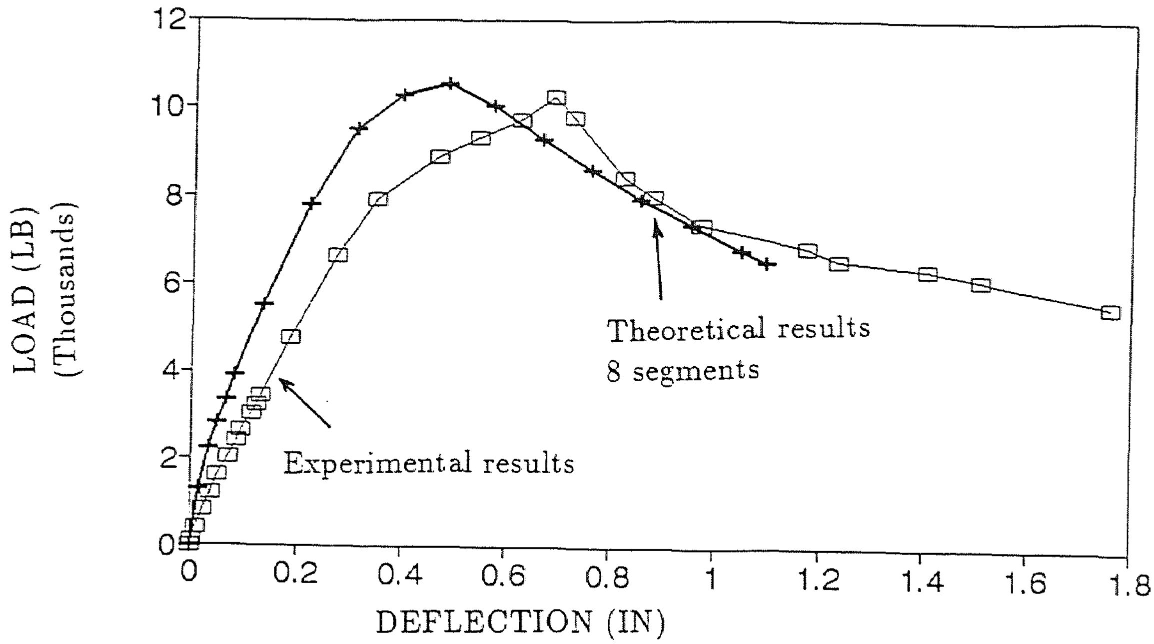

Figure. D.1 Comparison load-deflection curve (X-DIR.) for column B2.

COMPARISON LOAD-DEFLECTION CURVE (Y-DIR) FOR COLUMN B2.

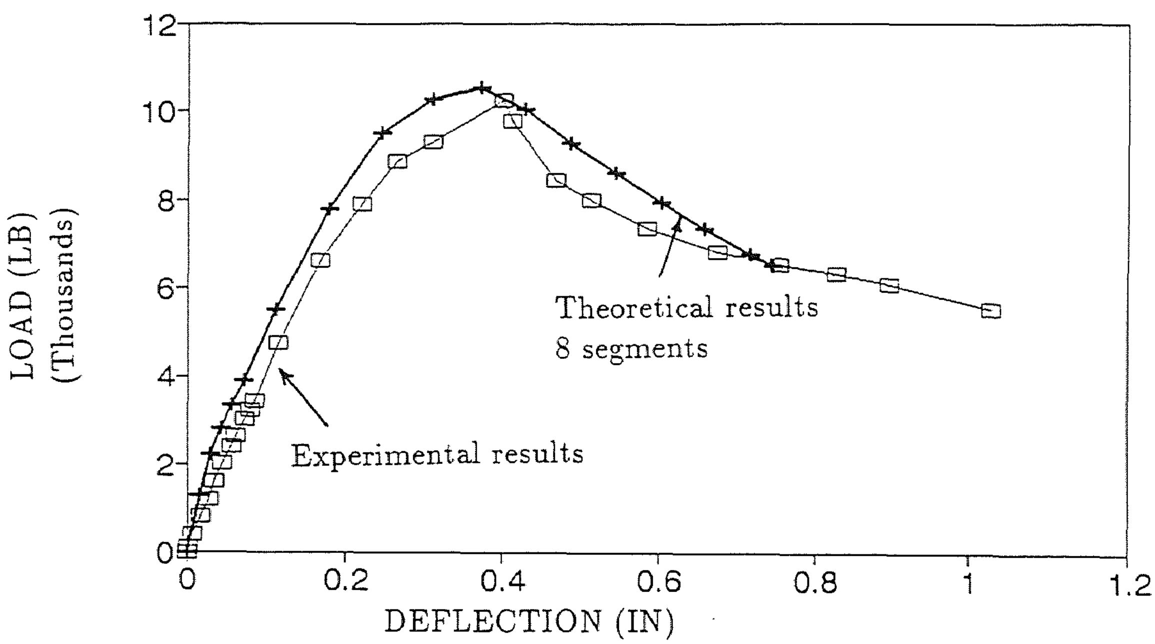

Figure. D.2 Comparison load-deflection curve (Y-DIR.) for column B2.

COMPARISON LOAD-DEFLECTION CURVE (X-DIR) FOR COLUMN B3.

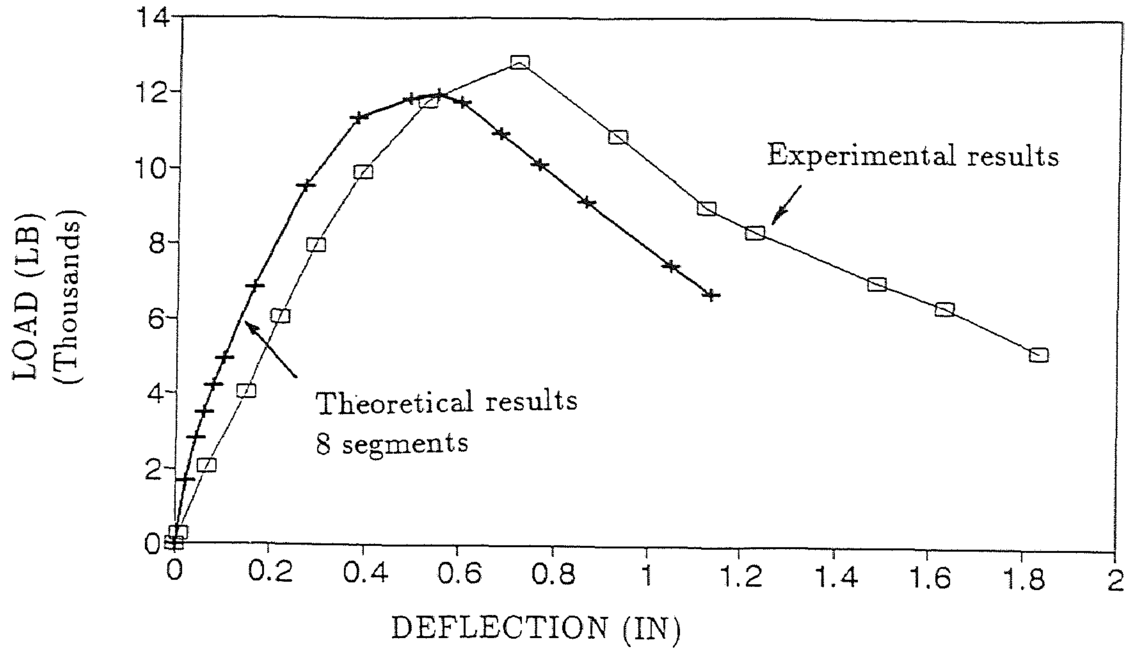

Figure. D.3 Comparison load-deflection curve (X-DIR.) for column B3.

COMPARISON LOAD-DEFLECTION CURVE (Y-DIR) FOR COLUMN B3.

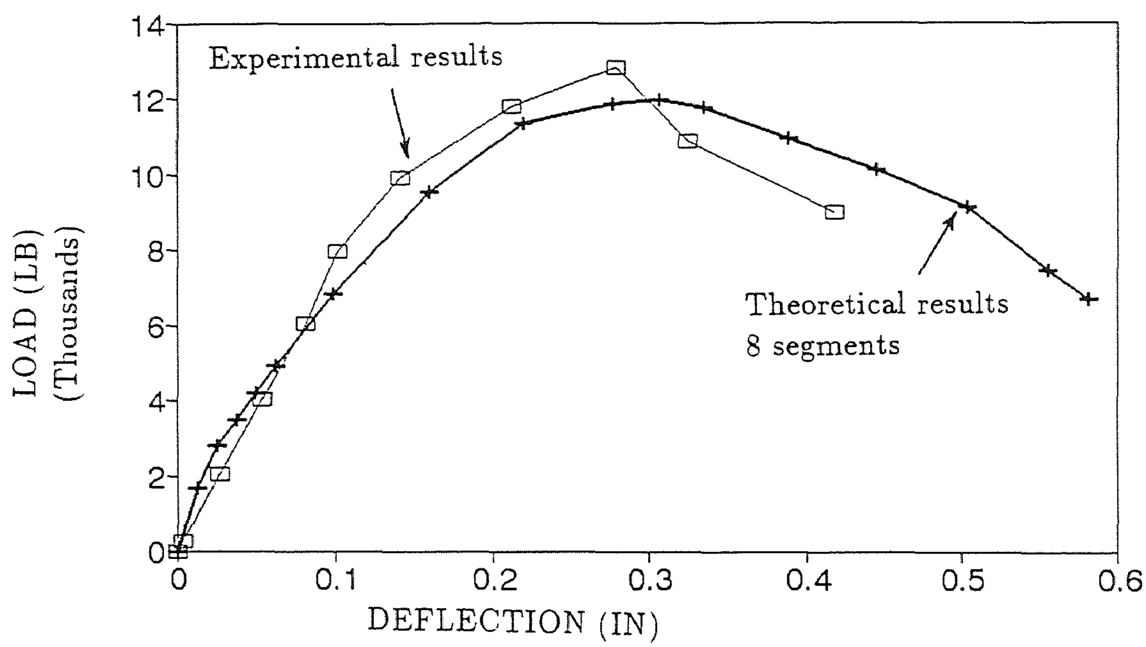

Figure. D.4 Comparison load-deflection curve (Y-DIR.) for column B3.

COMPARISON LOAD-DEFLECTION CURVE (X-DIR) FOR COLUMN B4.

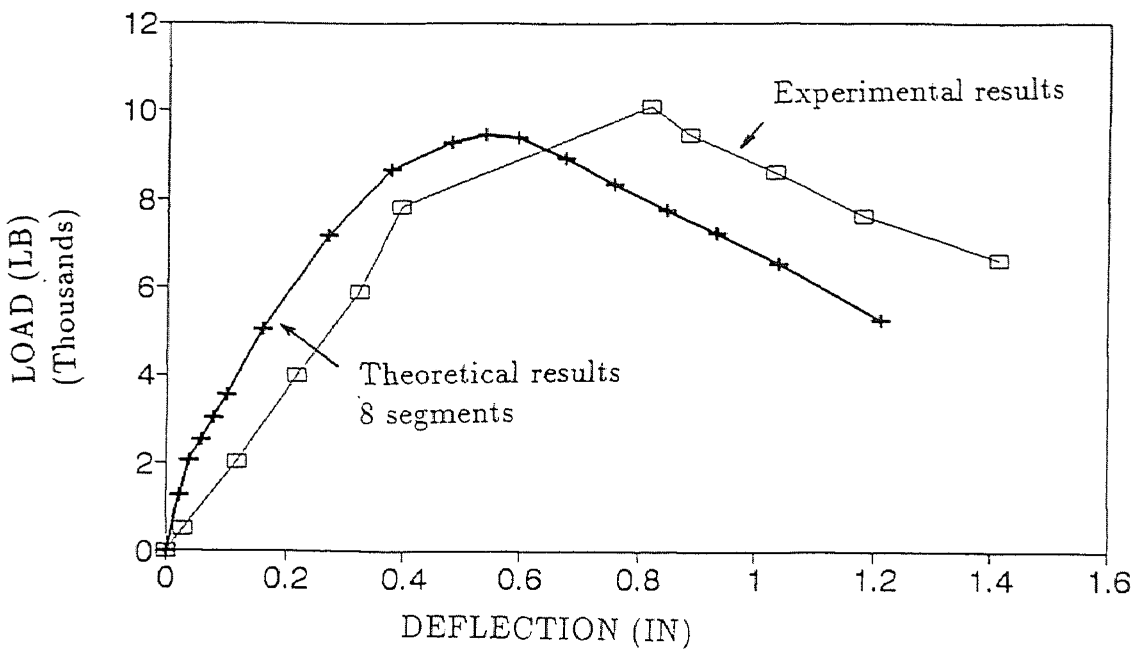

Figure. D.5 Comparison load-deflection curve (X-DIR.) for column B4.

COMPARISON LOAD-DEFLECTION CURVE (Y-DIR) FOR COLUMN B4.

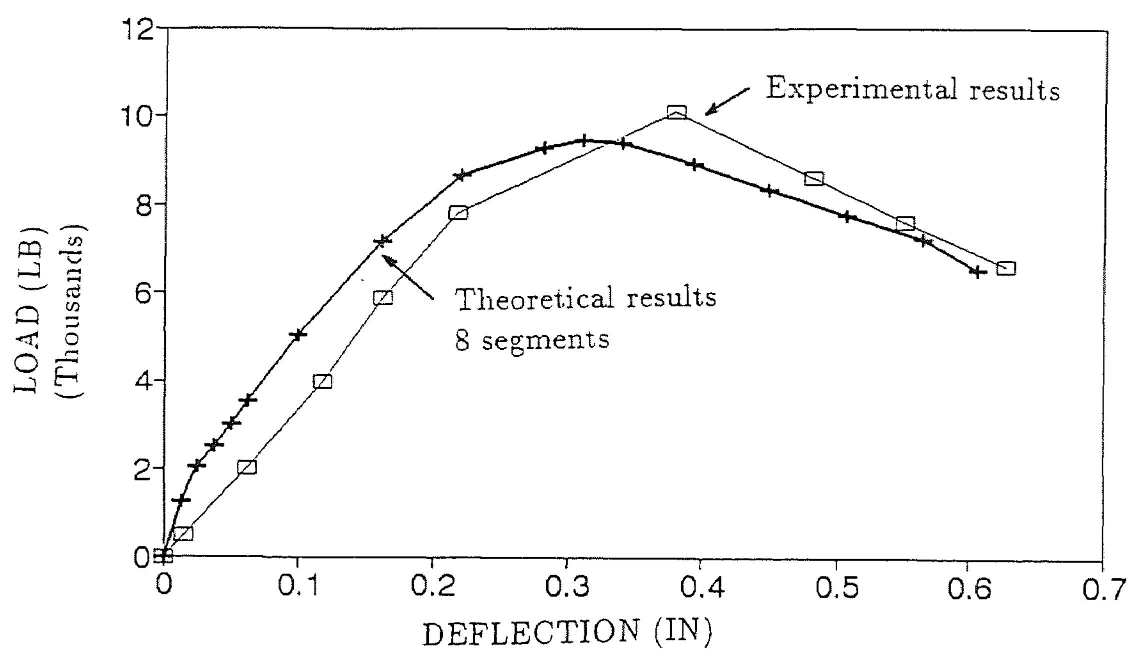

Figure. D.6 Comparison load-deflection curve (Y-DIR.) for column B4.

COMPARISON LOAD-DEFLECTION CURVE (X-DIR) FOR COLUMN B5.

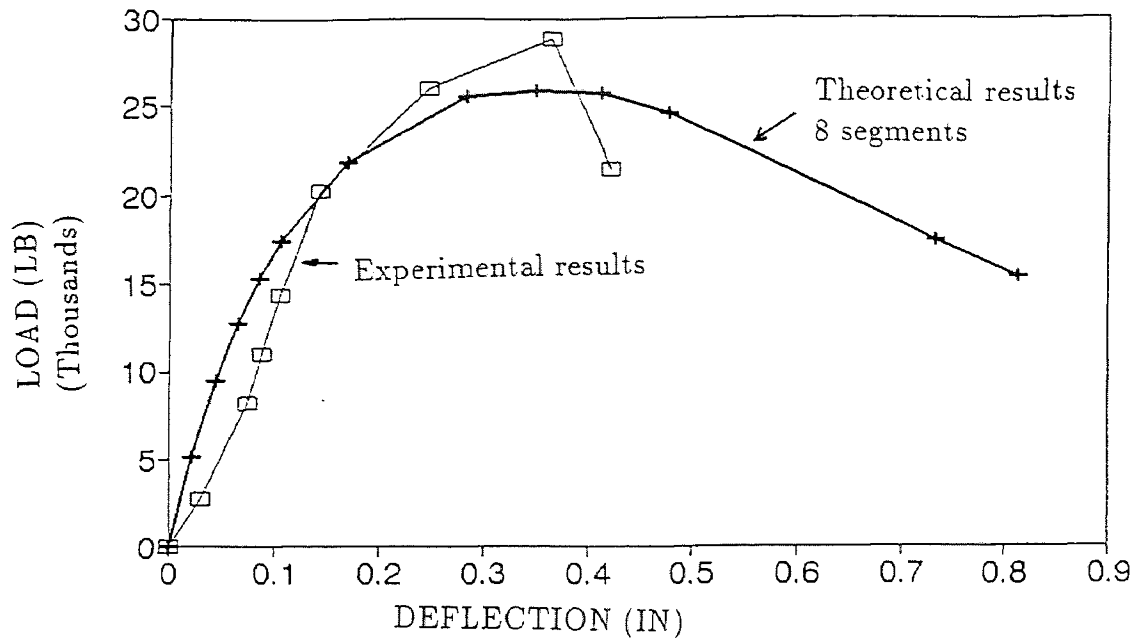

Figure. D.7 Comparison load-deflection curve (X-DIR.) for column B5.

COMPARISON LOAD-DEFLECTION CURVE (Y-DIR) FOR COLUMN B5.

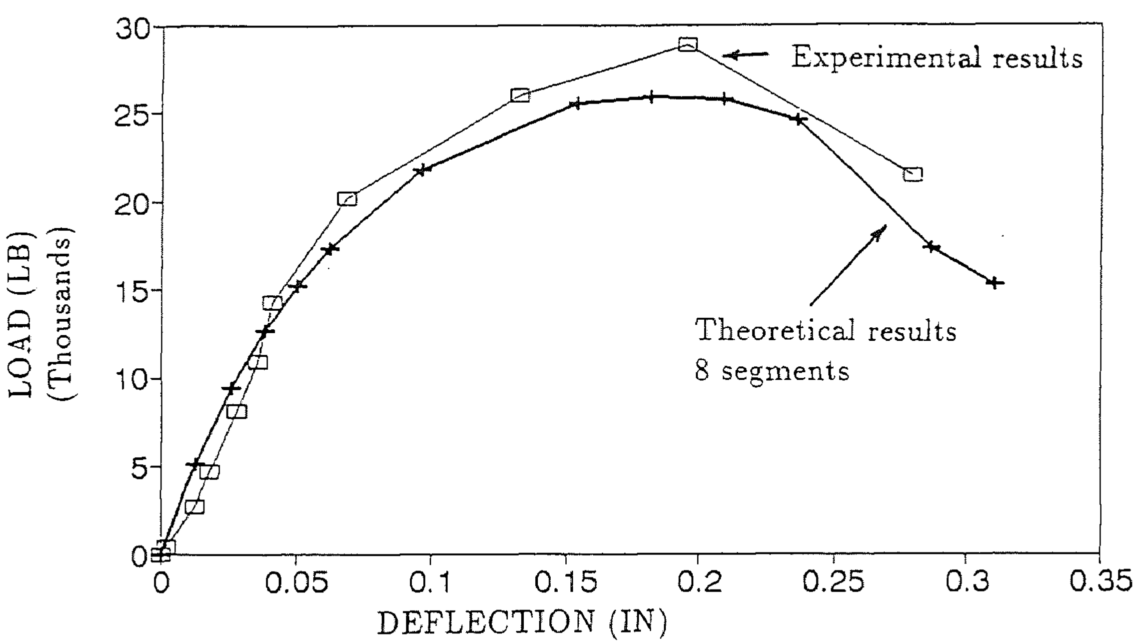

Figure. D.8 Comparison load-deflection curve (Y-DIR.) for column B5.

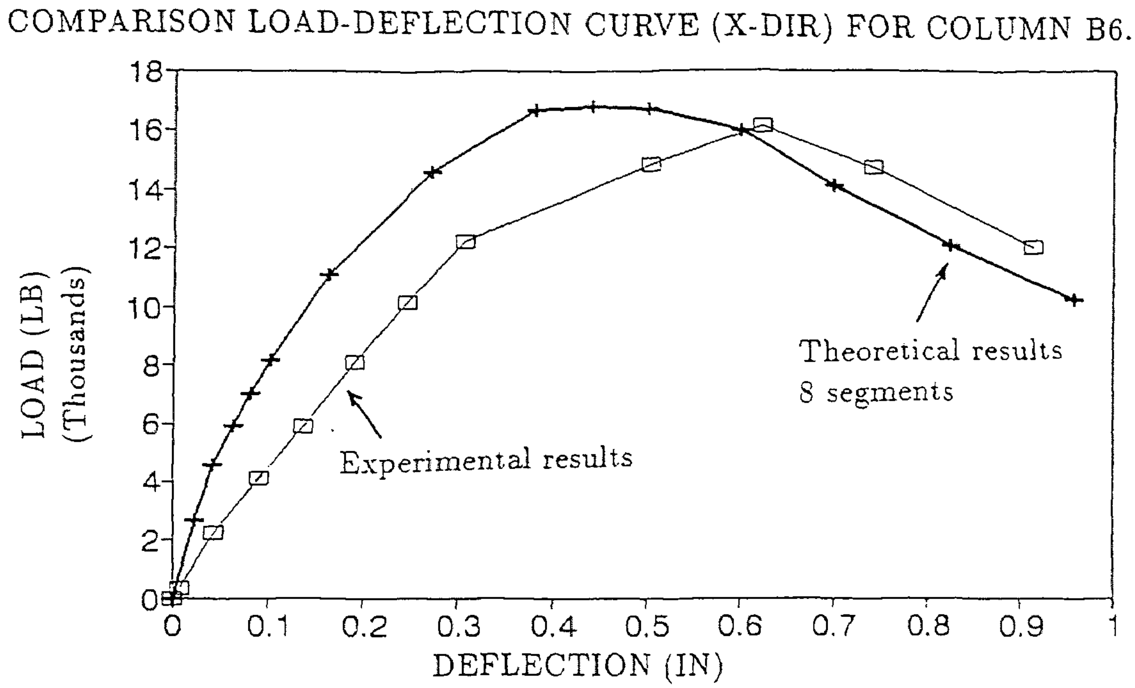

Figure. D.9 Comparison load-deflection curve (X-DIR.) for column B6.

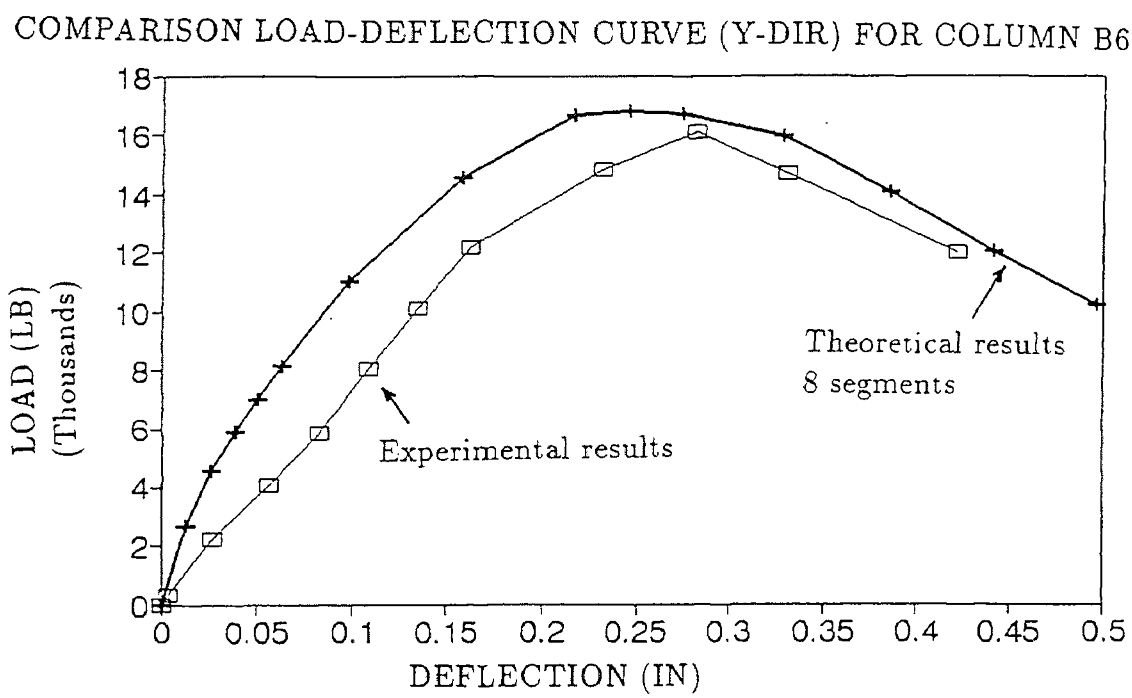

Figure. D.10 Comparison load-deflection curve (Y-DIR.) for column B6.

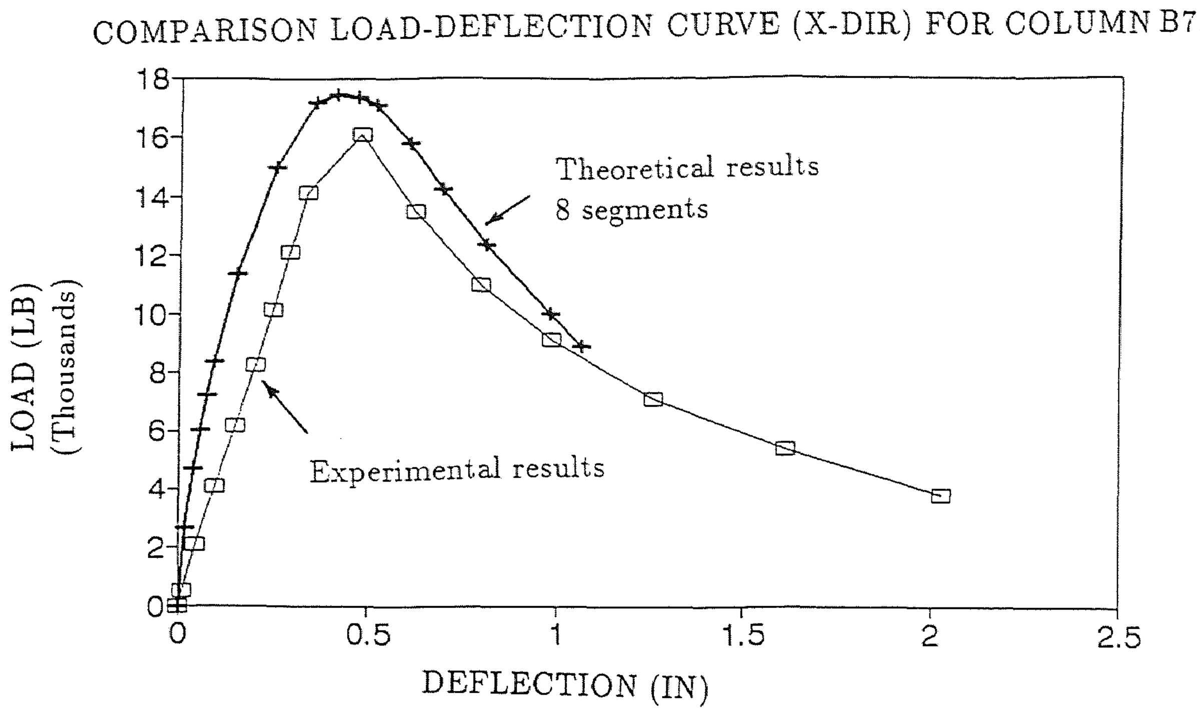

Figure. D.11 Comparison load-deflection curve (X-DIR.) for column B7.

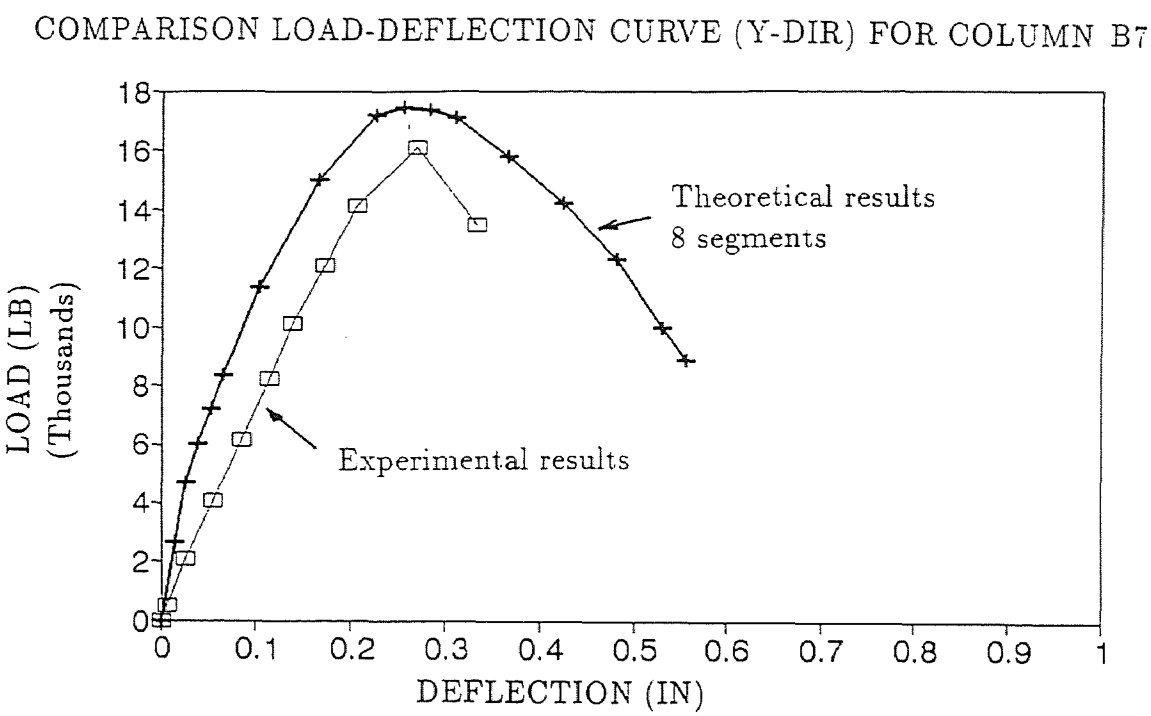

Figure. D.12 Comparison load-deflection curve (Y-DIR.) for column B7.

COMPARISON LOAD-DEFLECTION CURVE (X-DIR) FOR COLUMN B8.

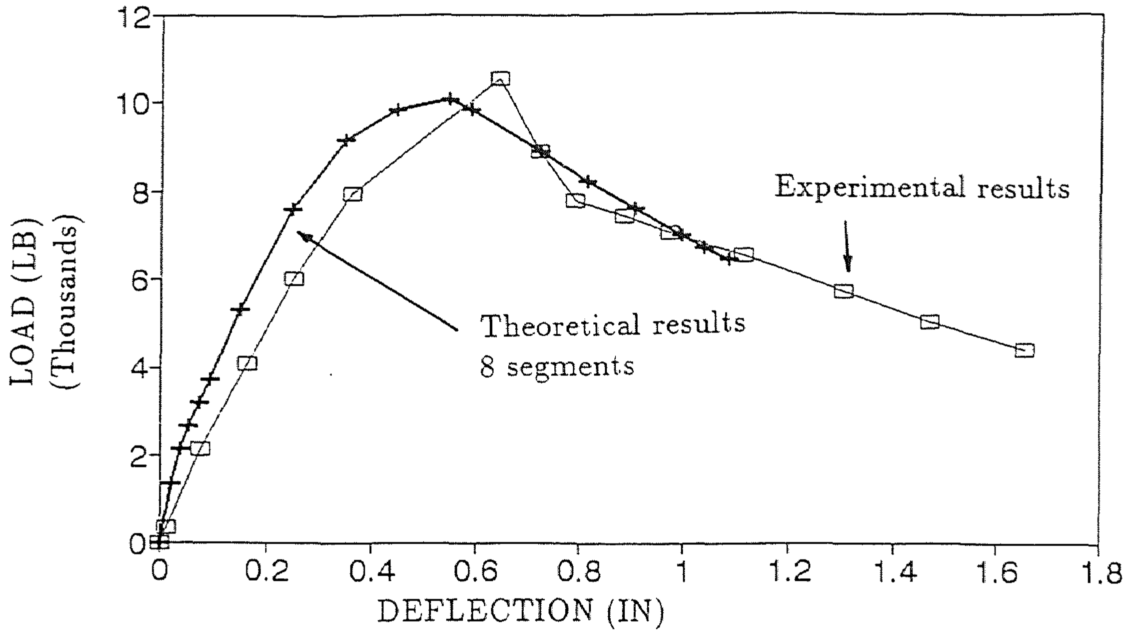

Figure. D.13 Comparison load-deflection curve (X-DIR.) for column B8.

COMPARISON LOAD-DEFLECTION CURVE (Y-DIR) FOR COLUMN B8.

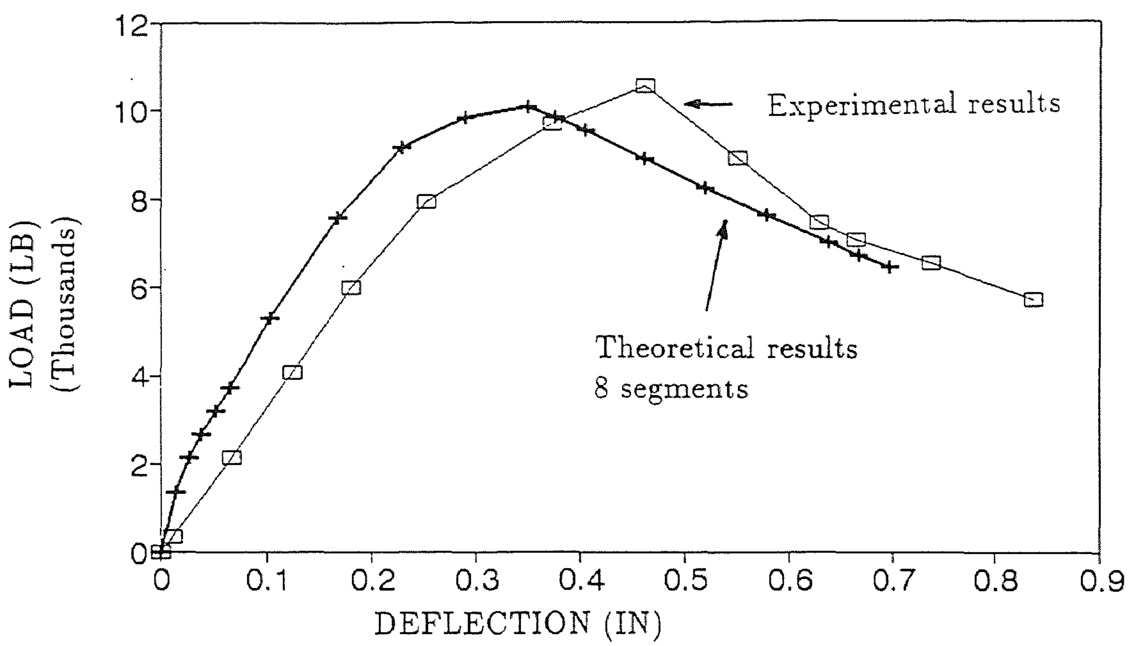

Figure. D.14 Comparison load-deflection curve (Y-DIR.) for column B8.

COMPARISON MOMENT-CURVATURE CURVE (M_x&ϕ_x) FOR COLUMN B2.

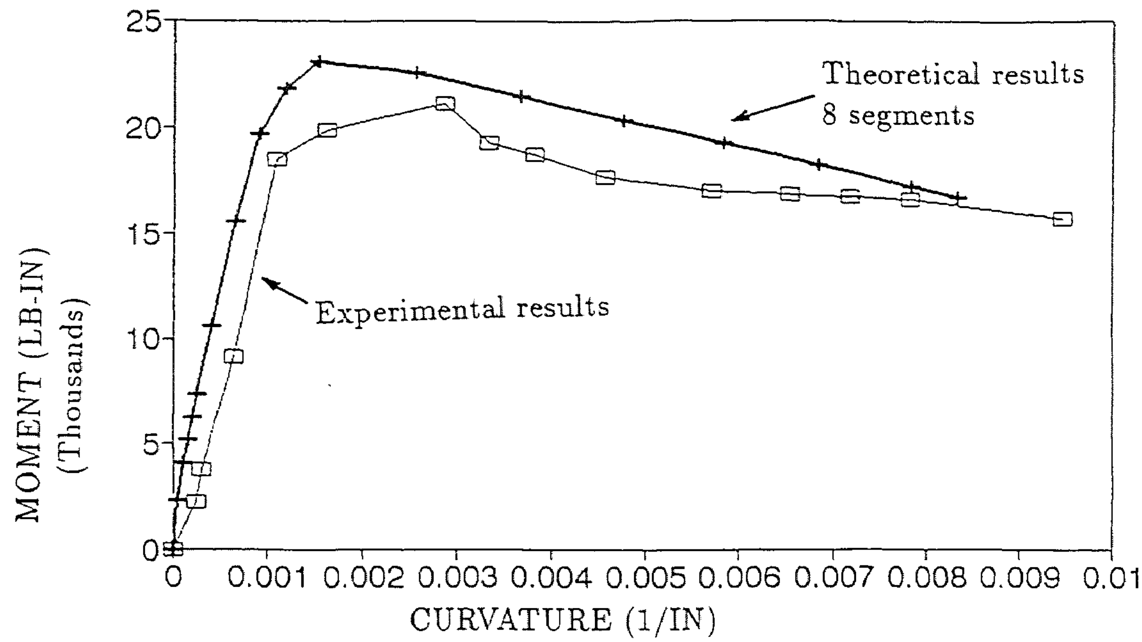

Figure. D.15 Comparison moment-curvature curve (M_x&ϕ_x) column B2.

COMPARISON MOMENT-CURVATURE CURVE (M_y&ϕ_y) FOR COLUMN B2.

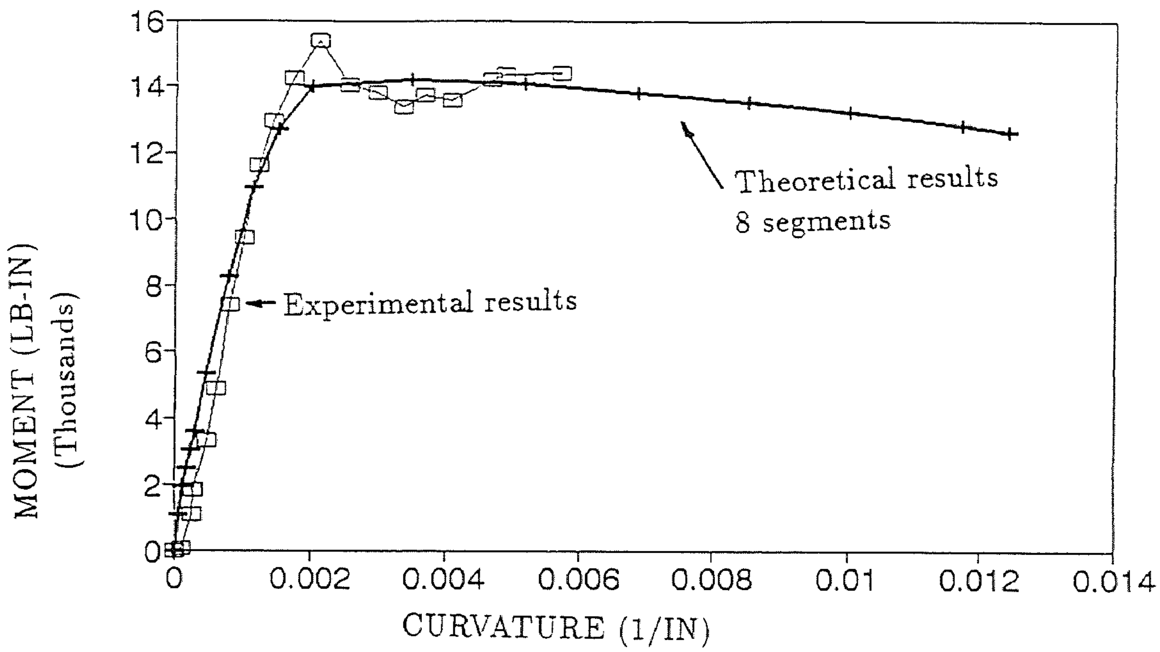

Figure. D.16 Comparison moment-curvature curve (M_y&ϕ_y) column B2.

COMPARISON MOMENT-CURVATURE CURVE (M_x&ϕ_x) FOR COLUMN B3.

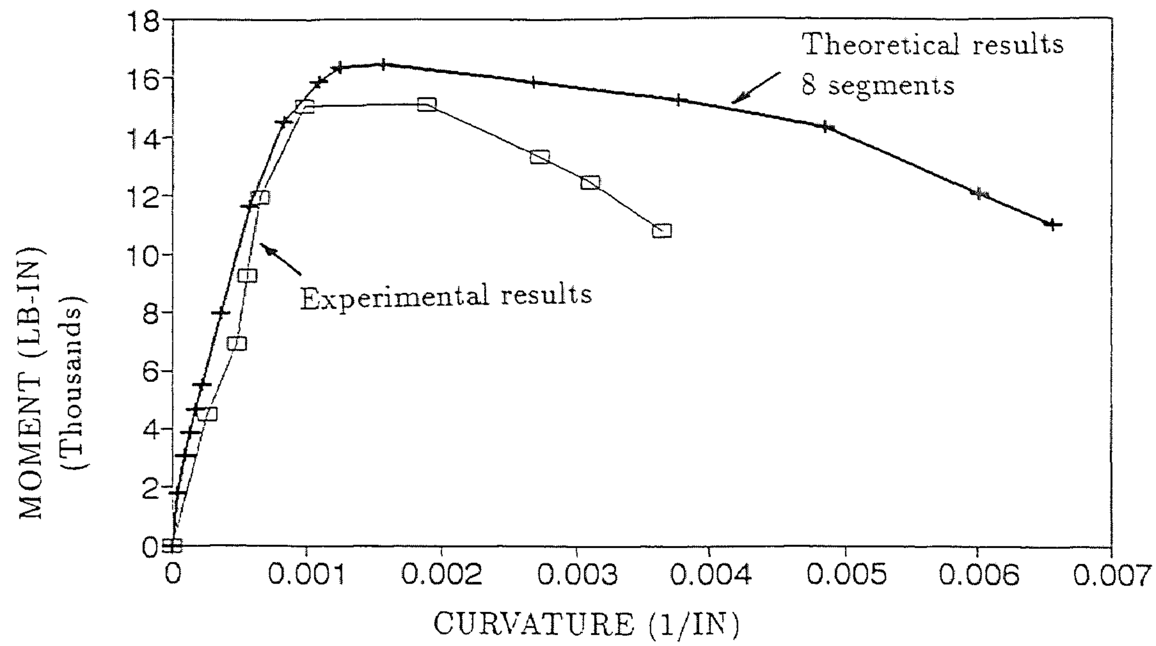

Figure. D.17 Comparison moment-curvature curve (M_x&ϕ_x) column B3.

COMPARISON MOMENT-CURVATURE CURVE (M_y&ϕ_y) FOR COLUMN B3.

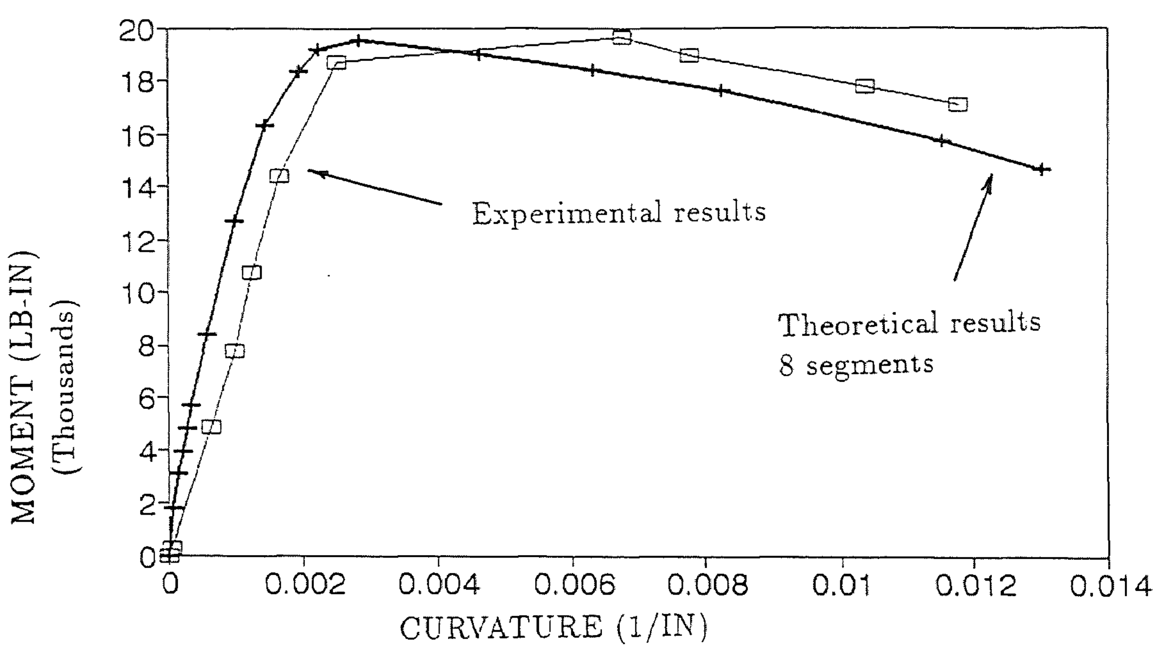

Figure. D.18 Comparison moment-curvature curve (M_y&ϕ_y) column B3.

COMPARISON MOMENT-CURVATURE CURVE (M_x&ϕ_x) FOR COLUMN B4.

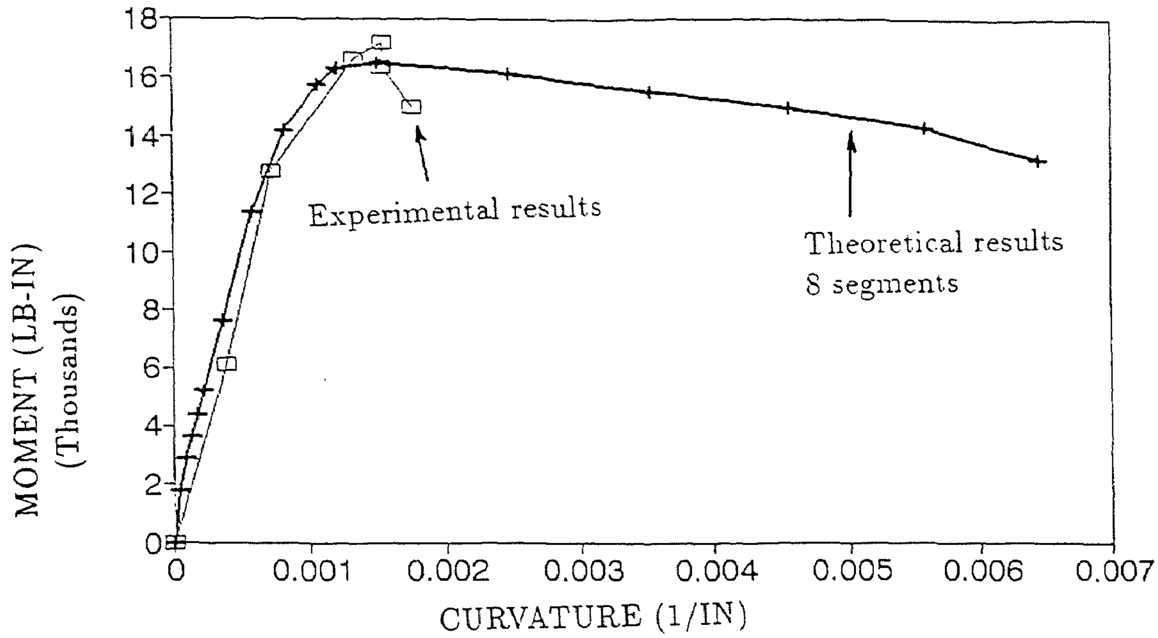

Figure. D.19 Comparison moment-curvature curve (M_x&ϕ_x) column B4.

COMPARISON MOMENT-CURVATURE CURVE (M_y&ϕ_y) FOR COLUMN B4.

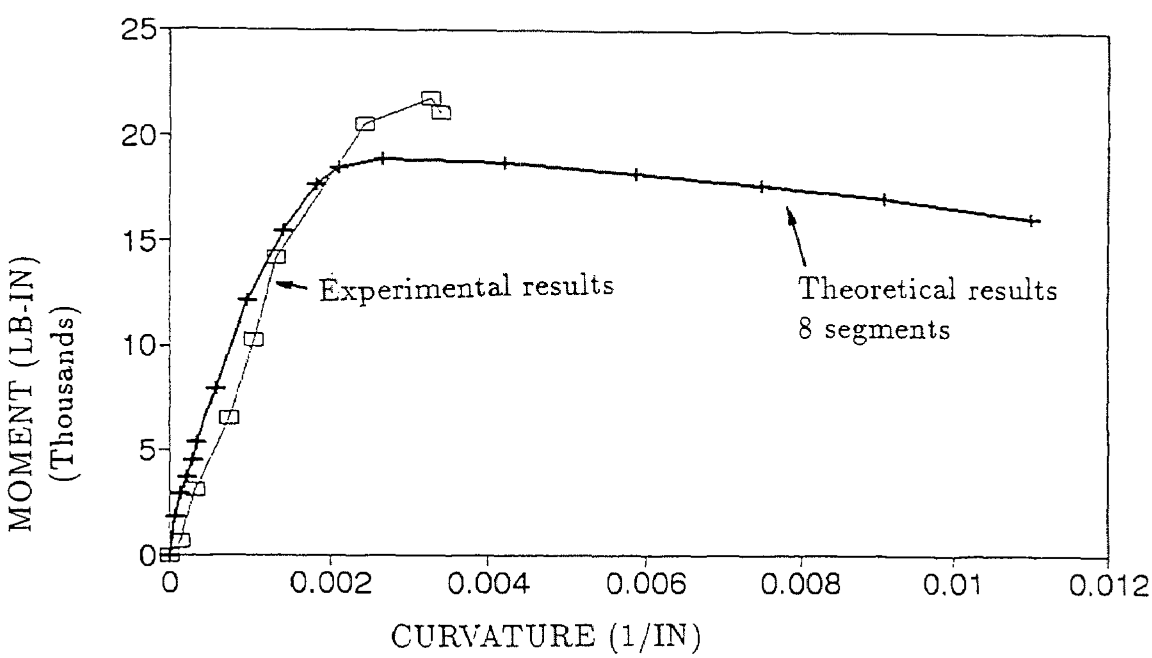

Figure. D.20 Comparison moment-curvature curve (M_y&ϕ_y) column B4.

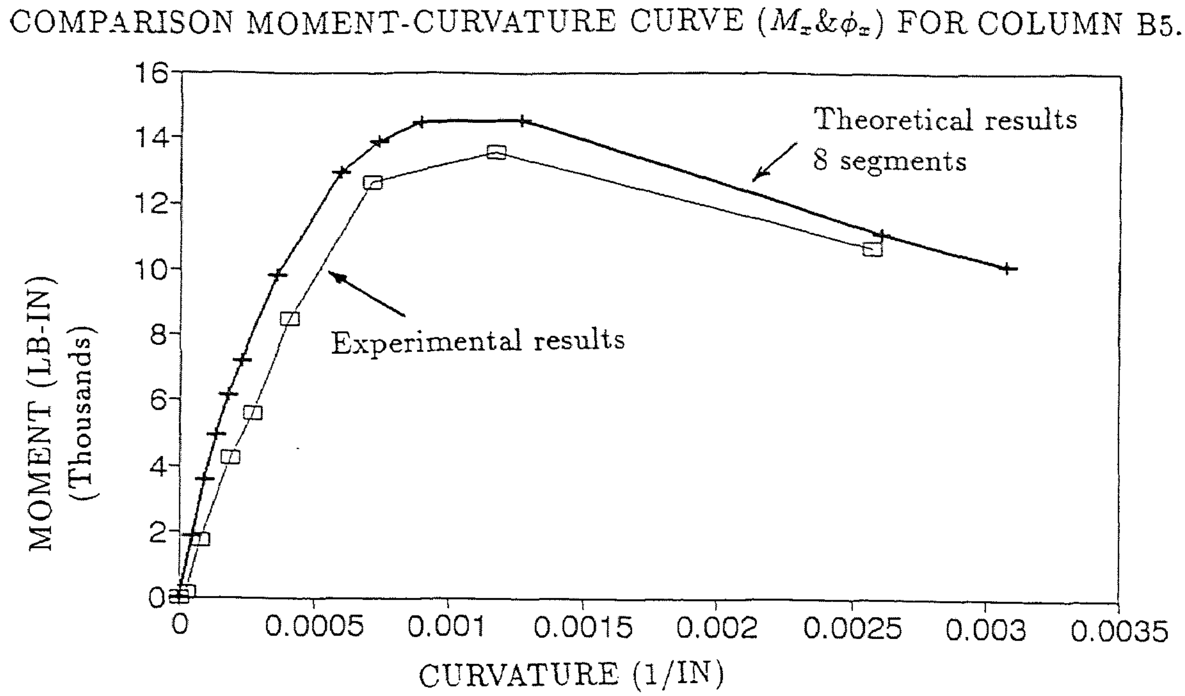

Figure. D.21 Comparison moment-curvature curve (M_x&ϕ_x) column B5.

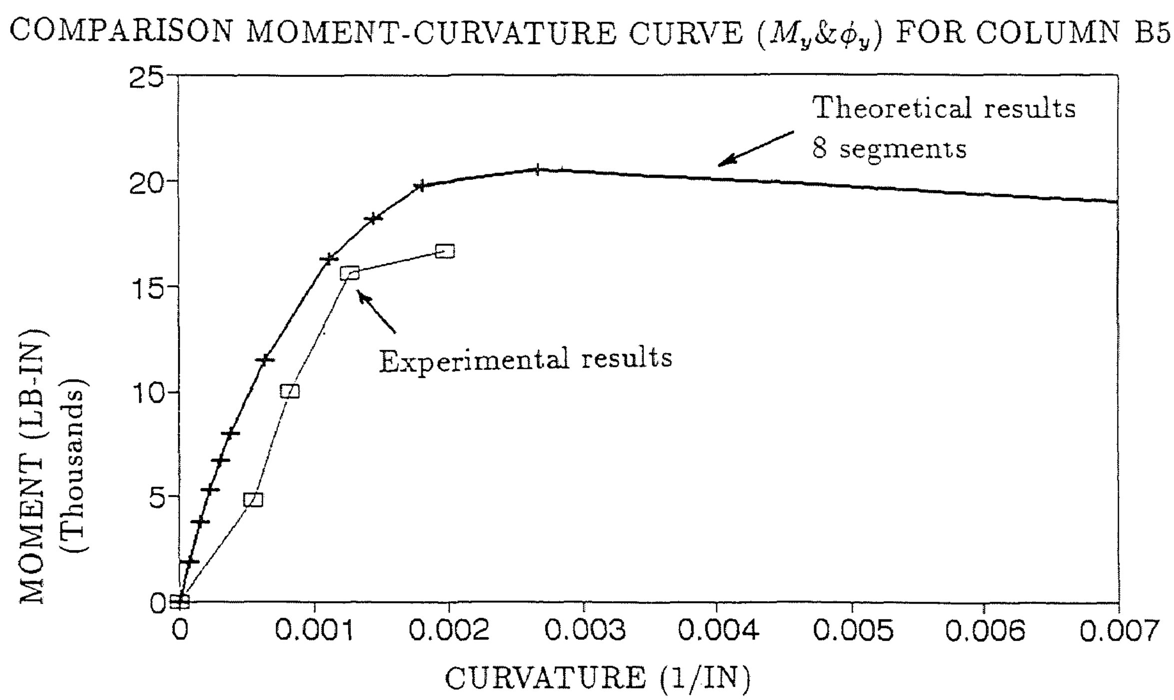

Figure. D.22 Comparison moment-curvature curve (M_y&ϕ_y) column B5.

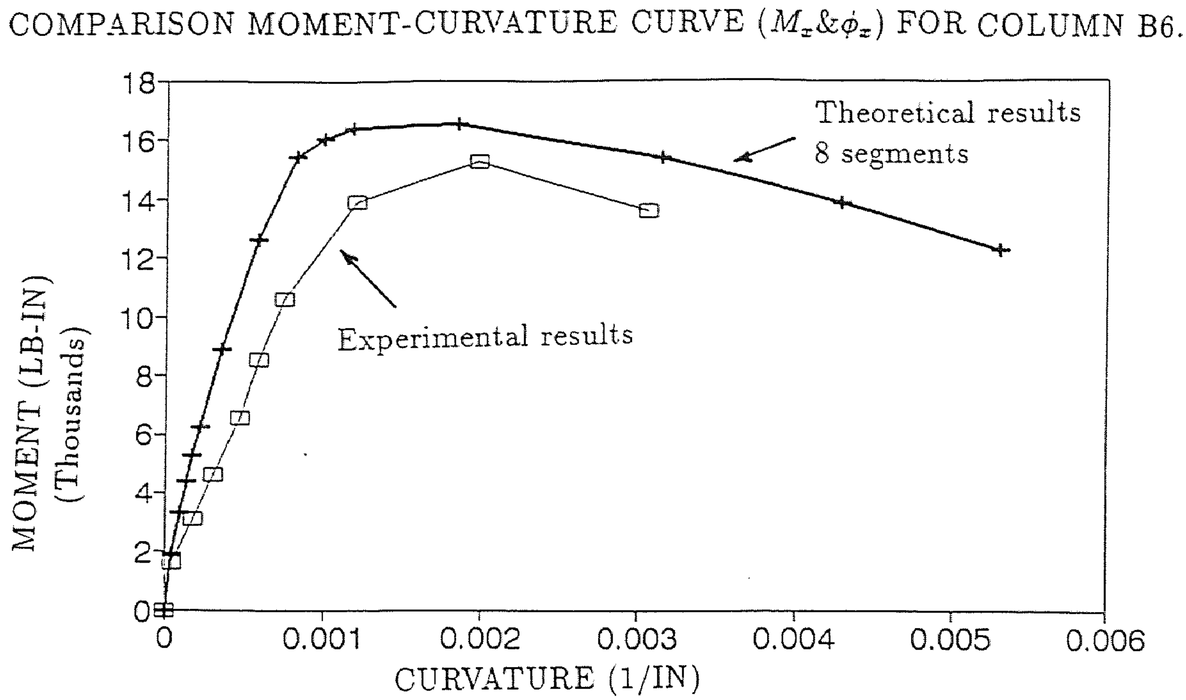

Figure. D.23 Comparison moment-curvature curve (M_x&φ_x) column B6.

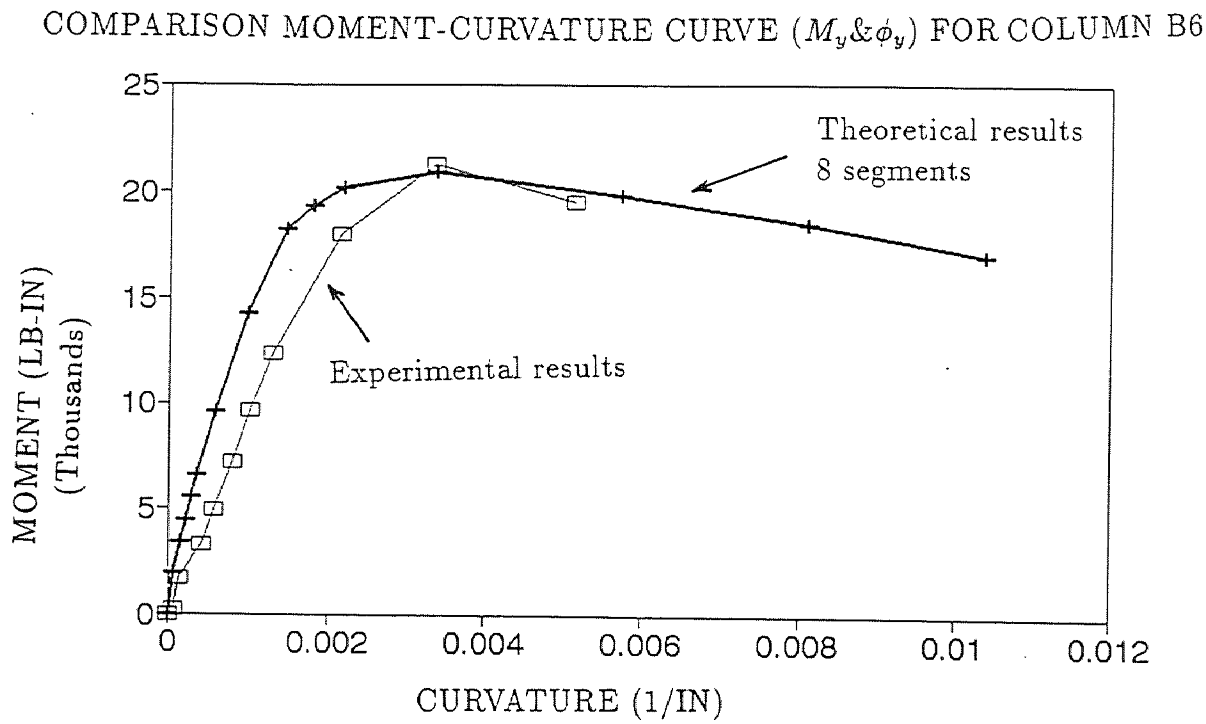

Figure. D.24 Comparison moment-curvature curve (M_y&ϕ_y) column B6.

COMPARISON MOMENT-CURVATURE CURVE (M_x&ϕ_x) FOR COLUMN B7.

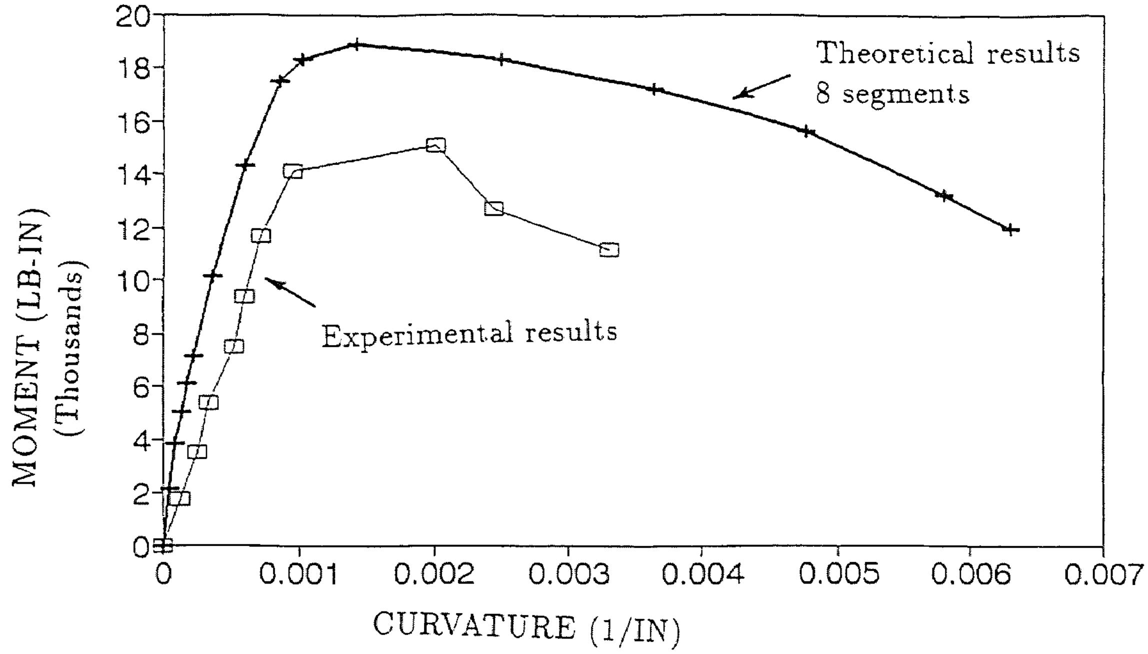

Figure. D.25 Comparison moment-curvature curve (M_x&ϕ_x) column B7.

COMPARISON MOMENT-CURVATURE CURVE (M_y&ϕ_y) FOR COLUMN B7.

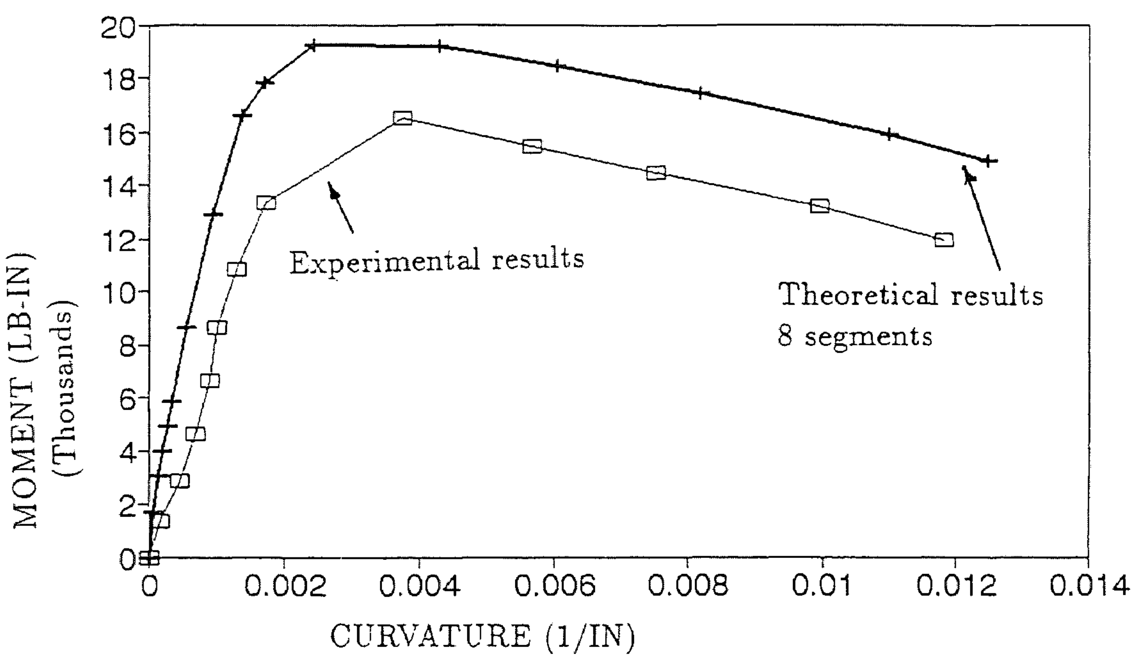

Figure. D.26 Comparison moment-curvature curve (M_y&ϕ_y) column B7.

COMPARISON MOMENT-CURVATURE CURVE (M_x&ϕ_x) FOR COLUMN B8.

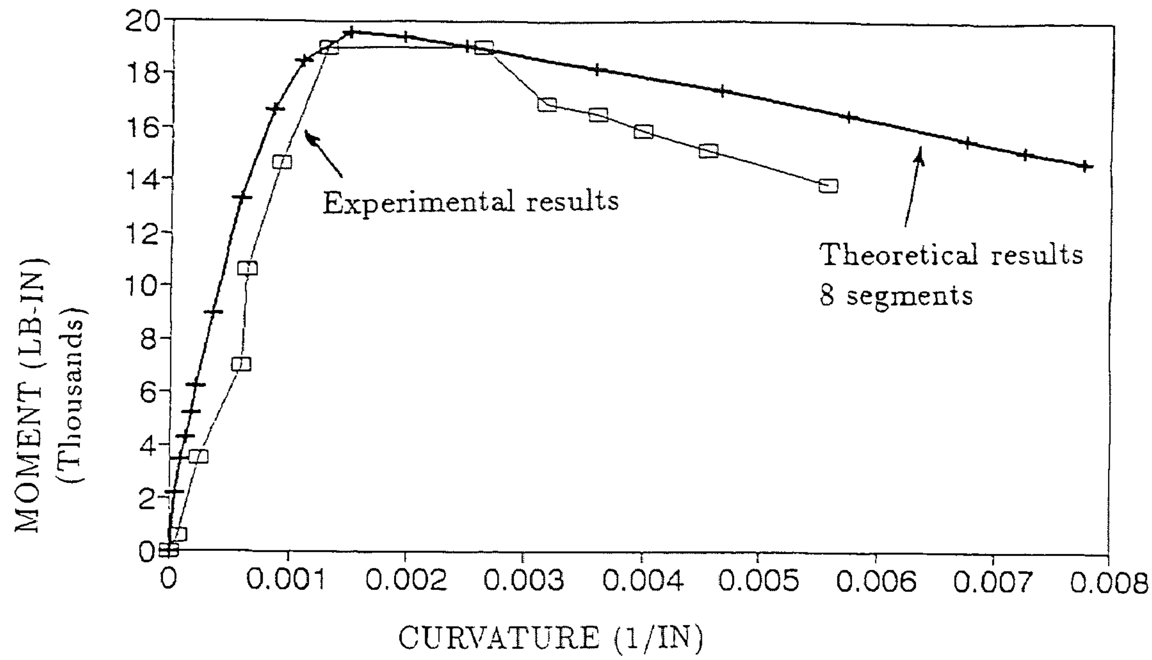

Figure. D.27 Comparison moment-curvature curve (M_x&ϕ_x) column B8.

COMPARISON MOMENT-CURVATURE CURVE (M_y&ϕ_y) FOR COLUMN B8.

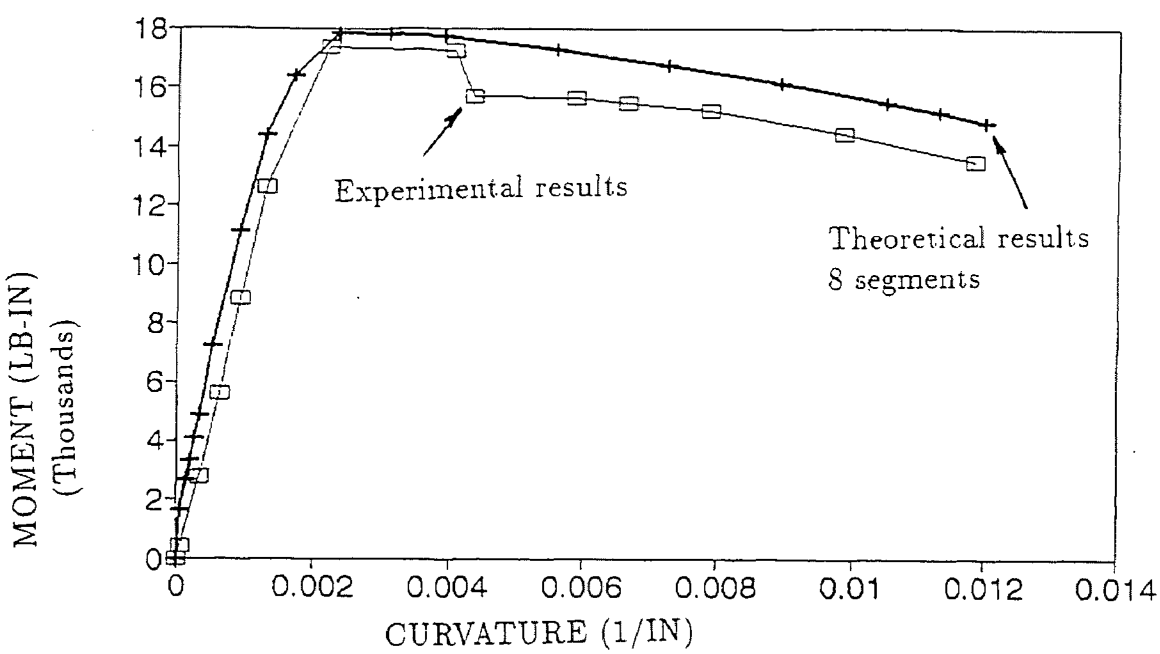

Figure. D.28 Comparison moment-curvature curve (M_y&ϕ_y) column B8.

Appendix E.

Theoretical and Experimental Comparisons for C-series Square Slender Columns.

Fig. E.1 through E.12 present theoretical and experimental comparisons of load-deflection curves and Fig. E.13 through E. 26 present theoretical and experimental comparisons of moment-curvature curves.

-⊟- Experimental results.

—+— Theoretical results. (8 segments)

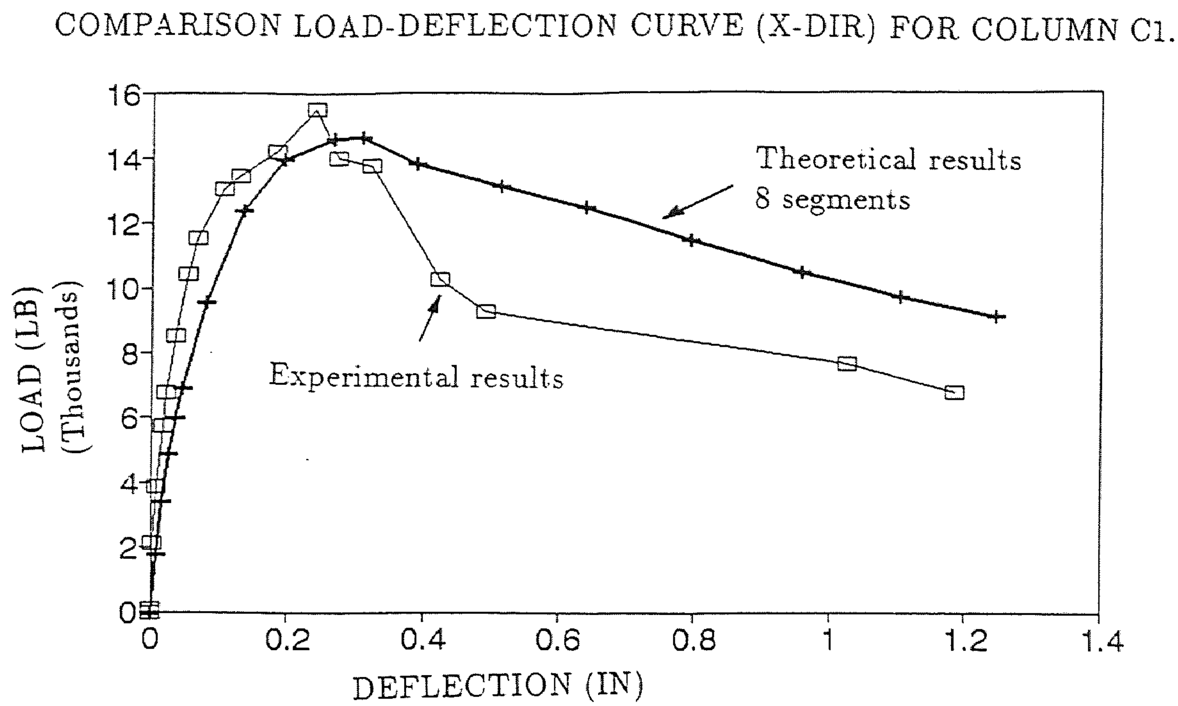

Figure. E.1 Comparison load-deflection curve (X-DIR.) for column C1.

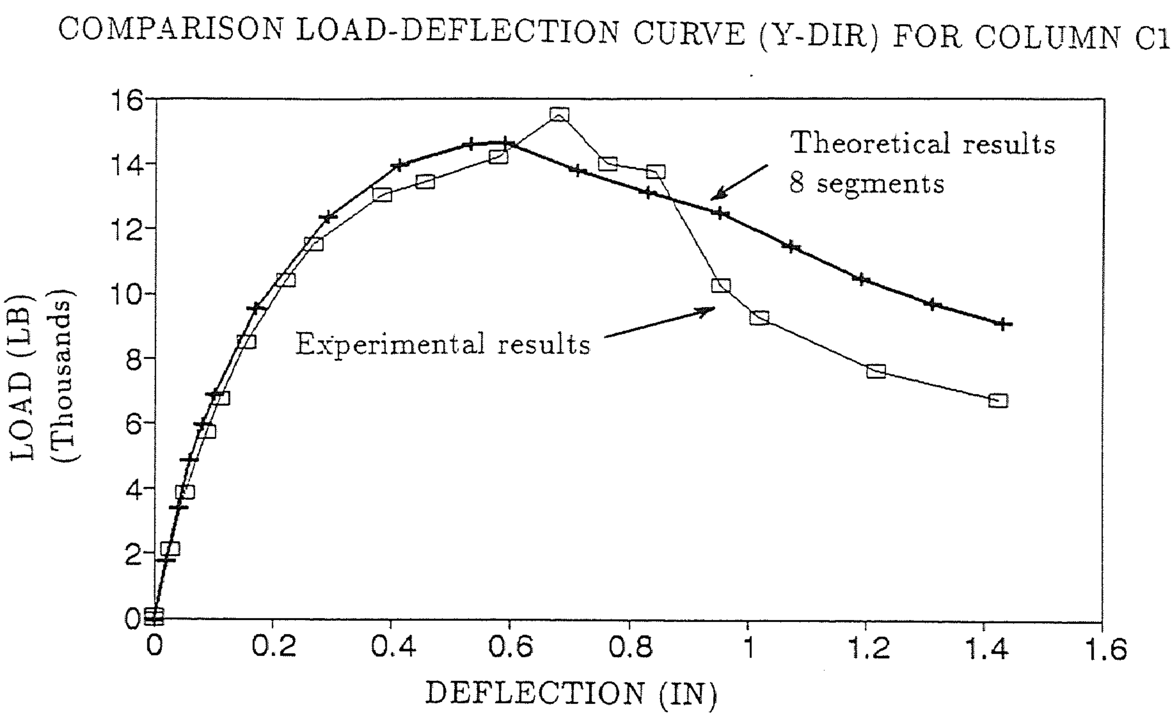

Figure. E.2 Comparison load-deflection curve (Y-DIR.) for column C1.

COMPARISON LOAD-DEFLECTION CURVE (X-DIR) FOR COLUMN C2.

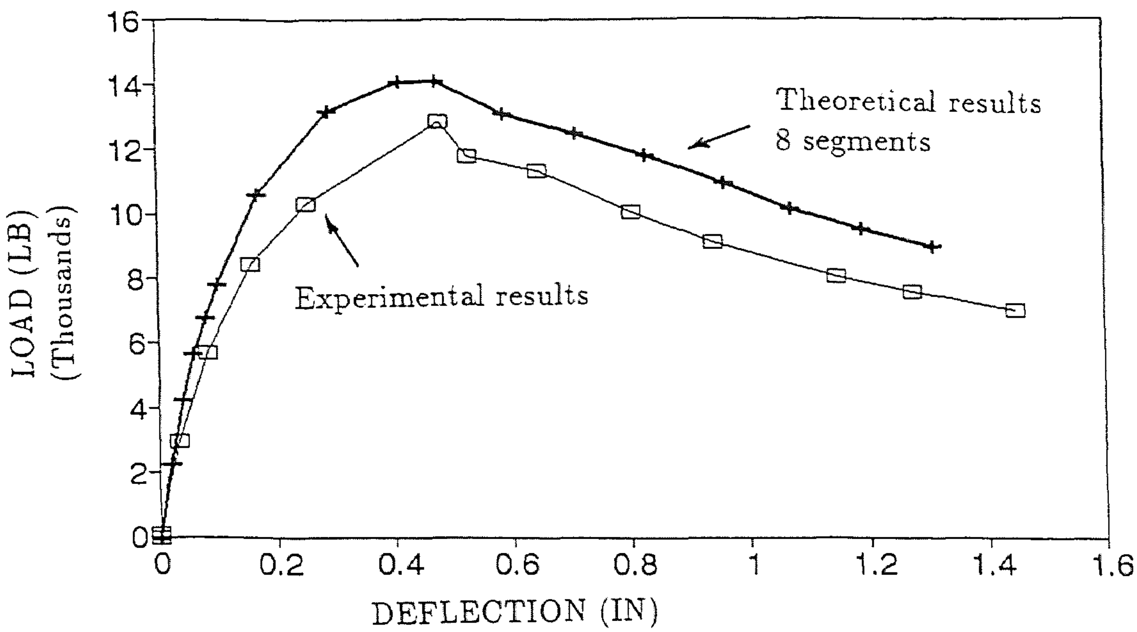

Figure. E.3 Comparison load-deflection curve (X-DIR.) for column C2.

COMPARISON LOAD-DEFLECTION CURVE (Y-DIR) FOR COLUMN C2.

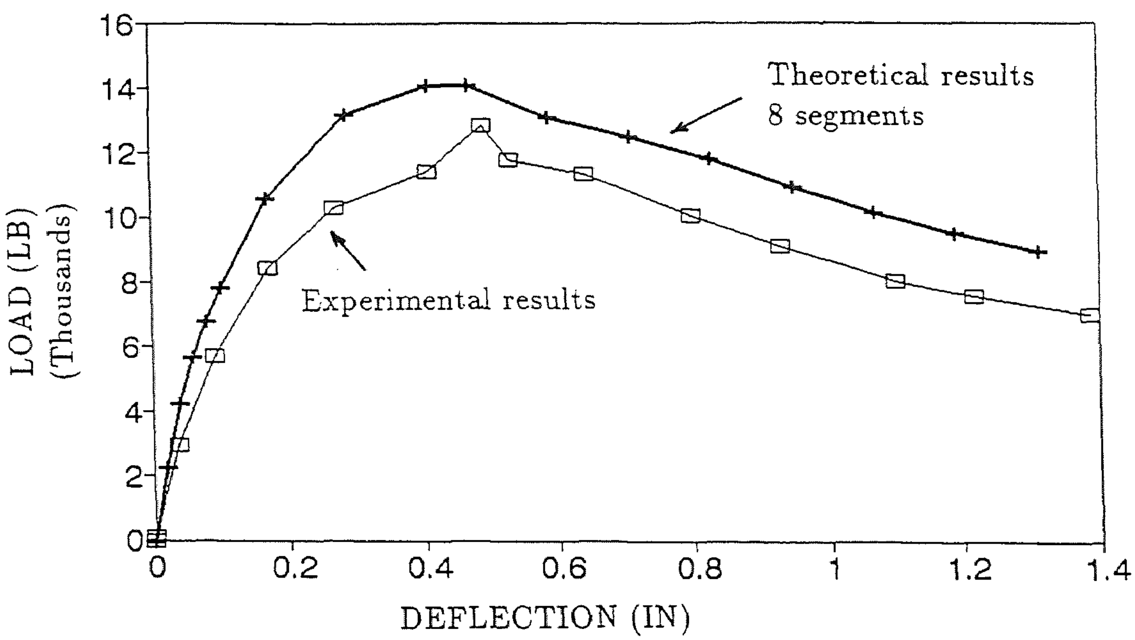

Figure. E.4 Comparison load-deflection curve (Y-DIR.) for column C2.

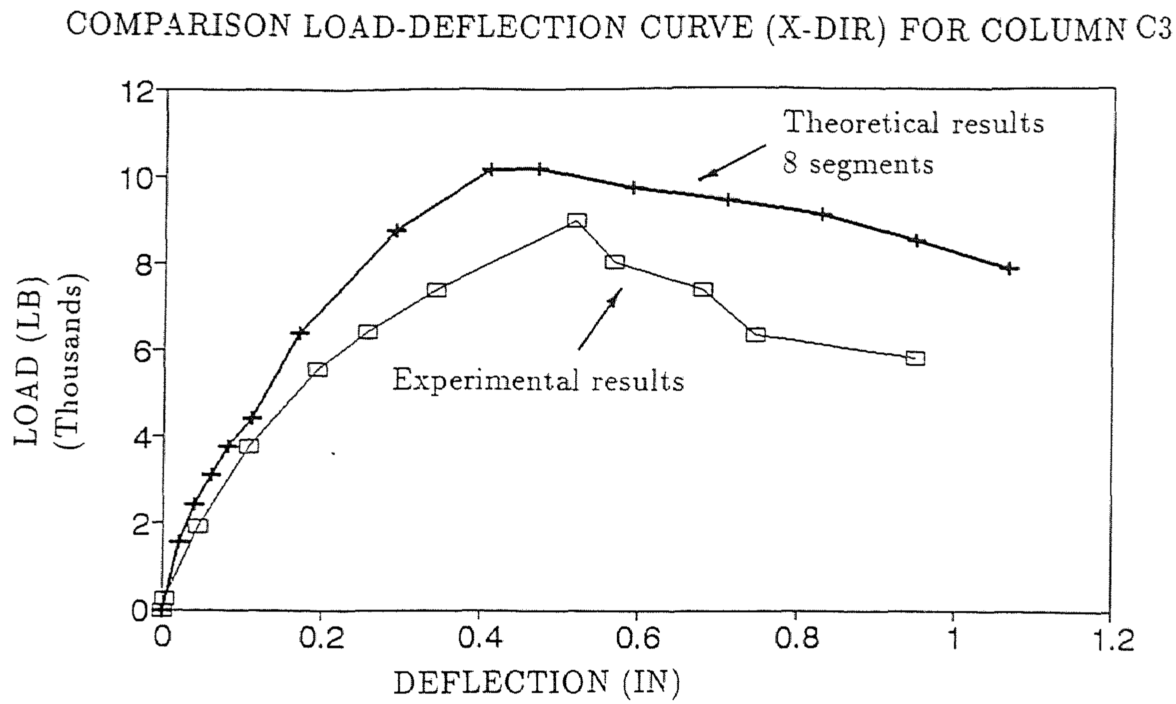

Figure. E.5 Comparison load-deflection curve (X-DIR.) for column C3.

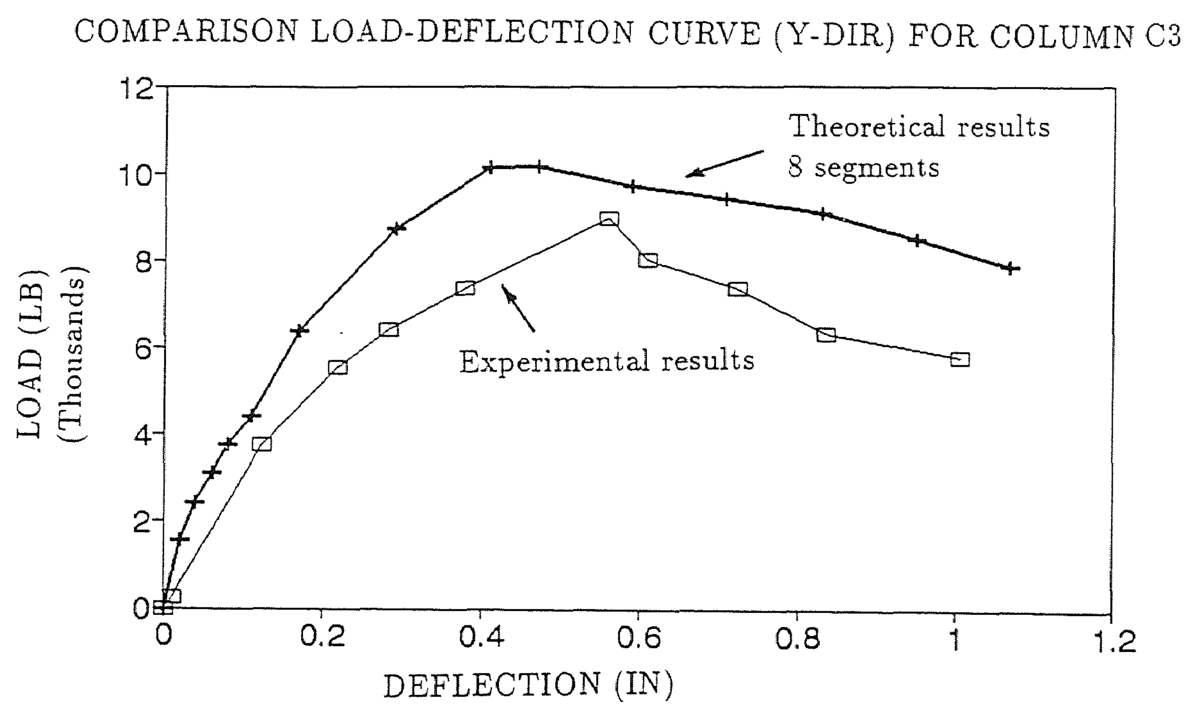

Figure. E.6 Comparison load-deflection curve (Y-DIR.) for column C3.

COMPARISON LOAD-DEFLECTION CURVE (X-DIR) FOR COLUMN C4.

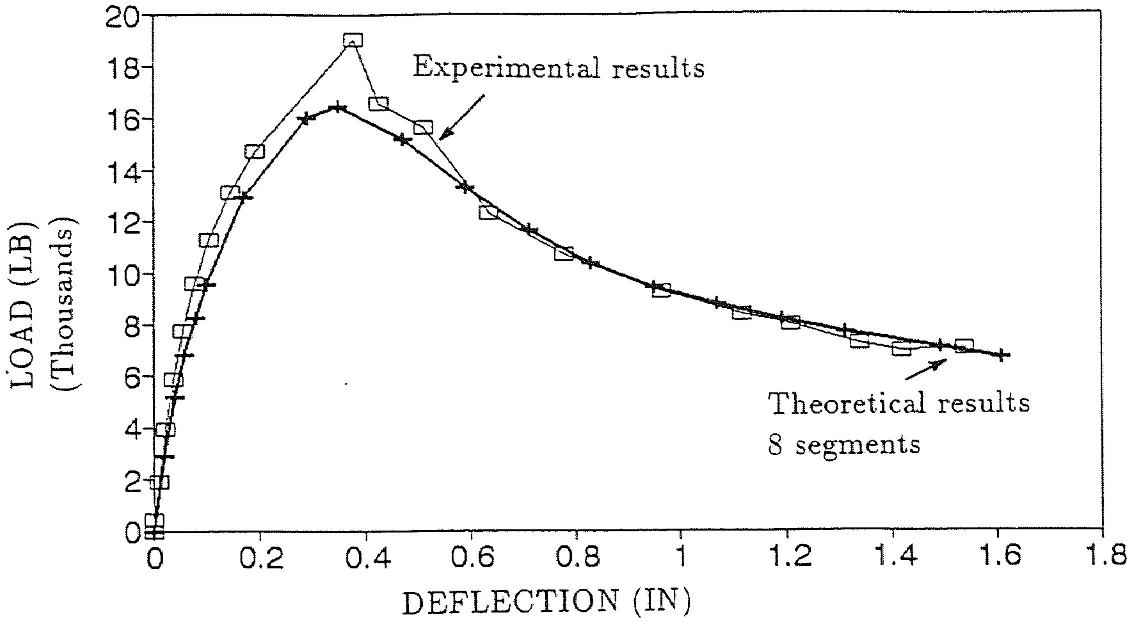

Figure. E.7 Comparison load-deflection curve (X-DIR.) for column C4.

COMPARISON LOAD-DEFLECTION CURVE (Y-DIR) FOR COLUMN C4.

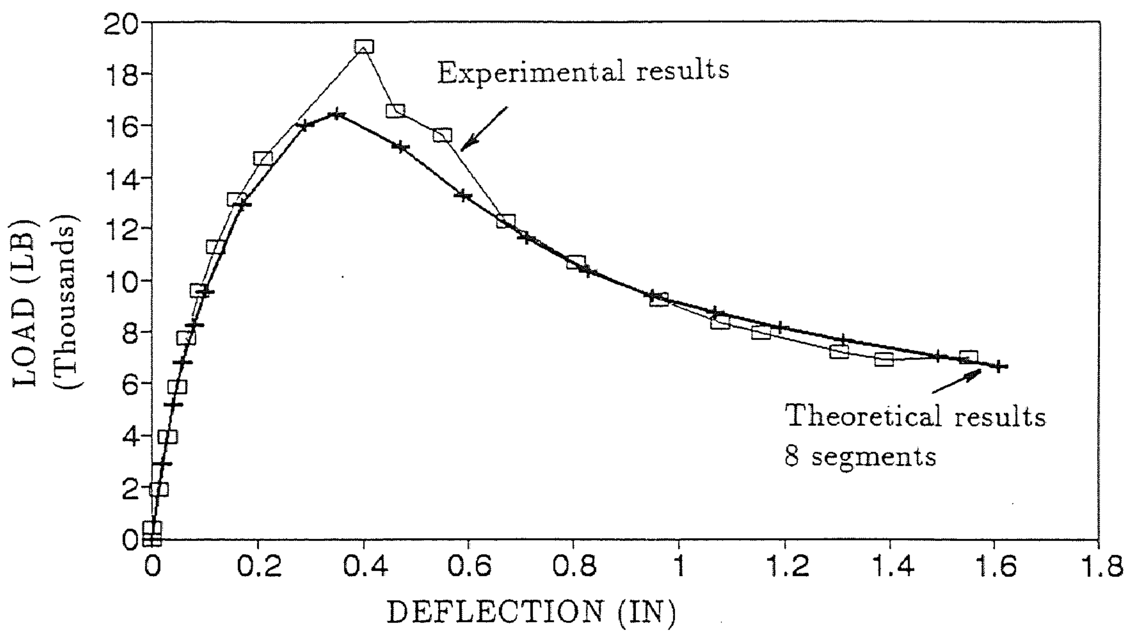

Figure. E.8 Comparison load-deflection curve (Y-DIR.) for column C4.

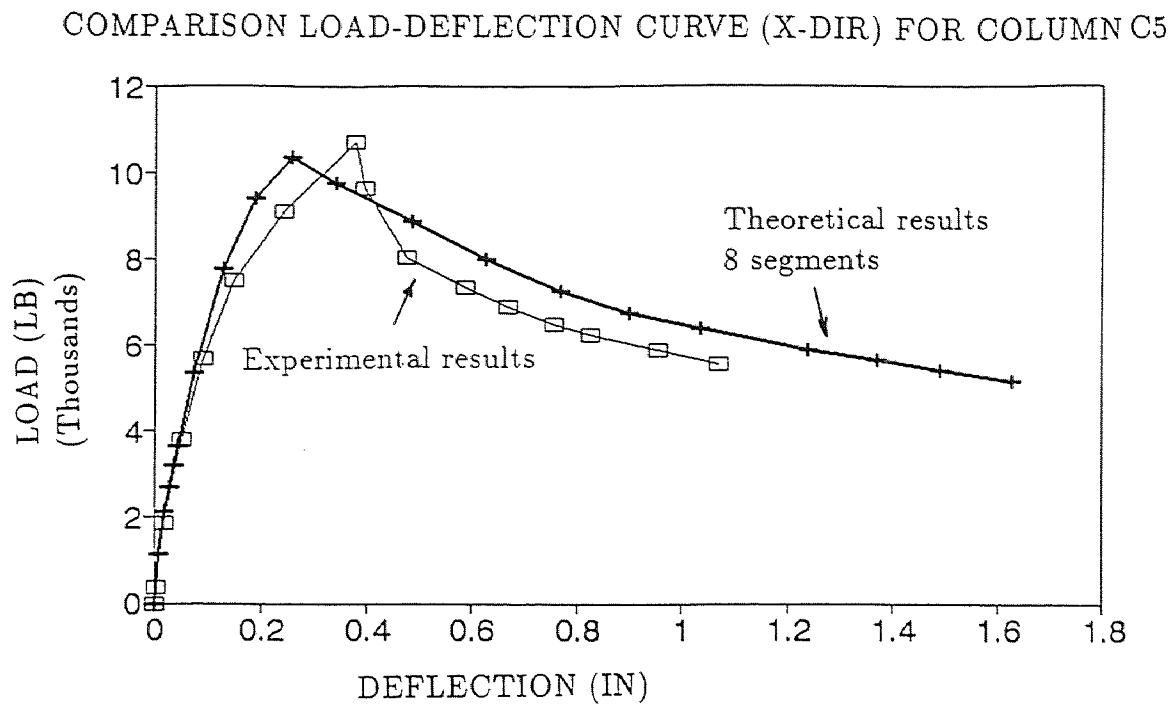

Figure. E.9 Comparison load-deflection curve (X-DIR.) for column C5.

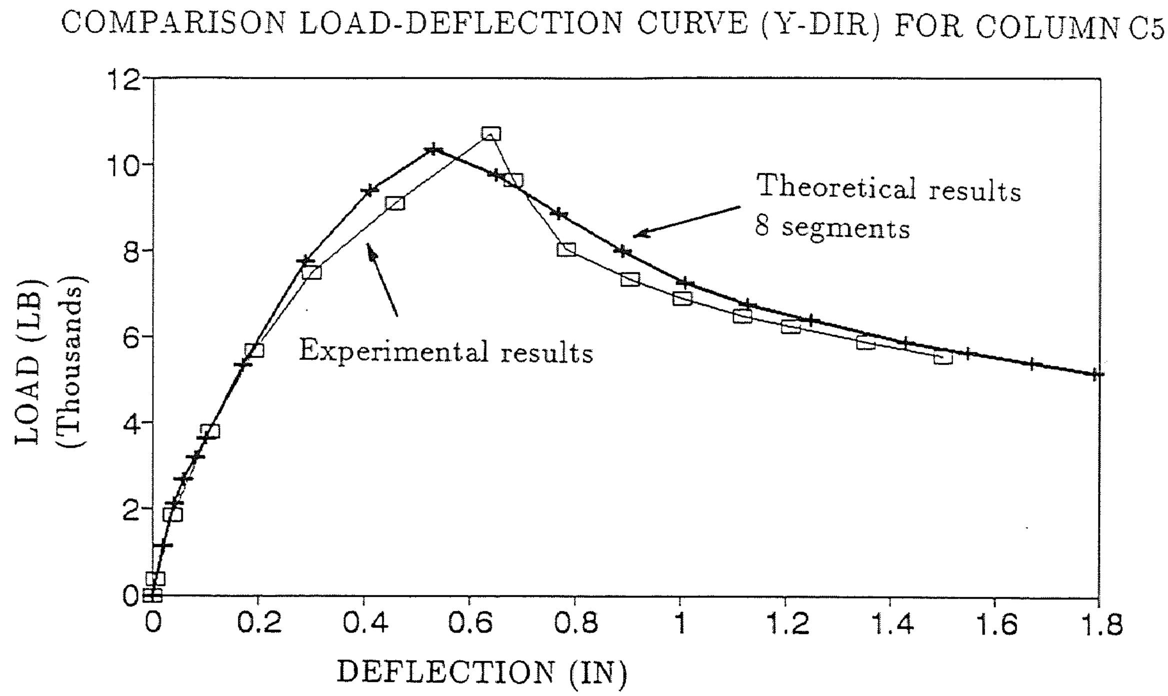

Figure. E.10 Comparison load-deflection curve (Y-DIR.) for column C5.

COMPARISON LOAD-DEFLECTION CURVE (X-DIR) FOR COLUMN C6.

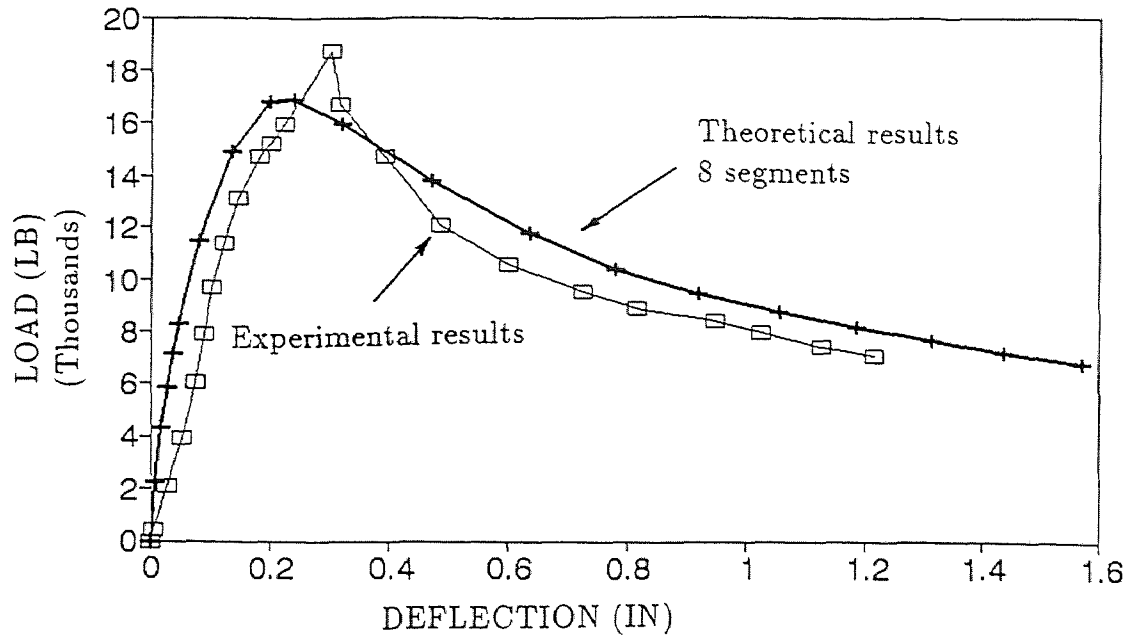

Figure. E.11 Comparison load-deflection curve (X-DIR.) for column C6.

COMPARISON LOAD-DEFLECTION CURVE (Y-DIR) FOR COLUMN C6.

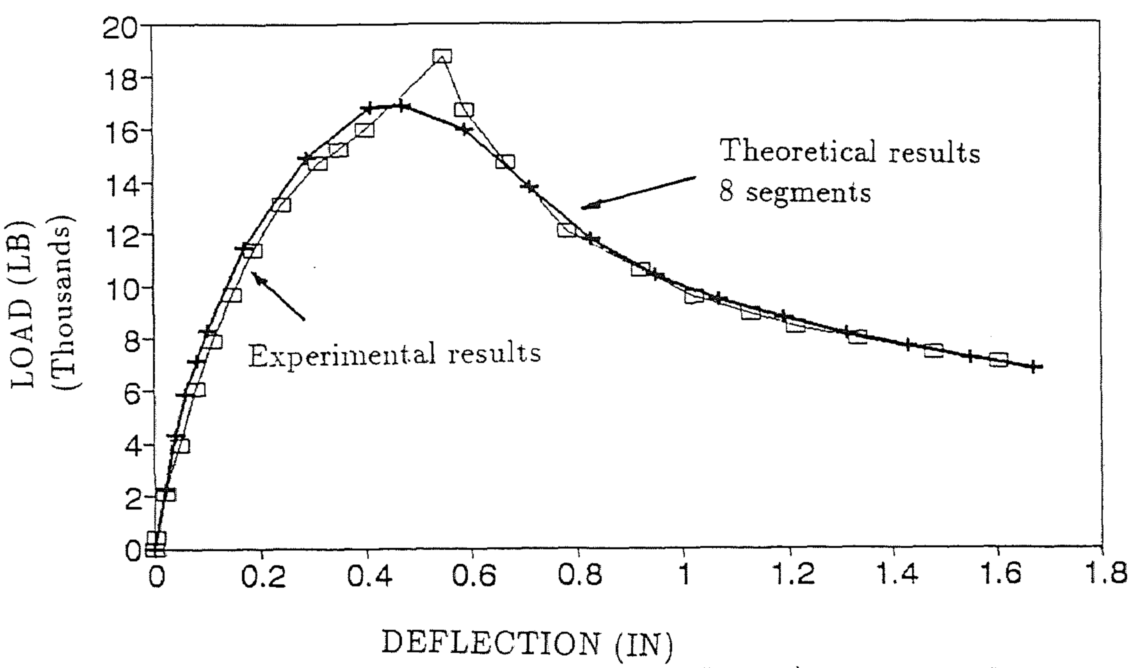

Figure. E.12 Comparison load-deflection curve (Y-DIR.) for column C6.

COMPARISON MOMENT-CURVATURE CURVE (M_x&ϕ_x) FOR COLUMN C1.

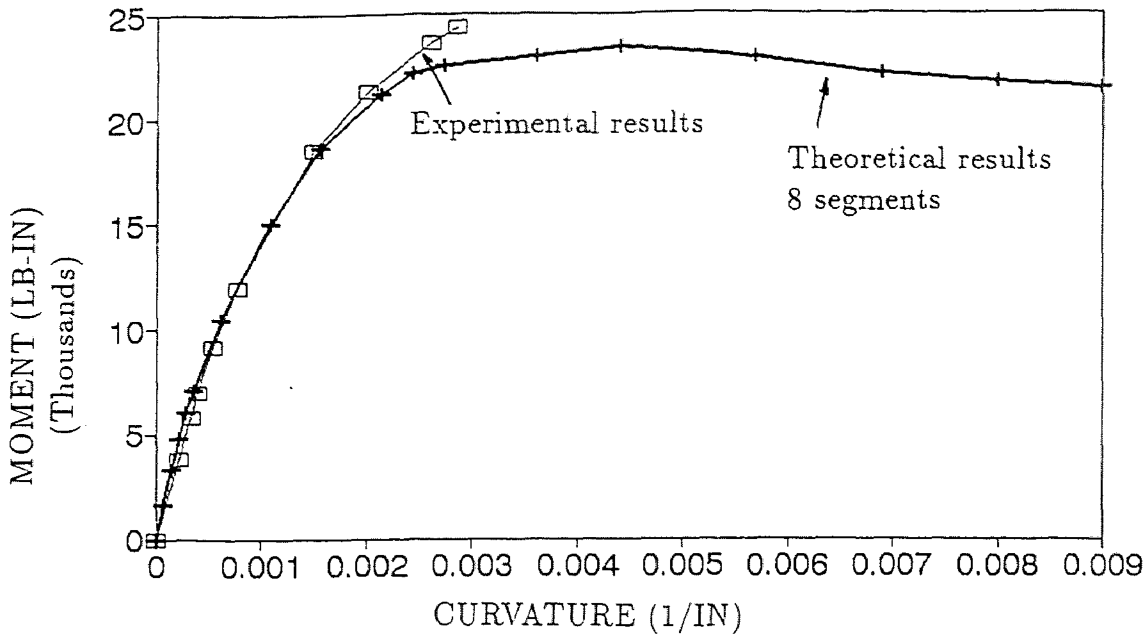

Figure. E.13 Comparison moment-curvature curve (M_x&ϕ_x) column C1.

COMPARISON MOMENT-CURVATURE CURVE (M_y&ϕ_y) FOR COLUMN C1.

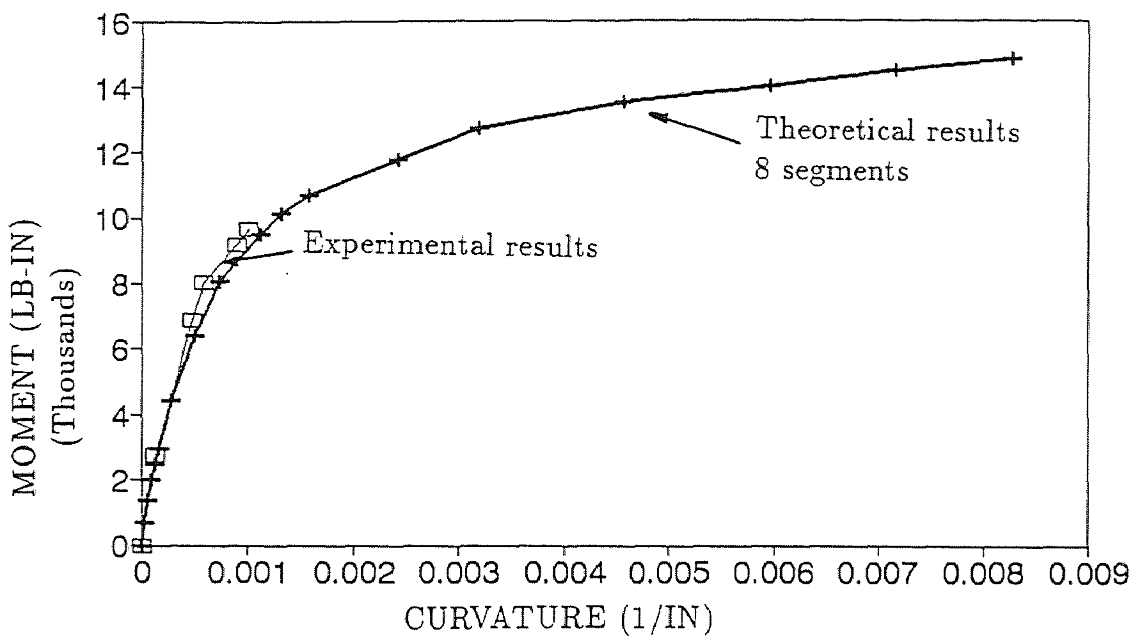

Figure. E.14 Comparison moment-curvature curve (M_y&ϕ_y) column C1.

COMPARISON MOMENT-CURVATURE CURVE (M_x&ϕ_x) FOR COLUMN C2.

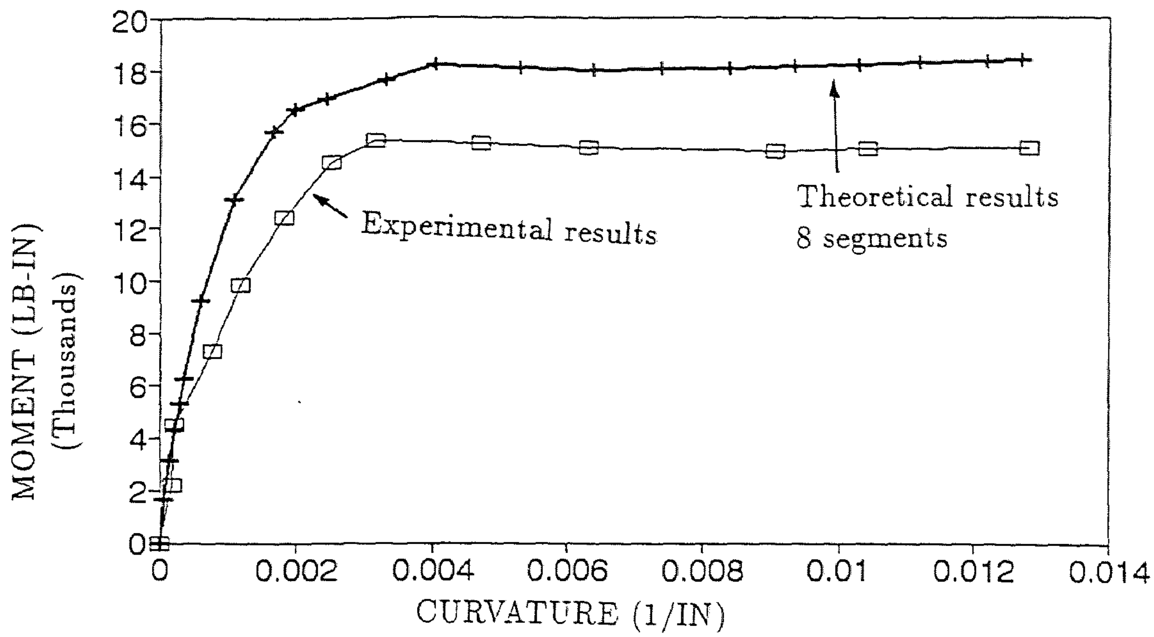

Figure. E.15 Comparison moment-curvature curve (M_x&ϕ_x) column C2.

COMPARISON MOMENT-CURVATURE CURVE (M_y&ϕ_y) FORCOLUMN C2.

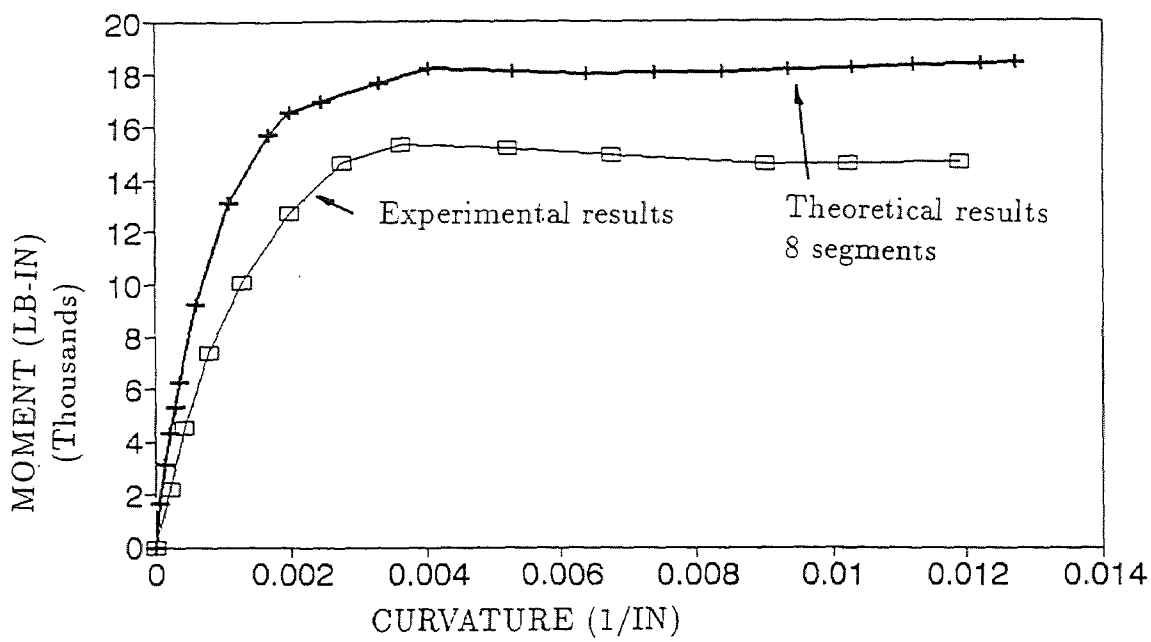

Figure. E.16 Comparison moment-curvature curve (M_y&ϕ_y) column C2.

COMPARISON MOMENT-CURVATURE CURVE (M_x&ϕ_x) FOR COLUMN C3.

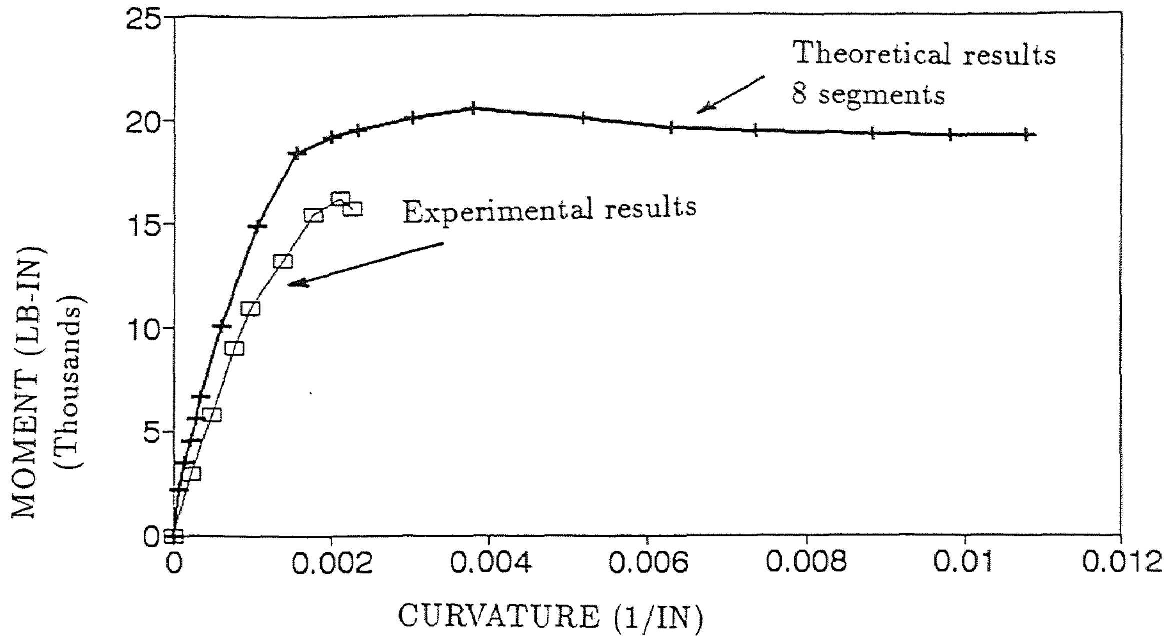

Figure. E.17 Comparison moment-curvature curve (M_x&ϕ_x) column C3.

COMPARISON MOMENT-CURVATURE CURVE (M_y&ϕ_y) FOR COLUMN C3.

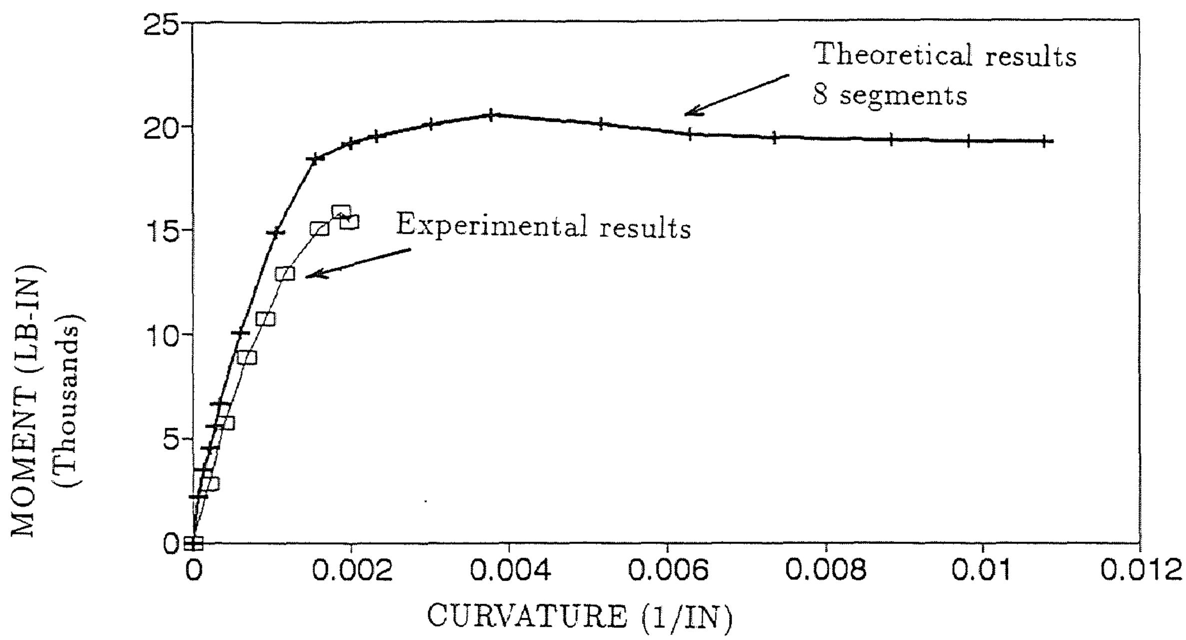

Figure. E.18 Comparison moment-curvature curve (M_y&ϕ_y) column C3.

COMPARISON MOMENT-CURVATURE CURVE (M_x&ϕ_x) FOR COLUMN C4.

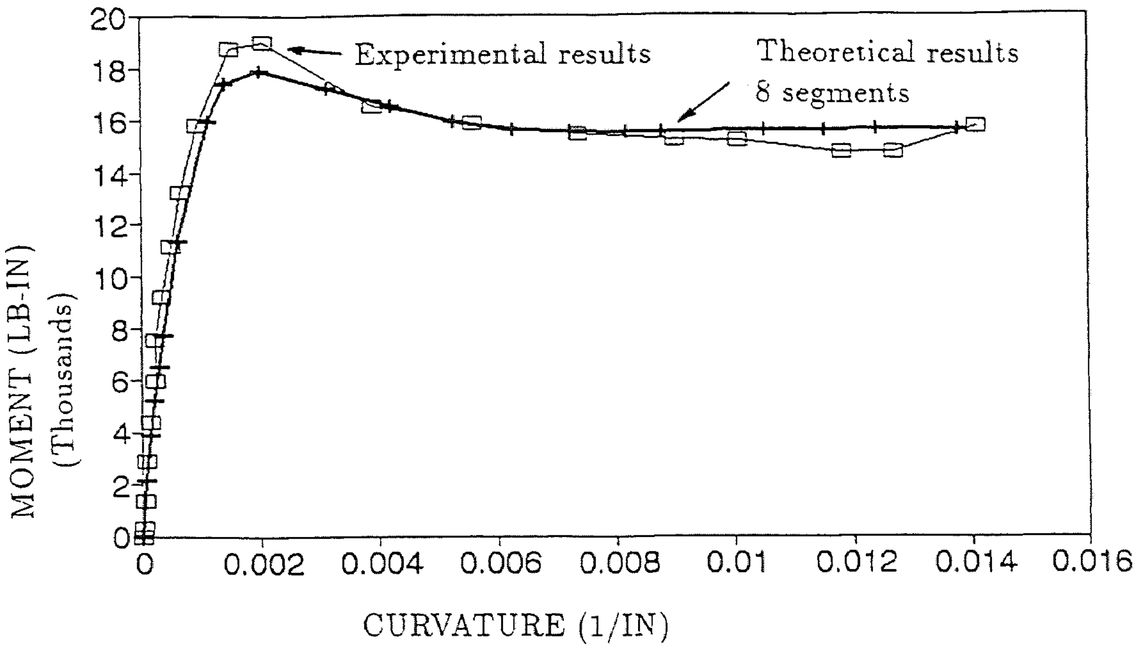

Figure. E.19 Comparison moment-curvature curve (M_x&ϕ_x) column C4.

COMPARISON MOMENT-CURVATURE CURVE (M_y&ϕ_y) FOR COLUMN C4.

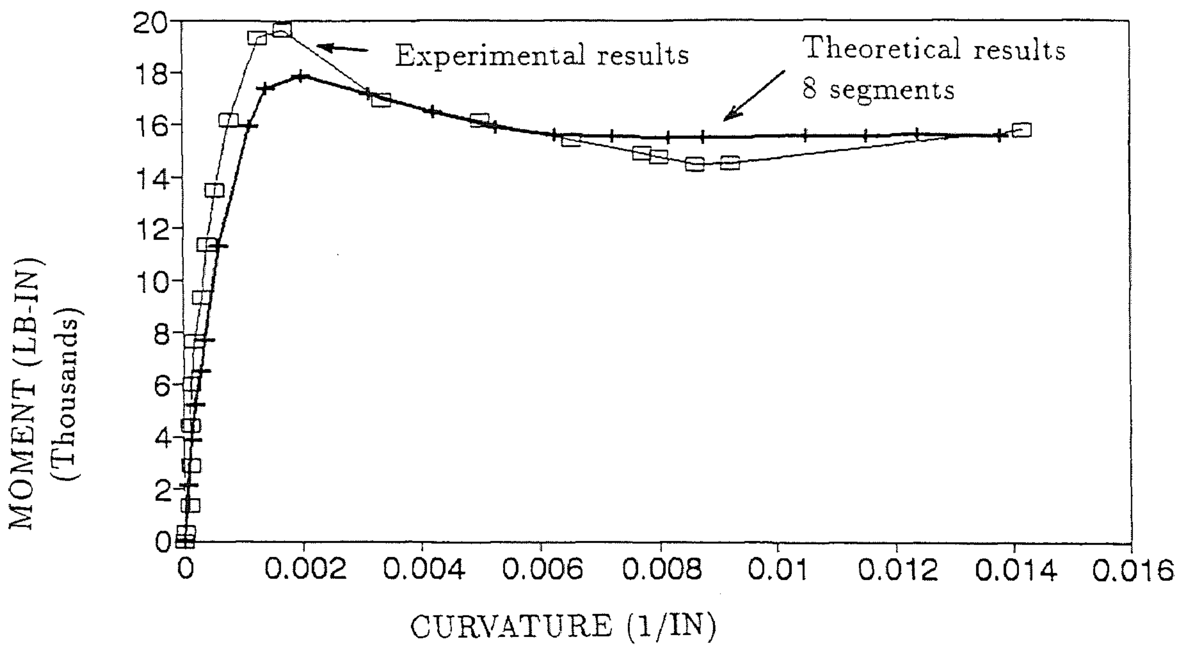

Figure. E.20 Comparison moment-curvature curve (M_y&ϕ_y) column C4.

COMPARISON MOMENT-CURVATURE CURVE (M_x&ϕ_x) FOR COLUMN C5.

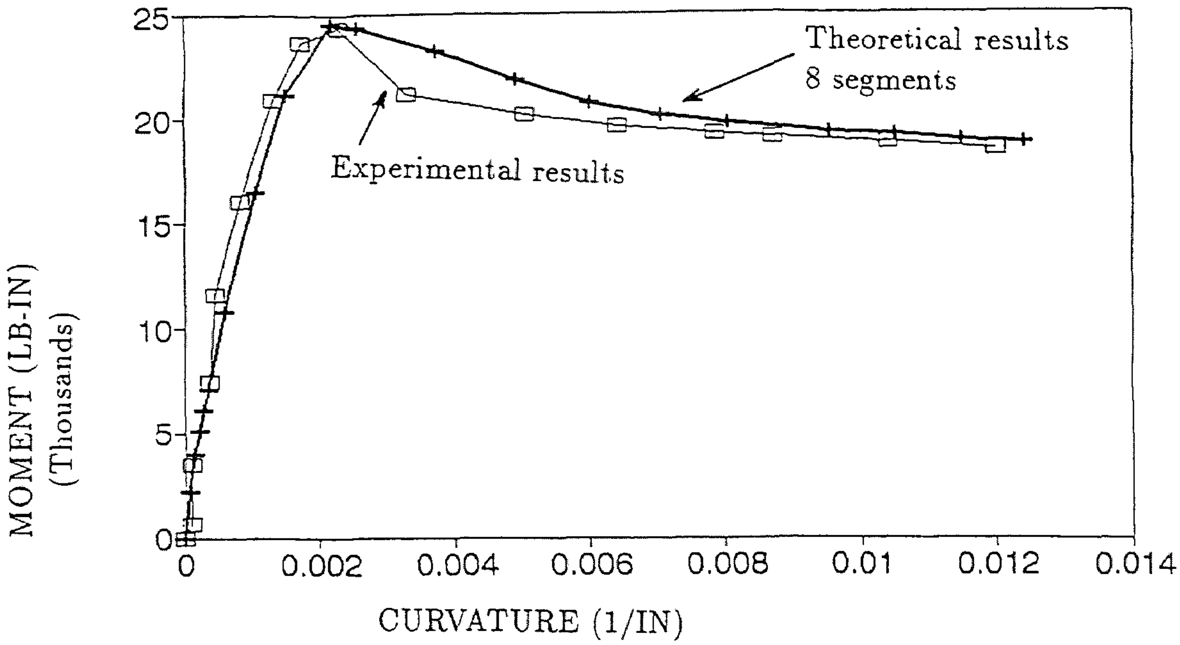

Figure. E.21 Comparison moment-curvature curve (M_x&ϕ_x) column C5.

COMPARISON MOMENT-CURVATURE CURVE (M_y&ϕ_y) FOR COLUMN C5.

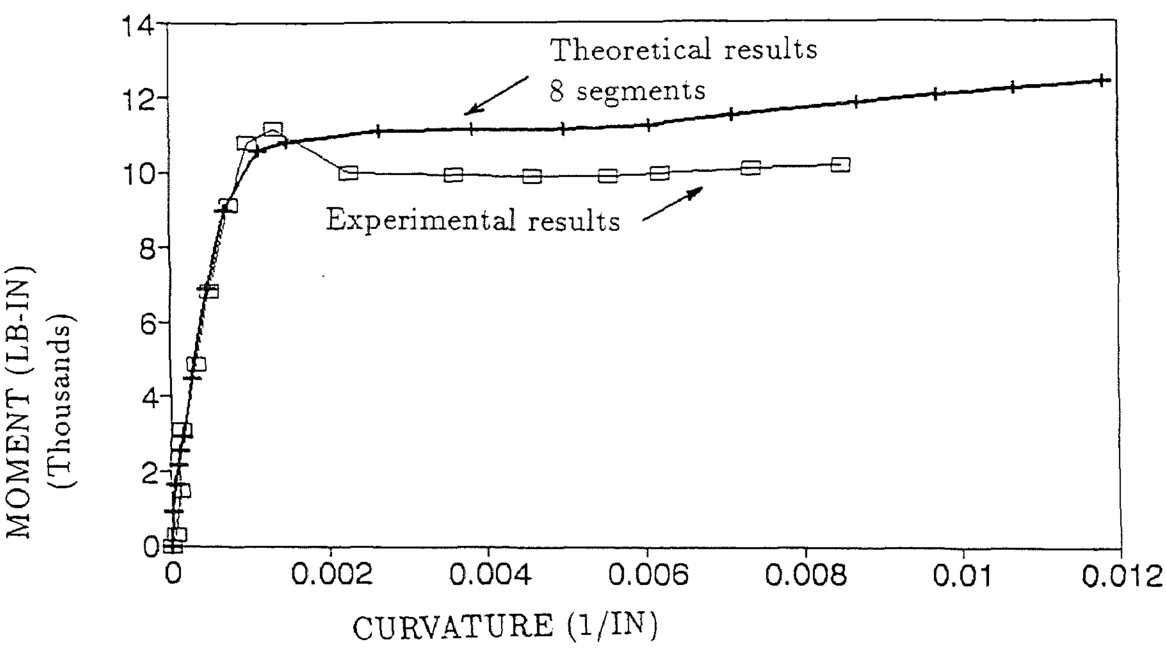

Figure. E.22 Comparison moment-curvature curve (M_y&ϕ_y) column C5.

COMPARISON MOMENT-CURVATURE CURVE (M_x&ϕ_x) FOR COLUMN C6.

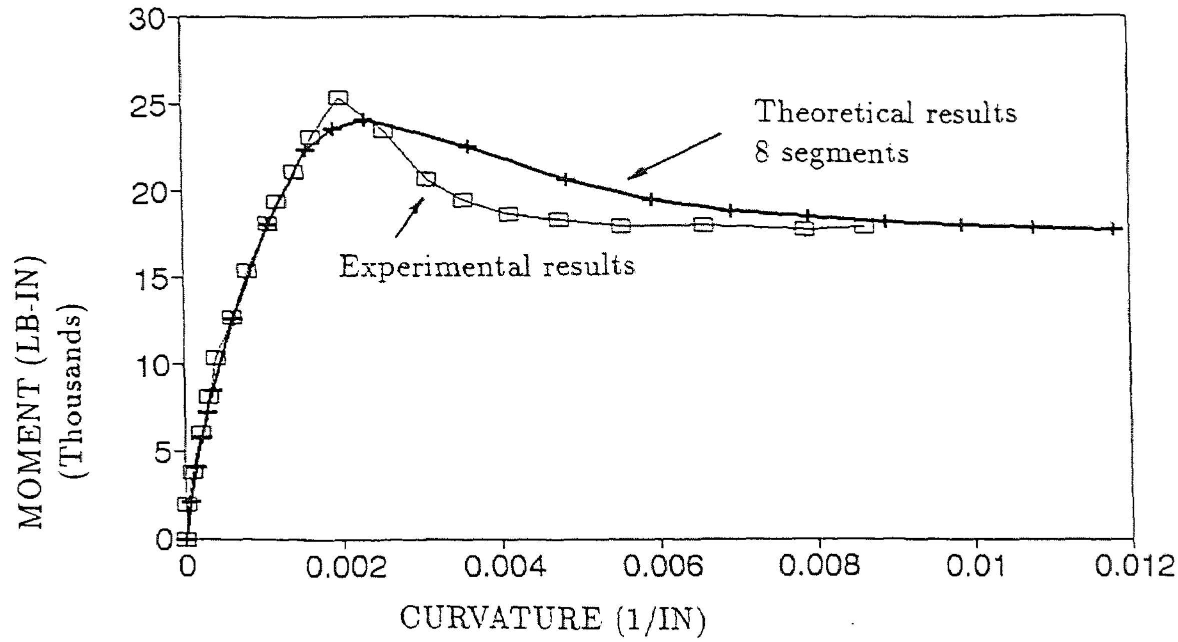

Figure. E.23 Comparison moment-curvature curve (M_x&ϕ_x) column C6.

COMPARISON MOMENT-CURVATURE CURVE (M_y&ϕ_y) FORCOLUMN C6.

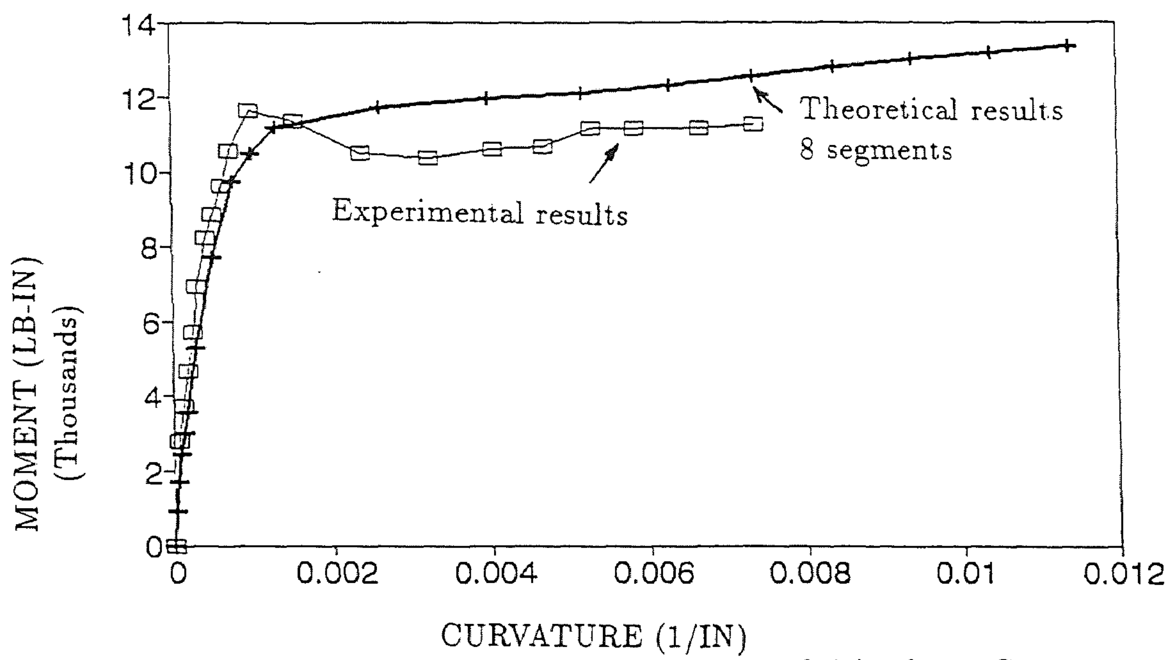

Figure. E.24 Comparison moment-curvature curve (M_y&ϕ_y) column C6.

Appendix F.

Modified Cranston-Chatterji stress-strain curve

Ritter's parabola:

$$f = f_c' \, (2 \, \frac{\epsilon}{\epsilon_0} - (\frac{\epsilon}{\epsilon_0})^2)$$

$$p'' = \frac{2(B2 + D2) AS2}{B2 \; D2 \; SP}$$

$$\epsilon_{cu}'' = \epsilon_0 + \frac{(P'')^{1/3}}{24.5}$$

$$\epsilon_{cu}'''' = \epsilon_0 + \frac{(P'' + 0.05)^{1/3}}{24.5}$$

$$f_t = 500psi, E_c = \frac{500}{\epsilon_t} = 1000 \; f_c'$$

$$\epsilon_{ct} = \frac{500}{1000 \; f_c'} = \frac{1}{2 \; f_c'}$$

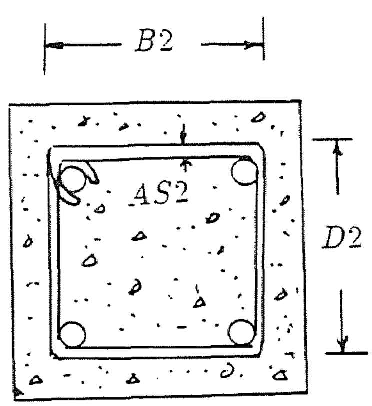

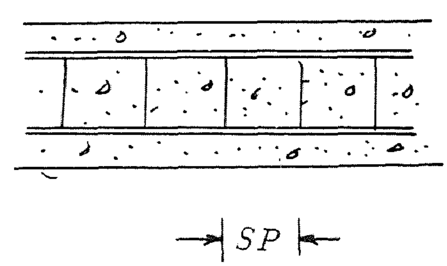

Appendix G. DETAILS OF SCHEME FOR REDIVISION OF SEGMENTS

$$\left\{ \begin{array}{c} P_{(c)} \\ P_{(c)}(e_v + d_v) \\ P_{(c)}(e_u + d_u) \end{array} \right\} = \begin{bmatrix} B_{11} & B_{12} & B_{13} \\ B_{21} & B_{22} & B_{23} \\ B_{31} & B_{32} & B_{33} \end{bmatrix} \left\{ \begin{array}{c} \epsilon_0 \\ \phi_u \\ \phi_v \end{array} \right\} \qquad (19)$$

The finite difference method is again used to solve the three dimensional behavior of slender columns after the plastic hinge forms. Fig. (10) shows segments are redivided.

For symmetrical case, the analysis can be further simplified. Let

lc =(nnod/2)+1

where lc = nodal number for the middle segment of column.

nnod= number of segments in slender column.

For segment (i),

$$\frac{d_{v_{(i+1)}} - 2d_{v_{(i)}} + d_{v_{(i-1)}}}{(CL)^2} = -(\phi_u)_i \qquad (20)$$
$$\frac{d_{u_{(i+1)}} - 2d_{u_{(i)}} + d_{u_{(i-1)}}}{(CL)^2} = -(\phi_v)_i$$

For segment (lc),

$$\frac{d_{v_{(lc+1)}} - 2d_{v_{(lc)}} + d_{v_{(lc-1)}}}{(CL2)^2} = -(\phi_u)_{lc} \qquad (G.1)$$
$$\frac{d_{u_{(lc+1)}} - 2d_{u_{(lc)}} + d_{u_{(lc-1)}}}{(CL2)^2} = -(\phi_v)_{lc}$$

For segment ($lc - 1$),

$$\frac{2(CL)d_{v_{(lc)}} - 2(CL2+CL)d_{v_{(lc-1)}} + 2(CL2)d_{v_{(lc-2)}}}{(CL2+CL)(CL)(CL2)} = -(\phi_u)_{lc-1} \quad (G.2)$$

$$\frac{2(CL)d_{u_{(lc)}} - 2(CL2+CL)d_{u_{(lc-1)}} + 2(CL2)d_{u_{(lc-2)}}}{(CL2+CL)(CL)(CL2)} = -(\phi_v)_{lc-1}$$

Substitute Eq. (20),(G.1),(G.2) in Eq. (18),

For segment (i),

$$\left\{ \begin{array}{c} P_{(c)} \\ P_{(c)}(e_v + d_{v_{(i)}}) \\ P_{(c)}(e_u + d_{u_{(i)}}) \end{array} \right\} = \begin{bmatrix} B_{11} & B_{12} & B_{13} \\ B_{21} & B_{22} & B_{23} \\ B_{31} & B_{32} & B_{33} \end{bmatrix} \left\{ \begin{array}{c} \epsilon_{0_{(i)}} \\ -(d_{v_{(i+1)}} - 2d_{v_{(i)}} + d_{v_{(i-1)}})/(CL)^2 \\ -(d_{u_{(i+1)}} - 2d_{u_{(i)}} + d_{u_{(i-1)}})/(CL)^2 \end{array} \right\} \quad (G.3)$$

For segment (lc),

$$\left\{ \begin{array}{c} P_{(c)} \\ P_{(c)}(e_v + d_{v_{(lc)}}) \\ P_{(c)}(e_u + d_{u_{(lc)}}) \end{array} \right\} = \begin{bmatrix} B_{11} & B_{12} & B_{13} \\ B_{21} & B_{22} & B_{23} \\ B_{31} & B_{32} & B_{33} \end{bmatrix} \left\{ \begin{array}{c} \epsilon_{0_{(lc)}} \\ -(d_{v_{(lc+1)}} - 2d_{v_{(lc)}} + d_{v_{(lc-1)}})/(CL2)^2 \\ -(d_{u_{(lc+1)}} - 2d_{u_{(lc)}} + d_{u_{(lc-1)}})/(CL2)^2 \end{array} \right\} \quad (G.4)$$

For segment $(lc-1)$,

$$\left\{ \begin{array}{c} P_{(c)} \\ P_{(c)}(e_v + d_{v_{(lc-1)}}) \\ P_{(c)}(e_u + d_{u_{(lc-1)}}) \end{array} \right\} = \begin{bmatrix} B_{11} & B_{12} & B_{13} \\ B_{21} & B_{22} & B_{23} \\ B_{31} & B_{32} & B_{33} \end{bmatrix}$$

$$\left\{ \begin{array}{c} \epsilon_{0_{(lc-1)}} \\ -2(CL)d_{v_{(lc)}} + 2(CL2+CL)d_{v_{(lc-1)}} - 2(CL2)d_{v_{(lc-2)}}/(CL2+CL)(CL)(CL2) \\ -2(CL)d_{u_{(lc)}} + 2(CL2+CL)d_{u_{(lc-1)}} - 2(CL2)d_{u_{(lc-2)}}/(CL2+CL)(CL)(CL2) \end{array} \right\} \quad (G.5)$$

Expand Eq. (18) and rearrange it, and for segment (i),

$$(CL)^2 \left\{ \begin{array}{c} P_{(c)} \\ P_{(c)}(e_v + d_{v_{(i)}}) \\ P_{(c)}(e_u + d_{u_{(i)}}) \end{array} \right\} =$$

$$\left[\begin{array}{ccccccc} (CL)^2 B_{11_{(i)}} & -B_{12_{(i)}} & -B_{13_{(i)}} & 2B_{12_{(i)}} & 2B_{13_{(i)}} & -B_{12_{(i)}} & -B_{13_{(i)}} \\ (CL)^2 B_{21_{(i)}} & -B_{22_{(i)}} & -B_{23_{(i)}} & 2B_{22_{(i)}} & 2B_{23_{(i)}} & -B_{22_{(i)}} & -B_{23_{(i)}} \\ (CL)^2 B_{31_{(i)}} & -B_{32_{(i)}} & -B_{33_{(i)}} & 2B_{32_{(i)}} & 2B_{33_{(i)}} & -B_{32_{(i)}} & -B_{33_{(i)}} \end{array} \right] \left\{ \begin{array}{c} \epsilon_{0_{(i)}} \\ d_{v_{(i-1)}} \\ d_{u_{(i-1)}} \\ d_{v_{(i)}} \\ d_{u_{(i)}} \\ d_{v_{(i+1)}} \\ d_{u_{(i+1)}} \end{array} \right\} \tag{G.6}$$

For segment (lc),

$$(CL2)^2 \left\{ \begin{array}{c} P_{(c)} \\ P_{(c)}(e_v + d_{v_{(lc)}}) \\ P_{(c)}(e_u + d_{u_{(lc)}}) \end{array} \right\} =$$

$$\left[\begin{array}{ccccccc} (CL2)^2 B_{11_{(lc)}} & -B_{12_{(lc)}} & -B_{13_{(lc)}} & 2B_{12_{(lc)}} & 2B_{13_{(lc)}} & -B_{12_{(lc)}} & -B_{13_{(lc)}} \\ (CL2)^2 B_{21_{(lc)}} & -B_{22_{(lc)}} & -B_{23_{(lc)}} & 2B_{22_{(lc)}} & 2B_{23_{(lc)}} & -B_{22_{(lc)}} & -B_{23_{(lc)}} \\ (CL2)^2 B_{31_{(lc)}} & -B_{32_{(lc)}} & -B_{33_{(lc)}} & 2B_{32_{(lc)}} & 2B_{33_{(lc)}} & -B_{32_{(lc)}} & -B_{33_{(lc)}} \end{array} \right] \left\{ \begin{array}{c} \epsilon_{0_{(lc)}} \\ d_{v_{(lc-1)}} \\ d_{u_{(lc-1)}} \\ d_{v_{(lc)}} \\ d_{u_{(lc)}} \\ d_{v_{(lc+1)}} \\ d_{u_{(lc+1)}} \end{array} \right\} \tag{G.7}$$

Let

C_0 =CL

$C_1 = (\mathrm{CL}+\mathrm{CL2})$

$C_2 = \mathrm{CL2}$

$C_3 = (\mathrm{CL}+\mathrm{CL2})(\mathrm{CL})(\mathrm{CL2})$

For segment $(lc-1)$,

$$C_3 \left\{ \begin{array}{c} P_{(c)} \\ P_{(c)}(e_v + d_{v_{(lc-1)}}) \\ P_{(c)}(\epsilon_u + d_{u_{(lc-1)}}) \end{array} \right\} = \left[\begin{array}{cccc} C_3 B_{11_{(lc-1)}} & -2(C_2)B_{12_{(lc-1)}} & -2(C_2)B_{13_{(lc-1)}} & \cdots \\ C_3 B_{21_{(lc-1)}} & -2(C_2)B_{22_{(lc-1)}} & -2(C_2)B_{23_{(lc-1)}} & \cdots \\ C_3 B_{31_{(lc-1)}} & -2(C_2)B_{32_{(lc-1)}} & -2(C_2)B_{33_{(lc-1)}} & \cdots \end{array} \right.$$

$$\left. \begin{array}{ccccc} \cdots & 2(C_1)B_{12_{(lc-1)}} & 2(C_1)B_{13_{(lc-1)}} & -2(C_0)B_{12_{(lc-1)}} & -2(C_0)B_{13_{(lc-1)}} \\ \cdots & 2(C_1)B_{22_{(lc-1)}} & 2(C_1)B_{23_{(lc-1)}} & -2(C_0)B_{22_{(lc-1)}} & -2(C_0)B_{23_{(lc-1)}} \\ \cdots & 2(C_1)B_{32_{(lc-1)}} & 2(C_1)B_{33_{(lc-1)}} & -2(C_0)B_{32_{(lc-1)}} & -2(C_0)B_{33_{(lc-1)}} \end{array} \right] \left\{ \begin{array}{c} \epsilon_{0_{(lc)}} \\ d_{v_{(lc-2)}} \\ d_{u_{(lc-2)}} \\ d_{v_{(lc-1)}} \\ d_{u_{(lc-1)}} \\ d_{v_{(lc)}} \\ d_{u_{(lc)}} \end{array} \right\} \quad (G.8)$$

Rearrange above Eq. (G.8) and for segment (i),

$$(C_0)^2 \left\{ \begin{array}{c} P_{(c)} \\ P_{(c)}(e_v + d_{v_{(i)}}) \\ P_{(c)}(e_u + d_{u_{(i)}}) \end{array} \right\} =$$

$$\begin{bmatrix} 0 & -B_{12_{(i)}} & -B_{13_{(i)}} & (C_0)^2 B_{11_{(i)}} & 2B_{12_{(i)}} & 2B_{13_{(i)}} & 0 & -B_{12_{(i)}} & -B_{13_{(i)}} \\ 0 & -B_{22_{(i)}} & -B_{23_{(i)}} & (C_0)^2 B_{21_{(i)}} & 2B_{22_{(i)}} & 2B_{23_{(i)}} & 0 & -B_{22_{(i)}} & -B_{23_{(i)}} \\ 0 & -B_{32_{(i)}} & -B_{33_{(i)}} & (C_0)^2 B_{31_{(i)}} & 2B_{32_{(i)}} & 2B_{33_{(i)}} & 0 & -B_{32_{(i)}} & -B_{33_{(i)}} \end{bmatrix} \begin{Bmatrix} 0 \\ d_{v_{(i-1)}} \\ d_{u_{(i-1)}} \\ \epsilon_{0_{(i)}} \\ d_{v_{(i)}} \\ d_{u_{(i)}} \\ 0 \\ d_{v_{(i+1)}} \\ d_{u_{(i+1)}} \end{Bmatrix} \qquad (G.9)$$

And let

$$G_{(i)} = \begin{bmatrix} 0 & -B_{12_{(i)}} & -B_{13_{(i)}} \\ 0 & -B_{22_{(i)}} & -B_{23_{(i)}} \\ 0 & -B_{32_{(i)}} & -B_{33_{(i)}} \end{bmatrix}$$

$$H_{(i)} = \begin{bmatrix} (C_0)^2 B_{11_{(i)}} & 2B_{12_{(i)}} & 2B_{13_{(i)}} \\ (C_0)^2 B_{21_{(i)}} & 2B_{22_{(i)}} & 2B_{23_{(i)}} \\ (C_0)^2 B_{31_{(i)}} & 2B_{32_{(i)}} & 2B_{33_{(i)}} \end{bmatrix}$$

For segment (lc),

$$G_{(lc)} = \begin{bmatrix} 0 & -B_{12_{(lc)}} & -B_{13_{(lc)}} \\ 0 & -B_{22_{(lc)}} & -B_{23_{(lc)}} \\ 0 & -B_{32_{(lc)}} & -B_{33_{(lc)}} \end{bmatrix}$$

$$H_{(lc)} = \begin{bmatrix} (C_2)^2 B_{11_{(lc)}} & 2B_{12_{(lc)}} & 2B_{13_{(lc)}} \\ (C_2)^2 B_{21_{(lc)}} & 2B_{22_{(lc)}} & 2B_{23_{(lc)}} \\ (C_2)^2 B_{31_{(lc)}} & 2B_{32_{(lc)}} & 2B_{33_{(lc)}} \end{bmatrix}$$

For segment $(lc-1)$,

$$G1_{(lc-1)} = \begin{bmatrix} 0 & -2(C_2)B_{12_{(lc-1)}} & -2(C_2)B_{13_{(lc-1)}} \\ 0 & -2(C_2)B_{22_{(lc-1)}} & -2(C_2)B_{23_{(lc-1)}} \\ 0 & -2(C_2)B_{32_{(lc-1)}} & -2(C_2)B_{33_{(lc-1)}} \end{bmatrix}$$

$$G2_{(lc-1)} = \begin{bmatrix} 0 & -2(C_0)B_{12_{(lc-1)}} & -2(C_0)B_{13_{(lc-1)}} \\ 0 & -2(C_0)B_{22_{(lc-1)}} & -2(C_0)B_{23_{(lc-1)}} \\ 0 & -2(C_0)B_{32_{(lc-1)}} & -2(C_0)B_{33_{(lc-1)}} \end{bmatrix}$$

$$H_{(lc-1)} = \begin{bmatrix} (C_3)B_{11_{(lc-1)}} & 2(C_1)B_{12_{(lc-1)}} & 2(C_1)B_{13_{(lc-1)}} \\ (C_3)B_{21_{(lc-1)}} & 2(C_1)B_{22_{(lc-1)}} & 2(C_1)B_{23_{(lc-1)}} \\ (C_3)B_{31_{(lc-1)}} & 2(C_1)B_{32_{(lc-1)}} & 2(C_1)B_{33_{(lc-1)}} \end{bmatrix}$$

Add i=2 to $i = lc$, it results in the following equations :

$$\left\{ \begin{array}{c} (C_0)^2 P_{(c)} \\ (C_0)^2 P_{(c)}(e_v + d_{v_{(2)}}) \\ (C_0)^2 P_{(c)}(e_u + d_{u_{(2)}}) \\ \vdots \\ (C_0)^2 P_{(c)} \\ (C_0)^2 P_{(c)}(e_v + d_{v_{(i)}}) \\ (C_0)^2 P_{(c)}(e_u + d_{u_{(i)}}) \\ \vdots \\ (C_3)P_{(c)} \\ (C_3)P_{(c)}(e_v + d_{v_{(lc-1)}}) \\ (C_3)P_{(c)}(e_u + d_{u_{(lc-1)}}) \\ (C_2)^2 P_{(c)} \\ (C_2)^2 P_{(c)}(e_v + d_{v_{(lc)}}) \\ (C_2)^2 P_{(c)}(e_u + d_{u_{(lc)}}) \end{array} \right\} =$$

$$
\begin{bmatrix}
H_{(2)} & G_{(2)} & & & & & & & \\
G_{(3)} & H_{(3)} & G_{(3)} & & & & & & \\
& \ddots & \ddots & \ddots & & & & & \\
& & G_{(i)} & H_{(i)} & G_{(i)} & & & & \\
& & & \ddots & \ddots & \ddots & & & \\
& & & & G1_{(lc-1)} & H_{(lc-1)} & G2_{(lc-1)} & \\
& & & & & & 2G_{(lc)} & H_{(lc)}
\end{bmatrix}
\begin{Bmatrix}
\epsilon_{0_{(2)}} \\ d_{v_{(2)}} \\ d_{u_{(2)}} \\ \vdots \\ \epsilon_{0_{(i)}} \\ d_{v_{(i)}} \\ d_{u_{(i)}} \\ \vdots \\ \epsilon_{0_{(lc)}} \\ d_{v_{(lc)}} \\ d_{u_{(lc)}}
\end{Bmatrix}
\tag{G.10}
$$

Select the deflection $d_{v_{(lc)}}$ as the control increment for each iteration step and interchange $d_{v_{(lc)}}$ and $P_{(c)}$ from Eq. (G.10), one has

$$
-d_{v_{(lc)}}
\begin{Bmatrix}
0 \\ 0 \\ 0 \\ \vdots \\ \vdots \\ -2(C_0)B_{12_{(lc-1)}} \\ -2(C_0)B_{22_{(lc-1)}} \\ -2(C_0)B_{32_{(lc-1)}} \\ 2B_{12_{(lc)}} \\ 2B_{22_{(lc)}} \\ 2B_{32_{(lc)}}
\end{Bmatrix}
=
$$

known

$$
\begin{bmatrix}
(C_0)^2 B_{11_{(2)}} & 2B_{12_{(2)}} & 2B_{13_{(2)}} & \cdots & -(C_0)^2 & 0 \\
(C_0)^2 B_{21_{(2)}} & 2B_{22_{(2)}} & 2B_{23_{(2)}} & \cdots & -(C_0)^2(e_v + d_{v_{(2)}}) & 0 \\
(C_0)^2 B_{31_{(2)}} & 2B_{32_{(2)}} & 2B_{33_{(2)}} & \cdots & -(C_0)^2(e_u + d_{u_{(2)}}) & 0 \\
 & \ddots & \ddots & \ddots & \vdots & \vdots \\
 & & & & -(C_3) & -2(C_0)B_{13_{(lc-1)}} \\
 & & & & -(C_3)(e_v + d_{v_{(lc-1)}}) & -2(C_0)B_{23_{(lc-1)}} \\
 & & & & -(C_3)(e_u + d_{u_{(lc-1)}}) & -2(C_0)B_{33_{(lc-1)}} \\
 & & & & -(C_2)^2 & 2B_{13_{(lc)}} \\
 & 0 & & & -(C_2)^2(e_v + d_{v_{(lc)}}) & 2B_{23_{(lc)}} \\
 & & & & -(C_2)^2(e_u + d_{u_{(lc)}}) & 2B_{33_{(lc)}}
\end{bmatrix}
\begin{Bmatrix}
\epsilon_{0_{(2)}} \\ d_{v_{(2)}} \\ d_{u_{(2)}} \\ \vdots \\ \epsilon_{0_{(i)}} \\ d_{v_{(i)}} \\ d_{u_{(i)}} \\ \vdots \\ \epsilon_{0_{(lc)}} \\ P_{(c)} \\ d_{u_{(lc)}}
\end{Bmatrix}
\tag{1012}
$$

known unknown